INVESTIGATION OF THE EFFECT OF TIRE WASTE INCLUSIONS ON THE SHEAR STRENGTH PARAMETERS OF SAND

by

Ahmet Çağatay

B.S., Civil Engineering, İstanbul Technical University, 2006

Submitted to the Institute for Graduate Studies in
Science and Engineering in partial fulfillment of
the requirements for the degree of
Master of Science

Graduate Program in Civil Engineering

Boğaziçi University

2008

ACKNOWLEDGEMENTS

Foremost, I would like to thank my thesis supervisor Assoc. Prof. Ayşe Edinçliler, who shared with me a lot of her expertise and research insight. This thesis would not have been possible without her guidance.

I wish to thank all the research assistants in the Geotechnical Laboratory of Bogazici University, for helping me during my experimental study.

Finally, I would like to thank all my family and friends who stood behind me during my study, for I would not be able to accomplish this thesis without their support.

ABSTRACT

INVESTIGATION OF THE EFFECT OF TIRE WASTE INCLUSIONS ON THE SHEAR STRENGTH PARAMETERS OF SAND

Using tire wastes as lightweight materials in highway embankment construction has many benefits in environmental and geotechnical aspects. Tire waste additions to sand enhance the shear strength of soil for embankment construction leading to lower settlement and higher bearing capacity. The objective of this thesis is to investigate the effect of the tire waste inclusions to sand on shear strength of the mixture. In this study, three different parameters as tire waste shape, tire waste content, and tire waste aspect ratio are examined. By using granular shape and fiber shape tire wastes, three different experimental programs are performed. Quick and consolidated drained (CD) triaxial compression tests are conducted by using a standard triaxial test equipment, and CBR tests are conducted by using a standard CBR test equipment. In the first part, tire crumb, tire buffings and their mixtures with sand are tested in CBR test. In the second and third parts, the same materials are tested in the quick triaxial compression and consolidated drained (CD) triaxial tests. The quick triaxial compression tests are conducted on dry specimens. At the last part, the test results are compared with the literature. The results indicate that tire shape, tire aspect ratio, and tire content have a significant effect on the shear strength parameters and the CBR value of the composition. The triaxial test results show that the optimum results are obtained by 5 per cent tire buffings addition to the sand. It is concluded that fiber shaped tire inclusions influences the shear strength parameters and the CBR value better compared to granular tire inclusions. Also, the CBR test results indicated that as the aspect ratio increases, the effectiveness of the reinforcements increase. From the literature study and this study it is revealed that processing type of tire waste affects the shear strength values.

ÖZET

ATIK LASTİK İLAVELERİNİN KUMUN KESME MUKAVEMETİ PARAMETRELERİ ÜZERİNDEKİ ETKİLERİNİN ARAŞTIRILMASI

Atık lastiklerin hafif yapı malzemeleri olarak yol dolgularında kullanımının hem çevresel hem de geoteknik açıdan faydaları bilinmektedir. İşlenmiş atık lastiklerin kum ile karıştırılması sonucunda yüksek kesme kuvvetine sahip dolgu malzemesi elde edilebilir. Bu tezin amacı kum ile karıştırılan farklı özelliklerdeki atık lastik ilavelerinin malzemenin kesme kuvveti ve Kaliforniya Taşıma Oranı değerleri üzerindeki etkilerinin incelenmesidir. Bu çalışmada üç farklı değişken ele alınmıştır. Bunlar atık lastik ilavesinin şekli, miktarı ve en boy oranıdır. Granül ve lif şeklinde olan farklı atık lastikler kullanılarak üç farklı deneysel program uygulanmıştır. Hızlı üç eksenli basınç ve konsolidasyonlu drenajlı üç eksenli basınç deneyleri ve Kaliforniya Taşıma Oranı deneyi yapılmıştır. İlk bölümde farklı şekil ve en boy oranına sahip granül ve kırpıntı lastiklerin kum ile karıştırılması ile elde edilen numuneler üzerinde Kaliforniya Taşıma Oranı deneyi yapılmıştır. İkinci ve üçüncü bölümlerde aynı malzemeler üzerinde hızlı üç eksenli basınç ve konsolidasyonlu drenajlı üç eksenli basınç deneyleri yapılmıştır. Hızlı üç eksenli deneyleri kuru numuneler üzerinde yapılmıştır. Son bölümde ise deney sonuçlarının literatür ile kıyaslaması yapılmıştır. Deney sonuçlarına göre atık lastik şeklinin, en boy oranının ve karıştırılan miktarın kumun kesme kuvveti ve Kaliforniya Taşıma Oranı değeri üzerinde önemli ölçüde etkileri olmaktadır. Üç eksenli basınç deneyi sonuçlarına göre en uygun dolgu malzemesi ağırlıkça yüzde 5 kırpıntı lastiğin kum ile karıştırılması sonucu elde edilebilir. Lif şeklindeki lastik katkısı, granül şeklindeki lastik katkısına kıyasla daha yüksek kesme kuvveti ve Kaliforniya Taşıma Oranı değeri vermektedir. Kaliforniya Taşıma Oranı deneyi sonuçlarına göre lastiklerin en boy oranı arttıkça katkı maddeleri daha efektif çalışmaktadır. Literatür çalışması ve bu çalışmanın sonucunda, atık lastiklerin üretim şeklinin kesme mukavemeti üzerinde önemli bir etkisinin olduğu görülmektedir.

TABLE OF CONTENTS

LIST OF FIGURES

LIST OF TABLES

LIST OF SYMBOLS / ABBREVIATIONS

c	Cohesion value
Φ	Angle of internal friction
Φ_{eq}	Equivalent angle of internal friction
σ_1	Major principle stress
σ_2	Intermediate principle stress
σ_3	Minor principle stress
ΔS_R	Increase in shear strength caused by the addition of reinforcement
t_R	Mobilized tensile strength of inclusions per unit area of soil
θ	Angle of shear distortion
i	Initial orientation angle with respect to shear surface
σ_R	Tensile stress developed in the inclusion at the shear plane
x	Horizontal shear displacement
z	Thickness of shear zone
k	Shear distortion ratio

ADU	Autonomous Data Acquisition Unit
ASTM	American Society of Testing Materials
CBR	California Bearing Ratio
CD	Consolidated Drained
DS7	Data System 7
RMA	Rubber Manufacturers Association
TOC	Total Organic Carbon
UU	Unconsolidated Undrained

1. INTRODUCTION

1.1. General

Millions of scrap tires are discarded annually and even larger numbers are currently stockpiled all around the world. The disposal of scrap tire stockpiles address to be a serious problem as tires do not decompose. These large amounts of scrap tire stockpiles are consuming valuable landfill space, and the improperly disposed ones constitute environmental and health hazards by producing air pollution from tire stockpile fires and by providing breeding grounds for disease carrying mosquitoes and vermin. Because of these reasons the recycling and reuse of tire wastes are getting more important each year. Waste tires can mainly be reused as rubber products, retreads, or fuel for energy production, and tires can be recycled for civil engineering or ground rubber applications.

The use of tire waste in civil engineering applications can reduce the tire disposal problem in an economically and environmentally beneficial way. In addition to these, tire wastes have unique properties for many geotechnical applications. Tire wastes can be used in highway and earthwork construction as lightweight fill material for retaining wall backfills and embankments, or in landfill applications as drainage material, leachate treatment medium, and thermal insulator. Properties of tire wastes such as durability, strength, resiliency, and high frictional resistance are of significant value for the design of highway embankments. The mixture of processed tires with soil for embankment construction may not only provide alternative means of reusing tires to address economic and environmental concerns, but also help solve geotechnical problems associated with low soil shear strength. By using different processing techniques different sized and shaped tire waste can be obtained, like granular or fiber shaped tire wastes.

The concept of reinforcing soil with natural fiber materials originated in ancient times. However, the use of randomly distributed fibers as soil reinforcement has recently attracted extra attention in geotechnical engineering. The use of fibers in geotechnical engineering is a major focus in the recent years because fiber materials are competitive with other materials in geotechnical aspects. Commonly used fiber reinforcement materials

are geosynthetics, wood, and steel. However, the use of fiber shaped tire waste inclusions is getting more popular because they are as effective as other reinforcements, and they may lead to cost-savings in some of the countries.

The aim of this thesis is to investigate the effect of the tire waste inclusions on the shear strength of tire waste – sand mixtures containing tire buffings and tire crumb and to determine the optimum tire waste inclusion to be used in highway embankment constructions. For this reason, samples prepared with various tire content, shape, and aspect ratio are tested using the triaxial compression tests. Also, CBR tests are formed to determine the CBR values of mixtures.

1.2. Problem Statement

The amount of waste tire deposits are increasing each year all over the world, and this issue is threatening the environment and economy of many countries. For this reason, new ways of recycling and reusing waste tires is a popular research in today's world. An alternative way to consume large amounts of waste tires is using them in geotechnical applications. Besides overcoming the environmental problems, use of scrap tires in embankment constructions helps solving geotechnical problems. Lightweight embankments composed of soil and tire waste inclusions are especially useful for highways constructed over soft soils, where large settlements can occur. The use of tire waste inclusions will lower the amount of settlement. The slopes of the embankment can also be made steeper than usual with the use of tire waste-sand composition. In addition to this, the use of tire wastes as reinforcement materials will result in savings of natural materials like sand or gravels.

1.3. Objective of the Thesis

The objective of this thesis is to determine the tire waste shape and size effect on the shear strength of the sand-tire waste mixtures for highway embankments. The addition of fiber shaped tire buffings with an aspect ratio of 3.5-4, and granular tire crumb with an aspect ratio of 1-1.5 to sand at varying contents is investigated to determine the shear strength parameters of the compositions. Triaxial compression tests are performed to

determine the shear strength parameters. By studying the experimental results, an optimum tire content, tire shape, and tire aspect ratio are chosen to be used in embankment constructions. Literature study is also performed to be able to assess this study with the experimental studies of other researchers.

1.4. Organization of the Thesis

In the first part of the thesis, a literature review about the general characteristics and civil engineering applications of tire wastes is presented. The next part contains general information about lightweight reinforcement materials, including different types of reinforcement materials and background information about previous studies. These parts are followed by the experimental procedures, in which detailed information about the conducted tests is gathered. The experimental results part of the thesis contains the results of the conducted tests. Finally, the results obtained from the experiments are summarized, the optimum lightweight composition and further study is proposed, and comparison with the literature is presented.

2. LITERATURE REVIEW

2.1. General Information About Scrap Tires

Number of scrap tire stockpiles continues to increase each year all over the world. In Europe approximately 2.5 million tons of scrap tire arise every year. In the United States, according to the last recorded data by Rubber Manufacturers Association (RMA, 2006), 299 million tires were discarded in 2005. On the other hand, in 2005, 87 per cent of the scrap tires were consumed in end-use markets in the U.S., which is approximately 259 million scrap tires. Although each year the amount of scrap tire stockpiles increase, the utilized amounts of scrap tires also increase with the growing market of scrap tires. The ratio of the amount of utilized scrap tires in 2005 to that in 1990 is 8:1 (RMA, 2006). Figure 2.1 shows the scrap tire management trends in the U.S. between 1990 and 2005. Scrap tires are consumed by a variety of scrap tire markets, including tire-derived fuel, civil engineering and ground rubber applications, as well as other smaller markets and legal landfilling (RMA, 2006).

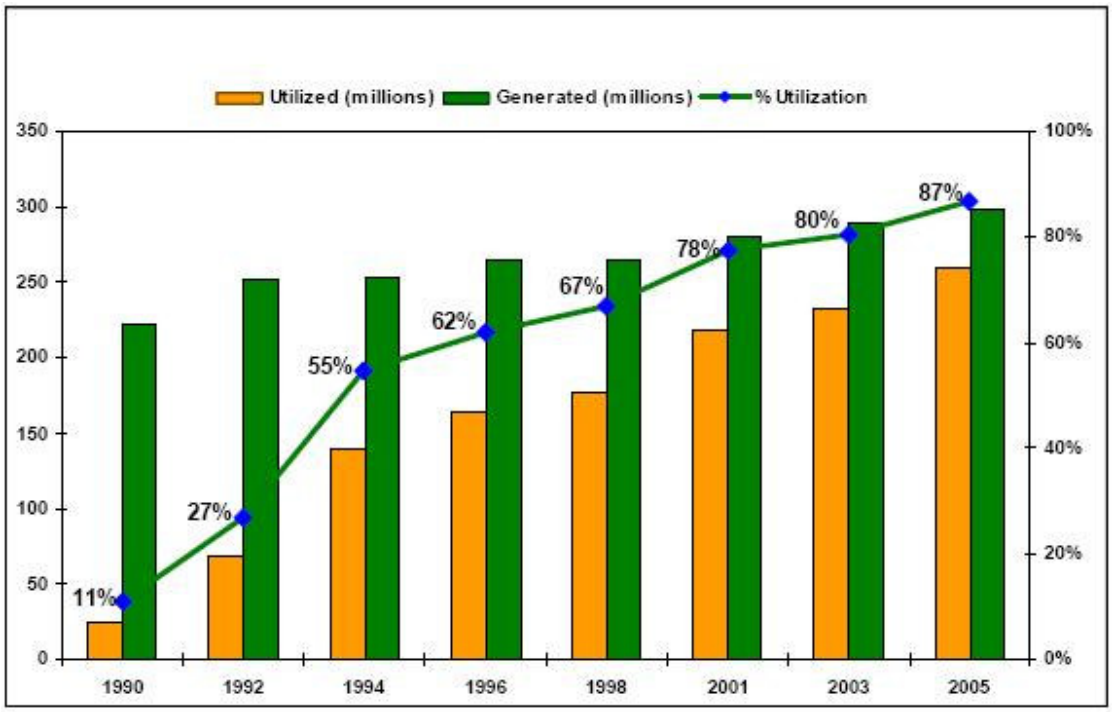

Figure 2.1. U.S. scrap tire management trends, 1990-2005 (RMA, 2006)

2.1.1. Tire-Derived Fuel

In this application, scrap tires are used as a cleaner and more economical alternative to coal as fuel. They are used as fuel in cement kilns, pulp and paper mills, and industrial and utility boilers. Tire-derived fuel accounted for about 155 million scrap tires in the U.S. in 2005, which corresponds to the 52 per cent of the total scrap tires generated (Figure 2.2). Due to increasing fuel prices and improvements in the quality, this market is anticipated to experience continued growth in the future.

2.1.2. Civil Engineering Applications

The civil engineering market consumed over 49 million tires in 2005, about 16 per cent of the total tires. The applications are mainly consist of use of tire shreds in road and landfill construction, septic tank leach fields, and other construction applications. Tires add beneficial properties in these applications, such as vibration and sound control, lightweight fill to prevent erosion and landslides, and facilitate drainage in leachate systems.

2.1.3. Ground Rubber Applications

This market consumed nearly 38 million tires in 2005, which is about 12 per cent of the scrap tires generated. Ground rubber applications include new rubber products, playground and other sports surfacing, and rubber-modified asphalt. The sports surfacing market was the most dynamic segment between these applications in 2005. The asphalt market uses ground rubber to modify the asphalt binder used in road paving, resulting in more durable roads.

2.1.4. Other Markets

Other markets include scrap tire exports, punched and stamped products and agricultural and miscellaneous uses. The export of tires was about 6.5 million tires in 2005. Punched and stamped products market used about 6.1 million tires. For agricultural and miscellaneous uses about 3 million tires were used.

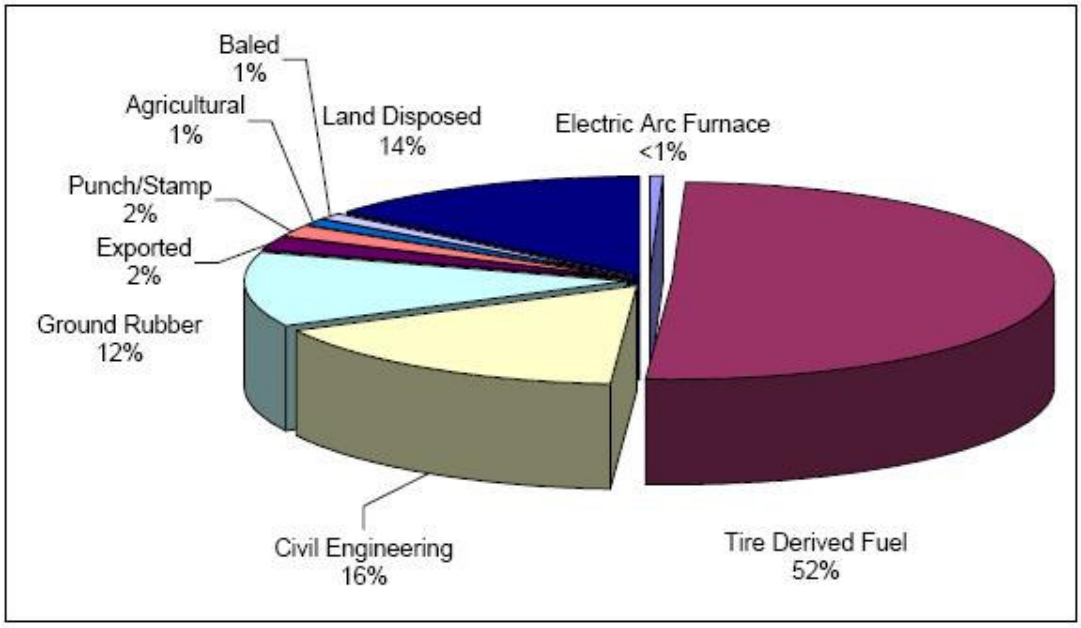

Figure 2.2. U.S. scrap tire disposition in 2005 (RMA, 2006)

2.2. Types of Processed Tires

Waste tires can be processed as whole, slit, shred, chip, ground rubber, crumb rubber, or rubber buffings. Examples of different shapes and sizes of processed tires are shown in Figure 2.3. A typical scrap automobile tire weighs 9.1 kg. Roughly 5.4 kg to 5.9 kg consists of recoverable rubber, composed of 35 per cent natural rubber and 65 per cent synthetic rubber. A typical truck tire weighs 18.2 kg and also contains about 60 per cent recoverable rubber. Truck tires typically contain 65 per cent natural rubber, and 35 per cent synthetic rubber. Tire cutting machines produce slit tires by first cutting it into halves and then separating the sidewall from the tread of the tire.

Tire shreds are pieces of scrap tires that have a basic geometrical shape in terms of cross section and are generally between 50 and 305 mm in size according to ASTM D6270-98. They are flat irregularly shaped tire chunks that may contain steel belts or beads. The production of tire shreds or tire chips involves primary and secondary shredding. Tire chips are pieces of scrap tires that have a basic geometrical shape and are generally between 12 and 50 mm in size and have most of the wires removed (ASTM D6270-98). A tire shredder is a machine with a series of oscillating or reciprocating cutting edges, moving

back and forth in opposite directions to create a shearing motion, that effectively cuts or shreds tires as they are fed into the machine.

Ground and crumb rubber have particle sizes ranging from 19 to 0.15 mm and 4.75 to 0.075 mm, respectively (ASTM D6270-98). The production of ground rubber is achieved by granulators, hammermills, or fine grinding machines. Granulators typically produce particles that are regularly shaped and cubical with a comparatively low-surface area. The steel belt fragments are removed by a magnetic separator. Fiberglass belts or fibers are separated from the finer rubber particles by an air separator. For converting scrap tires to crumb rubber, three methods are currently used. The crackermill process is the most commonly used method. The crackermill process tears apart or reduces the size of tire rubber by passing the material between rotating corrugated steel drums. This process creates an irregularly shaped torn particle with a large surface area. The second method is the granulator process, which shears apart the rubber with revolving steel plates that pass at close tolerance. The third process is the micro-mill process, which produces a very fine ground crumb rubber.

In addition to these, another type of processed waste tire is tire buffings. According to ASTM D6270-98, a buffing is a vulcanized rubber usually obtained from a worn or used tire in the process of removing the old tread in preparation for retreading. Tire buffings are the by-product of the tire retread process.

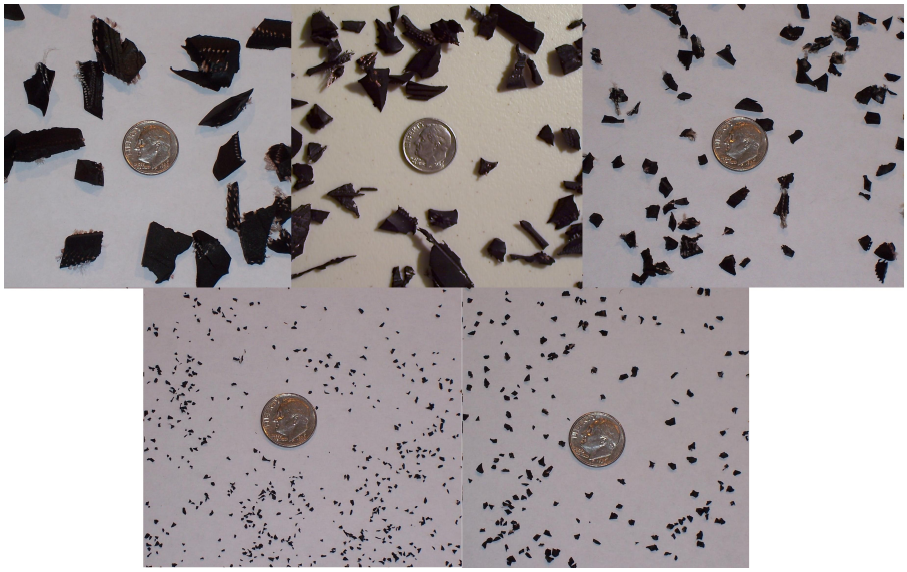

Figure 2.3. Example of different shapes and sizes of processed tires

2.3. Typical Tire Characteristics

Tires are composed of a combination of natural rubber and synthetic rubber elastomers derived from oil and gas. Multiple carbon blacks, extender oils, waxes, antioxidants, and other materials are added to enhance performance characteristics and manufacturing efficiency. To optimize performance characteristics, different polymers and additives are utilized in each section of a tire. Due to the composition and curing process, tires retain their basic chemical properties even when shredded into smaller pieces (Gray, 1997).

Steel or fabric reinforcement will have been added to improve strength of the tire, especially in the bead area bordering the rim. Steel belts and beads in the tire shreds can be exposed, which can be hazardous for the personnel.

Dissolution of exposed steel and zinc oxide can occur in aqueous environments depending upon pH conditions (Gray, 1997). The source of zinc leached from tire shreds can probably be zinc oxide in the rubber or zinc coating on the steel belt.

The tire composition may vary by manufacturer, but the main inorganic constituents are steel from reinforcing wire (5-15 per cent of total weight), titanium dioxide used in white sidewalls and letters, and zinc oxide and sulfur distributed uniformly within the polymer matrix to achieve vulcanization. Smaller concentrations of calcium and aluminum are also present, with very little magnesium, phosphorus, potassium, silica, sodium, and chloride. Tires are combustible if exposed to a continuous source generating temperatures around 322ºC (Gray, 1997).

2.4. Properties of Tire Wastes

Studies were made by Moo-Young et al. (2003) to determine the physical and chemical properties of tire shreds for use in engineering construction as a replacement for aggregates in embankments or as backfill. In general, test results revealed that tire shreds can be utilized in construction applications. As the size of tire shreds increases, physical properties such as specific gravity remained constant. As the tire shred size increased, the

hydraulic conductivity increased from 0.2 to 0.85 cm/s. Increasing the compaction energy had little effect on the final compaction density. The angle of friction and cohesion ranged from 15° to 32° and 349 to 394 N/m², respectively. As the particle size of the tire shreds increased, the shear strength of the scrap tire increased. Moreover, as the tire shred size increased, compressibility increased. Water absorption capacity of tire shreds generally ranges from 2 per cent to 4 per cent (Humphrey, 1997). Absorption capacity is the amount of water absorbed onto the surface of the tire shreds.

Water adsorption and specific gravity tests were performed on random samples of tire shreds by Moo-Young et al. (2003). The water adsorption of the tire shreds ranged from 6.7 per cent to 7 per cent, which are similar to the results reported by other researchers (Humprey and Manion, 1992). The specific gravity of tire shreds tested ranged from 1.06 to 1.12. These values show a good relation with the results of other researchers (Edil and Bosscher, 1994; Zimmerman, 1997). The values are shown in Table 2.1. The specific gravity of soils typically ranges from 2.6 to 2.8, which is more than twice that of tire shreds.

Table 2.1 Specific gravity and water adsorption values (Moo-Young et al., 2003)

Tire size (mm)	Specific gravity	Water adsorption (%)
<50	1.10	6.70
50–100	1.10	6.95
100–200	1.06	7.10
200–300	1.10	7.00

Moo-Young et al. (2003) measured the amount of exposed steel belts in accordance to ASTM D6270. Random samples of tire shreds with steel belts were used. The percentage of exposed wire was obtained by dividing the area of the exposed wire by the area of the rubber and area of the exposed wire. Table 2.2 presents the results of this study. The tire shreds examined contained a high percentage of exposed steel, so if these materials are to be utilized in construction applications, then a shredded that removes steel belts must be utilized.

Table 2.2. Exposed steel belts (Moo-Young et al. 2003)

Samples	Average tire area (mm^2)	Average area of wire (mm^2)	Wire in the shred (%)
30	625	166	21.0
30	2167	183	7.8
20	4333	41.6	1.0
17	10000	576	5.5
11	10400	520	4.8

Compaction tests were performed on tire shreds and tire chips using a 30.48 cm compaction mold with a modified compaction hammer and a 222N weight dropped from 91.4 cm (Moo-Young et al., 2003). The test results for the compaction of tire shreds at various particle sizes and the dry maximum unit weight is shown in Figure 2.4. The modified compaction hammer using 60 per cent compaction energy produced similar results to the 222N weight using 100 per cent compaction energy. It was reported that the compaction energy has only a small effect on the resulting dry unit weight.

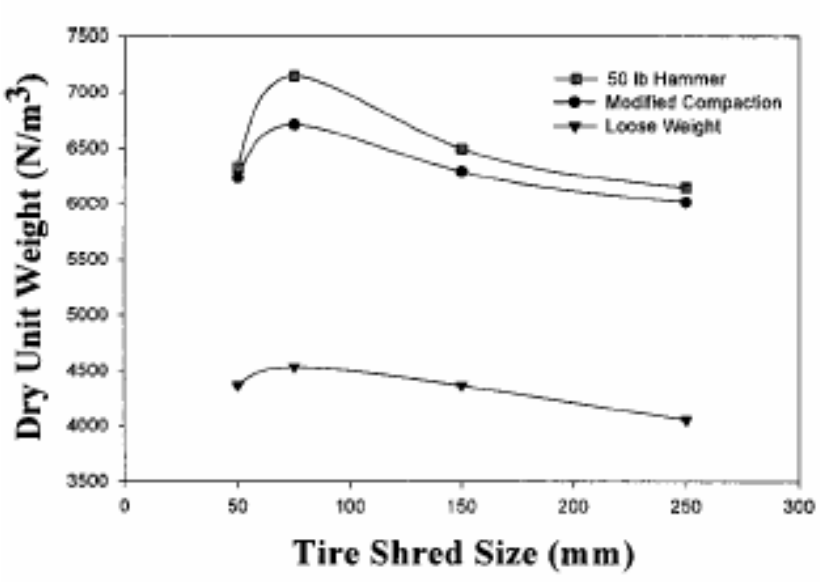

Figure 2.4. Compaction test results (Moo-Young et al., 2003)

Hydraulic conductivity tests were conducted on tire shreds to determine how the hydraulic conductivity of tire shreds change as the particle size increases (Moo-Young et al., 2003). The test results are shown in Figure 2.5. Hydraulic conductivity is defined as the rate of water flow under laminar flow conditions through a unit cross-sectional area of

porous medium under unit hydraulic gradient and standard temperature conditions. Hydraulic conductivity is of primary importance when assessing the feasibility of using tire shreds as a drainage material. According to the experimental results, as the tire shed increases in size, the hydraulic conductivity increases. The results are similar to the results obtained by other researchers (Edil and Bosscher, 1994). Various researchers also studied the hydraulic conductivity of different sized tire shreds (Humprey et al., 1992; Ahmed and Lovell, 1993; Duffy, 1995; Narejo and Shettima, 1995; Zimmerman, 1997; Lawrence et al., 1998). There is a wide range of hydraulic conductivities determined by different researchers varying from 0.0005 to 59.3 cm/s. The wide range of hydraulic conductivity values is attributed to the differences in shred size and composition, compaction level, and normal stress. The lowest conductivity was measured by Masad et al. (1996) as 0.002 to 0.0005 cm/s, when the tire shreds were less than 0.18 inches in size. Such a small tire shred size is not suitable due to the low hydraulic conductivity and high shredding cost. Reddy and Marella (2001) prepared a summary of the previous studies on the hydraulic conductivity of different sized tire shreds, which is shown in Table 2.3.

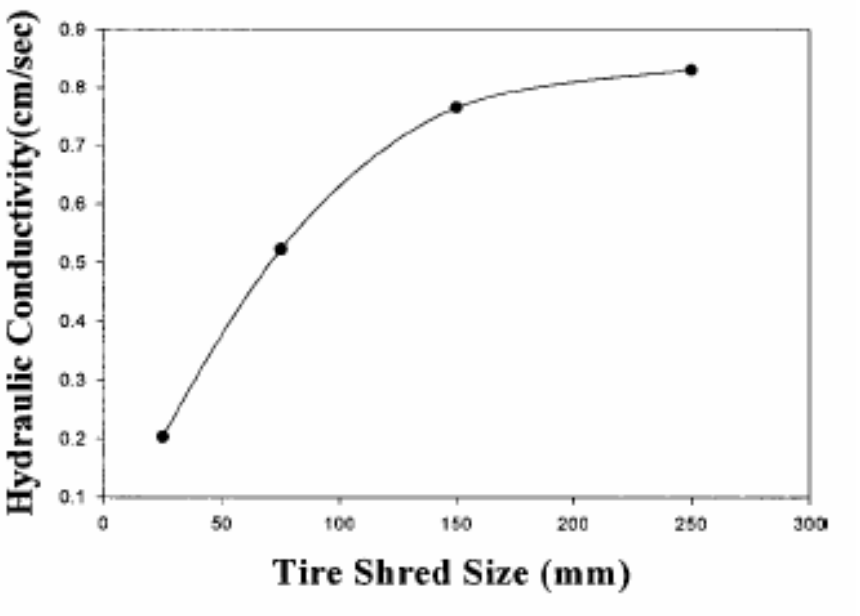

Figure 2.5. Hydraulic conductivity and tire size relationship (Moo-Young et al., 2003)

Table 2.3. Hydraulic conductivity of different size tire shreds (Reddy and Marella, 2001)

Reference	Tire Shred Size (inch)	Hydraulic Conductivity (cm/s)	Specific Test Conditions
Bressette, 1984 ASTM, 1998	1-2.5	2.9-23.5	-
	0.2-2.0	3.8-59.3	-
Hall, 1991	1.5	1.43-2.64	Simulated overburden of 0 to 35 feet of MSW
	0.75	0.79-2.74	Simulated overburden of 0 to 25 feet of MSW
Humphrey et al., 1992, Humphrey and Sandford, 1993 ASTM, 1998	0.4-2	7.7	Void ratio=0.925
	0.4-2	2.1	0.488
	0.75-3	15.4	1.114
	0.75-3	4.8	0.583
	0.4-1.5	6.9	0.833
	0.4-1.5	1.5	0.414
Edil et al., 1992 Edil and Bosscher, 1994	2-3	0.6	Stress (psf): 0
		0.45	1440
		0.4	2881
Ahmed and Lovell, 1993	0.5-1.5	0.58	-
Duffy, 1995	2	0.7	2500 psf (40 feet MSW)
		0.53	5000 psf (80 feet MSW)
		0.25	10000 psf (160 feet MSW)
		0.12	15000 psf (240 feet MSW)
Narejo and Shettima, 1995	2.4-4.0	55.0	1879
		20.0	3132
		10.0	7308
		6.0	11484
Andrews and Guay, 1996	1-2	1.0	-
Masad et al., 1996	0.18	0.002	3132
		$5x10^{-4}$	7308
Cecich et al., 1996	0.2-0.6	0.03	ASTM D2434
Bernal et al., 1996	2	1.2	-
Zimmerman, 1997	8-16	9.0	Void ratio=2.77
		3.2	1.53
		1.8	0.78
Lawrence et al., 1998	0.5-1.5	7.6	Void ratio=0.693
	0.5-1.5	1.5	0.328
	0.5-3	16.3	0.857
	0.5-3	5.6	0.546
Chu, 1998	0.25-0.5	0.16	-
	0.5-1.0	0.18	-
	1.0-1.5	0.18	-
Reddy and Saichek, 1998	0.5-5.5	0.65	3400 psf, Compression - 50%
	0.5-5.5	0.01	21000 psf Compression - 65%

Moo-Young et al. (2003) performed direct shear tests on tires of various particle sizes. The primary goal of the experiment was to determine the relation between shear strength and particle size. The shear strength between two particles is the force that must be applied to cause a relative movement between the particles, and it is a fundamental mechanical property that governs bearing capacity and slope stability. The Mohr-Coulomb failure envelopes and the corresponding shear strength parameters for various particle sizes are present in Figure 2.6. In general, as the particle size increased, the shear strength of tire particles increased. Several other researchers conducted direct shear and triaxial tests to

determine the shear strength parameters of tire shreds (Bresette, 1984; Ahmed and Lovell, 1993; Humprey et al., 1993; Foose et al., 1996; Edil and Bosscher, 1994; Bernal et al., 1996; Masad et al., 1996; Wu et al., 1997). The common result indicated by all researchers is that larger tire shred sizes possess shear strengths that are comparable to conventional drainage materials such as sand. A summary table was prepared by Reddy and Marella (2001) about the shear strength of tire shreds, which is shown in Table 2.4.

Table 2.4. Shear strength of different size tire shreds (Reddy and Marella, 2001)

Reference	Tire Shred Size (inch)	C (psf)	ϕ°	Specific Test Conditions/Normal Stress (psf)
Bresette, 1984	2-inch square	540	21	-
	2-inch shredded	660	14	
Ahmed and Lovell, 1993	0.5	747	20.5	Standard compaction & 20% strain as failure
	1.0	818	24.6	Modified compaction energy & 20% strain as failure
		694	25.3	Standard compaction energy & 20% strain as failure
		779	22.6	50% standard compaction energy & 20% strain as failure
Humphery et al., 1993	<1.5	180	25	Normal stress range: 400-1500 psf
	<2.0	90-160	21-26	
	<3.0	240	19	
Foose, 1993 Foose et al., 1996	<2 2-4 4-6	0-62.6	30	146-1460 psf
Edil and Bosscher, 1994	2-3	-	37-43	0
		-	85	Compacted Condition
Black and Shakoor, 1994	<0.04	100	30	Tested at dry unit weight of 33 pcf
	0.04-0.16	70	31	
	0.16-0.27	130	27	
Duffy, 1995	2	150	27	-
Cosgrove, 1995	1.5	69	38	Saturated
	3	90	32	
Bernal et al., 1996	2	0	17-35	17° at 5% strain 35° at 20% strain
Masad et al., 1996	0.18	1462	6	10% strain
		1482	11	15% strain
		1712	15	20% strain
Cecich et al., 1996	0.2-0.6	147	27	ASTM D3080
Andrews and Guay, 1996	1-2	80	27.5	-
Wu et al., 1997	<0.08	0	45	Tire shreds with out steel-triaxial tests under confining pressure of 720-1148 psf
	<0.37	0	47-60	
	<0.74	0	54	
	<1.5	0	57	
Gebhardt, 1997	1.5-55.1	65	38	115-585 psf Peak failure criterion
	1.5-55.1	0	38	115-585 psf 10% failure criterion

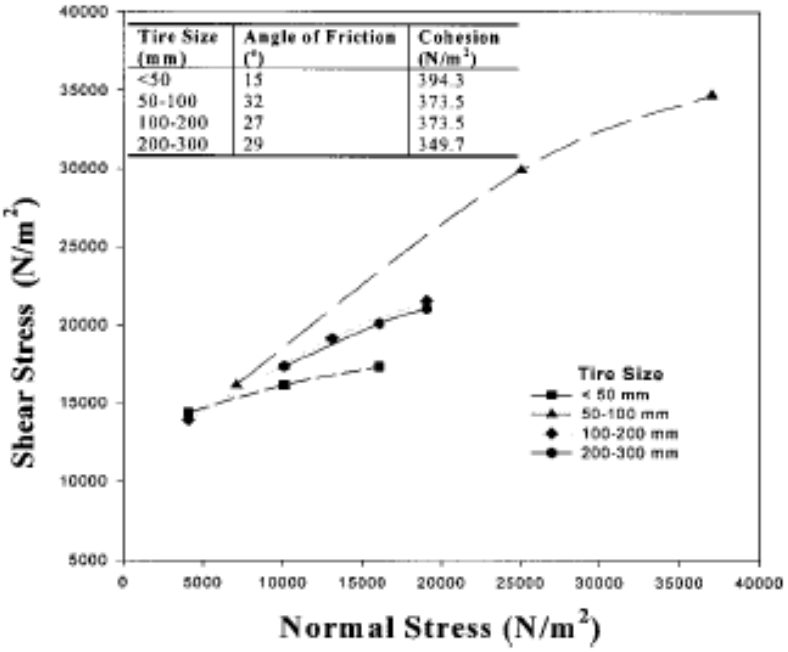

Figure 2.6. Failure envelope for tire particles (Moo-Young et al., 2003)

The property of a material pertaining to its susceptibility to volume change due to changes in stress is called compressibility. Tire shreds are highly compressible because of their high porosity and high rubber content. Compressibility tests were conducted on tires at various sizes, and on tire shreds mixed with soil at different mix ratios (Moo-Young et al., 2003). The primary reasons for conducting the tests were to determine the settlement that occurs during construction in the first couple of months to enable an adequate design that accounts for this settlement, to determine deflections caused by live or temporary loads post construction, and to determine the in-place unit weight of compressed scrap tire. The results indicated that as the tire shred size increases, the compressibility increases. This may be due to increased voids created by larger tire shreds. The test results are shown in Figure 2.7. Many other researchers investigated the compressibility of tire shreds (Hall, 1991; Humprey et al., 1992; Ahmed and Lovell, 1993; Edil and Bosscher, 1994; Zimmerman, 1997). The common reports of these researchers are that initially loosely placed tire shreds are compressed more than that of slightly compacted tire shreds, and that larger tire shreds are compressed more than smaller tire shreds. In addition, it was concluded that for stresses expected under landfill cover conditions, the compressibility of the tire shreds should range from 30 per cent to 50 per cent.

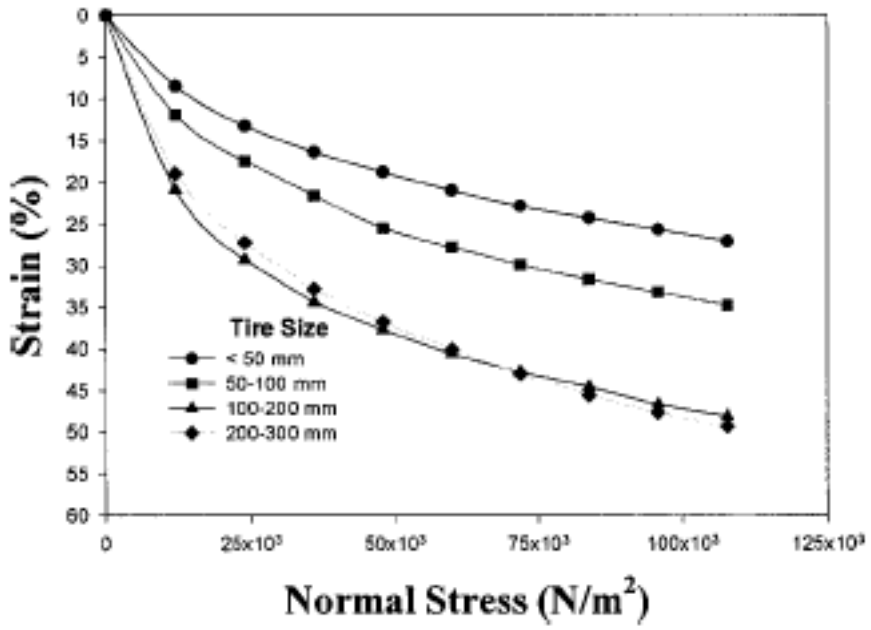

Figure 2.7. Compressibility test results (Moo-Young et al., 2003)

Chemical analysis of tire shreds was conducted to illustrate how properties such as total organic carbon, pH, and turbidity change with tire size (Moo-Young et al., 2003). Table 2.5 shows the results of chemical analysis. As tire shred size increases, the results illustrated a decrease in total organic carbon (TOC) and turbidity. Total organic carbon is the total amount of organic carbon molecules in the material, and turbidity is the amount of solid particles that are suspended in water. The pH also showed a slight decrease as tire size increased.

Table 2.5. TOC, pH, and turbidity results (Moo-Young et al., 2003)

Tire size (mm)	TOC (ppm)	pH	Turbidity (NTU)
<50	22.7	6.97	234
50–100	17.4	6.98	202
100–200	14.5	6.96	251
200–300	3.1	6.95	99

Continuous flow column tests were conducted on tire shreds by Moo-Young et al. (2003) for 7 days and showed improved water quality with time. The continuous flow column test results are present in Figure 2.8. However, pause flow column tests showed reduced water quality, which implies that placement of a tire embankment below the water

table where ponding can occur may reduced water quality. The pause flow experiment simulates a worst case scenario where waste tires are utilized to build an embankment below the water table or utilized as backfill below the water table where in both cases the drainage is inhibited by some physical mechanism. The results of pause flow column experiments are shown in Figure 2.9.

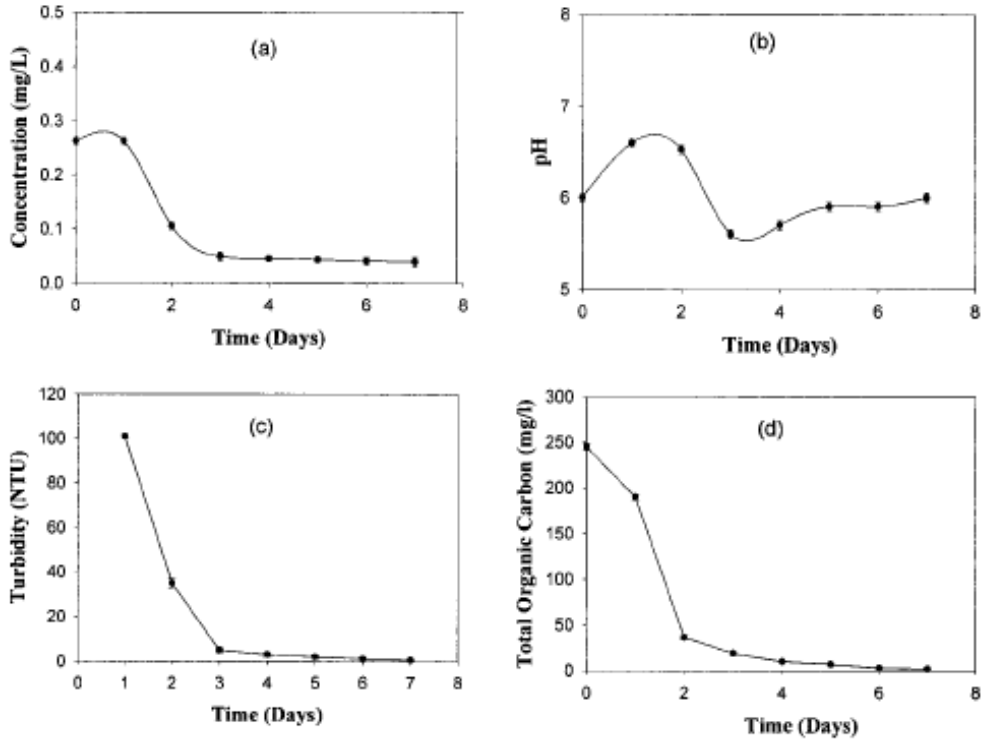

Figure 2.8. Continuous flow experiment results (a) Iron effluent concentrations, (b) pH, (c) turbidity, (d) TOC profiles (Moo-Young et al., 2003)

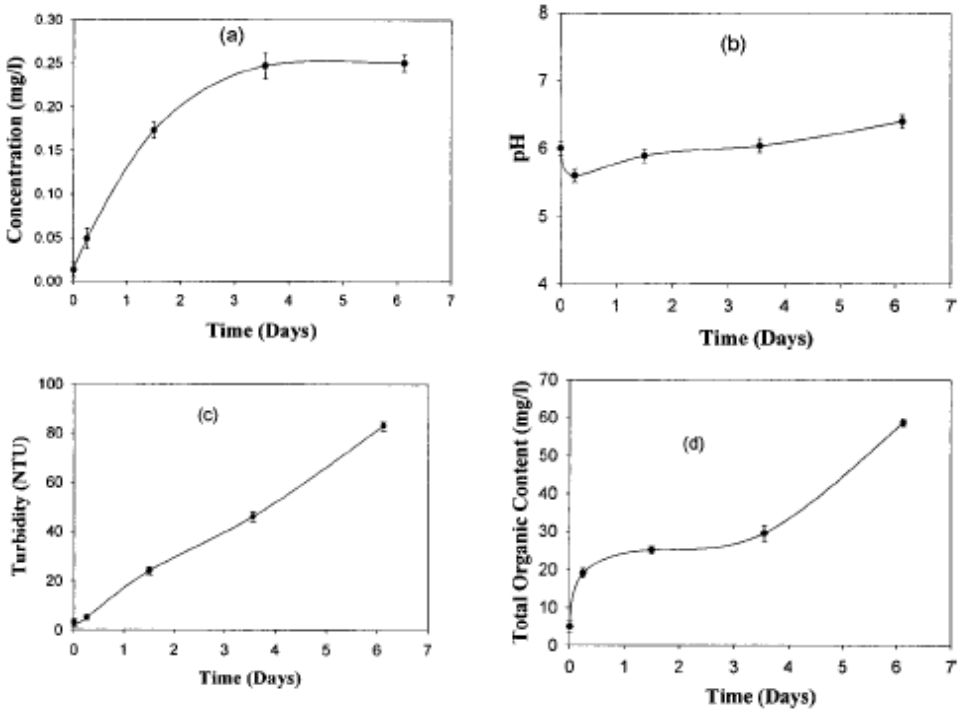

Figure 2.9. Pause flow experiment results (a) Iron effluent concentrations, (b) pH, (c) turbidity, (d) TOC profiles (Moo-Young et al., 2003)

TGA (thermal gravimetric analysis) were performed conducted to determine the thermal stability of tire shreds. The results showed that, tire shreds are stable up to temperatures of 200°C (Figure 2.10). This indicates that other mechanisms may be attributed to the exothermic reactions, which occurred in tire fills.

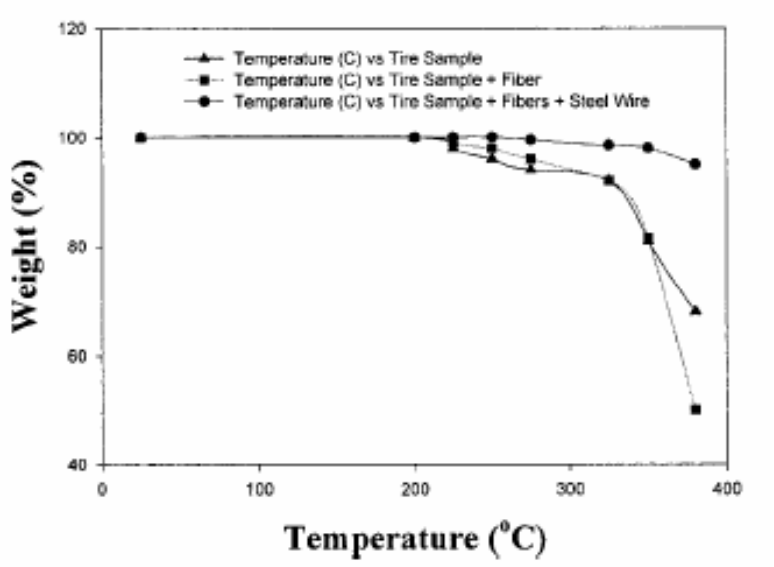

Figure 2.10. TGA weight curves (Moo-Young et al., 2003)

As an example, the properties of tire shreds used by Shalaby et al. (2004) are present in Table 2.6. Shalaby et al. (2004) constructed a shredded tire road embankment, to investigate the effect of sizes of tire shreds for determining a practical design model, and also to examine the potential environmental implications of the use of shredded rubber tires.

Table 2.6. Tire shred properties used in embankment construction (Shalaby et al., 2004)

Engineering property	Range of values	Remarks
Size (mm)	50–300	
Specific gravity	1.06–1.15	
Water absorption capacity (%)	3.9	Glass belted
	9.4	Steel belted
Uncompacted unit weight (kg/m^3)	300–500	For 25–75 mm shred size
Compacted unit weight (kg/m^3)	600–700	For 25–75 mm shred size
Compressibility (%)	40	At 400 kPa surcharge
Poisson's ratio	0.30	
Elastic modulus (kPa)	1100	75 mm size tire shreds
Internal friction angle (°)	19–25	
Cohesion intercept (kPa)	8–11	
Shear modulus (kPa)	2700	75 mm size tire shreds
Thermal conductivity (W/m°C)	0.20–0.30	At a density range of 0.58–0.79 mg/m^3
Permeability (cm/sec)	0.1	Compacted

2.5. Using Tire Wastes in Civil Engineering Applications

Usage of waste tires in construction projects is very useful for both civil engineers, and the environment. It is advantageous to use waste tires for civil engineers mainly because of the factors that they are valuable and cheap materials. On the other hand, many stockpiles of scrap tires exist in most of the countries, and some countries have banned the disposal of them. Using the tires in construction projects is a very good way to consume them, because large quantities of tires are being used in a single project. For this reason the usage of tire wastes in engineering projects is an important event for the environment.

2.5.1. Highway and Earthwork Applications

Highway and earthwork construction is an ideal application for using shredded tires because large volumes of scrap tires can be used in a single project. They can be used as a lightweight fill, as an admixture to increase the strength of soil, as a drainage material and a sound-deadening medium. Crumbed tires can also be added to asphalt, to improve the rheological properties at low and high temperatures and provide a longer lifetime.

2.5.1.1. Lightweight Fill. The use of shredded tires as lightweight fill is a particularly good method. Shredded tires or tire-soil mixtures can be used as backfill behind a highway retaining structure (Figure 2.11). The most significant advantage of shredded tires as a backfill material is that because of that the tires are lighter than soil, lower pressures are exerted on the retaining structure, and this results in a reduce in structural requirements. It is mentioned in ASTM D6270-98 that, the low-compacted dry density, high-hydraulic conductivity, and low-thermal conductivity makes tire shreds very attractive for use as retaining wall backfill. Lateral earth pressures for tire shred backfill can be about 50 per cent of values obtained for soil backfill. Tire shreds can also be used as backfill for geosynthetic-reinforced retaining walls (Benson, 1995).

Using shredded tires as lightweight fill material have many advantages. First, because of that shredded tires are non-biodegradable either above or below the water line, a stable road base with a longer duration is obtained compared to other lightweight fill materials. Next, shredded tires have a low density, and this property makes them useable to build roads over unstable soils. The transportation and placing of tire shreds on the job site is also easy to handle. They also display excellent porosity features, which is important for proper drainage of highway base grades. The high hydraulic conductivity of tire shreds makes them suitable for many drainage applications, including French drains, drainage layers in landfill liner and cover systems, and leach fields for on-site sewage disposal systems. Also there are many existing stockpiles of tires, and the material costs are low. The use of shredded tires will help to free up other valuable road building resources like sand and gravel for other use. Tire shreds are very inexpensive compared to other lightweight fill materials like cellular concrete and polystyrene. In addition, the use of shredded tires may also help complete a job faster and therefore save more money, because lightweight fill designs generally do not require a waiting period for settlement like other surcharge materials (Benson, 1995).

The disadvantage of using shredded tires as lightweight fill material is that, because of that the use of shredded tires as lightweight fill material is fairly a new concept, there is a lack of information and standards about their design. Next, waste tires require some preparation before they can be used as a road building material. The tires must be cleaned

of oils and grease in order to avoid soil and groundwater contamination. Also tire shreds may leach out heavy metals when subjected to highly acidic solutions (Bernal, 1996).

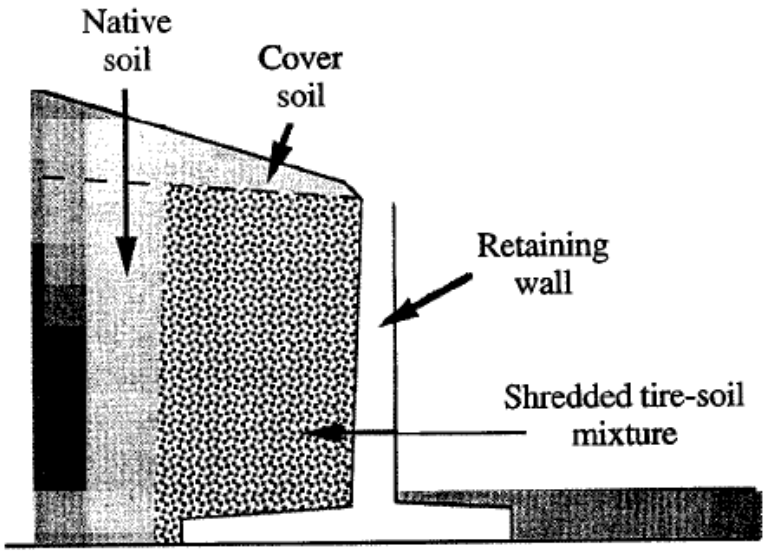

Figure 2.11. Shredded tires used as backfill for a highway retaining wall (Benson, 1995)

2.5.1.2. Admixture to Enhance Strength. When shredded tires are mixed with soil, the strength of the mixture is greater than the strength of the soil or the tires alone. In some cases the strength of the mixture can be twice as much as the strength of the soil alone. Because of this, the mixture has a greater capacity to support itself, and so it exerts less pressure on a wall. This results in construction material saving. In some cases, the tire-soil mixture can be self supporting up to 6 meters, where the retaining structure is designed more esthetically only to prevent erosion (Benson, 1995).

2.5.1.3. Lightweight Embankments. Shredded tires, and mixtures of soil and tires, can be used as fill material to construct lightweight embankments. These types of embankments are especially useful for highways constructed over soft soils, where large settlements can occur under high pressures. Usage of tire shred fills leads to less settlement. Because the fill is stronger, the slopes of the embankment can be made steeper, which saves construction effort. Large quantities of scrap tires are also used in such projects. According to ASTM D6270-98, tire shreds have a compacted dry density that is one-third to one-half of the compacted dry density of typical soil, and this makes them an attractive lightweight fill for embankment construction on weak, compressible soils where slope stability or excessive settlement are a concern. Constructing embankments with shredded scrap tires

results in a better product, has a similar or lower cost than an embankment built with soil, and large quantities of tires are consumed (Benson, 1995).

A tire shred-sand test embankment was constructed in the U.S.A. by Yoon et al. (2006). The schematic cross-section of the embankment is shown in Figure 2.12. The fill material was composed of tire shreds and a sandy soil mixed in equal proportions by volume. The height, length, and width of the test embankment were about 2.1, 20, and 17.7 m, respectively. After 200 days of road traffic, it was observed that the settlement stabilized at small values, and the maximum settlement observed was approximately 12mm. The maximum lateral movement with reference to the bottom of the embankment was only about 2 mm, and no evidence of significant differential settlement was observed. From the temperature measurements, no evidence of internal heat generation was detected. Finally, no evidence of slope stability problems, cracking of the road pavement or erosion was observed. They reported based on their findings that, the use of mixtures of tire shreds and soil in embankment fill construction is very promising and should be promoted, and the performance of the test embankment was quite satisfactory. They also added that, advantages of this material include the fact that it is lightweight, relatively cheap, easy to compact, free-draining, and relatively incompressible.

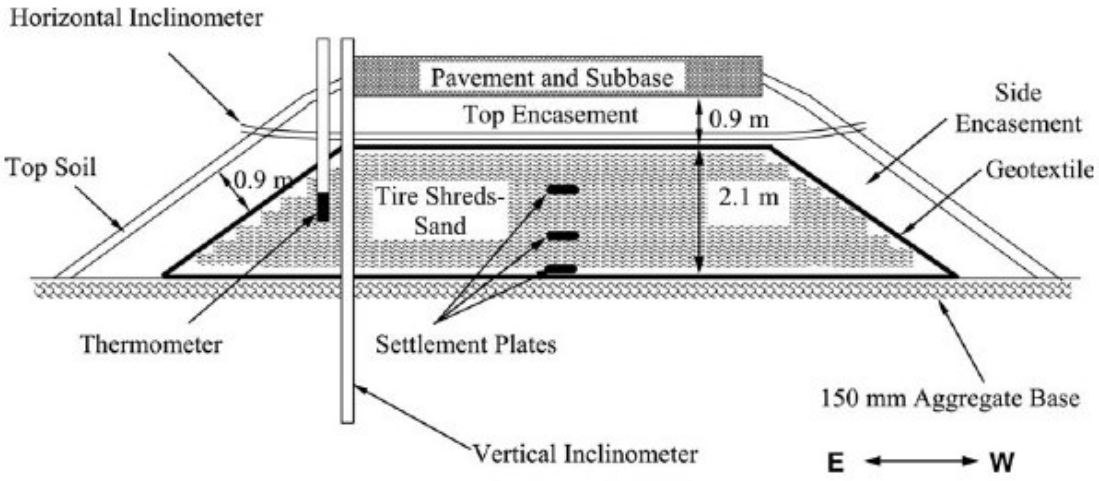

Figure 2.12. Schematic cross-section of an embankment constructed with tire shreds and sand (Yoon et al., 2006)

Humphrey et al. (1998), used tire shreds as lightweight fill for construction of two 32-ft high highway embankments. The site was underlain by about 40 ft of weak marine

clay. It was found that embankments built of conventional soil were too heavy resulting in an unacceptably low factor of safety against slope stability, so the designers had to make the embankment lighter. The designers of the project selected tire shreds as the fill material because they were about $300,000 cheaper than the other alternatives like expanded polystyrene and expanded shale. Plus, the project put about 1.2 million tires to a beneficial end use. ASTM standards required that a single tire shred layer should not be thicker than 1 ft, so the tire shred layer was broken into two layers, each up to 10 ft thick, separated by 3 ft of soil as shown in Figure 2.13. Low-permeability soil with a minimum of 30 per cent fines was placed on the outside and top of the fill to limit inflow of air and water. To limit heating, large shreds with a minimum of fines were used. The shreds had a maximum size measured in any direction of 12 inches to ensure that they could be easily placed with conventional construction equipment. The embankment was topped with 4 ft of granular soil plus 4 ft of temporary surcharge. The purpose of the surcharge was to increase the rate of consolidation of the soft clay foundation soils and was unrelated to the tire shred fill. The tire shreds were placed with conventional construction techniques. First the geotextile was placed on the prepared base to act as a separator between the tire shreds and surrounding soil. Then the tire shreds were spread in 12 inches thick lifts using a dozer. Each lift was compacted with six passes of a vibratory roller with a minimum 10 ton operating weight. After placing the shreds, the contractor placed a geotextile separator on the sides and top of the tire shred zone. Finally, the surrounding soil cover was placed.

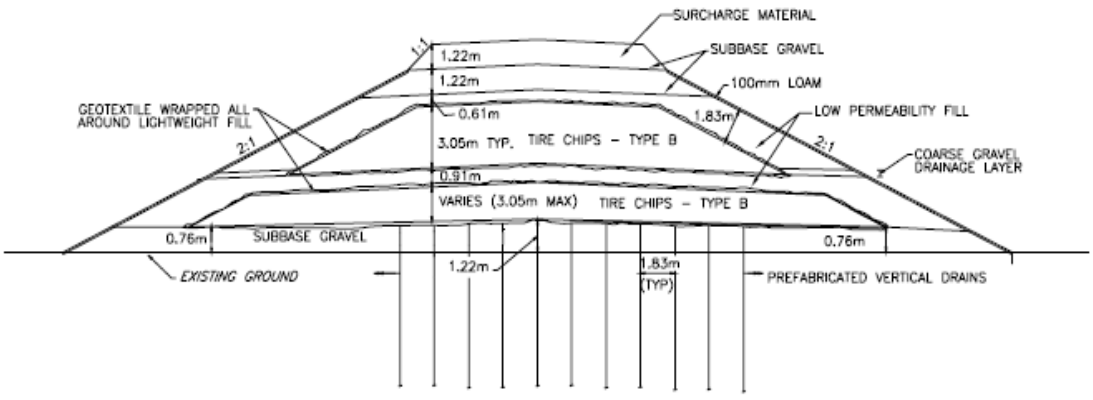

Figure 2.13. Cross-section of the embankment constructed on soft marine clay (Humphrey et al., 1998)

Another road embankment containing tire shreds was constructed by Shalaby et al. (2004). Initially, five layers of the whole tire sidewalls were manually placed on the subgrade in an overlapping pattern to provide a clear working surface and to raise tire shreds above the ground water table. Tire sidewalls were not processed by a shredder and contained an insignificant amount of exposed steel. The tire shreds were hauled to the site, unloaded directly over the sidewalls, and spread to the desired thickness of 1500 mm with a backhoe. The tire shreds were compacted in layers with five passes of a bulldozer. A gravel surface layer with a thickness of 450 mm was placed over the tires (Figure 2.14). In frost affected areas, the controlling factor for the thickness of a road embankment is the depth of frost penetration and not the expected traffic load. One of the climate related problems of interest in many regions of the world is that of damage caused to pavement structure by the freezing and thawing of subgrade and bases during winter and spring seasons. It was concluded that using tire shreds and incorporating the benefits of their lower thermal conductivity allows for reducing the thickness of the embankment.

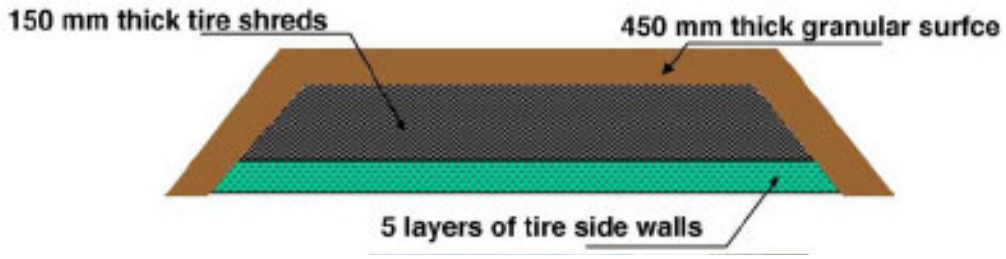

Figure 2.14. Cross section of the embankment (Shalaby et al., 2004)

2.5.2. Landfill Applications

Shredded waste tires can have valuable function in engineering landfill. They can be used as drainage material, leachate treatment medium, daily cover, or thermal insulation.

2.5.2.1. Leachate Collection Systems. Waste tires are more permeable than sands or gravels, which are normally used in leachate collection systems. Furthermore, waste tires can adsorb toxic organic chemicals normally found in leachate. Because of these two factors, when shredded tires are used the leachate is more readily removed and pre-treated (Benson, 1995). The performance of tire shreds as leachate drainage material is evaluated according to the following cases.

When used as a leachate drainage material, tire shreds will provide protection of public health by not containing leachable toxic materials or pathogens and being odorless. They will also provide environmental protection by not contributing to leachate generation and not contributing significant organics or inorganics to leachate or surface run off (Humprey et al. 1997).

Tire shreds used as leachate drainage material will provide adequate durability because they are not susceptible to puncture or tearing, and they are resistant to freeze-thaw cycles. Also, handling, transportation, and storage requirements of tire shreds are comparable to those for soil. Deployment of tire shreds during adverse weather conditions is easier compared to earthen material. The steel wire exposed at the cut edges of tire shreds can be a hazard to personnel walking on the shreds. Metal wires of tire shreds can cause flats in site vehicle tires. Track mounted or steel-wheeled equipment should be used to mitigate this problem. Adverse weather conditions, including hot and freezing temperatures and high wind, should not affect the installation rate of tire shreds. Tire shreds have a compressibility that is several orders of magnitude greater than the typical materials used as sand or gravel.

Using tire shreds as leachate drainage material is generally cost effective, compared to using granular materials or geosynthetics, despite additional labor requirements and costs to shred the scrap tires. Cost savings may result from collecting tipping fees for the scrap tires, saving airspace by using tire shreds as an engineered component of the landfill, and reducing costs associated with importing granular material or purchasing geosynthetics.

The leachate drainage layer is usually located near the base of the landfill, so overburden pressures can be high as waste is placed to its final grades and compression of the leachate drainage layer occurs. Tire shreds are relatively compressible material. The leachate drainage material must support heavy construction and operations equipment and be of sufficient thickness to prevent the damage of underlying components due to penetration of waste components. Compressibility of the tire shreds should be accounted in determining the minimum thickness and hydraulic conductivity of the leachate drainage material.

2.5.2.2. Daily Landfill Cover. Using shredded waste tires instead of soil as daily cover at a landfill is also very useful. They are as effective as soil cover in preventing the trash from blowing around, foraging by animals, and controlling landfill odors. Also, because the tires are permeable, pooling of leachate within the landfill is minimized. The shredded tires cleanse the leachate as it trickles through the trash (Benson, 1995).

2.5.2.3. Other Applications. Tire wastes can also be used as thermal insulation to protect landfill lining systems from freezing in winter months. Freezing has a serious detrimental effect on landfill liners, especially to the ones constructed with clay. When overlain by a layer of shredded tires, the temperature of a geomembrane liner is maintained above freezing throughout the entire winter. The thermal resistivity of tire shreds is approximately eight times greater than for a typical granular soil. For this reason, tire shreds can be used as a 150 to 450 mm thick insulating layer to limit the depth of frost penetration beneath roads, and this reduces frost heave in the winter and improves subgrade support during the spring thaw (ASTM D6270-98). Shredded tires can even be used to clean up hazardous waste sites. For example, at many sites where contaminated groundwater exists, a groundwater cut-off wall is installed to slow the flow (Figure 2.15). Most of these cut-off walls are constructed with clay. When shredded tires are mixed to clay, the ability to slow contaminant movement improves significantly (Benson, 1995).

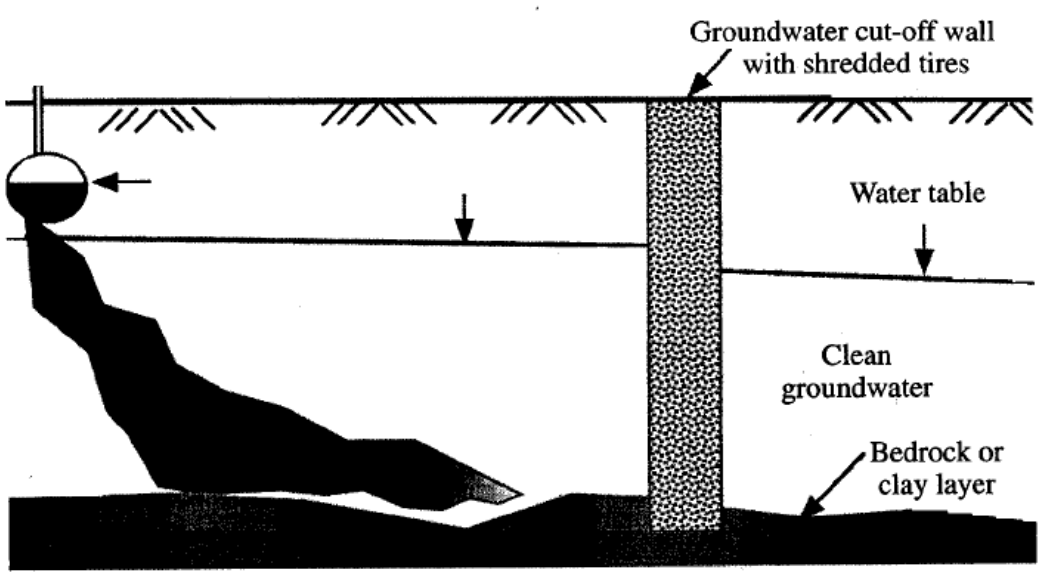

Figure 2.15. Groundwater cut-off wall with shredded tires (Benson, 1995)

2.6. Environmental Problems with Scrap Tire Stockpiles

First, scrap tire stockpiles can cause an increase in mosquito population. Mosquitoes are known as pests and vectors of disease. Discarded tires are breeding grounds for mosquitoes. Scrap tires can hold water for long periods of time because of their impermeability and geometric shape. For this reason, scrap tire stockpiles are very suitable for mosquito larva development (Jang et al., 1997).

Next, scrap tire stockpiles can cause fire hazards. An example of an open-air tire fire is shown in Figure 2.16. Tire fires are dangerous and hard to handle because of the difficulty with extinguishment. A whole scrap tire contains a void ratio of 75 per cent, which makes it difficult to either quench the fire with water or cut off the oxygen supply. Watering tire fires often increases the production of pyrolytic oil, provides a mode of transportation to carry oils off site, and aggravates contamination of soil and water. Air pollutants from tire fires include dense black smoke, which impairs visibility, and toxic gas emissions. Tire fire by-products may cause contamination of surface and subsurface water and soils (Jang et al., 1997).

Figure 2.16. Example of an open-air tire fire

3. GENERAL INFORMATION ABOUT FIBER REINFORCEMENT

3.1. Types of Fiber Reinforcement

Reinforcing soils with randomly distributed fiber materials have recently attracted increasing attention in geotechnical engineering. There have been many experimental researches on the reinforcement of soils with randomly distributed natural and synthetic fiber materials (Gray and Ohashi, 1983; Ranjan et al., 1996; Santoni et al., 2001; Michalowski et al., 2003; Yetimoglu and Salbas, 2003; Akbulut et al., 2007). The use of fiber materials in geotechnical design and application is advantageous because randomly distributed fibers offer strength isotropy and improve the soil performance and also fibers are cost-competitive with other materials. Commonly used fibers are obtained from geosynthetics, steel, wood, and tire wastes.

3.1.1. Geosynthetic Fibers

Most synthetic fibers are polymer-based, and are produced by a process known as spinning. This process involves extrusion of a polymeric liquid through fine holes known as spinnerets. After the liquid has been spun, the resulting fibers are oriented by stretching or drawing. This increases the polymeric chain orientation and degree of crystallinity, and has the effect of increasing the modulus and tensile strength of the fibers. Fiber manufacture is classified according to the type of spinning that the polymer liquid undergoes. Examples of geosynthetic fibers is shown in Figure 3.1. The three spinning types are melt spinning, dry spinning, and wet spinning.

Melt spinning is the simplest method, but it requires the polymer constituent to be stable above its melting temperature. The polymer is melted and forced through the spinnerets. During the cooling process, the fiber is drawn to induce orientation. Melt spinning is used with polymers such as nylon, polyethylene, polyvinyl chloride, and in the multifilament extrusion of polypropylene.

In dry spinning, the polymer is first dissolved in a solvent. The polymer solution is extruded through the spinnerets. The solvent is evaporated with hot air and collected for reuse. The fiber then passes over rollers, and is stretched to orient the molecules and increase the fiber strength. Cellulose acetate, modacrylic, aromatic nylon, and polyvinyl chloride are made by dry spinning.

In wet spinning, the polymer solution is spun into a coagulating solution to precipitate the polymer. This process has been used with acrylic, and polyvinyl chloride fibers.

Figure 3.1. Geosynthetic fibers

3.1.1.1. Polyamide (Nylon) Fibers. Polyamide polymers are characterized by the presence of an amide group. They are resistant to alkalies, molds, solvents, and moths. They can be damaged by strong acids, phenol, bleaches, and heat above 170ºC.

Michalowski et al. (2003) conducted triaxial compression tests on sand reinforced with polyamide monofilament fibers. Various diameters and lengths of fibers were used to determine the effect of aspect ratio. They reported that addition of polyamide monofilament fibers can increase the shear strength as 70 per cent.

Ghiassian et al. (2004) also performed drained triaxial tests on sand and polyamide fiver mixtures. The fibers had various lengths, and square cross-sections. They resulted that addition of nylon fibers increases the peak shear strength of sand.

3.1.1.2. Polypropylene Fibers. Polypropylene fibers are composed of at least 85 per cent of propylene by weight. These fibers have low melting points. They have a very low

specific gravity. They are softer, smoother, and lighter than nylon. They are resistant to alkalies, acids, solvents, insects, and mildew. They are damaged by heat above 110ºC.

Several researches (Yetimoglu et al., 2003; Santoni et al., 2001; Michalowski et al., 2003) conducted laboratory experiments using sand reinforced with polypropylene fibers. They all reported that up to a certain limit addition of polypropylene fibers resulted in an increase of shear strength of the specimens.

3.1.1.3. Polyethylene Fibers. Polyethylene fibers are composed of at least 85 per cent of ethylene by weight. They also have low melting points. These fibers are resistant to alkalies, acids, insects, and mildew. They are damaged by oil and grease, oxidizers, and heat above 100ºC.

Benson et al. (1994) investigated the effects of adding polyethylene fibers to sand by performing direct shear tests. They resulted that the addition of 2-4 per cent of fibers to sand results in the highest shear strength for the mixture.

3.1.2. Steel Fibers

Steel fibers are generally used in reinforcing concrete. They can be produced in various lengths and aspect ratios (Figure 3.2). Steel fibers have high tensile strengths.

Michalowski et al. (2003) conducted triaxial tests on steel galvanized fibers. They reported that steel fibers have a reinforcement effect only slightly higher than do polyamide fibers of the same geometry, due to the larger interface friction angle of steel fibers.

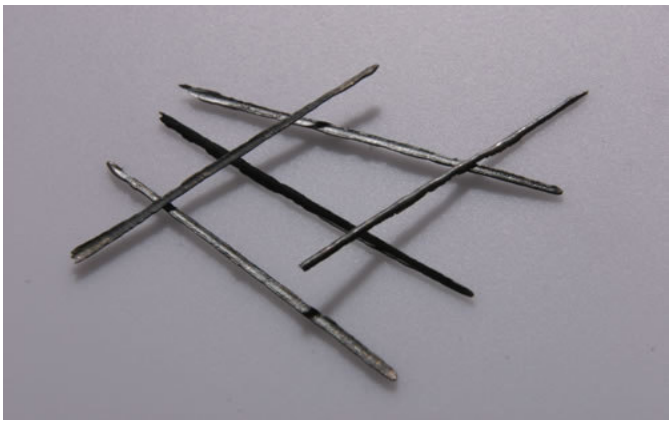

Figure 3.2. Steel fibers

3.1.3. Wood Fibers

Wood fiber is composed of layers of crystalline cellulose wrapped in a cylindirical shape with an open center. Wood fiber is broken down into five distinct layers and are referred to as layers ML, P, S1, S2, and S3. The fibrils in the S2 layer form the major strength-producing portion of the wood fiber. The fibril angle varies from over 35 degrees in juvenile and compression wood to 10 degrees or less in mature wood. Normal juvenile and mature wood fibers are approximately rectangular in cross-section with the wall thickness varying from 10 per cent of the total cross section in earlywood to about 80 per cent of the cross section in latewood. The gross wood structure is composed of fibers in the longitudinal direction bound together by a lignin and bundles of ray cells oriented in the radial direction in the wood which act as reinforcement rods to increase the radial strength. Compression wood fibers have a circular cross section with the S3 layer missing, have extreme fibril angle in the S2 layer and have short grain length. Dimensional stability is poor and strength is low in compression wood, making it a very undesirable structure element.

Kilian and Ferry (1993) investigated the long-term performance of wood fiber fills used in constructing an embankment. They reported that over half of the wood fiber samples were found to be nearly fresh after 15 years, and none after 5 or more than 19 years was found to be completely decomposed. They resulted that embankments constructed of wood fiber were found to perform well over an almost 20-year period, and a service life of more than 50 years can be expected of wood fiber fills.

Figure 3.3. Wood fibers

3.2. Types of Tire Reinforcement

Recovery of tire reinforcements differs slightly at different scrap tire processing plants. Basically, in the processing plant, passenger tires and truck tires are separated, and tires containing metallic rims are de-rimmed. The tires are re-introduced to the tire conveying system to reduce the whole tires through shredding and granulating down to various particle size, classified into three groups as coarse, mid-range, and fine. Metals are usually separated using magnets. Tire shreds are then vacuumed out from the crumb rubber. The appearance, shape, and size of the tire shreds depend on the type of processing. A sample appearance of processed tires is shown in Figure 3.4.

Figure 3.4. Processed tires

Wu et al. (1997) conducted triaxial compression tests to determine the shear strength of five processed scrap tire products having different gradations and particle shapes. The summary of the test results is shown in Table 3.1.

Table 3.1. Summary of test results (Wu et al., 1997)

Product (1)	Shape (2)	Maximum size (mm) (3)	Volume strain at 55 kPa (%) (4)	Young's modulus E (kPa) (5)	Friction angle ϕ (°) (6)	Interparticle friction ϕ_r (°) (7)
1	Flat	38	27.0	580–690	57	56
2	Granular	19	26.5	430–580	54	53
3	Elongated	9.5	31.6	350–480	60	53
4	Granular	9.5	25.4	450–600	47	47
5	Powder	2	27.0	450–820	45	44

3.2.1. Tire Shreds

Tire shreds are generally between 50 and 305 mm in size (ASTM D6270-98). The production of tire shreds involves primary and secondary shredding. Tire shreds have a basic geometrical shape as a cross section.

Several researchers (Zornberg et al., 2004; Moo-Young et al., 2003; Foose et al., 1996; Hataf and Rahimi, 2005; Attom, 2005) investigated the shear strength of mixtures

composed of sand and tire shreds. They all reported that up to a certain percentage addition of tire shreds increased the shear strength of sand.

3.2.2. Tire Chips

Tire chips are pieces of scrap tires that have a basic geometrical shape and are generally between 12 mm and 50 mm in size (ASTM D6270-98). Most of the wire is removed from the tire waste.

Several researchers (Gotteland et al., 2005; Venkatappa Rao et al., 2006; Humprey et al., 1993; Tatlisoz et al., 1998) conducted experimental studies to investigate the effect of tire chips addition to sand on the shear strength of the mixture. They all concluded that up to a certain level addition of tire chips increased the shear strength of sand.

3.2.3. Tire Buffings

Tire buffings are by-products of the tire retread process. A tire buffings is a particulate rubber produced as a by-product of the buffing operation in the carcass preparation stage of tire retreading. Tire buffings are characterized by a wide range of particulate sizes which are predominately elongated or acicular in shape. The lengths of fibers are generally smaller than 50 mm.

Edincliler et al. (2004) conducted large scale direct shear tests on specimens composed of sand and various percentages of tire buffings. It is reported that addition of tire buffings to sand increased the strength at low confinement pressures. Ozkul and Baykal (2007) conducted both consolidated drained and consolidated undrained triaxial tests to evaluate the drained and undrained shear strength of mixtures of clay and tire buffings. They reported that the addition of tire buffings to clay increased the shear strength up to a limiting confining stress.

3.3. Theory of Fiber Reinforcement

Modeling the behavior of fiber soil reinforcement during deformation and failure is very complex and difficult. Advanced finite element analysis and the setup of proper relationships are required. However, a simpler analysis can be accomplished to predict the shear behavior of fiber reinforced sand based on limit equilibrium of forces.

Wu (1976) developed a fiber reinforcement model considering only an inclusion oriented perpendicularly to the shear surface. The model assumes full mobilization of the tensile strength of the inclusions. Waldron (1977) also proposed a model which is based on partial mobilization of inclusion tensile strength depending upon the amount of inclusion elongation during shear. Both of these models do not set any constraint on the distribution or position of the fibers. The reinforcement model (Gray and Ohashi, 1983) is presented in Figure 3.5. Distortion can occur in the fibers during shearing, causing an increase in the shear resistance of the reinforcement. The tensile force of the fiber reinforcements is composed of a normal and a tangential component with respect to the shearing plane. The normal component increases the shear resistance by increasing the confining stress on the failure plant, and the tangential component directly resists shear.

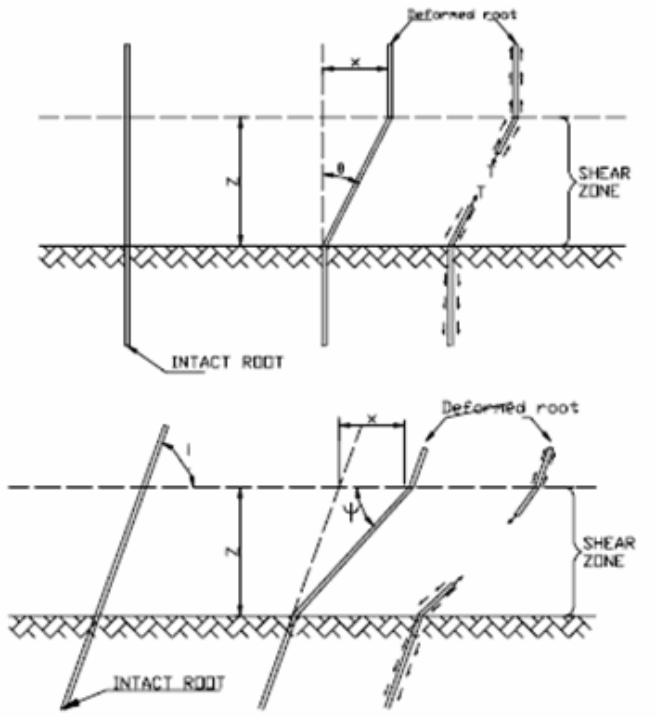

Figure 3.5. Fiber reinforcement model (Gray and Ohashi, 1983)

Hataf and Rahimi (2006) used the following equations to estimate the shear strength increase of sand reinforced with fibers:

$$\Delta S_R = t_R(\sin\theta + \cos\theta \tan\phi), \tag{3.1}$$

$$\Delta S_R = t_R(\sin(90-\psi) + \cos(90-\psi)\tan\phi), \tag{3.2}$$

$$\psi = \tan^{-1}\left[\frac{1}{k + (\tan^{-1} i)^{-1}}\right], \; k=(x/z), \tag{3.3}$$

$$t_R = \left(\frac{A_R}{A}\right)\sigma_R, \tag{3.4}$$

where, ΔS_R is the increase in shear strength caused by the addition of reinforcement; t_R is the mobilized tensile strength of inclusions per unit area of soil; ϕ is the friction angle of sand; θ is the angle of shear distortion; i is the initial orientation angle with respect to shear surface; x is the horizontal shear displacement; z is the thickness of shear zone; k is the shear distortion ratio; and σ_R is the tensile stress developed in the inclusion at the shear plane.

For a specimen containing more than one inclusion, the cross sectional areas of fiber reinforcements are calculated, and the total reinforcement concentration is expressed in terms of an inclusion area ratio (A_R/A).

Similarly, Maher and Gray (1990) predicted the following model to estimate the increase in shear strength of soil due to addition of fiber reinforcement:

$$\Delta S_R = N_S\left(\pi\frac{d^2}{4}\right)(2\sigma' \tan\delta)(\sin\theta + \cos\theta\tan\phi)(\xi), \tag{3.5}$$

$$N_S = \frac{2\beta_f}{\pi d^2}, \tag{3.6}$$

where, d is the diameter of the fiber; σ' is the effective normal stress; δ is the friction angle between the soil and the fiber; ξ is an empirical coefficient for the sand

granulometry and fiber properties; and β_f is the volumetric reinforcement content. The other parameters are same with the study of Hataf and Rahimi (2006) mentioned previously.

The assumptions that are used in this formulation are mentioned by Foose et al. (1996). The length and diameter of the fibers are assumed to be constant. In addition to this, the fibers do not provide any resistance to bending, and the smaller portion of each fiber that lies on either side of the shearing plane is uniformly distributed between zero and half the length of the fiber. It is also assumed that the orientation of fibers relative to a fixed axis follows a uniform distribution, the number of fibers in the soil mass and the number of fibers intersecting the failure plane are randomly distributed following a Poisson process, sand-fiver composites have a bilinear failure envelope, and at normal stresses less than the critical normal stress the fibers slip, at greater normal stresses they yield.

Failure of a single fiber is studied by Michalowski and Zhao (1996). It is stated that the failure can occur due to fiber slip or tensile rupture. Even if a tensile rupture occurs, the ends of the fiber will slip as the tensile strength of the fiber material can not be mobilized throughout the entire fiber length. Figure 3.6 represents the expected distribution of shear stress and axial stress in a rigid-perfectly plastic fiber.

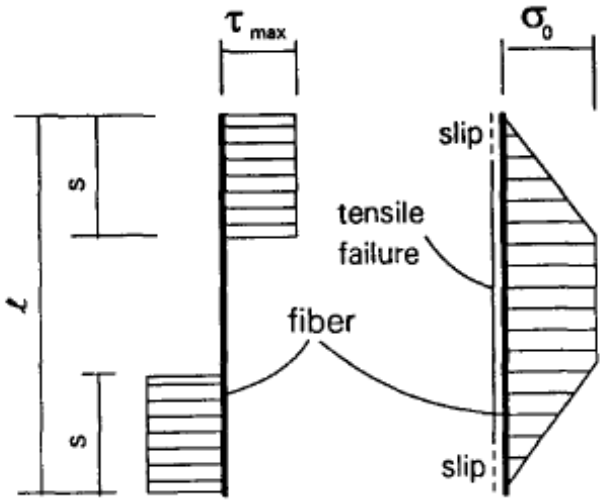

Figure 3.6. Fiber-matrix shear stress and axial stress in a rigid-perfectly plastic fiber (Michalowski and Zhao, 1996)

The following equation is used to study the distance of slip occurring by the fail of a single fiber:

$$s = \frac{r}{2}\frac{\sigma_0}{\sigma_n \tan\varphi_w}, \tag{3.7}$$

where, s is the distance occurring at both fiber ends after slip; σ_0 is the yield stress of the fiber material; σ_n is the stress normal to the fiber surface; and φ_w is the friction angle of the matrix-fiber interface. A pure slip failure mode would occur if the length of the fibers becomes less than $2s$, or when the aspect ratio becomes less than $\left(\frac{1}{2}\frac{\sigma_0}{\sigma_n \tan\varphi_w}\right)$.

Li and Zornberg (2003) defines the equivalent shear strength of fiber-reinforced soil as a function of the fiber-induced distribution tension, and the shear strength of the unreinforced soil as follows:

$$S_{eq} = S + \alpha t = c + \sigma_n \tan\phi + \alpha t \tag{3.8}$$

where, t is the fiber-induced distribution tension; S is the shear strength of the unreinforced soil, α is an empirical coefficient for the orientation of fiber and the mixing of fibers; ϕ is the value of angle of internal friction; c is the cohesion value; and σ_n is the normal stress acting on the fibers.

3.4. Background

Tires wastes can be used as lightweight material in the form of whole tires, or shredded tires, or in mix with soil. Many studies regarding the use of scrap tires in geotechnical applications have been done, including laboratory investigations, numerical and physical modeling, and field investigations. The summary of shear strength data obtained from previous studies is shown in Table 3.2.

Zornberg et al. (2004) conducted 15 series of consolidated drained (CD) triaxial compression tests on specimens composed of pure sand, pure tire shred, and tire shred-sand mixtures. A large-scale triaxial device was used with specimens having a diameter of 153 mm and a height of 305 mm. The aim of the study was to evaluate the optimum tire shred content and aspect ratio to be used in tire shred-sand mixtures. They reported that the shear strength increases with increasing tire shred content and reaches a maximum for a tire shred content value around 35 per cent, and then decreases for tire shred contents beyond this value. In addition to this result, they concluded that the shear strength of tire shred-sand mixtures increases with increasing aspect ratio.

Gotteland et al. (2005) carried out 9 series of consolidated drained (CD) triaxial compression tests using a large-scale triaxial cell with specimens 150 mm in diameter and 300 mm in height. Specimens were composed of mixing sand and tire chips by varying the tire content and the orientation of chips. The purpose of the study was to determine the optimum percentage mass of tires and the optimum unit weight which give the maximum shear strength. The results indicated that the strength increases with the increase of tire content up to an optimum percentage mass of 34 per cent, after which the shear strength decreases. The optimum percentage mass corresponds to a unit weight of 13.5 kN/m³. Plus, they found that the orientation of the tire chips also had an effect on the shear strength of the mixture. The strength was higher when the tire chips were placed horizontally, followed by the specimens made of alternately placed horizontal and vertical tires, tires placed only vertically, and finally the specimens where tire chips had no orientation.

Venkatappa Rao et al. (2006) performed a total of 28 compressibility tests, 4 repeated load tests, and 52 drained triaxial compression tests to investigate the behavior of sand with and without tire chips. The varying test parameters in triaxial tests were confining pressure, percentage of tire chips, and size of tire chips. The results of drained triaxial tests revealed that the tire chip-sand admixtures up to 20 per cent chip content behave like gravel-sand mixtures, the strength showing a marginal improvement. They stated that the use of tire chips and sand admixture is advantageous in construction of highway embankments up to a maximum height of 10m.

Ghiassian et al. (2004) conducted drained triaxial tests on specimens composed of silty sand and randomly distributed fiber strips obtained from carpet waste, to study the influence of synthetic fibrous materials for improving the strength characteristics of a fine sandy soil. The main test variables included the aspect ratio and the content of fiber strips. The results indicate that at a constant aspect ratio, increasing the strip content increases the peak strength. Similarly, at constant strip content, increasing the aspect ratio again increases the peak strength. They also reported that in both cases the rate of increase reduces with increasing one of the variables.

Michalowski et al. (2003) investigated the behavior of fiber-reinforced granular soils by performing 14 series of drained triaxial compression tests. Triaxial specimens were prepared at a height and diameter equal to 94.5 mm. Three types of fibers were used which are polyamide monofilament, steel galvanized wire, and polypropylene fibrillated fibers. The results showed that a substantial increase in the shear strength, compared to that in unreinforced sand, can be gained with a fiber concentration of 2 per cent by volume. They concluded that the reinforcing effect was also dependant on the fiber aspect ratio. The larger the aspect ratio, the more effective the fibers were and longer fibers contributed more to the composite strength than did the shorter fibers.

Li et al. (2003) performed triaxial tests on unreinforced and reinforced specimens obtained by mixing polypropylene fibers with both sand and clay. Consolidated drained (CD) triaxial tests were conducted on specimens prepared with sand, and consolidated undrained (CU) triaxial tests were conducted on specimens prepared with clay. They resulted that the addition of fibers can significantly increase the peak shear strength and limit the post peak strength loss of both cohesive and granular soil. They also added that the peak shear strength and the strain at peak deviator stress increases with increasing fiber aspect ratio.

A series of triaxial tests were performed by Michalowski and Zhao (1996) on specimens composed of fibers and sand. Both steel and polyamide fibers were used in the tests. The varying parameters were fiber concentration, aspect ratio, fiber diameter, and range of confining pressure. The results indicated that the increase in the content of steel fibers led to a clear increase in the peak shear stress, and also led to an increase in the

stiffness of the composite prior to reaching failure. On the other side, the increase in the content of polyamide fibers led to a very significant increase in the peak shear stress, a noticeable decrease in the stiffness, and an increase of the strain to failure. An increase in the aspect ratio of both the steel and polyamide fibers contributed to a significant increase in the peak shear stress.

Edincliler (2004) conducted large-scale direct shear tests to determine the shear strength parameters and deformation behavior of tire buffings-sand mixtures at varying tire buffings content. The test results indicated that addition of tire buffings to sand increased the strength at low confinement pressures. Plus, it is stated that an addition of 10 per cent by weight tire buffings to sand alters the deformation behavior of the mixture by stiffening the material at low strains and softening the mixture at large strains. It was reported that the use of tire buffings additive at the top one-two meters of the highway embankments would improve the performance of the embankments under the traffic load.

The feasibility of reinforcing sand with strips of high-density polyethylene was investigated by Benson et al. (1994). Strips that are prepared at aspect ratios of 4, 8, and 12 were mixed with Portage sand and tested to determine the California Bearing Ratio, secant modulus, resilient modulus, and shear strength. A large-scale direct shear device was constructed to examine the shear strength. In conclusion, they reported that addition of strips increased the peak and residual shear strength of the sand. They also added that the increase in residual strength was a function of strip content at higher confining pressures, but was independent of strip content at lower confining pressures. The peak values of CBR, secant modulus, resilient modulus, and shear strength parameters were obtained at an aspect ratio of 8. They concluded that strips cut from high-density polyethylene could prove useful as soil reinforcement in highway and light-duty geotechnical applications.

Humprey et al. (1993) performed large-scale direct shear tests to determine the shear strength of tire chips for use as retaining wall backfill. Three different sized tire chips were used. They concluded that, the friction angle of the tire chips was between 19 and 25 degrees, and the cohesion between 8 and 11 kPa. They also added that the amount of exposed steel belt appears to have a systematic effect on some of the engineering properties of tire chips. Large amounts of exposed steel belts tend to cause higher

compressibility during the first loading cycle, higher Young's modulus during unloading and reloading cycles, lower coefficient of earth pressure at rest, and lower shear strength. The tests suggested that there may be some advantage to using tire chips with large amounts of exposed steel belt as retaining wall backfill because of their low coefficient of earth pressure at rest.

Tatlisoz et al. (1998) conducted direct shear and pull-out tests to assess the shear strength and geosynthetic interaction of tire chip and soil-tire chip backfills that may be used for geosynthetic reinforced walls and embankments. The results showed that soil-tire chip mixtures had significantly higher shear strength than the soil used in the mixture. In addition, they point out that soil-tire chip mixtures did not exhibit a peak shear strength, but rather the shear strength continued to increase with increasing displacement.

A study was undertaken by Yetimoglu et al. (2003) to investigate the shear strength of sands reinforced with randomly distributed discrete fibers. The effect of the fiber reinforcement content on the shear strength was observed. A series of direct shear tests were performed. Polypropylene fibers with a diameter of 0.05 mm and a length of 20 mm were used as reinforcement. They reported that the peak shear stresses were insignificantly affected by fiber content, and the values of the peak shear strength angle could be considered identical for reinforced and unreinforced sand. They also mentioned that residual shear strength angle of the sand tend to be increased by adding the fiber reinforcements.

Foose et al. (1996) conducted a series of direct shear tests on mixtures of dry sand and shredded waste tires to investigate the feasibility of using shredded waste tires to reinforce sand. Normal stress, sand matrix unit weight, shred content, shred length, and shred orientation were the factors studied to evaluate their influence on shear strength. According to the test results, normal stress, shred content, and sand matrix unit weight were found to significantly affect the shear strength. They stated that in all cases, sand containing shredded tires had higher shear strength than sand alone. It was mentioned that the initial friction angle increased as the shred content increased. Finally, they suggested that shredded waste tires and mixtures of sand and shredded waste tires may be useful as

soil reinforcement in highway fills, leachate collection systems on steep slopes, and other applications where strong and lightweight fill is needed.

Attom (2005) performed direct shear tests to study the effect of the shredded tires on the shear strength properties of sand. Three different types of sand were used and each type of sand was mixed with four different percentages of shredded tires. As a result, it was reported that the increase in the content of shredded tire waste increased both the angle of internal friction and the shear strength of the sand. Additionally, it was stated that the increase in the initial dry density of the sand-shredded waste tire mixture increased the shear strength of the sand.

Ghazavi (2004) performed direct shear tests on sand-granular rubber mixtures to demonstrate the shear strength characteristics of the mixtures. The rubber particles were produced from waste garden hose and plastic shoes. It was reported that an apparent cohesion was obtained in samples containing rubber grains. It was mentioned that an addition of 10-20 per cent rubber to the sand was optimal to obtain the greatest friction angle.

Moo-Young et al. (2003) conducted large-scale direct shear and compression tests on pure tire shreds. The results showed an increase in shear strength as the particle size of tire shreds increased. They added that as the density of the tire shreds increased the shear strength increased. Finally, the compression tests showed that as the scrap tire size increased compressibility increased.

Santoni et al. (2001) conducted unconfined compression tests on sand specimens reinforced with randomly oriented discrete fibers to identify the effect of numerous variables on the performance of the specimens. The synthetic monofilament, fibrillated, tape, and mesh fibers used in the study were made of polypropylene. They concluded that the inclusion of all of the fiber types evaluated in the sand materials improved the unconfined compressive strength of the individual specimens. They reported that the performance of the various fiber types from best to worst was fibrillated, tape, monofilament, and mesh. The analysis showed that the optimum fiber length for discrete

fiber reinforcement was 51 mm, and the optimum dosage rate for the fiber stabilization of sand materials lies between 0.6 and 1.0 per cent dry weight.

A specially designed pullout test was conducted by Li and Zornberg (2005) to study the interface shear strength between individual fibers and soil. Polypropylene tape fiber was used as the fiber in the experiments. They reported that the coefficient of interaction was found to decrease with increasing confining pressure due to soil dilatancy.

Hataf and Rahimi (2005) carried out a series of laboratory model tests to investigate the using of shredded waste tires as reinforcement to increase the bearing capacity of soil. The main parameters investigated in the study were shred content and shreds aspect ratio. In conclusion, it was found that addition of 10 per cent shreds by volume increased BCR (bearing capacity ratio) from 1.17 to 1.83, 20 per cent tire shreds increases BCR from 1.6 to 2.2, 30 per cent tire shreds increase BCR from 2.15 to 3, 40 per cent tire shreds increase BCR from 3.2 to 3.9 and 50 per cent tire shreds increases BCR from 2.95 to 3.9 with respect to shreds width and aspect ratio. They reported that optimum shred content was found to be 40 per cent, and the best aspect ratio was found as 4.

Ghazavi and Sakhi (2005) investigated the advantage of optimizing aspect ratio of waste tire shreds on California Bearing Ratio (CBR) of sand-tire shred mixtures. The mixtures were composed of a relatively uniform sand and tire shreds with various widths and lengths. As a result, they concluded that the key factors affecting CBR values of the mixtures were shred content, shred with, shred aspect ratio, and compaction energy, which could increase the CBR value in the range of 14-850 per cent. They stated that the CBR values of mixtures increased with increasing shred contents.

Table 3.2. Summary of shear strength data obtained from previous studies

Reference	Test Type	Material	Unit Weight (kN/m³)	c (kPa)	Φ (º)	Φ_{eq} (º)
Edincliler et al. (2004)	Large Scale Direct Shear	Sand	15.3	6.9	33	-
		Tire Buffings	5.1	3.1	22	-
		5% Tire Buffings	15.19	10.4	28	-
		10%TireBuffings	14.89	8.7	29	-
		20% Tire Buffings	14.22	15.5	5	-
		30% Tire Buffings	13.56	10.7	8	-
Zornberg et al. (2004)	Large Scale Triaxial (CD) (48.3, 103.5, 207 kpa) Strain rate= 0.5 mm/min	Sand	15.64	7.8	36.8	37.9
		Sand	16.21	3.8	41.0	41.4
		Tire Shred (12.7mm)	-	22.8	21.4	26.5
		5% Tire Shred	-	7.0	36.1	37.1
		10% Tire Shred	-	21.7	35.7	38.9
		30% Tire Shred	-	30.4	35.7	40.2
		60% Tire Shred	-	18.2	34.4	37.3
		38.3% Tire Shred	-	41.2	36.1	42.0
Gotteland et al. (2005)	Large Scale Triaxial (CD) (50, 75, 100kPa) Strain rate= 2 mm/min	Sand	16.7	0	40.9	40.9
		Tire Chips	6.1	16.3	19	25
		14% Tire Chips	15.5	13.8	39	43
		14% Tire Chips (H)	15.9	15	42.6	44.5
		14% Tire Chips (V)	15.9	7.5	41.7	43.5
		15% Tire Chips (H&V)	15.5	10	41.1	44.5
		22% Tire Chips (H&V)	15.3	50	36.1	45
		50% Tire Chips	11.4	7.5	41.5	43.5

Venkatappa Rao et al. (2006)	Triaxial (CD) (34.5, 69, 138, 276 kPa) Strain rate= 1.016 mm/min (continued)	Sand	16.7 (max.)	0	38	-
		Type 1 Tire Chips (10mm*10mm)				
		5% Tire Chips	-	6.6	39.6	-
		10% Tire Chips	-	9.1	39.7	-
		15% Tire Chips	-	11.5	39.9	-
		20% Tire Chips	-	13.3	40	-
		Type 2 Tire Chips (20mm*20mm)				
		5% Tire Chips	-	9.2	39.5	-
		10% Tire Chips	-	11.6	39.7	-
		15% Tire Chips	-	14.1	39.9	-
		20% Tire Chips	-	15.8	40.1	-
		Type 3 Tire Chips (10mm*20mm)				
		5% Tire Chips	-	15.2	39.2	-
		10% Tire Chips	-	15.9	39.5	-
		15% Tire Chips	-	17.6	39.7	-
		20% Tire Chips	-	18.4	39.9	-
Tatlisoz et al. (1998)	Large Scale Direct Shear	Sandy Silt	18.3	11	30	-
		10% Tire Chips	17.6	8	55	-
		20% Tire Chips	17	38	54	-
		30% Tire Chips	16.3	39	53	-
		Sand	16.8	2	34	-
		Tire Chips	5.9	0	30	-
		10% Tire Chips	15.6	2	46	-
		20% Tire Chips	14.5	2	50	-
		30% Tire Chips	13.3	2	52	-

Humphrey et al. (1993)	Large Scale Direct Shear (continued)	Tire Chips-1 < 76 mm	7.01	8.6	25	-
		Tire Chips-1 < 76 mm	6.82	11.5	19	-
		Tire Chips-1 < 76 mm	7.24	7.7	21	-
		Tire Chips-2 < 76 mm	-	4.3	26	-
Wu et al. (1997)	Triaxial Compression	Tire Chips 38 mm-Flat	5.89	0	57	-
		Tire Chips 19 mm-Granular	5.69	0	54	-
		Tire Chips 9.5 mm-Elongated	4.95	0	54	-
		Tire Chips 9.5 mm-Granular	5.89	0	47	-
		Tire Chips 2 mm-Powder	5.69	0	45	-
Attom (2004)	Large Scale Direct Shear (Sand A)	Sand A	-	0	25	-
		10% Tire Shreds	-	0	30	-
		20% Tire Shreds	-	0	37	-
		30% Tire Shreds	-	0	41	-
		40% Tire Shreds	-	0	45	-
	Large Scale Direct Shear (Sand B)	Sand B	-	0	28	-
		10% Tire Shreds	-	0	35	-
		20% Tire Shreds	-	0	42	-
		30% Tire Shreds	-	0	47	-
		40% Tire Shreds	-	0	49	-
	Large Scale Direct Shear (Sand C)	Sand C	-	0	36	-
		10% Tire Shreds	-	0	42	-
		20% Tire Shreds	-	0	45	-
		30% Tire Shreds	-	0	48	-
		40% Tire Shreds	-	0	50	-

4. EXPERIMENTAL PROGRAM

4.1. General

The aim of the experimental program is to determine the shear strength of sand, tire waste, and various sand-tire waste mixtures and also CBR values. Tire crumb and tire buffings inclusions are used at varying contents as soil reinforcement. Both quick triaxial compression tests and consolidated drained (CD) triaxial tests are performed to analyze the effects of tire content, tire shape, and tire aspect ratio on the shear strength of sand. California bearing ratio (CBR) tests are also conducted to evaluate the effects of these parameters on CBR value. All tests are conducted in accordance with the ASTM standards.

4.2. Materials Used

4.2.1. Sand

Sand is used as soil in the experimental program. The selected sand was considered as a common type for use in highway embankments.

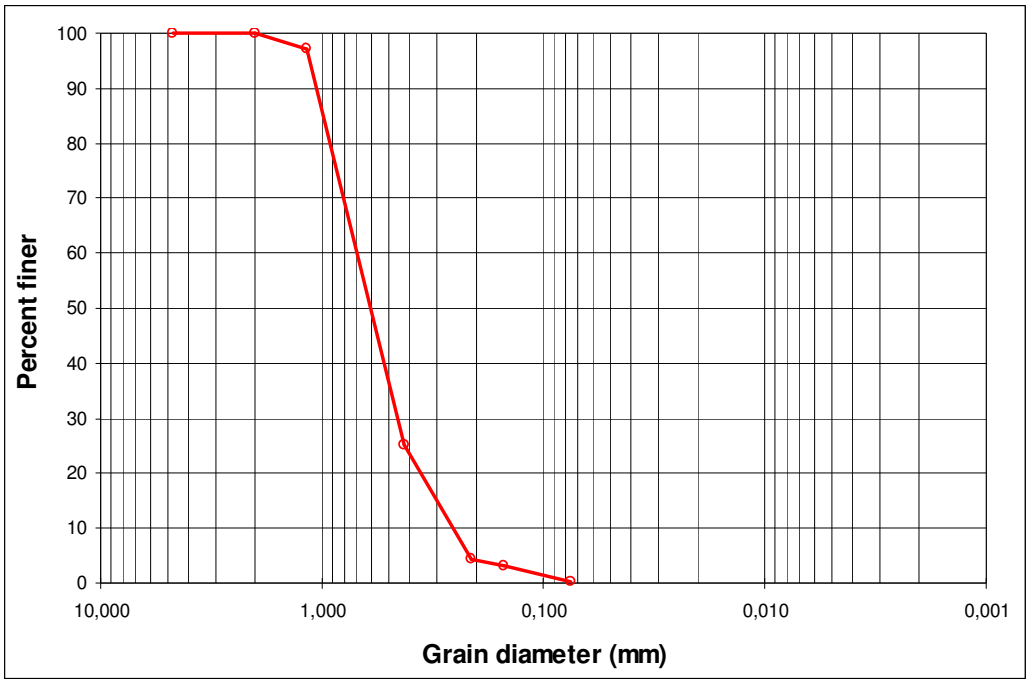

Figure 4.1. Grain size distribution of sand

Particle size analysis of sand is investigated in accordance to ASTM D422. According to the grain size distribution curve of the sand (Figure 4.1), the coefficient of uniformity (C_u) is calculated as 2,8, and the coefficient of curvature (C_c) is calculated as 1,16. Using these values and the Unified Soil Classification System the sand can be classified as SP, uniform graded sand. Sand used in this study is shown in Figure 4.2.

Figure 4.2. Sand used in the experiments

4.2.2. Tire Waste Material

4.2.2.1. Tire Crumb. Tire crumb is a granular material obtained by processing scrap tires. Tire crumb used in this study is purchased from a company in Istanbul (Figure 4.4). The grain size distribution curve of tire crumb is shown in Figure 4.3. The tire crumb used in the experiments has an aspect ratio of 1-1.5.

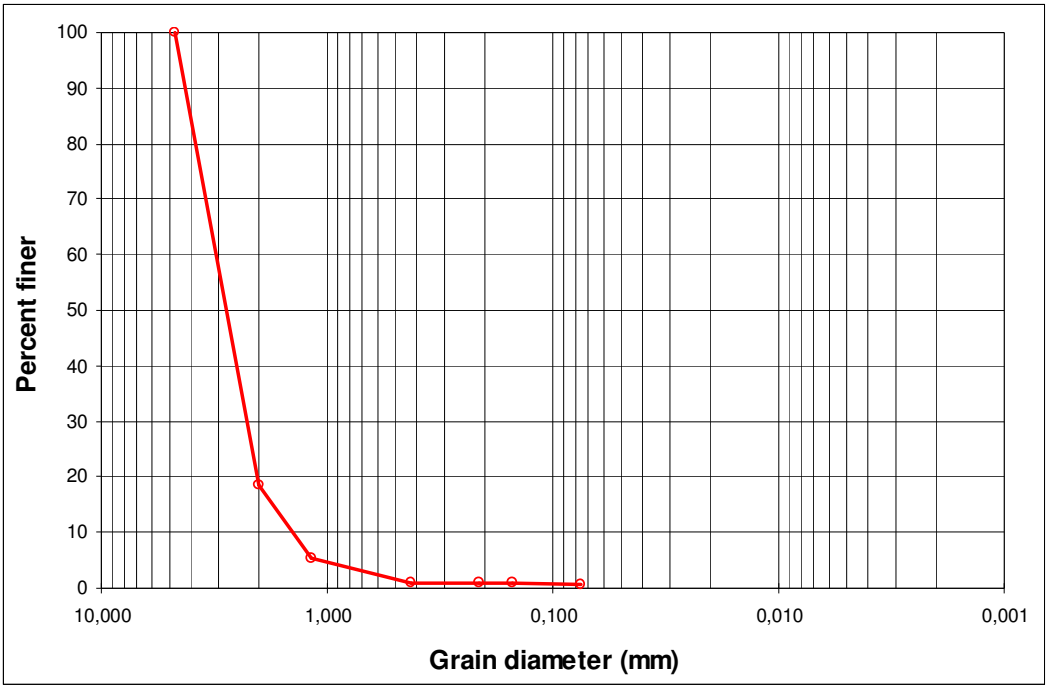

Figure 4.3. Grain size distribution of tire crumb

Figure 4.4. Tire crumb used in the experiments

4.2.2.2. Tire Buffings. Tire buffings are fiber shaped materials obtained from tire retread process. The grain size distribution of tire buffings is shown in Figure 4.5. Tire buffings used in this study are purchased from tire retread companies in Istanbul (Figure 4.6). Tire buffings had various lengths, so gradation is done according to ASTM D4767 – 04 standards to obtain buffings at the required length for the experimental study. All tire buffings used in this study were graded to have a length less than 5,8 mm. Because of that the buffings could pass through the sieves in the longitudinal direction, tire buffings used in this study are obtained by eliminating the ones left above sieve no 10 (2 mm) and the ones below sieve no 40 (0.425 mm). The tire buffings used in the triaxial tests have an aspect ratio of 3.5-4. In the CBR tests, both tire buffings having an aspect ratio of 3.5-4 and tire buffings having an aspect ratio of 7.5-8 are used. A comparison of tire buffings and tire crumb is shown in Figure 4.7.

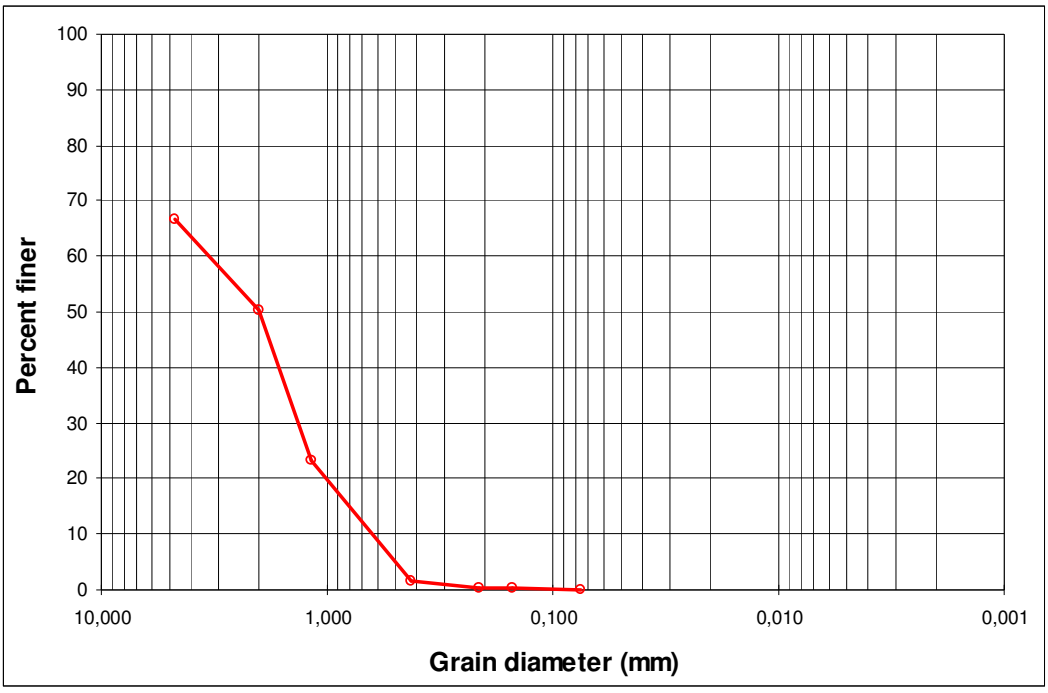

Figure 4.5. Grain size distribution of tire buffings

Figure 4.6. Tire buffings used in the experiments

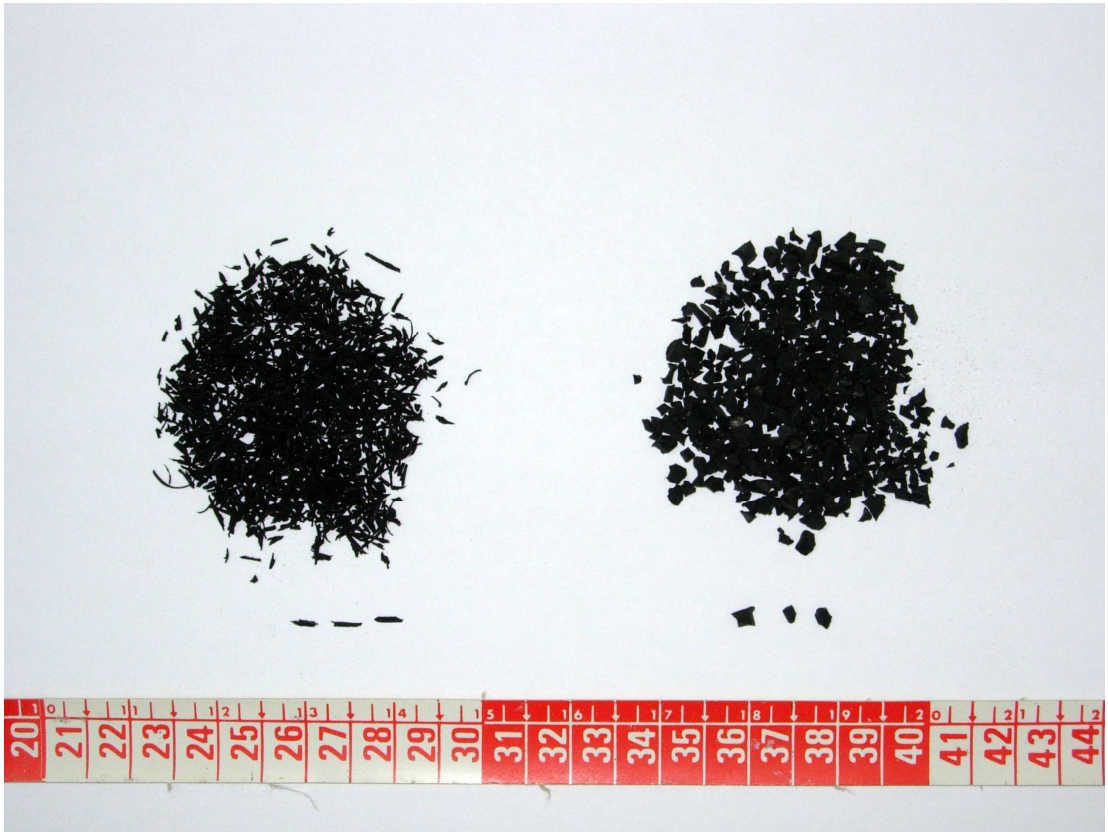

Figure 4.7. Tire buffings and tire crumb

4.3. Sample Preparation

4.3.1. Unit Weight Determination

Relative density determination tests are performed to determine the maximum, minimum, and relative densities of the specimens to be used in the triaxial tests. Sand, tire crumb, tire buffings, and various mixtures of these materials are tested. A standard compaction mold with a volume of 864 cm^3, and a standard compaction hammer is used (Figure 4.8). The test is done in accordance with ASTM D4253-83 and ASTM D4254-83. To determine the minimum density of a material, the compaction mold is filled with the material in the loose state and the density is calculated after measuring the weight. To determine the maximum density, the mold is filled with material in five layers with each layer hammered with fifteen blows. The maximum weight is measured and the corresponding density is calculated.

Figure 4.8. Compaction mold and hammer

After determining the maximum and minimum densities, a density between these values is selected for each specimen to be used in the triaxial tests that corresponds to the dense state. The relative densities are calculated using the selected densities. The density and relative density values of samples are shown in Table 4.1.

Table 4.1. Density and relative density values of samples

Sample	Min. (kN/m³)	Max. (kN/m³)	Used (kN/m³)	Dr
%100 sand	15.08	16.58	16.0	0.64
%5 crumb	13.72	15.90	15.1	0.67
%10 crumb	12.76	15.48	14.5	0.68
%20 crumb	11.62	14.19	13.3	0.70
%30 crumb	10.47	13.31	12.5	0.76
%40 crumb	9.46	12.55	11.2	0.63
%5 buffings	12.97	15.56	14.7	0.71
%10 buffings	11.97	14.48	13.7	0.73
%20 buffings	9.94	13.05	12.1	0.75
%30 buffings	8.33	11.26	10.3	0.74
%40 buffings	7.04	10.21	9.1	0.73
%100 crumb	5.29	7.16	6.5	0.71
%100 buffings	3.18	5.22	4.6	0.79

4.4. California Bearing Ratio (CBR) Test Procedure

A set of CBR tests are conducted on sand and mixtures of sand and tire waste. Tire crumb, and tire buffings are the types of tire wastes used in the experiments. Two different tire buffings having an aspect ratio of 3.5-4 and 7.5-8 are tested. The mixtures are prepared at tire contents of 5, 10, 20, 30, and 40 per cent tire waste by weight. A medium dense sand matrix is used with a unit weight of 15.79 kN/m³. The effect of tire content, tire shape, and tire aspect ratio on the CBR value of the soil is observed. The tests are performed in

the Geotechnical Laboratory of Bogazici University using a standard CBR machine with a penetration speed of 1.27 mm/min as described in ASTM D1883-07, a standard CBR mold with a diameter of 15.2 cm, a standard compaction hammer, a displacement measuring device, and a load measuring device (Figure 4.9).

Figure 4.9. Standard CBR machine

The procedure described in ASTM D1883-07 is employed for the tests. The specimens to be tested are prepared in optimum water contents obtained from previously conducted compaction tests. The mixture is placed in the CBR mold in three layers with compacting each layer by 25 blows using the standard compaction hammer. CBR tests are conducted on unsoaked specimens only. Load readings at penetrations of 0.64 mm, 1.27 mm, 1.91 mm, 2.54 mm, 3.18 mm, 3.81 mm, 4.45 mm, 5.08 mm, 7.62 mm, 10.16 mm,

12.70 mm are recorded. The CBR value is calculated as described in ASTM D1883-07 using the stress values at penetrations of 2.54 mm, and 5.08 mm.

4.5. Triaxial Test Procedure

Series of triaxial tests are performed on sand-tire waste mixtures to determine effect of tire reinforcement on the shear strength of soil specimens. A total of 26 sets of quick triaxial compression tests and consolidated drained (CD) triaxial tests are conducted at three different confining pressures of 40, 100, and 200 kPa. The rate of strain is selected as 0.5 mm/min, at which the pore pressure stays constant at zero in the consolidated drained (CD) triaxial tests. The specimens are prepared at a constant volume with a diameter of 35 mm and a height of 70 mm according to the ASTM D4767-04 and ASTM D2850-03a standards. The triaxial tests continued until a peak and fall is observed in the deviator stress or a maximum of 15 per cent axial strain is reached. All tests are carried out in the Geotechnical Laboratory of the Bogazici University. Test data is obtained by an Autonomous Data Acquisition Unit (ADU) with transducers and evaluated by using the software DataSystem 7. The cohesion (c) and the angle of internal friction (Φ) values are determined from the Mohr-failure envelopes. Using regression analysis the equivalent angle of internal friction (Φ_{eq}) values are also calculated. The equivalent angle of internal friction stands for the friction angle at which the cohesion is assumed as zero. It is calculated by regression analysis using the data obtained from the experiments. Several researchers (Zornberg et al. 2004, Gotteland et al. 2005) suggest the use of equivalent friction angle because it enables a straightforward comparison of experimental results to study the effect of variables like tire content, shape, and aspect ratio on shear strength parameters.

4.5.1. Principles of the Triaxial Compression Test

The triaxial compression test is used to measure the shear strength of a soil under controlled drainage conditions (ASTM D4767, ASTM D2850). In the conventional triaxial test, a cylindrical specimen of soil within a rubber membrane is placed in a triaxial compression chamber, subjected to a confining fluid, and then loaded axially to failure. Drainage of pore water is controlled throughout the test stages. Before shear, the principal

stresses are equal to the chamber fluid pressure which is also called as the confining pressure. During shear, the major principal stress (σ_1) is equal to the sum of applied axial stress and the chamber pressure (σ_3). The applied axial stress (σ_1 - σ_3) is called the "deviator stress". The intermediate principal stress (σ_2), and the minor principal stress (σ_3) are identical and equal to the confining pressure.

4.5.2. Triaxial Test Apparatus

A standard triaxial test apparatus in the Geotechnical Laboratory of the Bogazici University which is purchased from ELE International Company is used. The apparatus is composed of a load frame (Digital Tritest 50), a triaxial cell, a specimen base adapter, a de-aired water apparatus, a bladder type air/water pressure system, a universal pump and pressure indicating panel, a two-way pneumatic pressure reducing panel, a water distribution panel, a volume-change unit, a twin-burette, transducers (displacement, load, and pressure), an Autonomous Data Acquisition Unit (ADU), and a computer with DataSystem 7 (DS7) and Microsoft Office Word software installed. The equipments also used are rubber membranes, filter paper, porous stones, two-way split mold, and rubber O-rings. The triaxial cell used has a diameter of 50 mm, a maximum piston load of 45 kN, and a working pressure limit of 1700 kPa. The general components of the triaxial test and the test equipment used in this study are shown in Figure 4.10 and Figure 4.11.

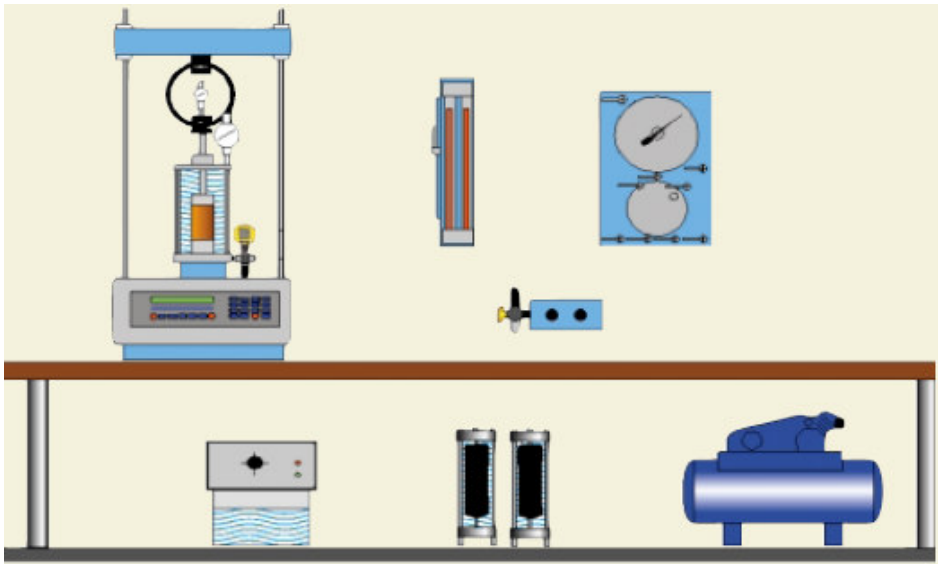

Figure 4.10. General layout of components for the triaxial test

Figure 4.11. Triaxial test equipment

4.5.3. Specimen Preparation

The specimen has a constant volume of 67.35 cm³ calculated from a diameter of 35 mm and a height of 70 mm. Using the densities selected from the relative density test and the constant volume of specimen, required material weights are calculated. From the total material weight, the amount of required sand and tire weights are calculated, and corresponding amounts of materials are taken and mixed in a dish (Figure 4.12). The sample preparation is done in accordance with ASTM D4767 and ASTM D2850.

Figure 4.12. Example of materials mixed in a dish

A rubber membrane with a thickness of 0.5 mm and a diameter of 35 mm is taken and is attached to the cleaned base platen using two rubber “O” rings (Figure 4.13). A porous stone is placed on the base inside the rubber membrane, and a filter paper with the proper diameter is placed on the porous stone.

Figure 4.13. Rubber membrane attached to the base platen using “O” rings

The rubber membrane is then covered with a specimen mold having a diameter of 35 mm and a height of 70 mm, and the top portion of the membrane is folded down over the mold. A vacuum machine is attached to the mold, and vacuum is applied to pull the membrane against the side of the mold (Figure 4.14).

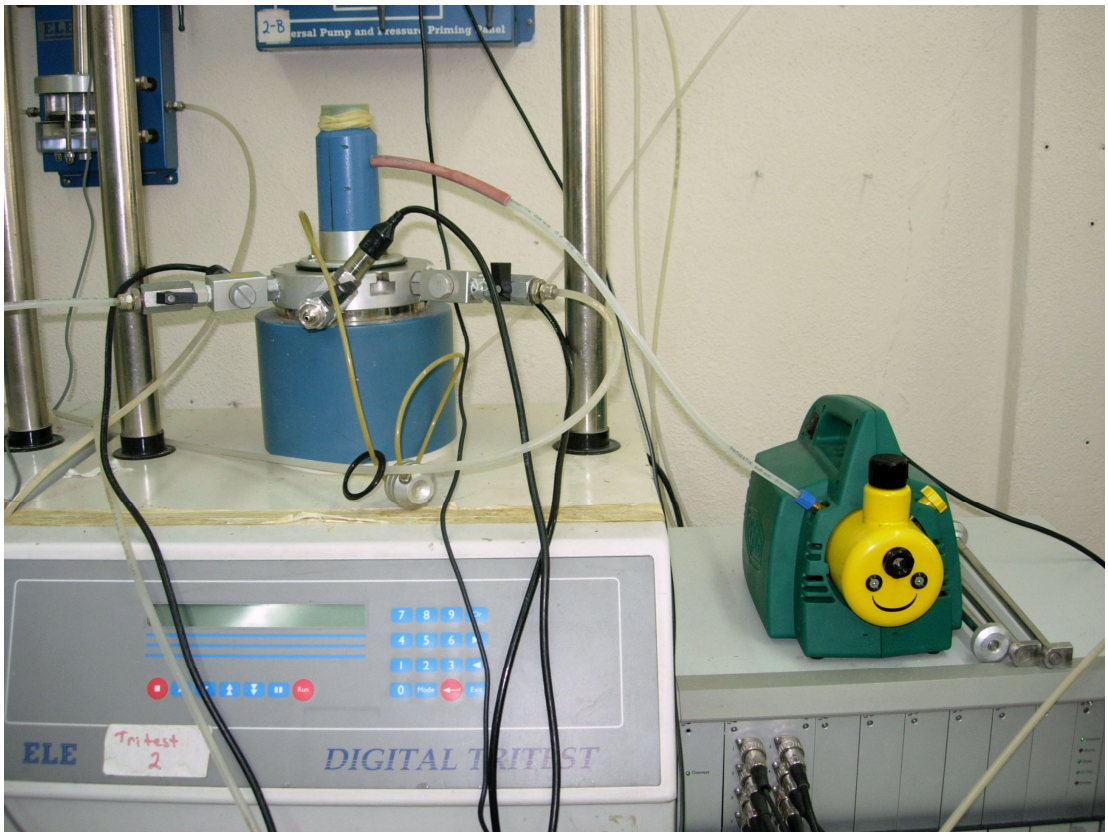

Figure 4.14. Vacuum machine attached to the mold

The sand-tire mixture is poured into the mold carefully in six layers with each layer tampered using a tamper to achieve the required density as described in the ASTM standards. A piece of filter paper is placed on the top of the sample and a porous stone is placed on the filter paper. Finally, the top platen is placed on the porous stone and the folded membrane is rolled on the top platen and sealed using two rubber "O" rings. The vacuum is then released, and the mold is taken off the sample (Figure 4.15). Exceeded membrane is folded down on the sample, and the membrane is checked for any deformations or holes. Three height measurements 120º apart and three diameter measurements are done to check if the sample meets the required dimensions.

Figure 4.15. Mold taken off the specimen

The lucite cylinder is placed on the base platen and an airtight seal is applied (Figure 4.16). The cell is placed in the compression machine.

Figure 4.16. Lucite cylinder sealed on the base plated

Finally, the cell is filled with de-aired water obtained from the de-aired water apparatus while the top valve of the cell is open (Figure 4.17). After the chamber is completely filled the top valve is closed.

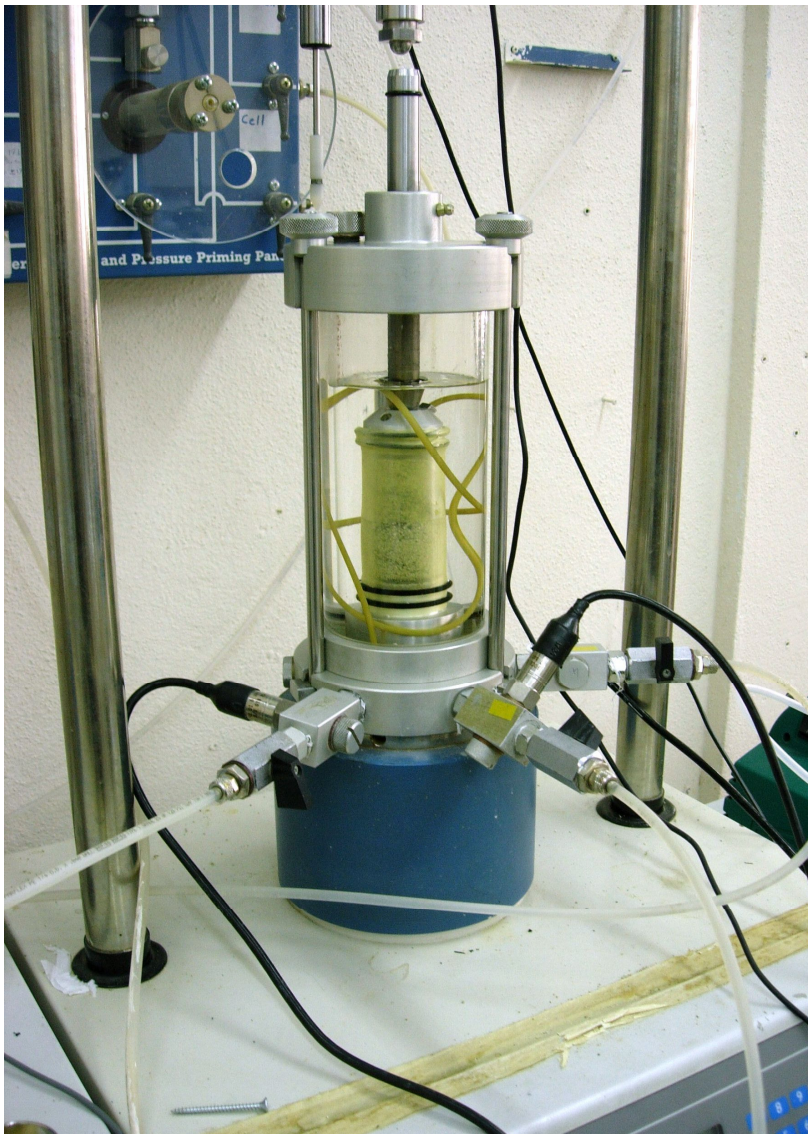

Figure 4.17. Cell filled with de-aired water

4.5.4. Quick Triaxial Compression Test Procedure

The quick triaxial compression test is performed on dry specimens. The test is performed with the drainage valve closed for all phases of the test. Axial loading takes place immediately after the chamber pressure is stabilized. The test consists mainly of three stages, test initialization, compression, and final measurements (Figure 4.18). The test procedure is performed in accordance to ASTM D2850-03a.

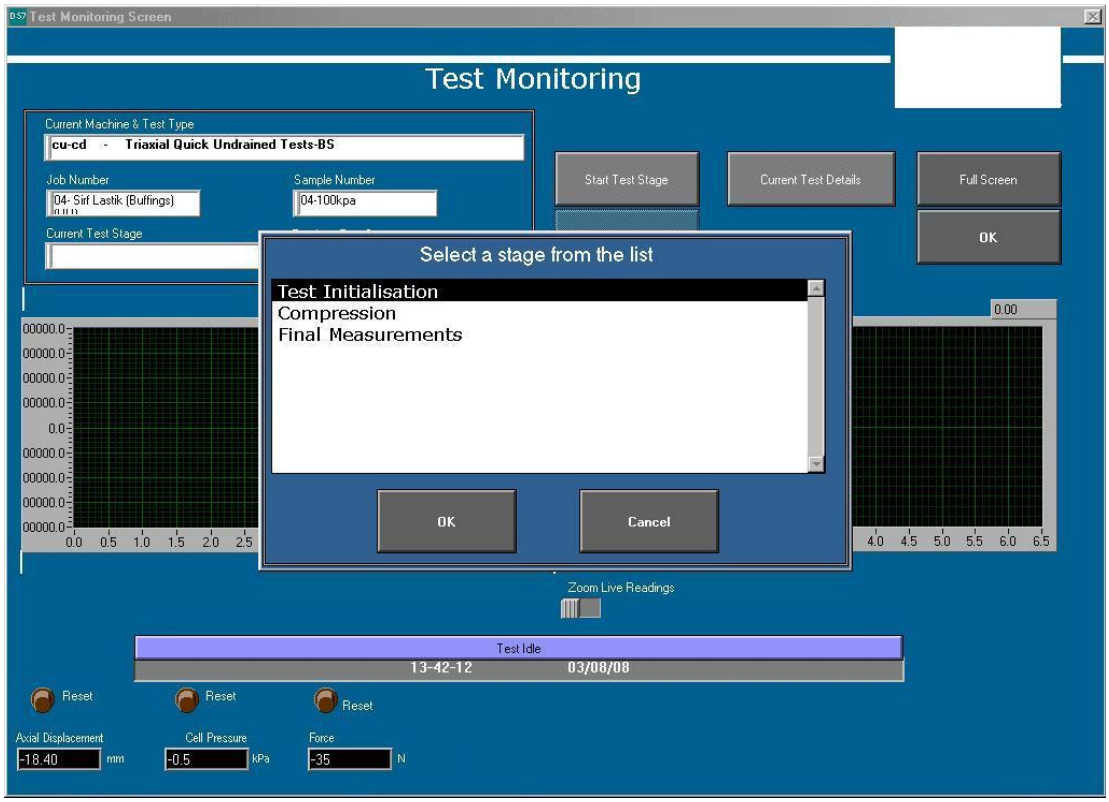

Figure 4.18. Stages of quick triaxial compression test

After the specimen is prepared and the cell is filled with de-aired water as described in the previous section, the cell pressure (confining pressure) is adjusted to the desired value (40, 100, or 200 kPa). The compression machine is turned on and adjusted to 0.5 mm/min. Finally, the loading is started and the test continues until the load peaks or the 15 per cent strain is reached.

4.5.5. Consolidated Drained (CD) Triaxial Test Procedure

In the consolidated drained test, the drainage valve is left open for the duration of the test, and complete sample drainage takes places before the compression stage. The load is applied at a strain rate at which the particle readjustments in the specimen do not induce any excess pore water pressure. The total stresses will equal to the effective stresses since there is no excess pore water pressure. The volume change of the specimen can also be measured if desired. The test consists of five stages that are test initialization, saturation, consolidation, compression, and final measurements (Figure 4.19). The test is conducted in accordance to ASTM D4767-04.

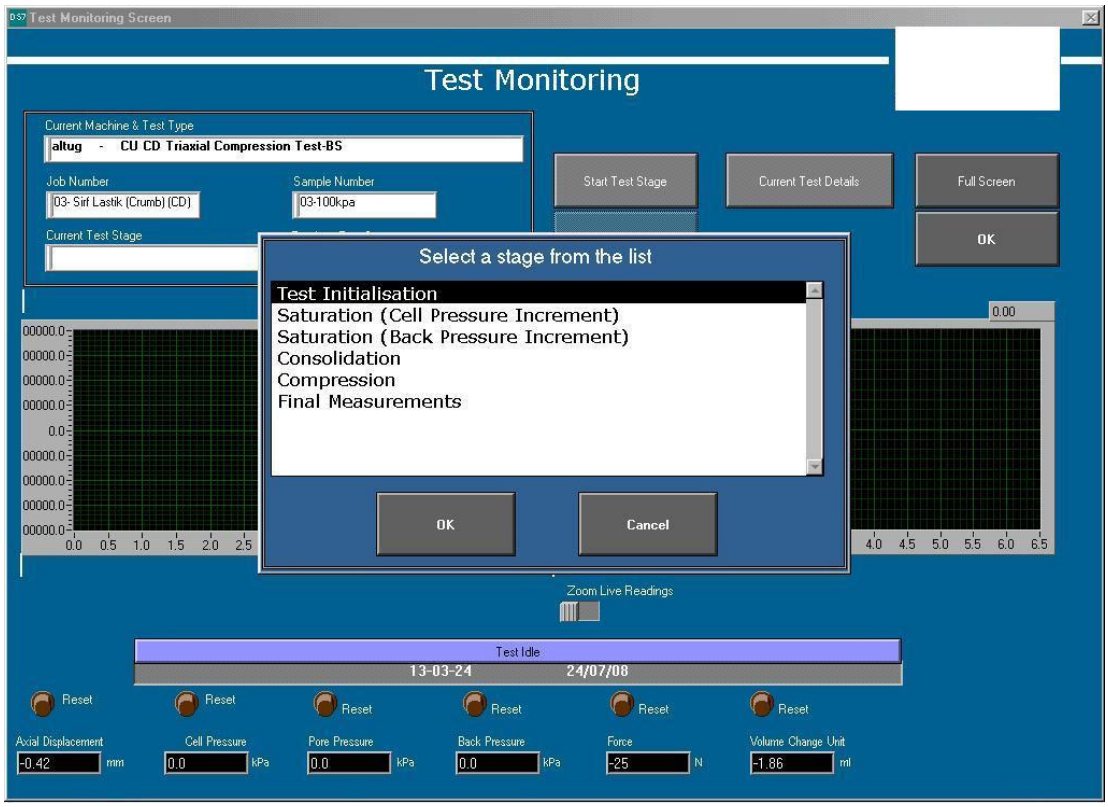

Figure 4.19. Stages of consolidated drained triaxial test

The specimen is prepared and the cell is filled as indicated in the section 4.5.3. Before saturating the specimen, the cell pressure is raised for deformation not to occur with the water flow. And then water is flowed from the bottom sample drainage line until the sample and the top drainage line are saturated. The de-aired water supply system is shown in Figure 4.20.

In the saturation stage cell and back pressures are applied until all the air in the specimen is dissolved. In order to establish this, the cell and back pressures are increased in steps. In the first increment the cell pressure is raised to 50 kPa. The pressure is applied until the pore water pressure gets steady. Then the back pressure is raised to 40 kPa, with a differential of 10 kPa in between. When the pore pressure change ends, these steps are repeated until the B value gets around 0.97, at the point where all air in the sample dissolves (ASTM D4767-04). Usually this happens when the back pressure is increased to around 200 kPa.

In the consolidation stage the back and pore pressure valves are closed, and the cell pressure is increased to the specific value in which the effective stress becomes 60 kPa. And then the back pressure valve is opened, and the consolidation process runs until 95 per cent of the pore water pressure dissipates (ASTM D4767-04).

Finally, at the compression stage the cell pressure (confining pressure) is set to either 40, 100, or 200 kPa and the sample is loaded under a strain rate of 0.5 mm/min, while the drainage valve is open. The strain rate is selected so that the pore water pressure will remain unchanged at the value of zero for the rest of the test. The compression stage continues until the load peaks or the 15 per cent strain is reached. An example of a failed specimen is shown in Figure 4.21.

Figure 4.20. De-aired water supply

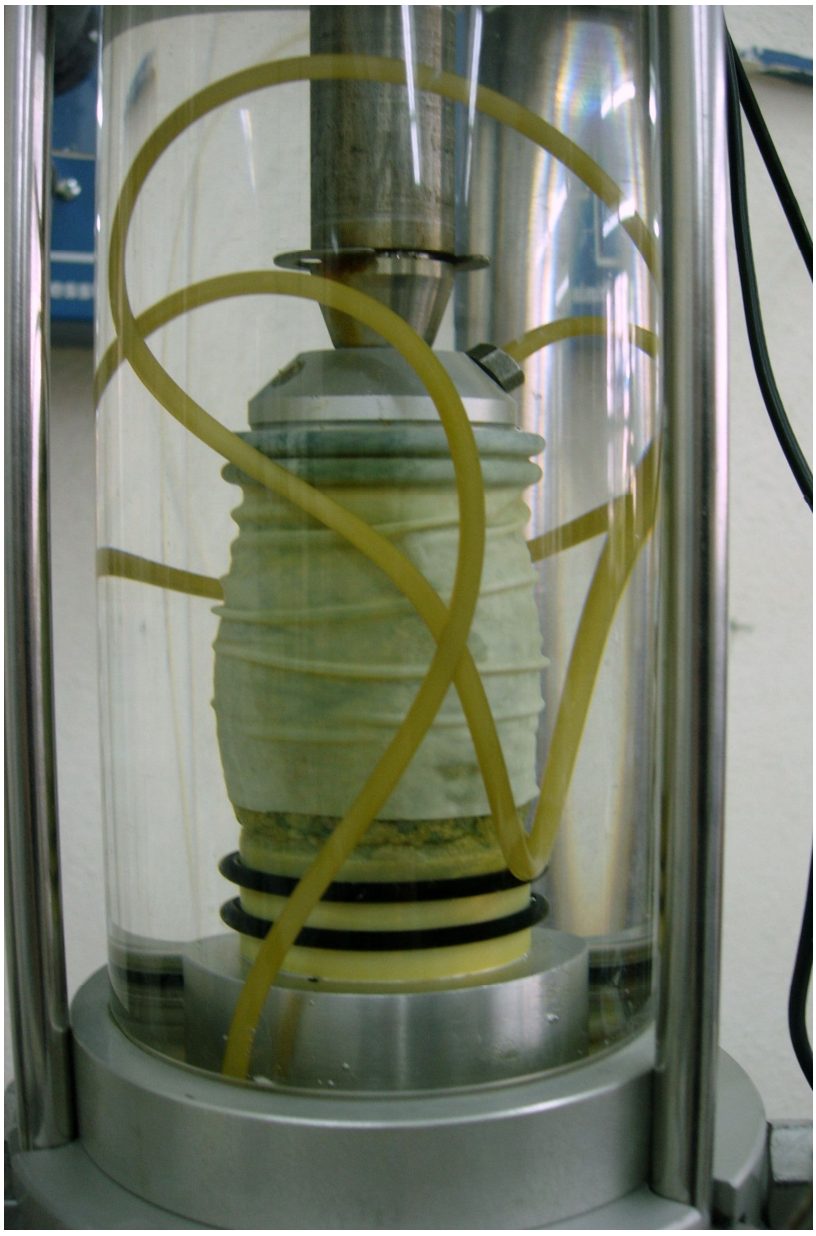

Figure 4.21. Example of a failed specimen

5. EXPERIMENTAL RESULTS

5.1. California Bearing Ratio (CBR) Test Results

A set of CBR tests are performed on sand alone and mixtures composed of sand and varying amounts of tire waste. Tire crumb, and two different types of tire buffings are used as tire inclusions in the experiments. Tire crumb is a granular material, and tire buffings is a fiber shaped material. Tire buffings-(H) represents the tire buffings having a higher aspect ratio. Tire crumb have an aspect ratio of 1-1.5, tire buffings have an aspect ratio of 3.5-4, and tire buffings-(H) have an aspect ratio of 7.5-8. The mixtures are prepared at tire contents of 5, 10, 20, 30, and 40 per cent tire waste by weight. The effect of tire content, tire shape, and tire aspect ratio on the CBR value of the soil is observed. The tests are conducted in accordance with ASTM D1883-07. The test results are shown in Table 5.1.

Table 5.1. CBR test results

Specimen	Unit Weight (kN/m^3)	Water Content (%)	CBR Value	General Rating
100% Sand	15.79	15.0	7.98	Fair
5% Tire Crumb	15.03	14.1	6.86	Poor to Fair
10% Tire Crumb	14.72	13.4	7.58	Fair
20% Tire Crumb	14.03	11.8	6.73	Poor to Fair
30% Tire Crumb	13.41	10.9	5.92	Poor to Fair
40% Tire Crumb	12.85	9.7	4.99	Poor to Fair
5% Tire Buffings	14.82	13.8	8.56	Fair
10% Tire Buffings	14.07	13.0	9.85	Fair
20% Tire Buffings	12.96	11.2	10.74	Fair
30% Tire Buffings	12.09	10.1	11.48	Fair
40% Tire Buffings	11.15	8.9	10.93	Fair
5% Tire Buffings-(H)	15.18	14.3	11.21	Fair
10% Tire Buffings-(H)	14.80	13.8	12.88	Fair
20% Tire Buffings-(H)	14.23	12.5	14.24	Fair
30% Tire Buffings-(H)	13.71	11.7	15.77	Fair
40% Tire Buffings-(H)	13.02	10.4	14.08	Fair

5.1.1. Analysis of California Bearing Ratio Test Results

The values of CBR of sand alone and sand-tire waste mixtures containing tire crumb and tire buffings as tire inclusions with different percentages have been obtained. Figure 5.1 shows the change in CBR value of the specimens with changing tire content. It can be seen that the addition of tire crumb decreased the CBR value of soil, however the addition of tire buffings increased the CBR value, and tire buffings with a higher aspect ratio resulted in a higher CBR value. The addition of 30 per cent tire buffings with an aspect ratio of 3.5-4 to sand resulted in a 44 per cent increase in the CBR value of the soil, and the addition of 30 per cent tire buffings with an aspect ratio of 7.5-8 to sand resulted in a 98 per cent increase in the CBR value of the soil. Similar results are obtained by Benson and Khire (1994), who mixed high-density polyethylene fibers at different aspect ratios with sand. They concluded that when the aspect ratio is small, the strips are too short to develop sufficient friction angle at the end of the strips, and little tensile force is generated in the strip.

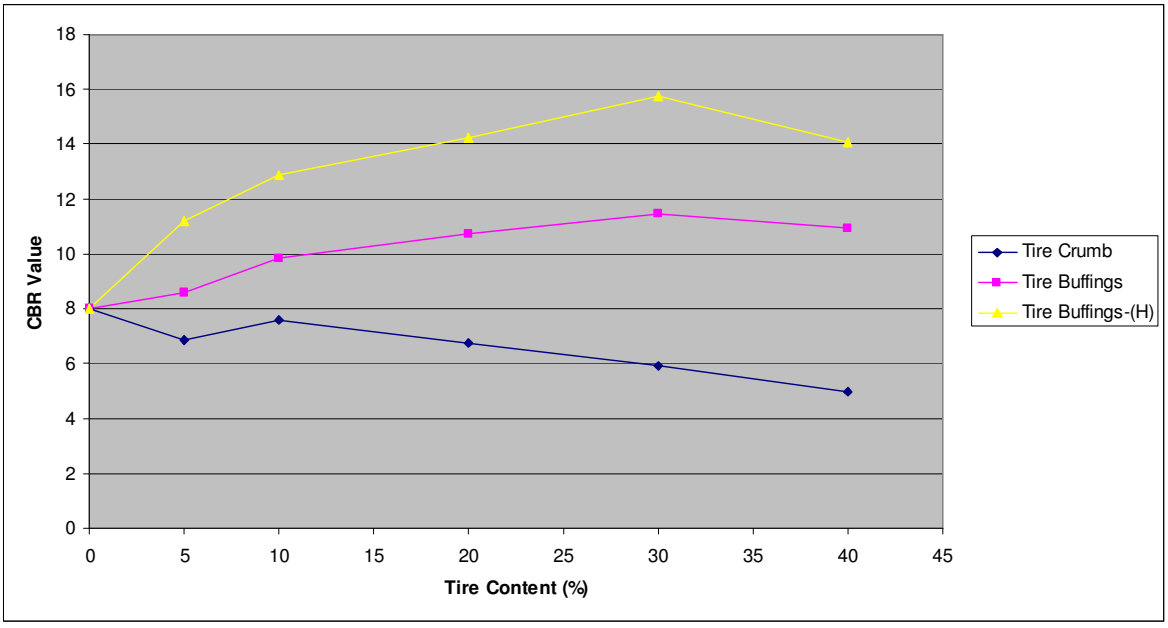

Figure 5.1. Tire content-CBR value graph

Figure 5.2 shows the change in the CBR value of soil with changing the aspect ratio of the tire waste. It can be seen that for all tire contents the higher aspect ratio results in a higher CBR value. The highest CBR values are obtained by using tire buffings having an

aspect ratio of 7.5-8 as tire inclusions. Ghazavi and Sakhi (2005) conducted CBR tests on sand mixed with tire shreds to investigate the effect of tire aspect ratio on the CBR value of the soil. They used two different compaction levels that the loose state corresponds to a sand unit weight of 15.5 kN/m³ and a CBR value around 2, and the dense state corresponds to a sand unit weight of 16.8 kN/m³ and a CBR value around 13. They also concluded that the aspect ratio of tire shreds had a significant influence on CBR values. The sand used in this study is a medium dense sand with a CBR value of 7.98 which is in good correlation with the results of Ghazavi and Sakhi (2005).

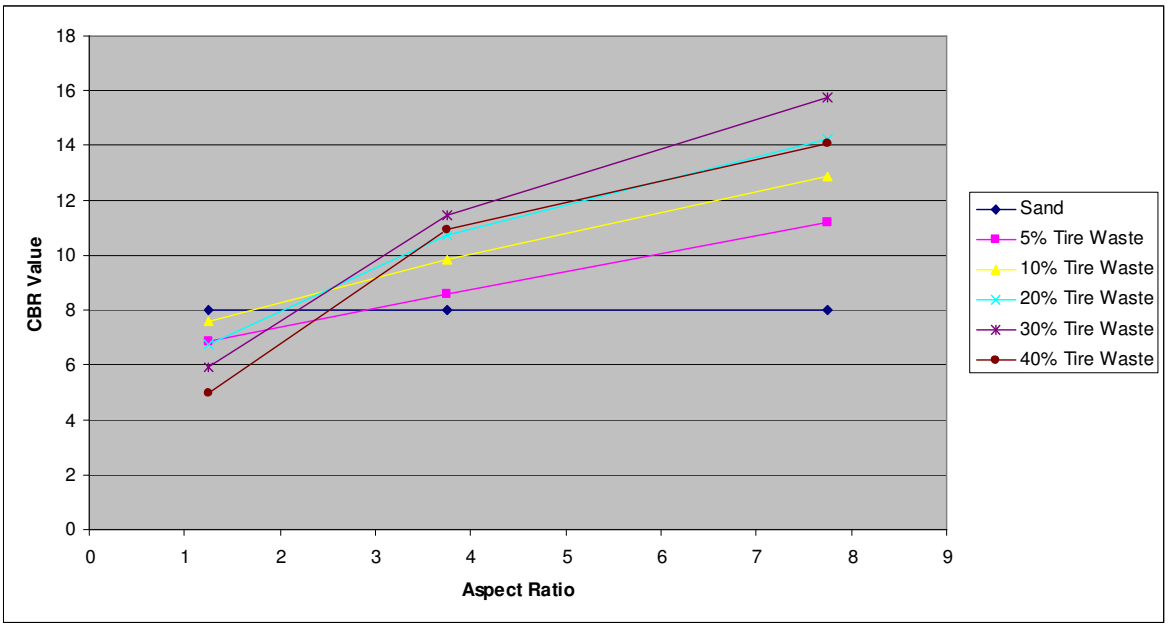

Figure 5.2. Aspect ratio-CBR value graph

In conclusion, the test results indicate that addition of tire crumb which is a granular material with an aspect ratio about 1-1.5 do not have an important effect on the CBR value, however the addition of tire buffings which is a fiber shaped material increases the CBR value. Tire buffings having an aspect ratio of 7.5-8 increases the CBR value of soil greater compared to tire buffings having an aspect ratio of 3.5-4. Up to 30 per cent tire buffings addition by weight the CBR value of soil increases, beyond this content it decreases. The optimum mixture with the highest CBR value is obtained by the addition of 30 per cent tire buffings having an aspect ratio of 7.5-8, which results in a 98 per cent increase in the CBR value of the soil.

5.2. Quick Triaxial Compression Test Results

Quick triaxial compression tests are performed on dry specimens of sand, tire crumb, tire buffings, and sand-tire waste mixtures at different tire contents. A total of 13 sets of tests are done, with each test repeated at three different confining pressures of 40, 100, and 200 kPa. Tire waste-sand mixtures are prepared at 5, 10, 20, 30, and 40 per cent of tire waste by weight. The strain rate is selected as 0.5 mm/min, a value within proper limits of ASTM D2850. The correction for rubber membrane with a thickness of 0.5 mm is calculated by Data System 7. The corrected deviator stress is calculated by Data System 7 using the area corrections for the rubber membrane as described in ASTM D2850. The shear strength obtained from the quick triaxial compression test is used where the loading is assumed to take place so rapidly that there is no time for the induced excess pore water pressure to dissipate or for consolidation to occur, for example in rapidly constructed embankments.

5.2.1. Mixture Containing 100 per cent Sand

Sand alone is tested. The unit weight of the sand specimen is 16.0 kN/m³. The deviator stress-strain behavior of the specimen is shown in Figure 5.3. The peak values of deviator stress are obtained around an axial strain of 5 per cent. At 0 per cent axial strain, the sample tested at 40 kPa confining pressure shows a sudden increase in deviator stress. The failure conditions are 221 kPa deviator stress and 5.35 per cent axial strain at 40 kPa confining pressure, 462 kPa deviator stress and 5.39 per cent axial strain at 100 kPa confining pressure, and 810 kPa deviator stress and 4.88 per cent axial strain under 200 kPa confining pressure. According to the failure envelope (Figure 5.4), the cohesion value is 9.97 kPa and the internal friction angle is 41.48 degrees. The same cohesion and friction angle values can be obtained from the p-q graph of the specimen, which is shown in Figure 5.5. Using regression analysis the equivalent angle of internal friction is calculated as 43.02 degrees.

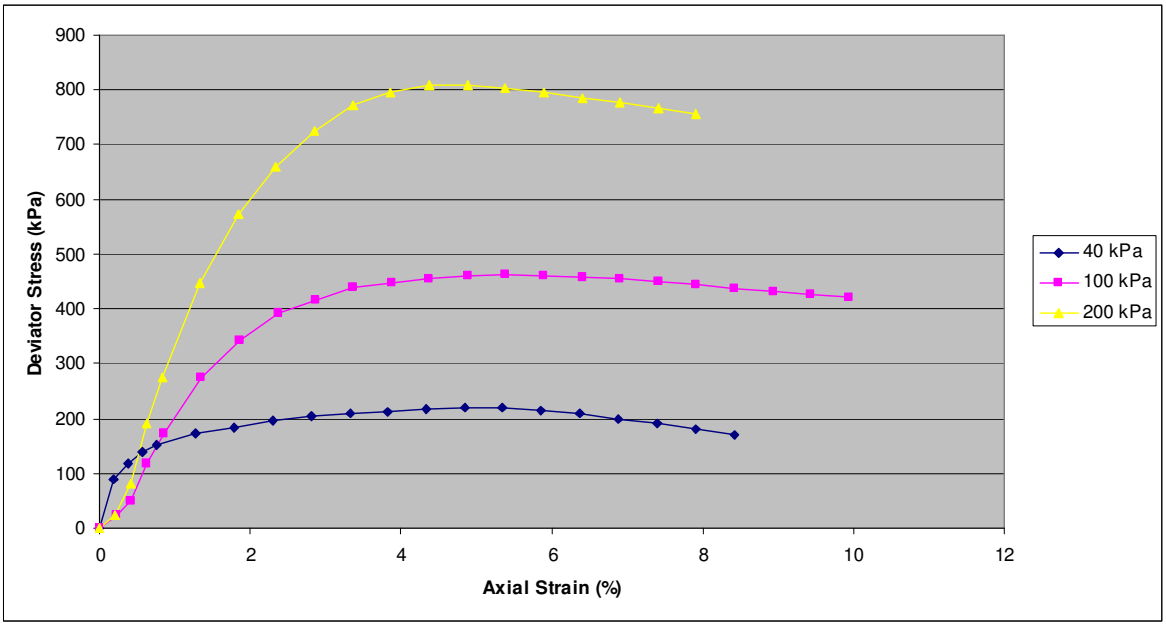

Figure 5.3. Deviator stress-axial strain behavior of specimen containing 100 per cent sand

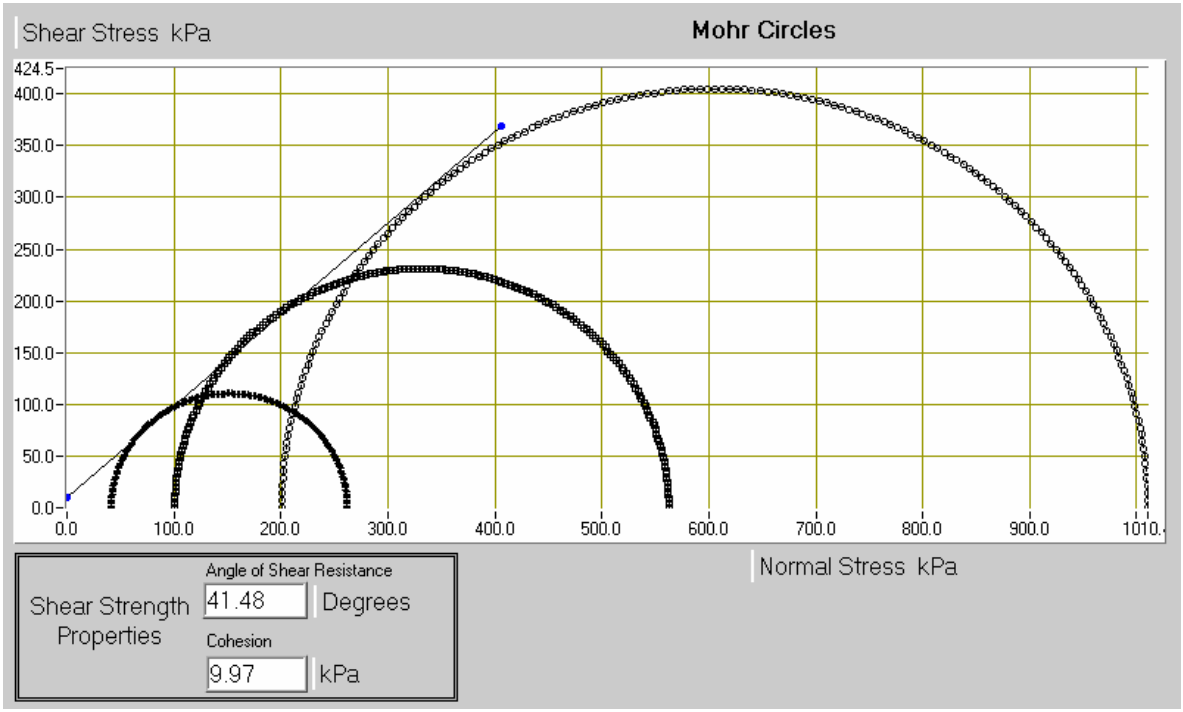

Figure 5.4. Shear strength envelope of specimen containing 100 per cent sand

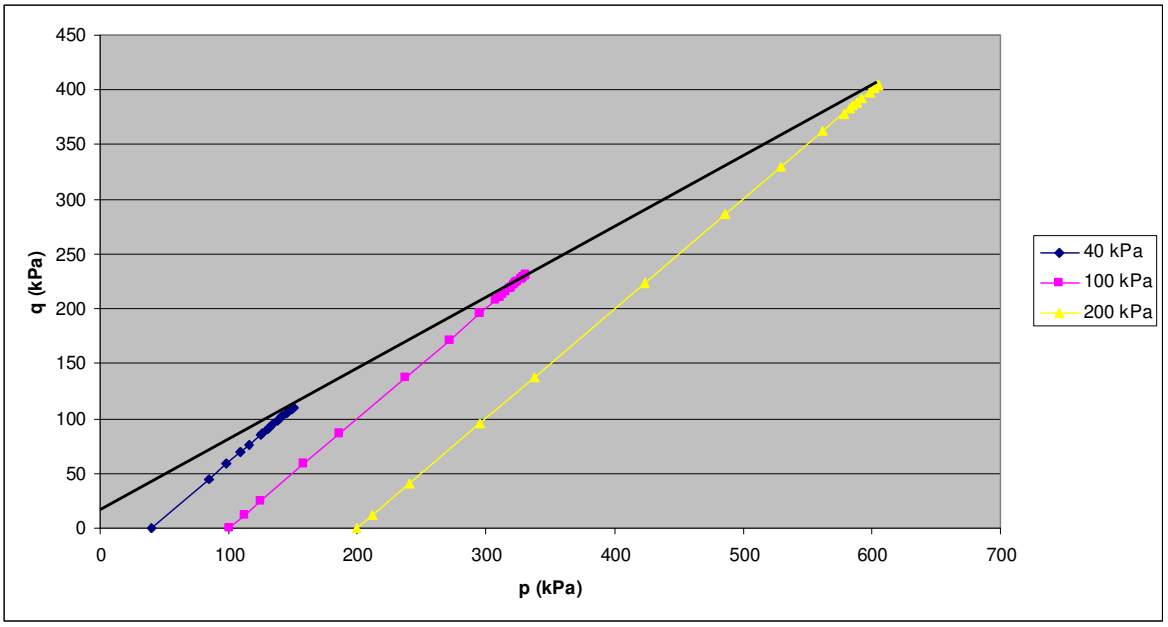

Figure 5.5. p-q graph of specimen containing 100 per cent sand

5.2.2. Mixture Containing 100 per cent Tire Crumb

The specimen is prepared using only tire crumb. The unit weight of the sample is 6.5 kN/m³. The deviatoric stress-strain behavior of the specimen is shown in Figure 5.6. The deviator stress continued to increase with increasing axial strain, so the failure envelope is drawn according to the stress values corresponding to an axial strain of 15 per cent as mentioned in the ASTM standards. It is observed that the samples tested at 100 and 200 kPa confining pressures show similar behavior up to 2 per cent axial strain. At 15 per cent axial strain the corresponding deviator stresses are 54, 102, and 184 kPa for the tests done at confining pressures 40, 100, and 200 kPa. The shear strength envelope is shown in Figure 5.7. The cohesion value is determined as 8.10 kPa and the angle of internal friction is 16.89 degrees. Same shear strength parameters can be obtained from the p-q graph shown in Figure 5.8. The equivalent angle of internal friction is calculated as 19.71 degrees.

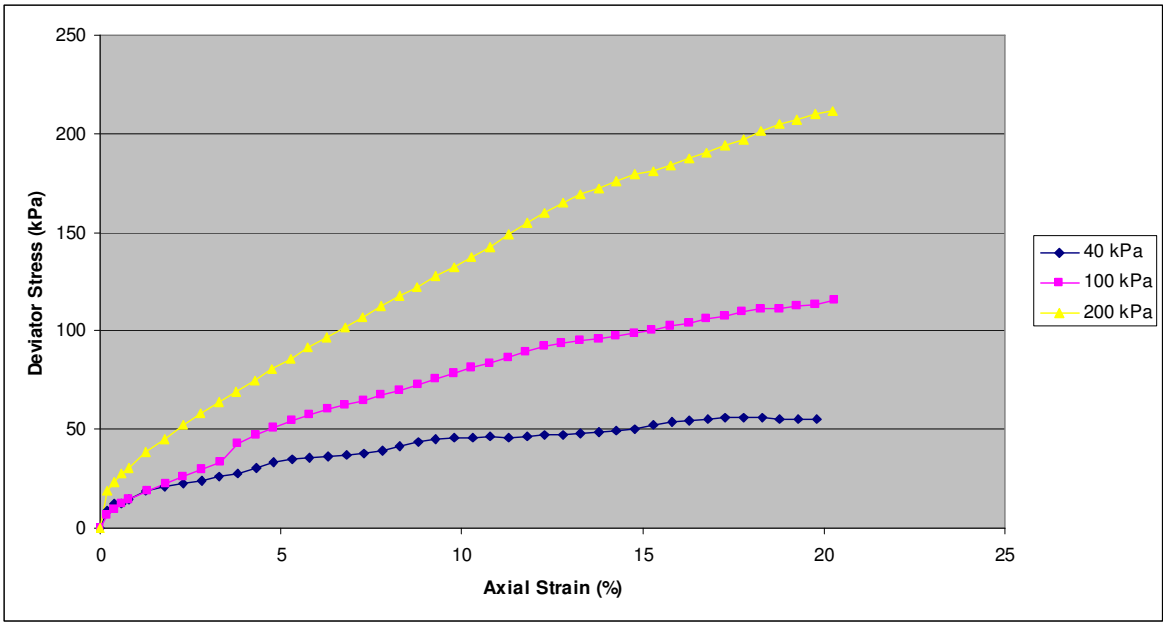

Figure 5.6. Deviator stress-axial strain behavior of specimen containing 100 per cent tire crumb

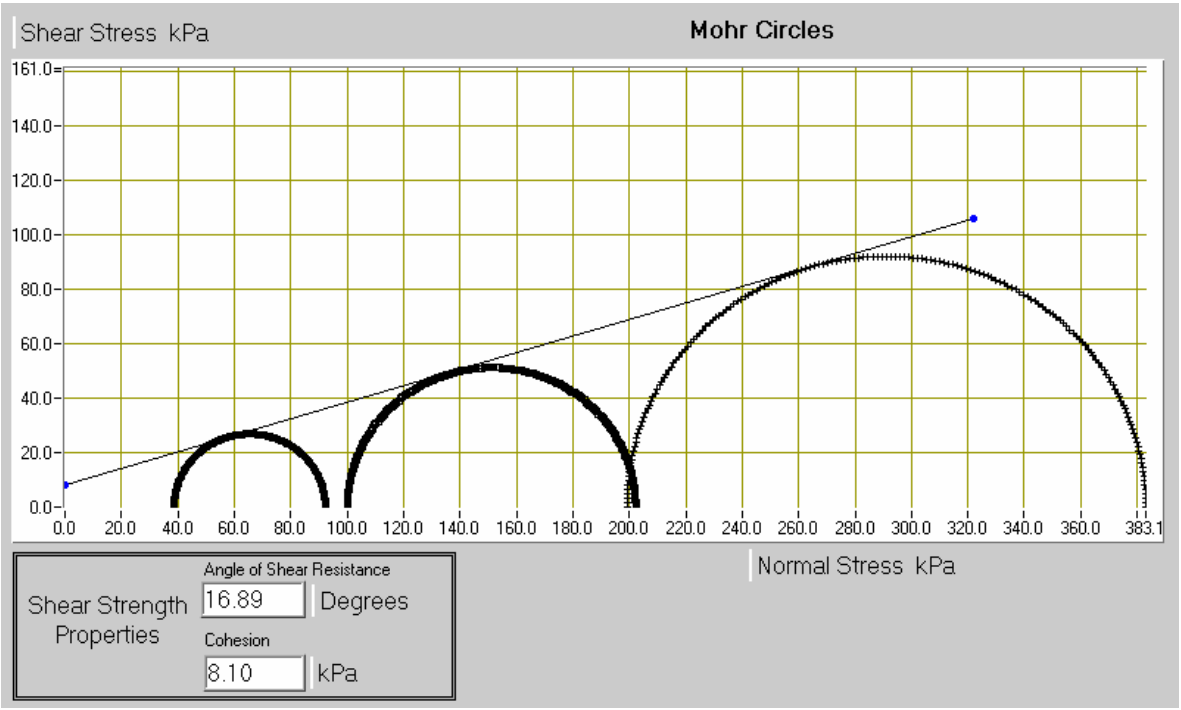

Figure 5.7. Shear strength envelope of specimen containing 100 per cent tire crumb

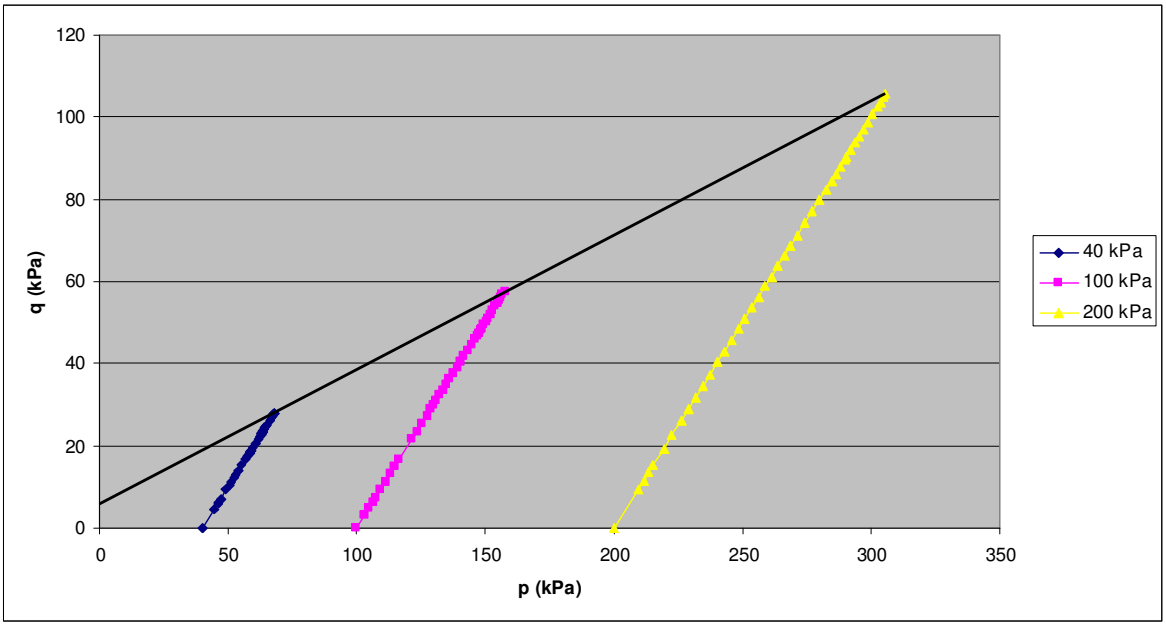

Figure 5.8. p-q graph of specimen containing 100 per cent tire crumb

5.2.3. Mixture Containing 5 per cent Tire Crumb

The specimen is prepared by mixing 5 per cent of tire crumb by weight with sand. The unit weight of the sample is 15.1 kN/m³. Figure 5.9 shows the deviator stress-strain behavior of the specimen. The peak deviator stresses are obtained at about 6-7 per cent axial strain. The stress-strain graph indicates that up to 0.5 per cent axial strain, the tests at 100 and 200 kPa confining pressures show similar behavior. Maximum deviator stresses observed are 191, 408, and 692 kPa for the tests at confining pressures 40, 100, and 200 kPa. According to the Mohr-failure envelope (Figure 5.10) the cohesion value is 15.10 kPa and the angle of internal friction is 38.19 degrees. These shear strength parameters can also be obtained from the p-q graph of the specimen (Figure 5.11). By regression analysis, the equivalent friction angle is calculated as 40.88 degrees. In Figure 5.12, a mixture containing 5 per cent tire crumb by weight is shown.

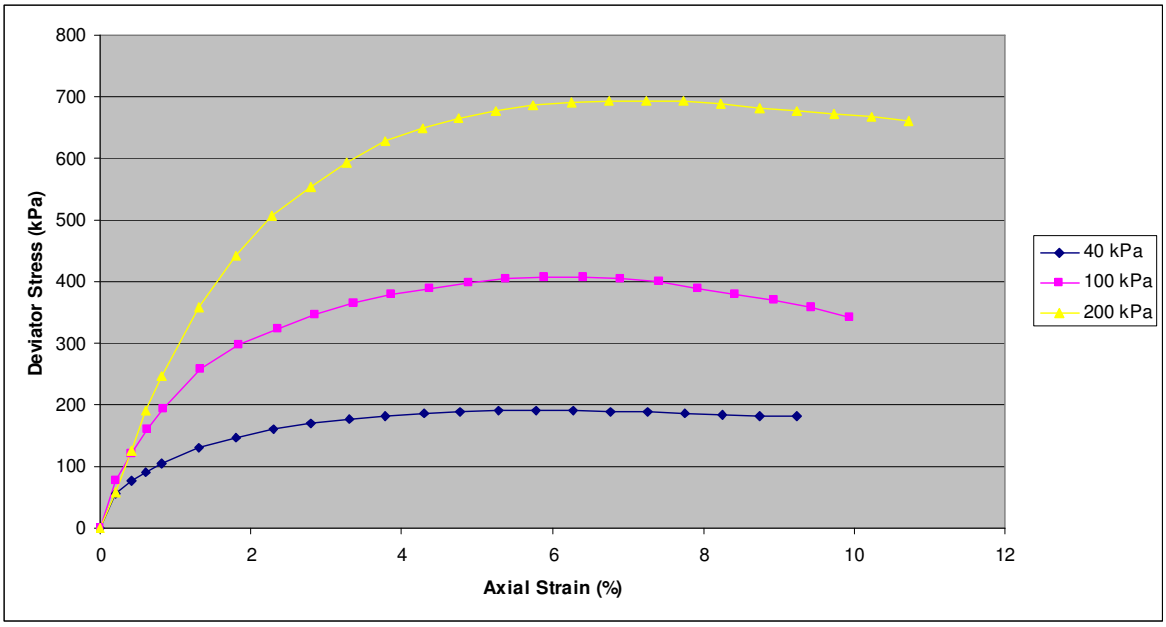

Figure 5.9. Deviator stress-axial strain behavior of specimen containing 5 per cent tire crumb

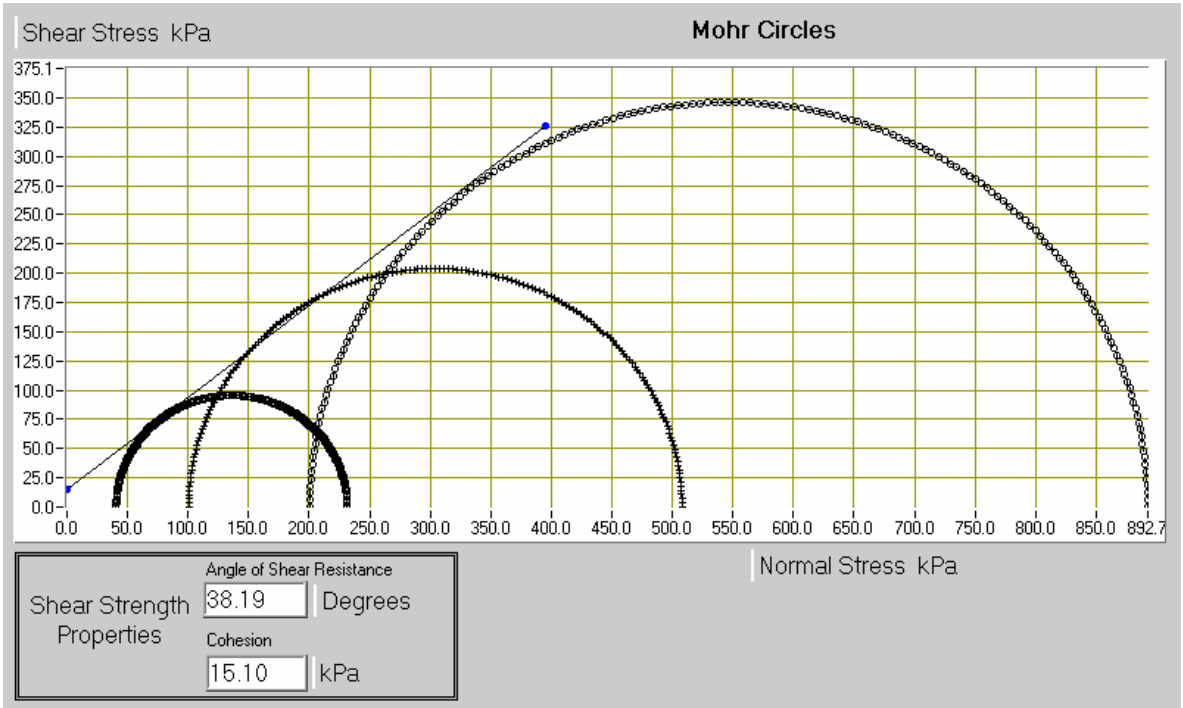

Figure 5.10. Shear strength envelope of specimen containing 5 per cent tire crumb

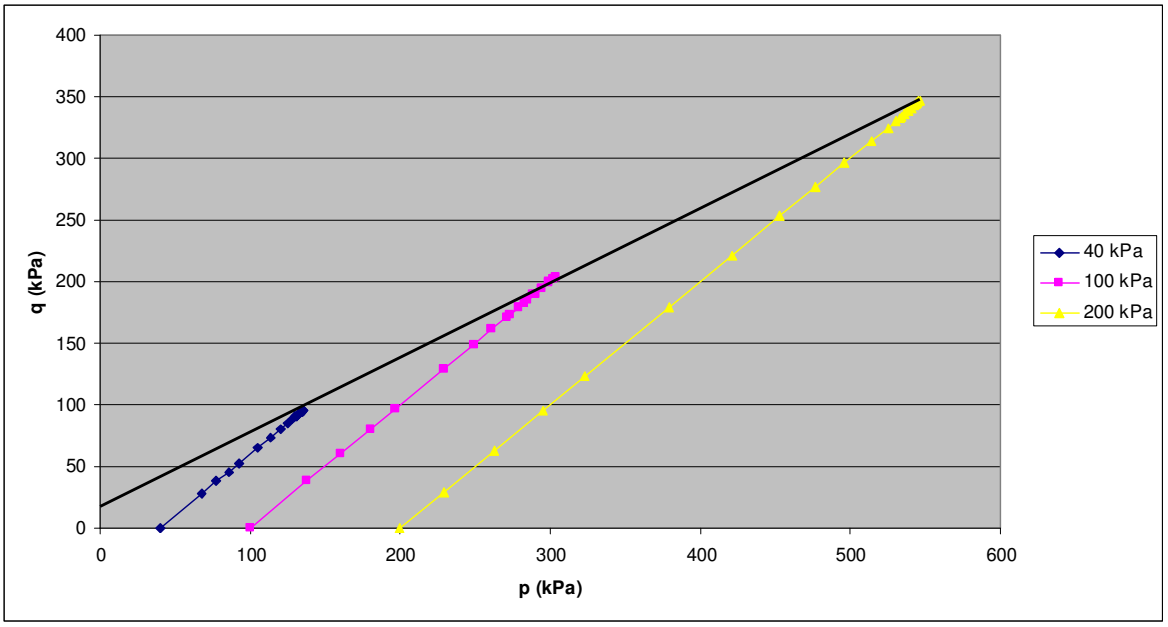

Figure 5.11. p-q graph of specimen containing 5 per cent tire crumb

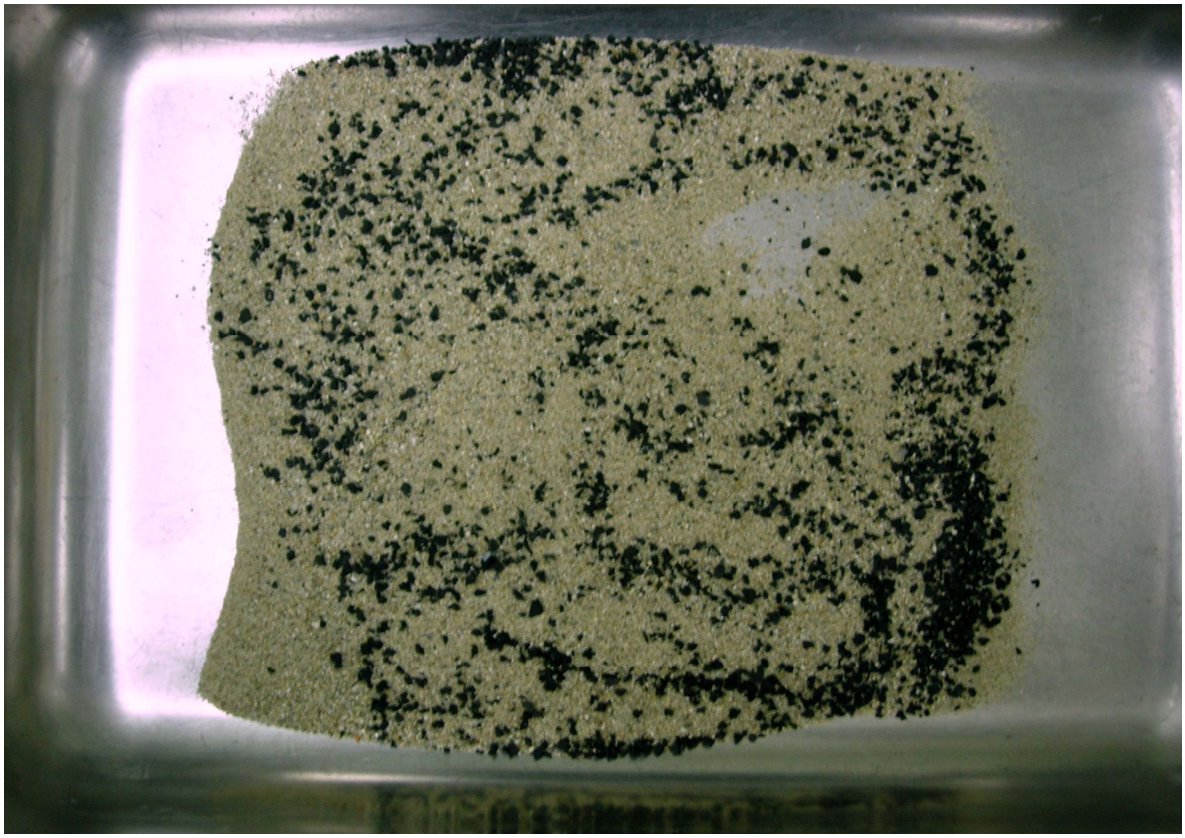

Figure 5.12. Mixture containing 5 per cent tire crumb by weight

5.2.4. Mixture Containing 10 per cent Tire Crumb

10 per cent tire crumb by weight is mixed with sand. The unit weight of the specimen is 14.5 kN/m³. The deviator stress-strain graph is drawn (Figure 5.13), and it is found that the peak stresses are obtained between 6 per cent and 8 per cent of axial strain. All of the samples show similar behavior between 0 per cent and 0.5 per cent axial strain. At failure, the peak deviator stresses recorded are 233, 428, and 731 kPa, for the tests performed at 40, 100, and 200 kPa confining pressures. From the failure envelope (Figure 5.14), the cohesion value is found as 21.02 kPa and the friction angle as 38.16 degrees. These values can also be determined from the p-q graph of the specimen which is shown in Figure 5.15. The equivalent friction angle is calculated as 41.57 degrees. A mixture containing 10 per cent tire crumb by weight is shown in Figure 5.16.

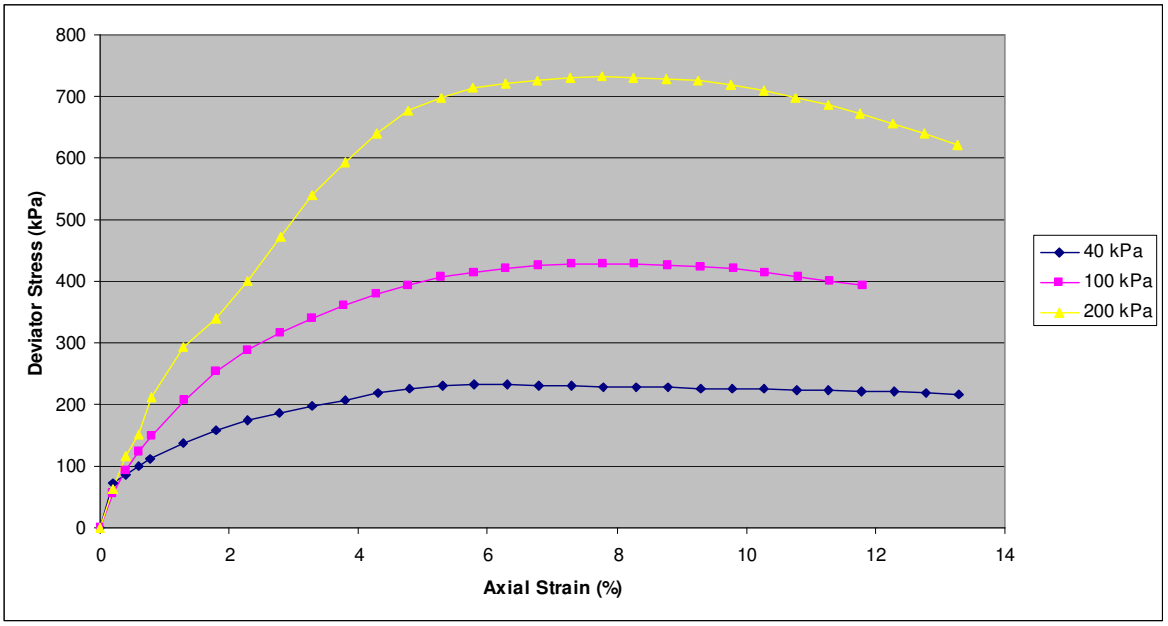

Figure 5.13. Deviator stress-axial strain behavior of specimen containing 10 per cent tire crumb

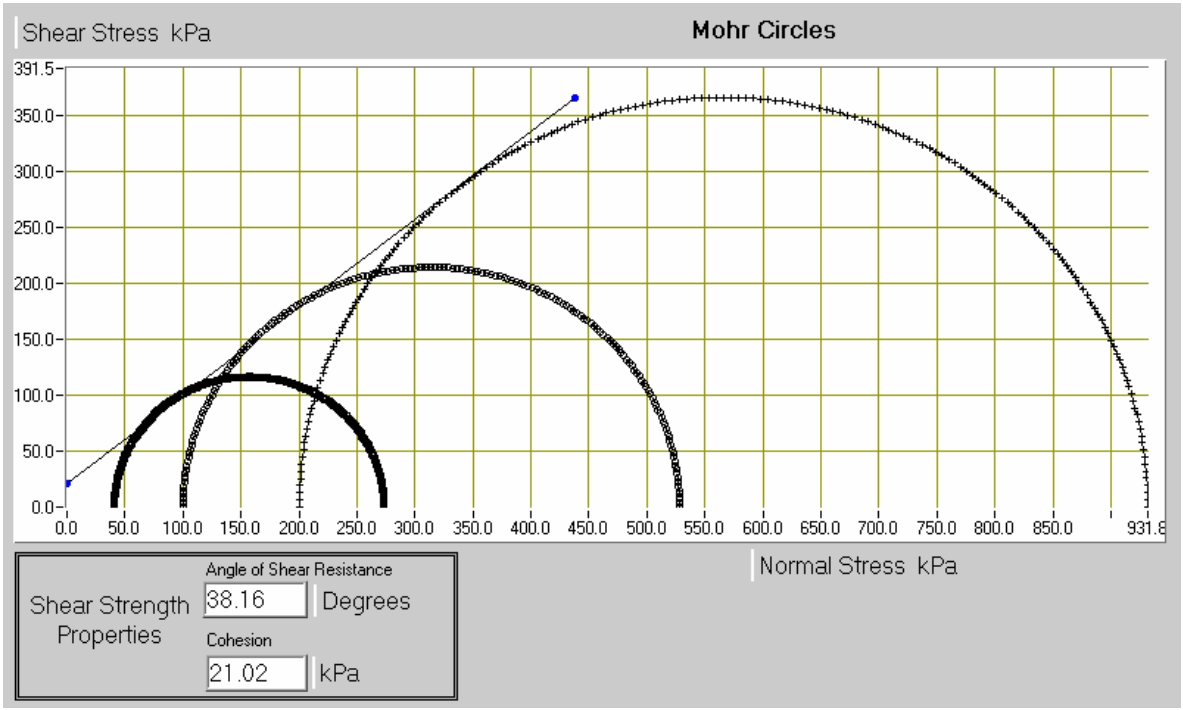

Figure 5.14. Shear strength envelope of specimen containing 10 per cent tire crumb

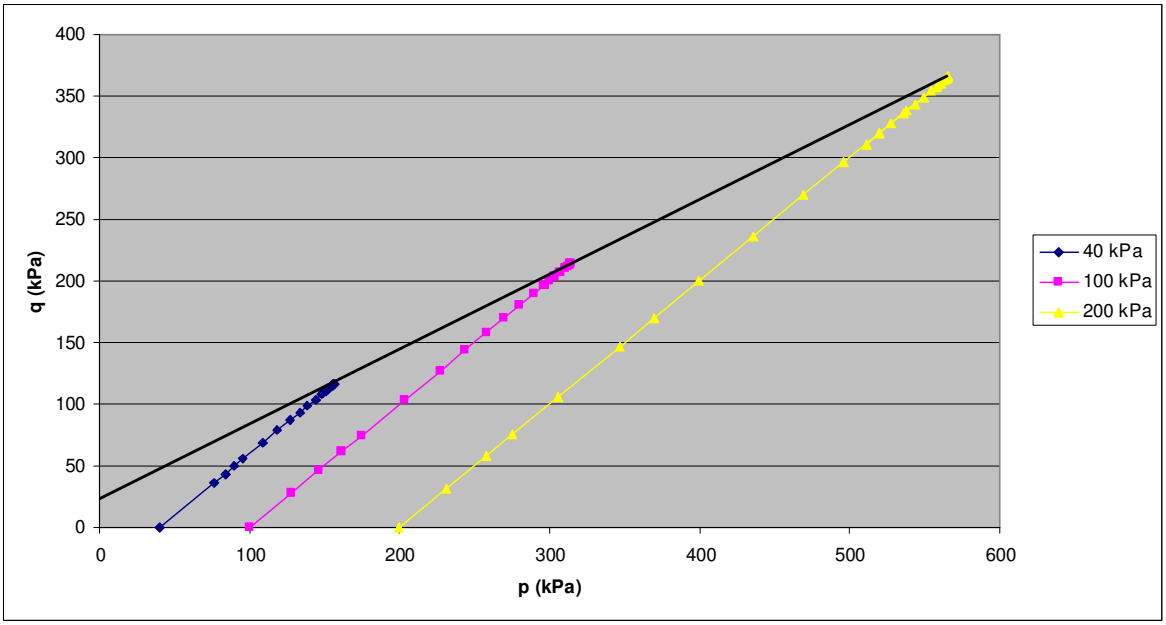

Figure 5.15. p-q graph of specimen containing 10 per cent tire crumb

Figure 5.16. Mixture containing 10 per cent tire crumb by weight

5.2.5. Mixture Containing 20 per cent Tire Crumb

The specimen to be tested is prepared by mixing 20 per cent tire crumb by weight with sand. The unit weight of the sample is found as 13.3 kN/m³. The deviator stress-strain behavior of the specimen is shown in Figure 5.17. The peak deviator stresses are obtained between 10 per cent and 12 per cent axial strain. A steep increase in the deviator stress is observed for the test at a confining pressure of 200 kPa between 0 per cent and 1 per cent axial strain. At failure, the maximum deviator stresses observed are 210, 355, and 632 kPa. According to the shear strength envelope (Figure 5.18), the cohesion value is determined as 24.65 kPa and the friction angle as 35.12 degrees. The shear strength parameters can also be obtained from the p-q graph shown in Figure 5.19. Using regression analysis, the equivalent friction angle is calculated as 39.57 degrees. A mixture containing 20 per cent tire crumb by weight is shown in Figure 5.20.

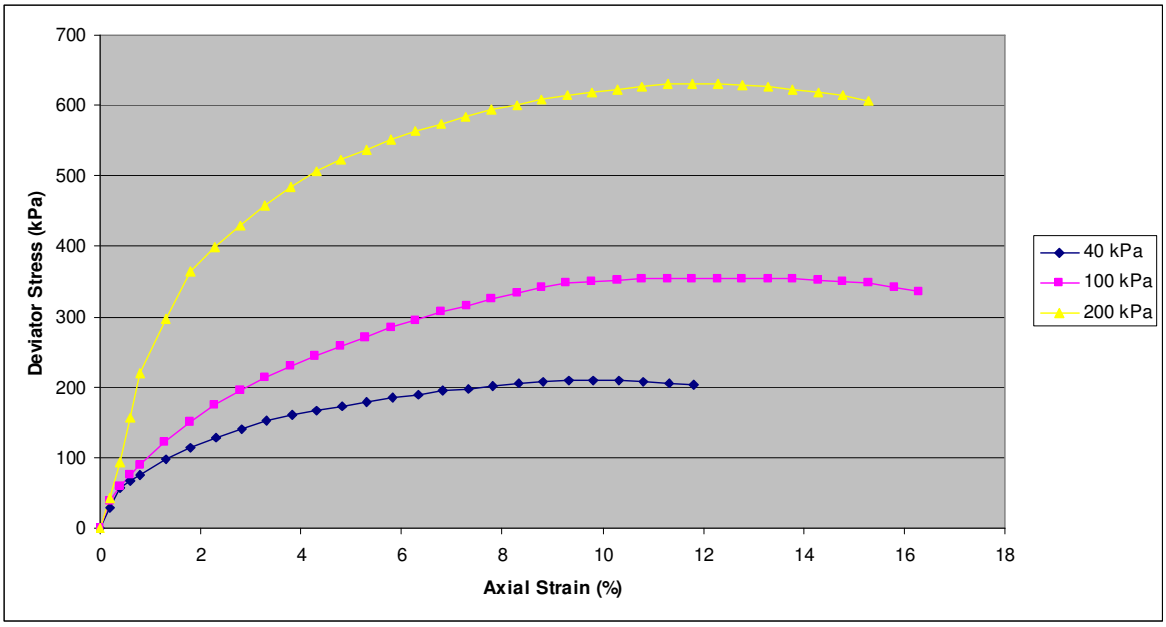

Figure 5.17. Deviator stress-axial strain behavior of specimen containing 20 per cent tire crumb

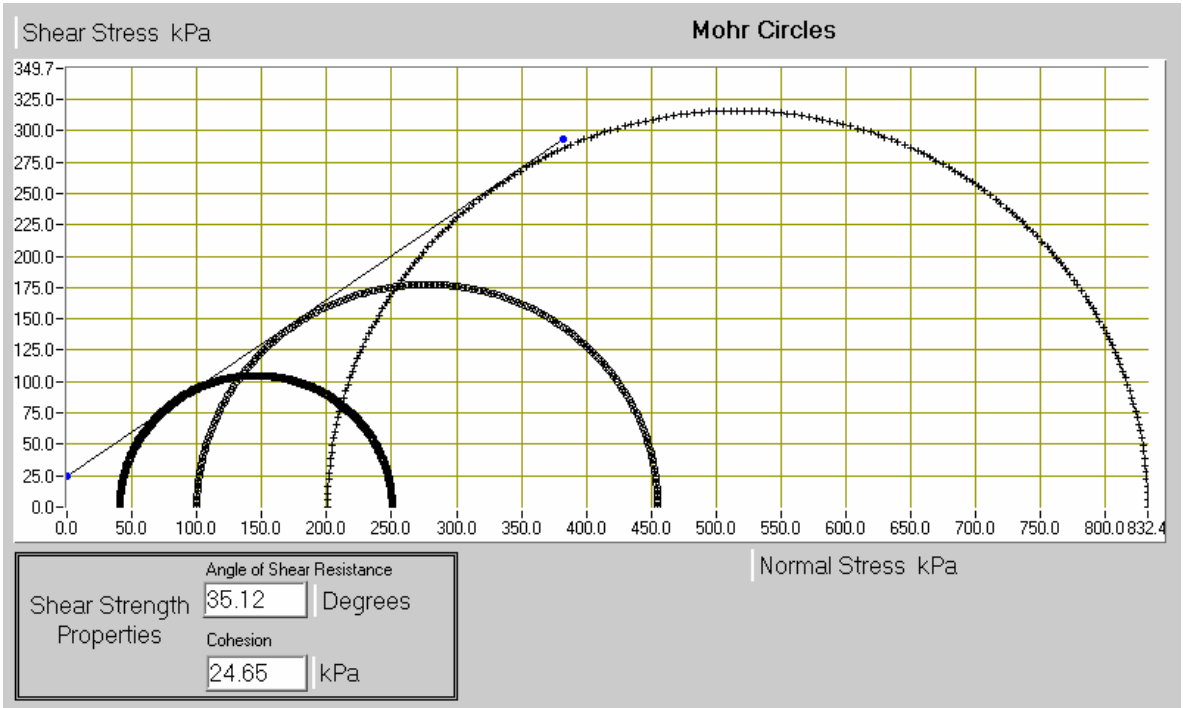

Figure 5.18. Shear strength envelope of specimen containing 20 per cent tire crumb

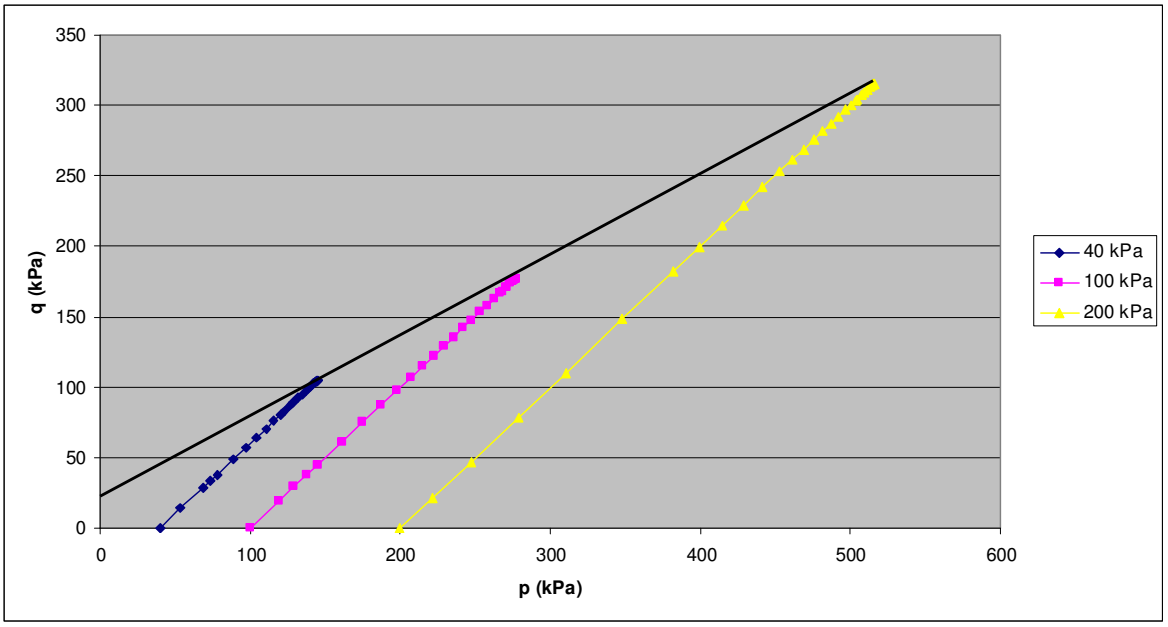

Figure 5.19. p-q graph of specimen containing 20 per cent tire crumb

Figure 5.20. Mixture containing 20 per cent tire crumb by weight

5.2.6. Mixture Containing 30 per cent Tire Crumb

30 per cent tire crumb by total weight is mixed with sand. The unit weight of the specimen is 12.5 kN/m³. Figure 5.21 shows the deviatoric stress-strain behavior of the specimen. Between 0 per cent and 2 per cent axial strain, samples tested under 40 and 100 kPa confining pressures show similar stress behavior, and the sample tested at a confining pressure of 200 kPa shows a sharp increase in deviator stress. At failure, the maximum deviator stresses observed are 134, 262, and 472 kPa, and the corresponding axial strains are 15 per cent, 13.32 per cent, and 10.74 per cent. According to the Mohr-failure envelope (Figure 5.22) the cohesion value is found as 14.21 kPa and the angle of internal friction as 31.02 degrees. Figure 5.23 shows the p-q graph of the specimen. Same cohesion and friction angle values are also obtained from the p-q graph. In addition to these, the equivalent angle of internal friction is calculated as 34.19 degrees. A mixture containing 30 per cent tire crumb by weight is shown in Figure 5.24.

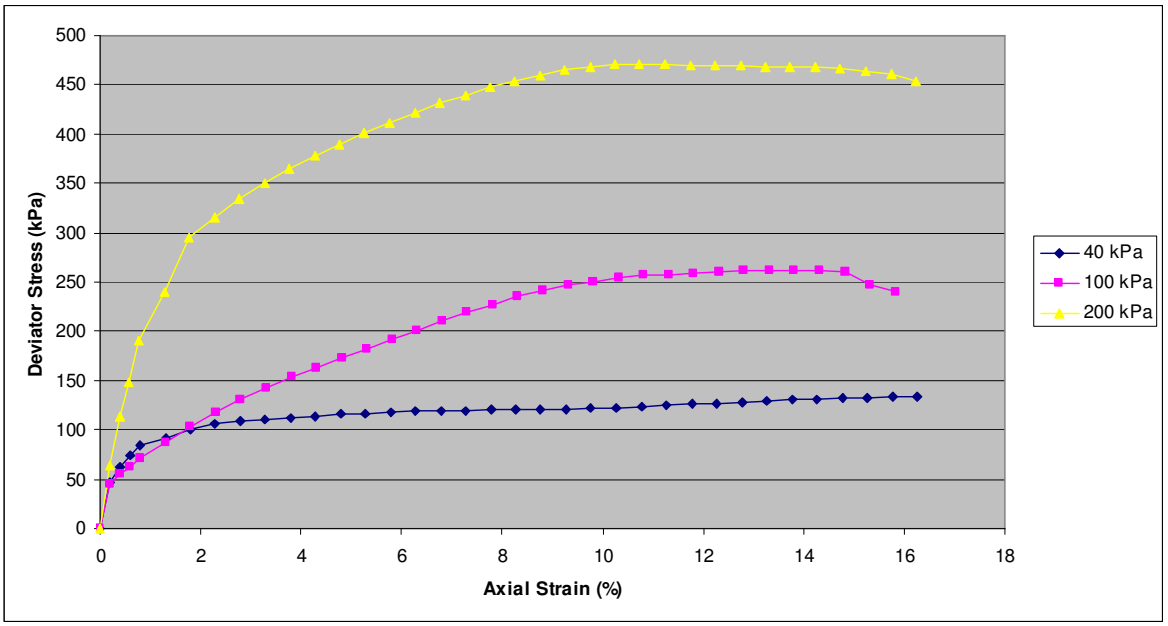

Figure 5.21. Deviator stress-axial strain behavior of specimen containing 30 per cent tire crumb

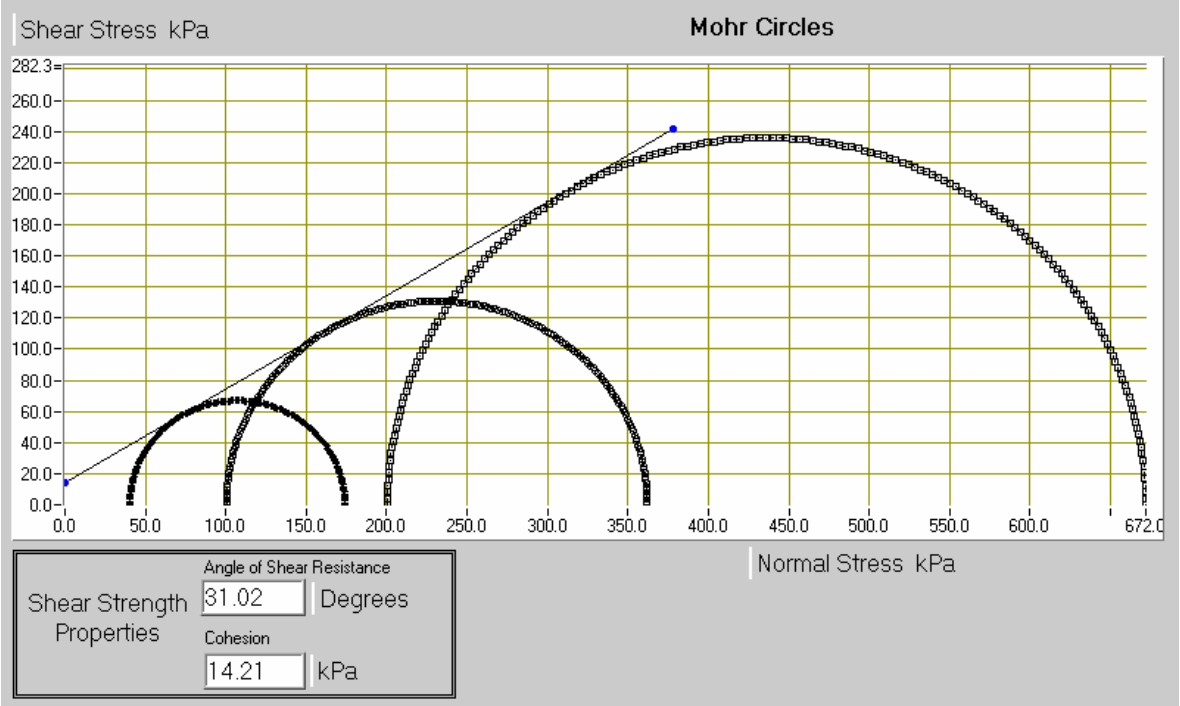

Figure 5.22. Shear strength envelope of specimen containing 30 per cent tire crumb

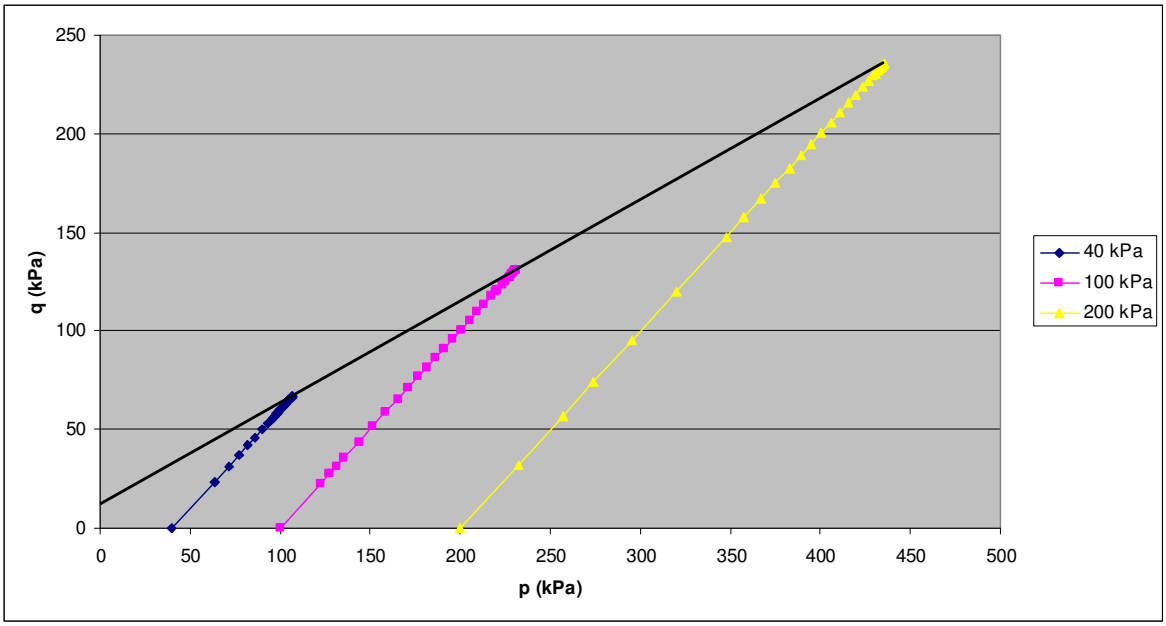

Figure 5.23. p-q graph of specimen containing 30 per cent tire crumb

Figure 5.24. Mixture containing 30 per cent tire crumb by weight

5.2.7. Mixture Containing 40 per cent Tire Crumb

The specimen is prepared by mixing 40 per cent tire crumb by weight with sand. The unit weight of the mixture is 11.2 kN/m. The deviator stress-strain behavior of the specimen is shown in Figure 5.25. With this amount of tire addition, the specimen acts more like tire crumb, and the deviator stress continues to increase with increasing axial strain. Between 0 per cent and 1 per cent axial strain, the specimens tested under 40 and 100 kPa confining pressures show a similar stress-strain behavior. The corresponding deviator stresses at 15 per cent axial strain are 108, 210, and 398 kPa. Using the Mohr circle diagram (Figure 5.26), the cohesion value is determined as 9.28 kPa, and the internal friction angle as 28.69 degrees. Figure 5.27 shows the p-q graph of the specimen. The p-q graph leads to the same shear strength parameters with the Mohr circle diagram. The equivalent angle of internal friction is calculated as 30.96 degrees. A mixture containing 40 per cent tire crumb by weight is shown in Figure 5.28.

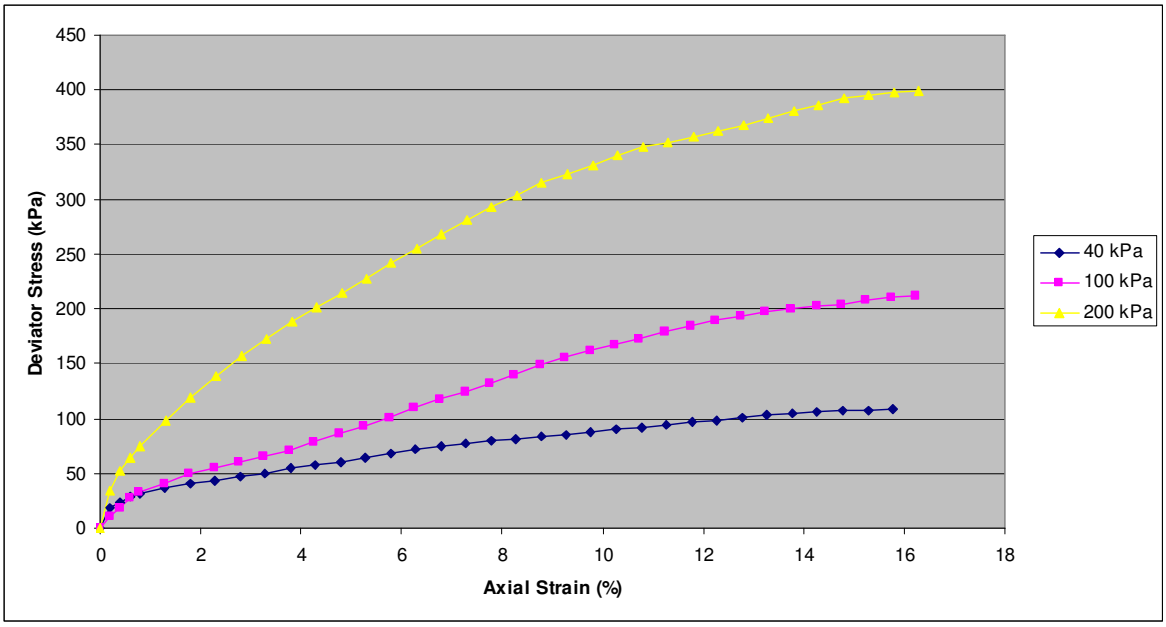

Figure 5.25. Deviator stress-axial strain behavior of specimen containing 40 per cent tire crumb

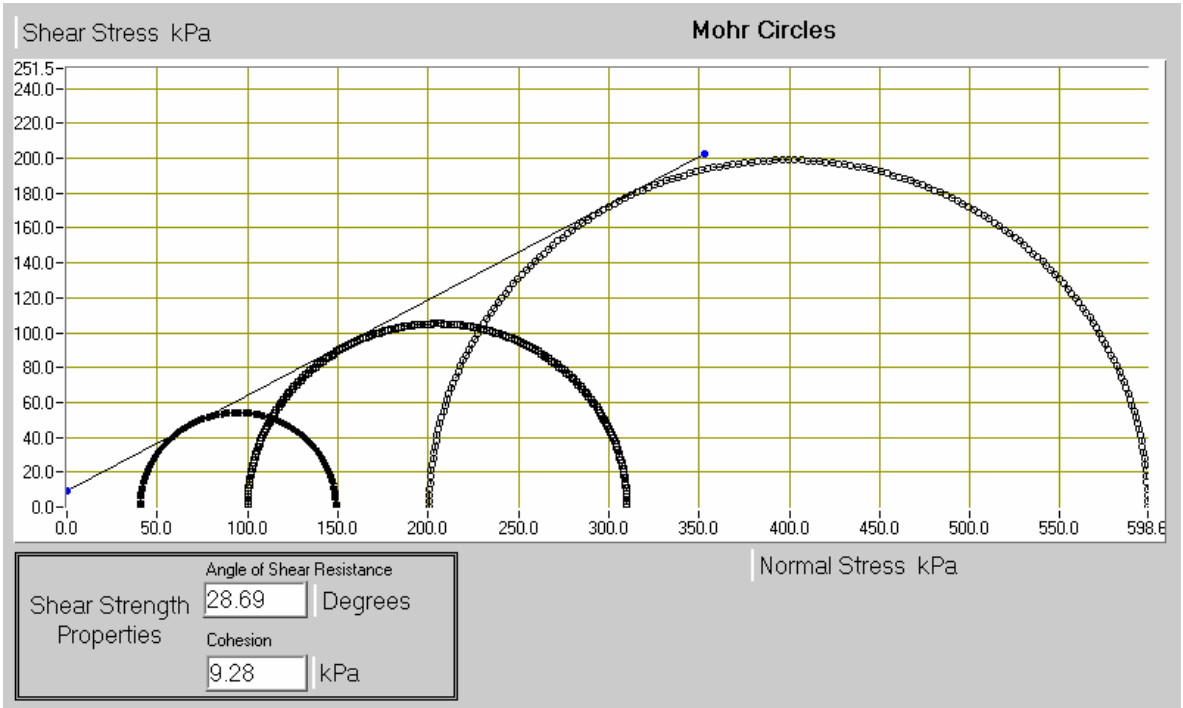

Figure 5.26. Shear strength envelope of specimen containing 40 per cent tire crumb

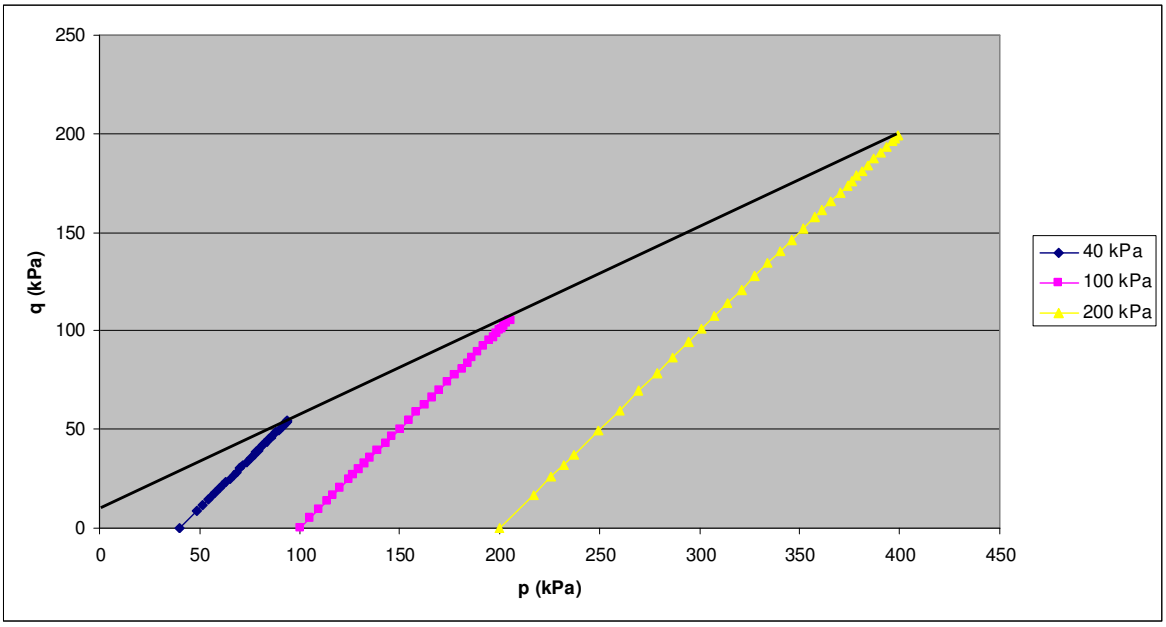

Figure 5.27. p-q graph of specimen containing 40 per cent tire crumb

Figure 5.28. Mixture containing 40 per cent tire crumb by weight

5.2.8. Mixture Containing 100 per cent Tire Buffings

Tire buffings alone is tested. The unit weight of the sample is 4.6 kN/m³. Similar like tire crumb, in the experiment done with tire buffings the deviator stress-strain diagram (Figure 5.29) does not show any peak values. The deviator stress continues to increase as the axial strain increases. The deviator stress values at 15 per cent axial strain are 52, 89, and 156 kPa. According to the failure envelope (Figure 5.30), the cohesion value is determined as 9.54 kPa and the angle of internal friction is 14.35 degrees. The same cohesion and friction values are also found from the p-q graph of the specimen (Figure 5.31). Using regression analysis, the equivalent internal friction angle is calculated as 17.74 degrees.

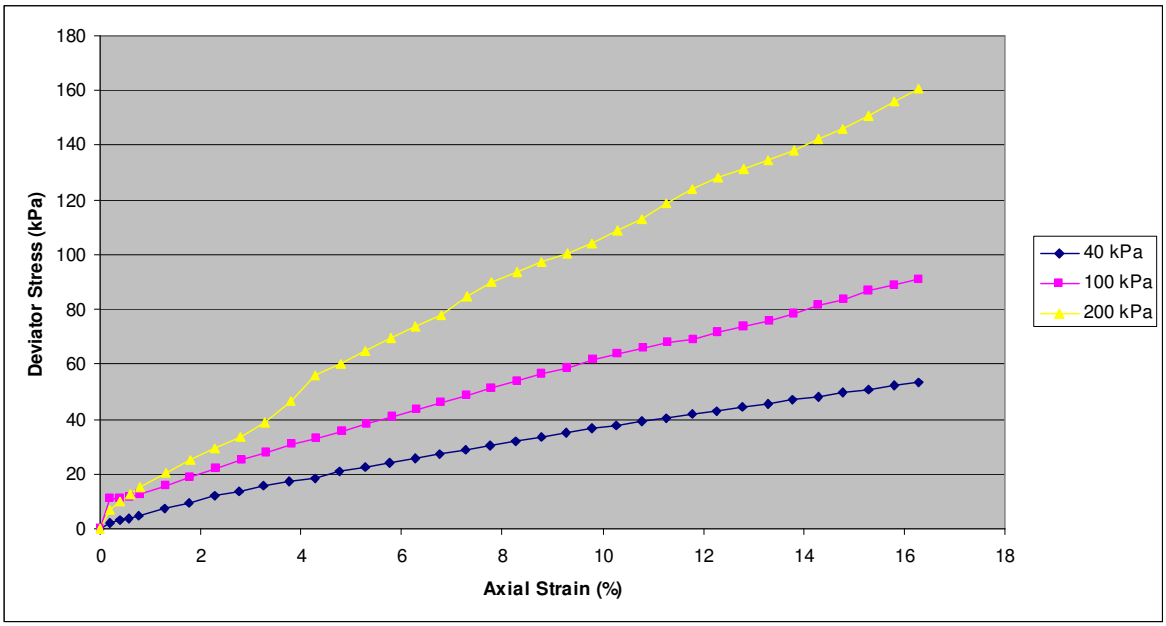

Figure 5.29. Deviator stress-axial strain behavior of specimen containing100 per cent tire buffings

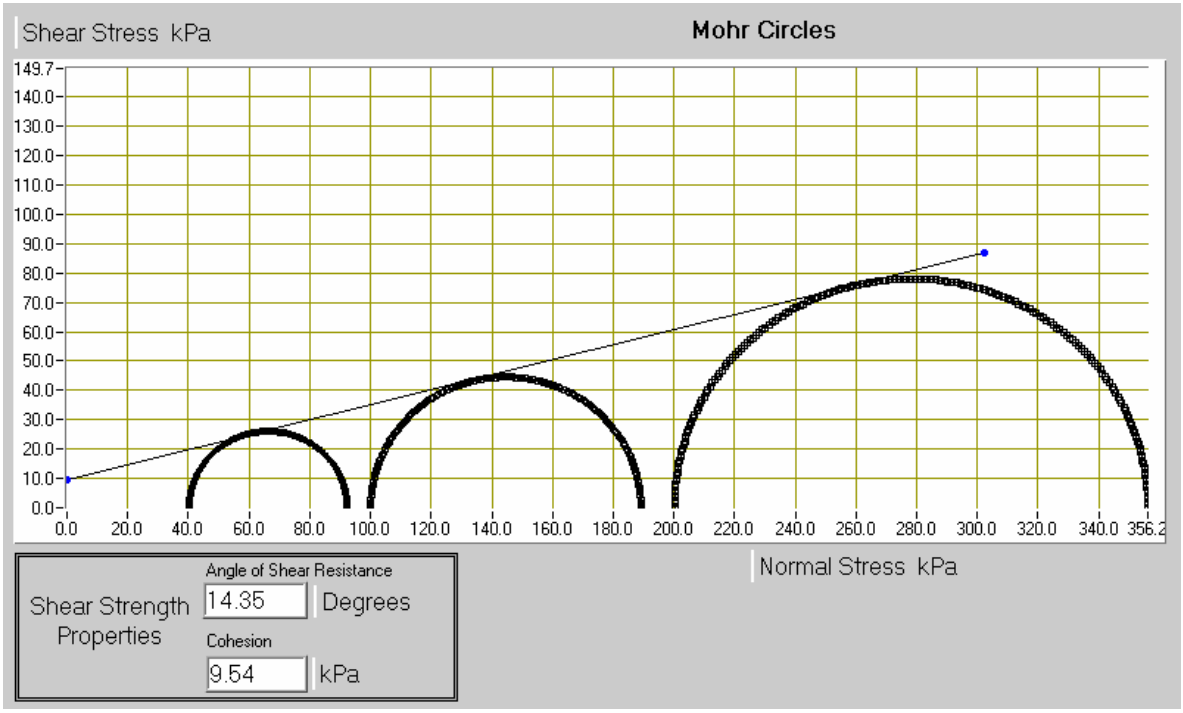

Figure 5.30. Shear strength envelope of specimen containing 100 per cent tire buffings

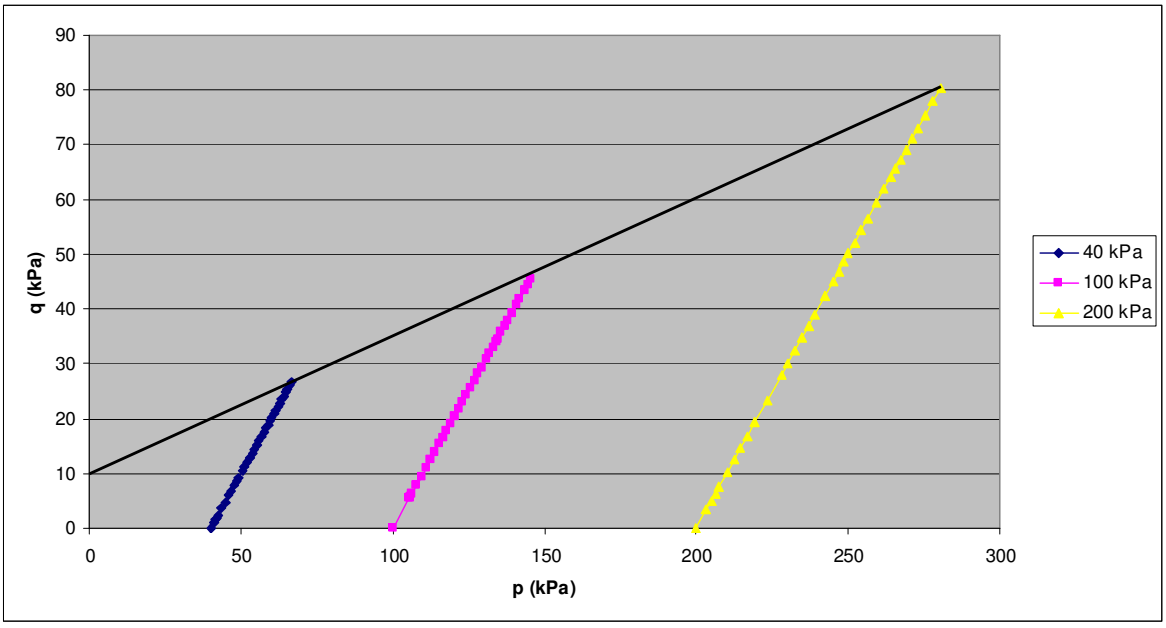

Figure 5.31. p-q graph of specimen containing 100 per cent tire buffings

5.2.9. Mixture Containing 5 per cent Tire Buffings

The specimen is composed of 5 per cent tire buffings by weight and sand. The unit weight of the specimen is 14.7 kN/m³. The deviator stress-strain graph (Figure 5.32) shows that the peak values of deviator stress are obtained at different axial strains for different confining pressures. At failure, the deviator stresses observed are 218, 454, and 813 kPa, corresponding to axial strains of 9.26 per cent, 8.78 per cent, and 10.81 per cent. The corresponding Mohr circle diagram is drawn (Figure 5.33), and the cohesion value is obtained as 11.43 kPa, while the angle of internal friction is found as 41.28 degrees. The same shear strength parameters can also be obtained using the p-q graph shown in Figure 5.34. The equivalent friction angle is calculated as 43.18 degrees. A mixture containing 5 per cent tire buffings by weight is shown in Figure 5.35.

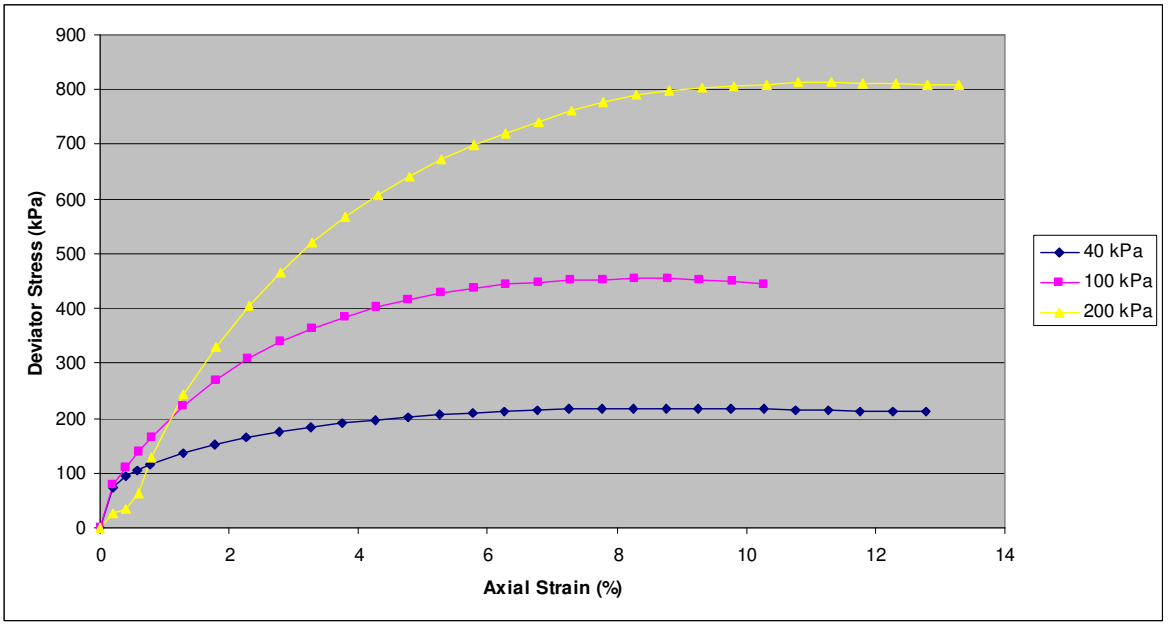

Figure 5.32. Deviator stress-axial strain behavior of specimen containing 5 per cent tire buffings

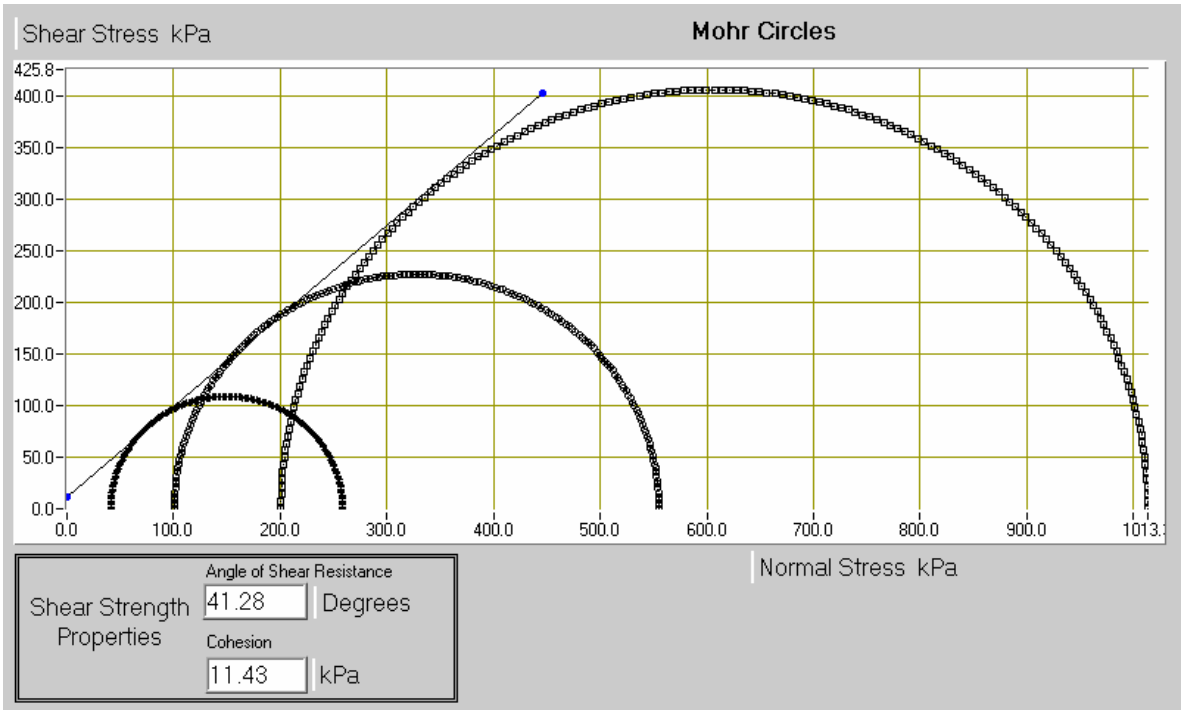

Figure 5.33. Shear strength envelope of specimen containing 5 per cent tire buffings

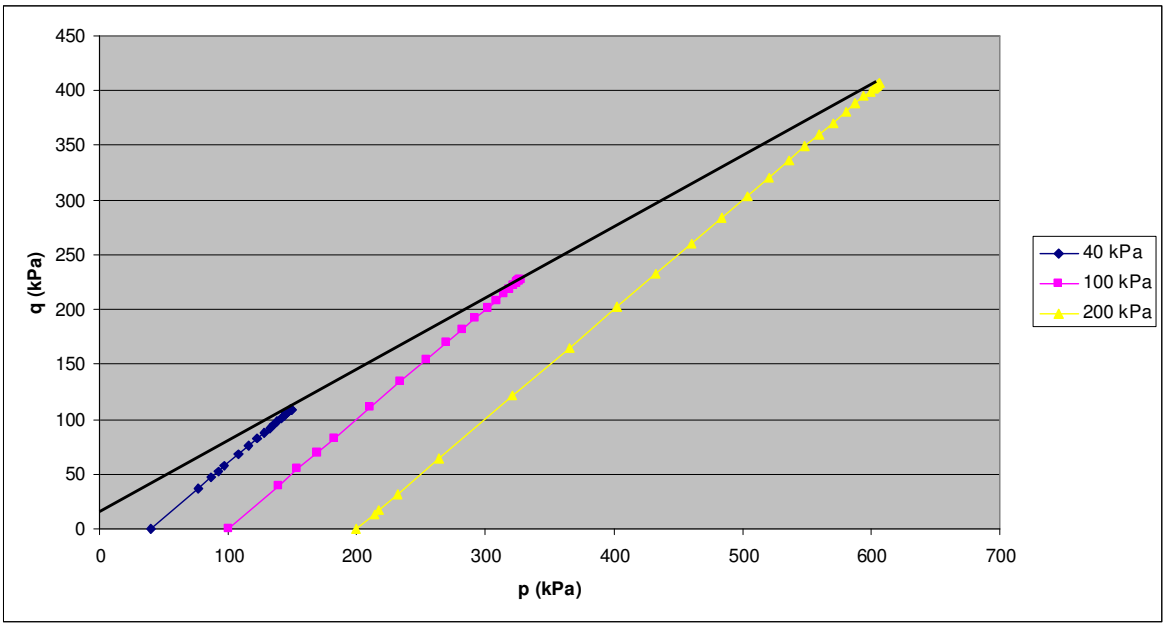

Figure 5.34. p-q graph of specimen containing 5 per cent tire buffings

Figure 5.35. Mixture containing 5 per cent tire buffings by weight

5.2.10. Mixture Containing 10 per cent Tire Buffings

10 per cent tire buffings by weight is added to sand. The unit weight of the mixture is 13.7 kN/m³. The deviatoric stress-strain diagram is shown in Figure 5.36. Peak stresses are found at different axial strains for tests performed under different confining pressures. At 0 per cent axial strain the sample tested under 200 kPa confining pressure shows a sharp increase in the deviator stress. At failure, the maximum deviator stresses observed are 181, 336, and 616 kPa, corresponding to 10.28 per cent, 8.77 per cent, and 11.31 per cent axial strains. The shear strength envelope of the specimen is shown in Figure 5.37. The cohesion value is determined as 14.98 kPa and the internal friction angle as 35.93 degrees. The p-q graph is shown in Figure 5.38. The p-q graph gives the same shear strength parameters with the Mohr failure diagram. The equivalent friction angle is calculated as 38.78 degrees. A mixture containing 10 per cent tire buffings by weight is shown in Figure 5.39.

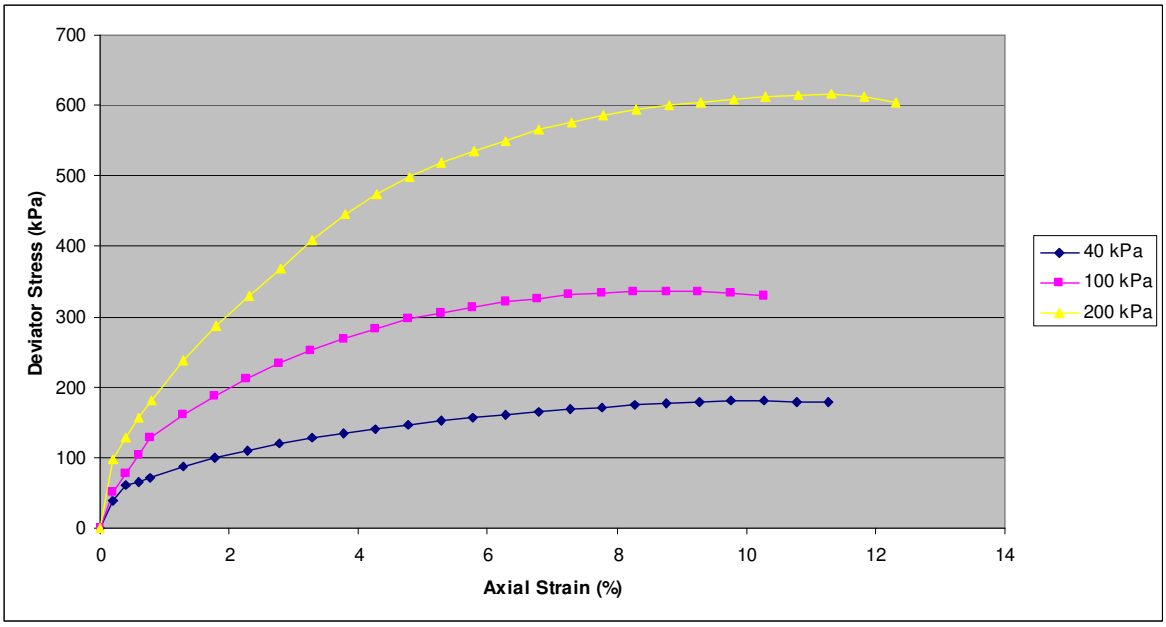

Figure 5.36. Deviator stress-axial strain behavior of specimen containing 10 per cent tire buffings

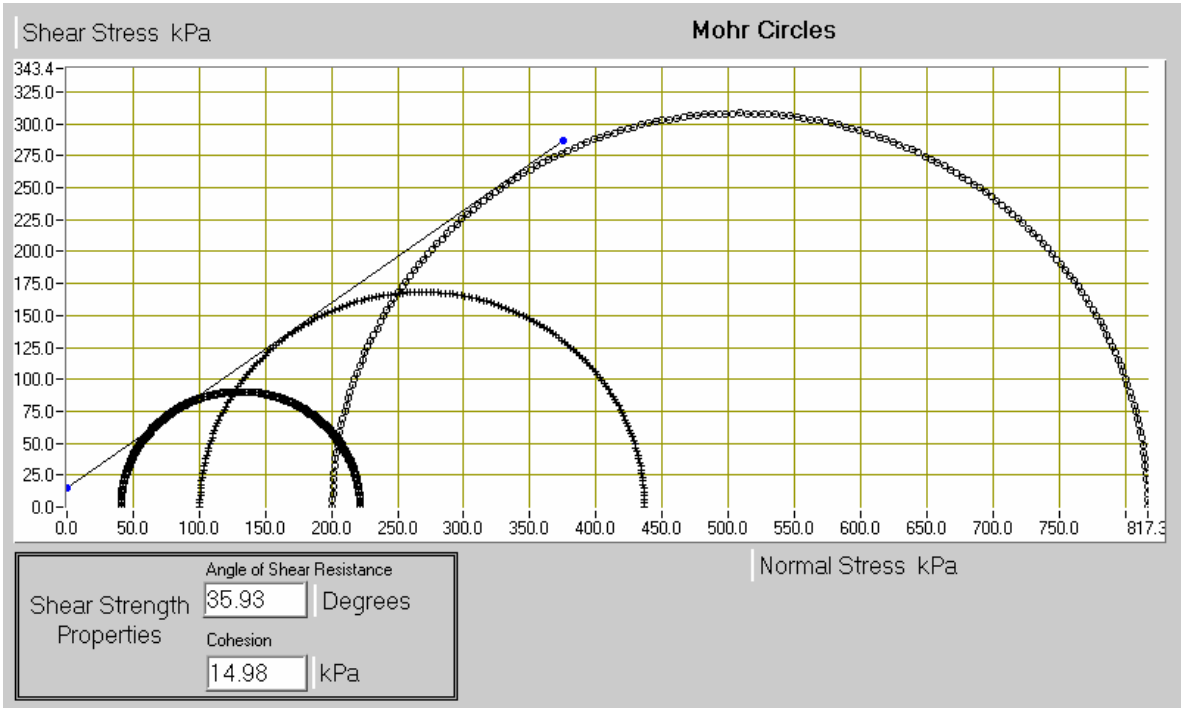

Figure 5.37. Shear strength envelope of specimen containing 10 per cent tire buffings

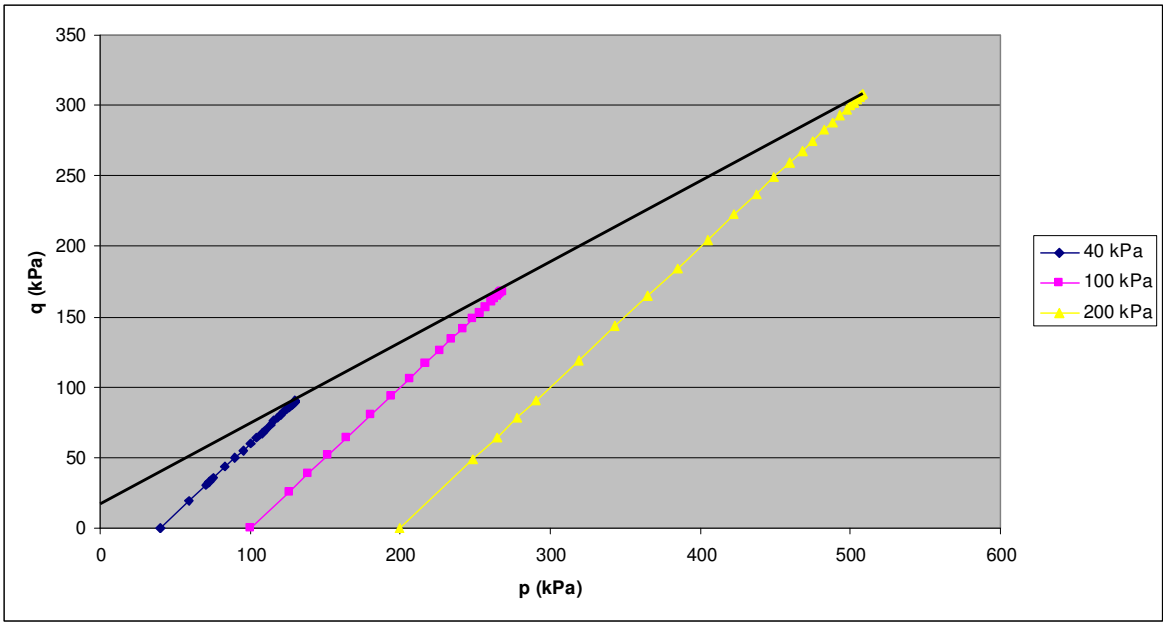

Figure 5.38. p-q graph of specimen containing 10 per cent tire buffings

Figure 5.39. Mixture containing 10 per cent tire buffings by weight

5.2.11. Mixture Containing 20 per cent Tire Buffings

The specimen is composed of 20 per cent tire buffings by weight and sand. The unit weight of the sample is calculated as 12.1 kN/m³. The deviatoric stress-strain behavior of the specimen is shown in Figure 5.40. The peak deviator stresses are found between the axial strain values of 12 per cent and 15 per cent. The maximum deviator stresses observed at failure are 140, 275, and 463 kPa, for tests under 40, 100, and 200 kPa confining pressures. From the failure envelope (Figure 5.41) the cohesion is found as 14.04 degrees, and the friction angle as 30.99 degrees. Using the data obtained from the experiment the equivalent friction angle is calculated as 34.07 degrees. The p-q graph of the specimen is shown in Figure 5.42 which leads to the same shear strength values with the Mohr failure envelope. A mixture containing 20 per cent tire buffings by weight is shown in Figure 5.43.

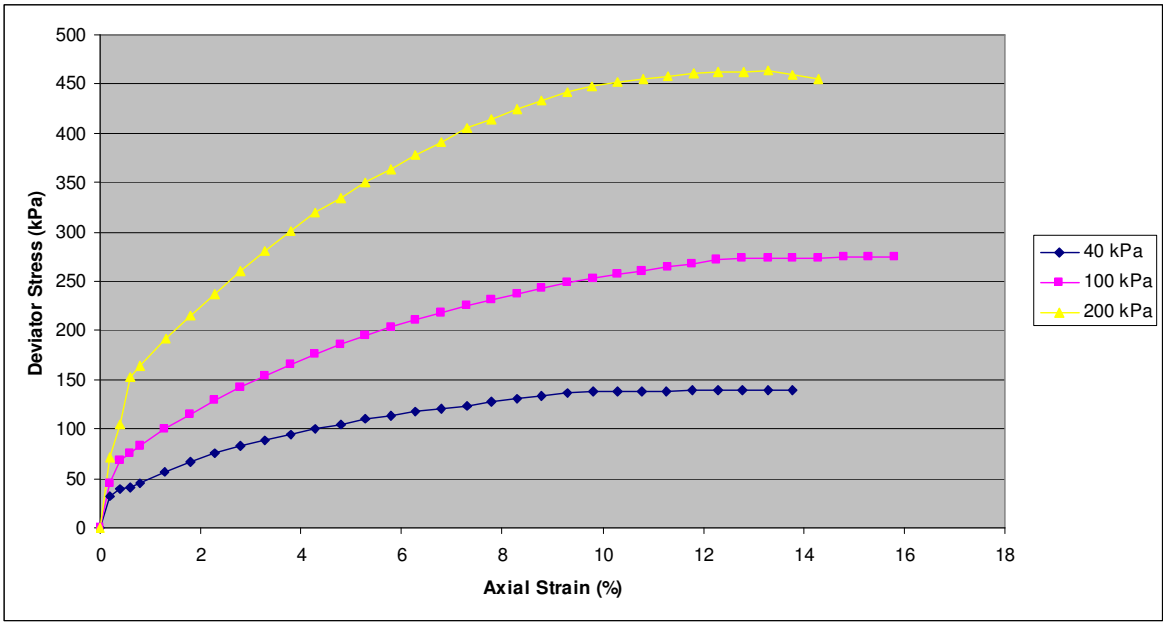

Figure 5.40. Deviator stress-axial strain behavior of specimen containing 20 per cent tire buffings

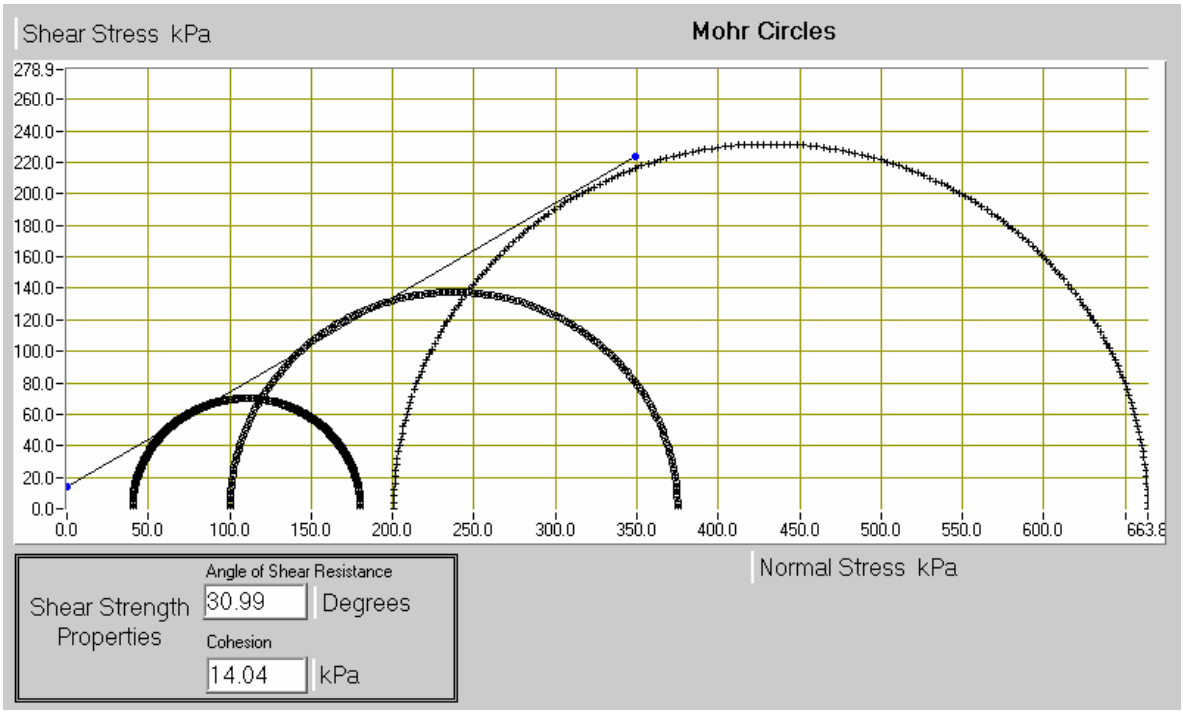

Figure 5.41. Shear strength envelope of specimen containing 20 per cent tire buffings

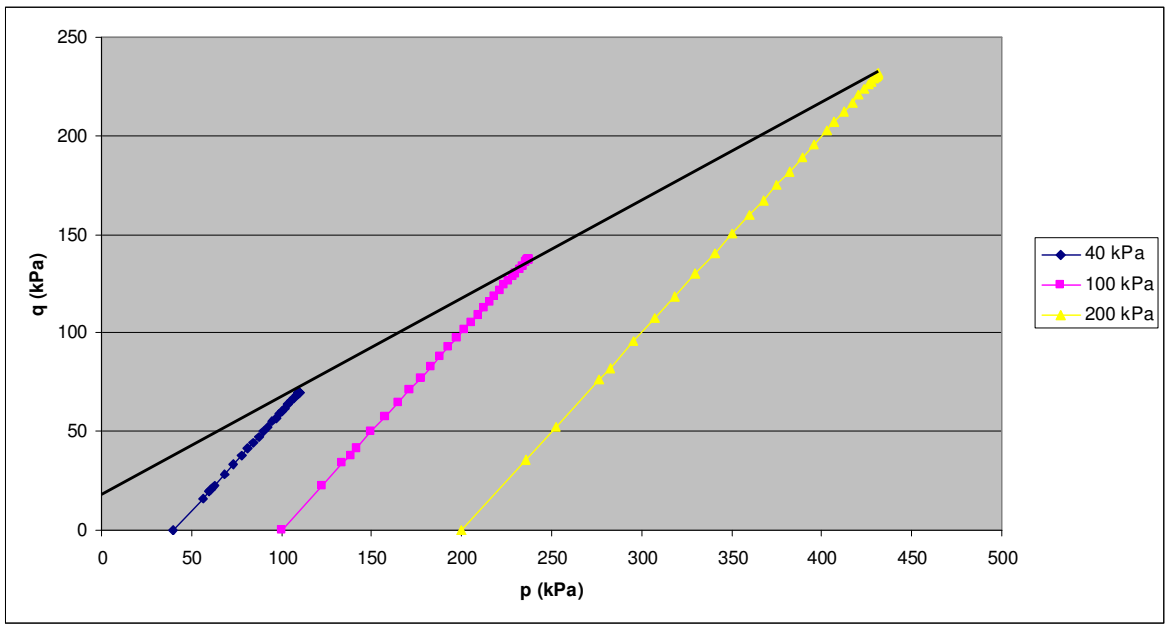

Figure 5.42. p-q graph of specimen containing 20 per cent tire buffings

Figure 5.43. Mixture containing 20 per cent tire buffings by weight

5.2.12. Mixture Containing 30 per cent Tire Buffings

The mixture to be tested is prepared by adding 30 per cent tire buffings by weight to sand. The unit weight of the specimen is 10.3 kN/m³. The deviator stress-strain graph is shown in Figure 5.44. Maximum deviator stresses correspond to 15 per cent axial strain. The maximum stress values recorded are 116, 218, and 368 kPa. According to the Mohr-failure envelope (Figure 5.45) the cohesion is 13.63 kPa, and the angle of internal friction is 26.89 degrees. These values can also be obtained from the p-q graph (Figure 5.46). The corresponding equivalent friction angle is calculated as 30.33 degrees. A mixture containing 30 per cent tire buffings by weight is shown in Figure 5.47.

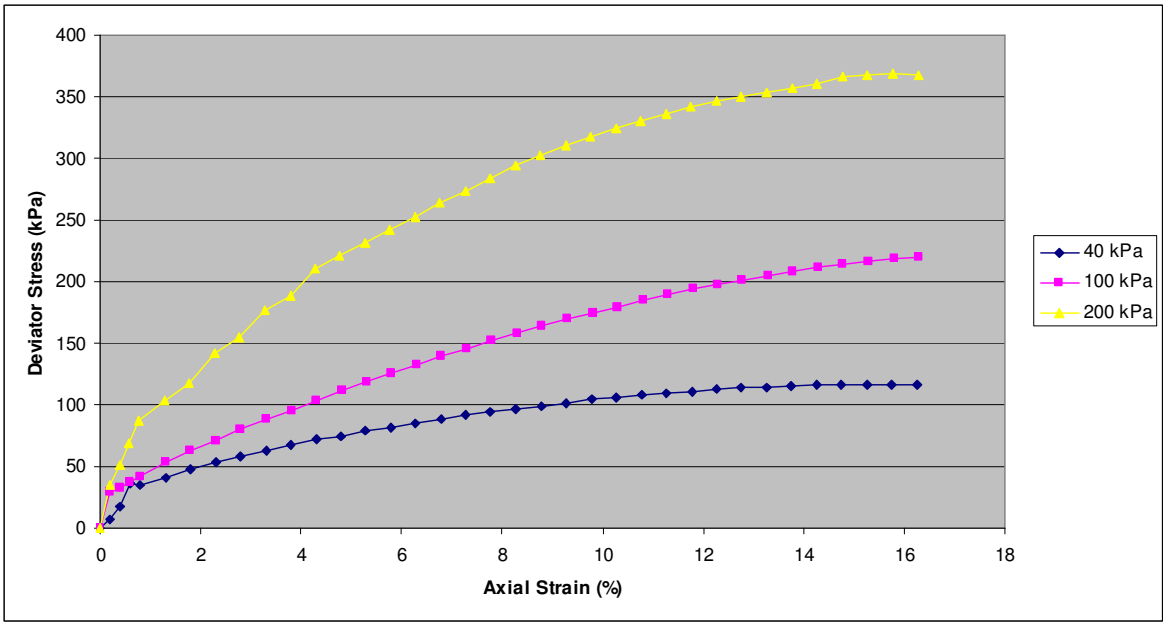

Figure 5.44. Deviator stress-axial strain behavior of specimen containing 30 per cent tire buffings

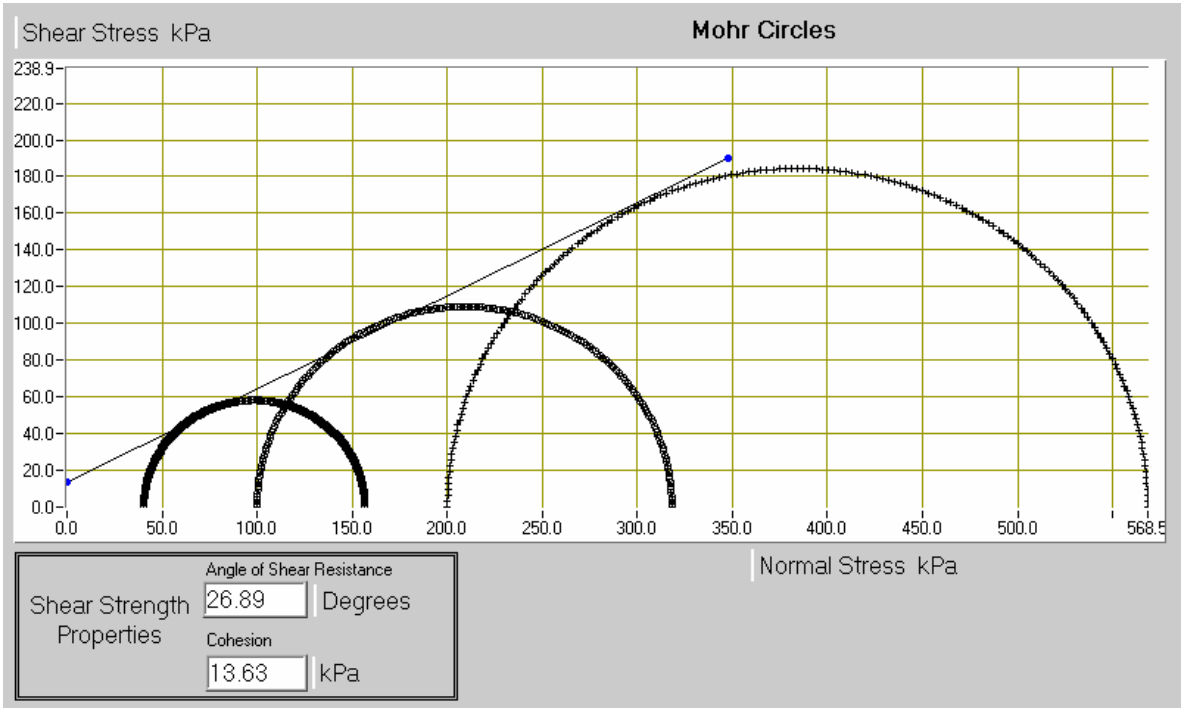

Figure 5.45. Shear strength envelope of specimen containing 30 per cent tire buffings

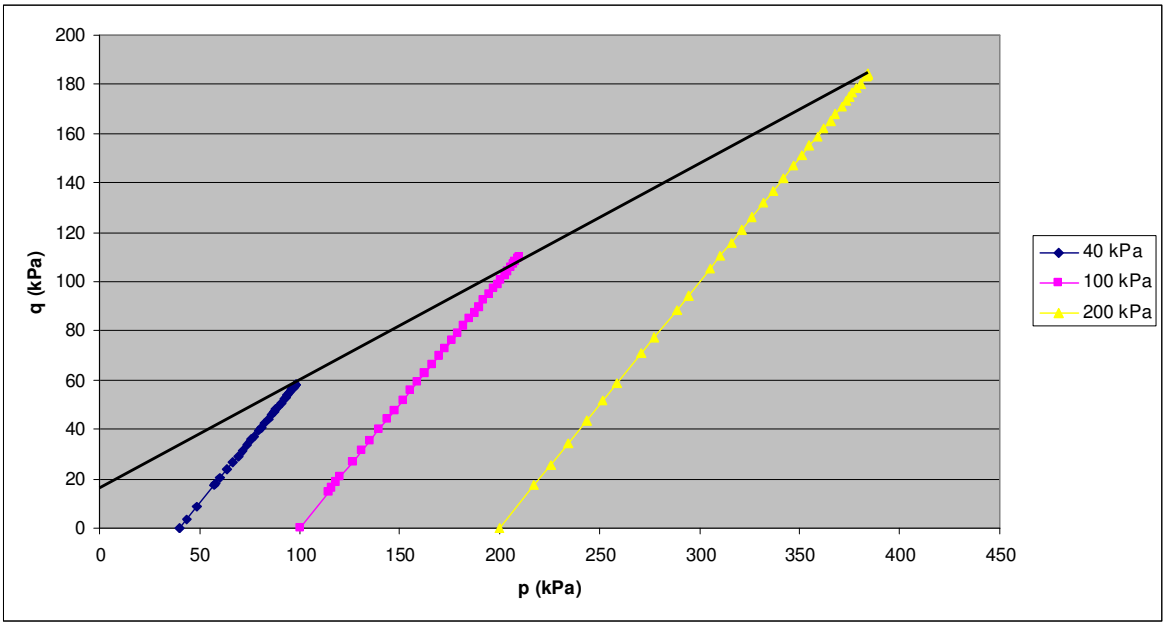

Figure 5.46. p-q graph of specimen containing 30 per cent tire buffings

Figure 5.47. Mixture containing 30 per cent tire buffings by weight

5.2.13. Mixture Containing 40 per cent Tire Buffings

In order to prepare the specimen to be tested, 40 per cent tire buffings by weight is mixed with sand. The unit weight of the sample is found as 9.1 kN/m³. The deviator stress-axial strain diagram is shown in Figure 5.48. It is determined that the deviator stress does not show any peaks, and continues to increase as the axial strain increases. The samples under 100, and 200 kPa confining pressures show similar stress behaviour up to 1.5 per cent axial strain. The corresponding stress values at 15 per cent axial strain are 99, 174, and 328 kPa. From the failure envelope (Figure 5.49), cohesion is found to be 11.18 kPa, and the angle of internal friction is found to be 24.70 degrees. Figure 5.50 shows the p-q graph of the specimen. The same cohesion and friction angle values are also obtained from the p-q graph. Using regression analysis the equivalent angle of internal friction is calculated as 27.72 degrees. A mixture containing 40 per cent tire buffings by weight is shown in Figure 5.51.

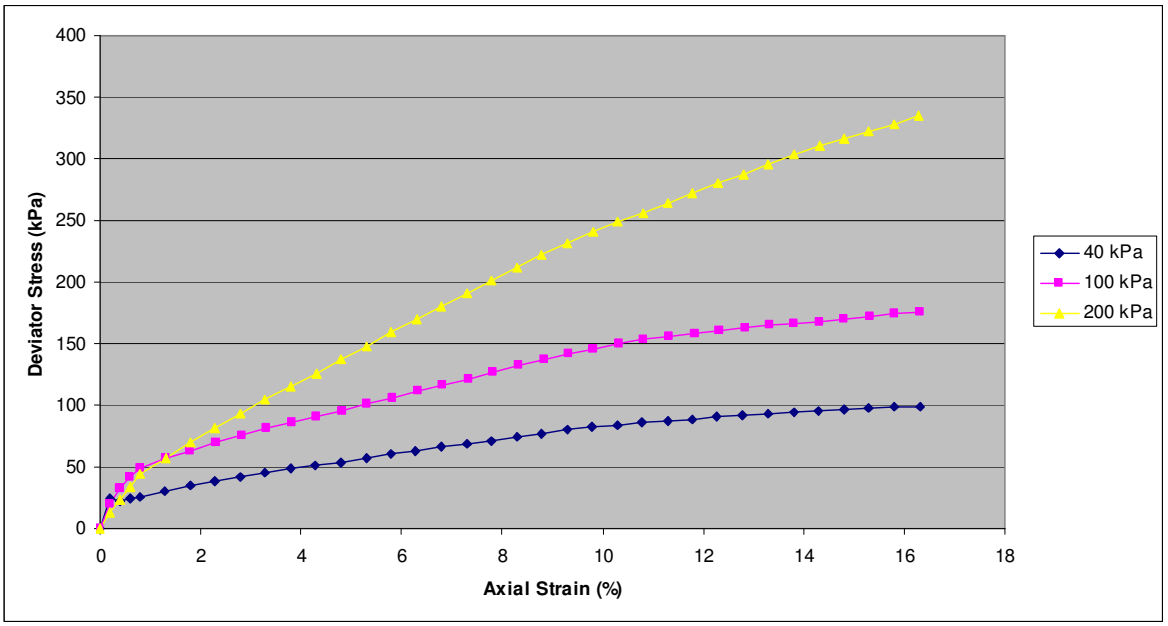

Figure 5.48. Deviator stress-axial strain behavior of specimen containing 40 per cent tire buffings

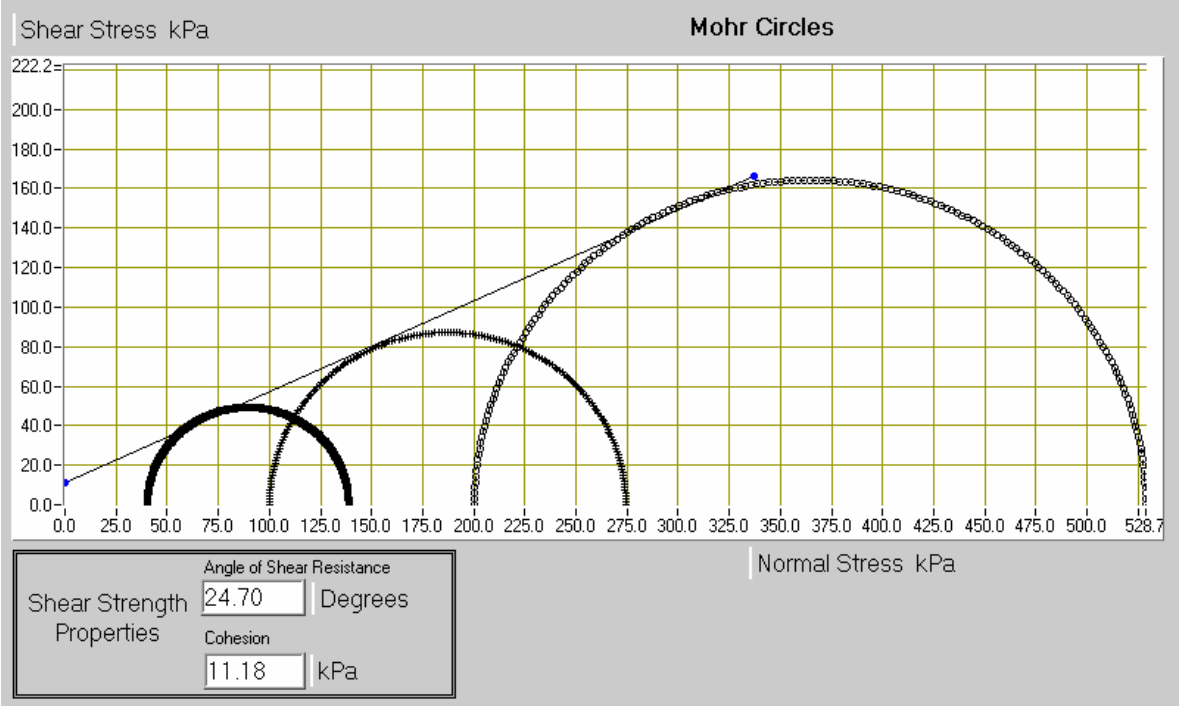

Figure 5.49. Shear strength envelope of specimen containing 40 per cent tire buffings

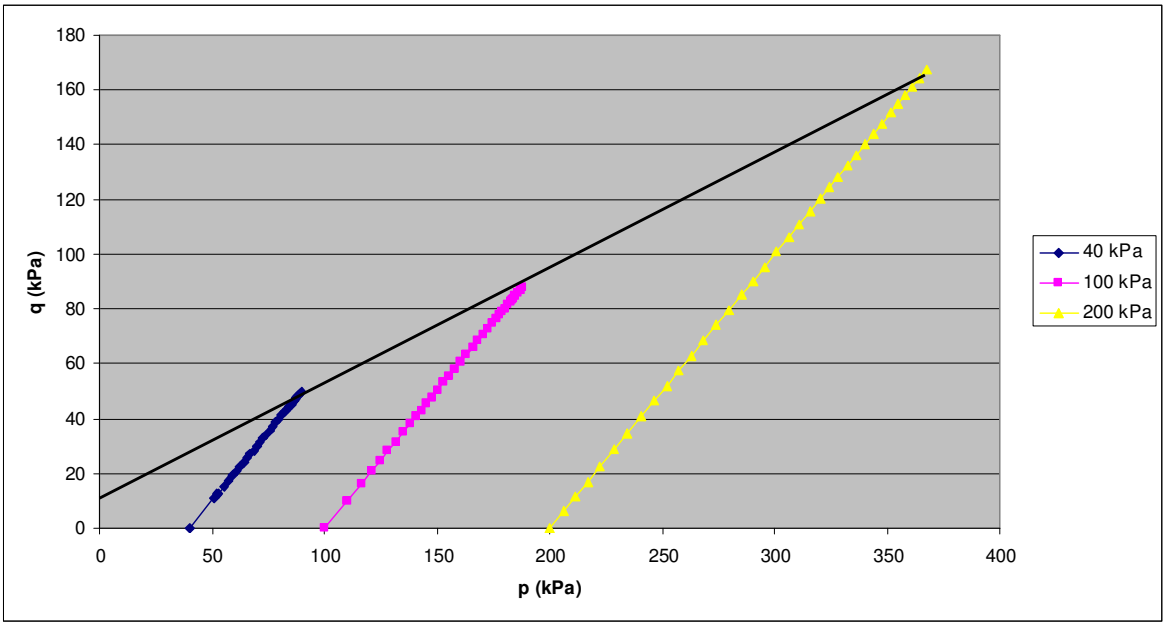

Figure 5.50. p-q graph of specimen containing 40 per cent tire buffings

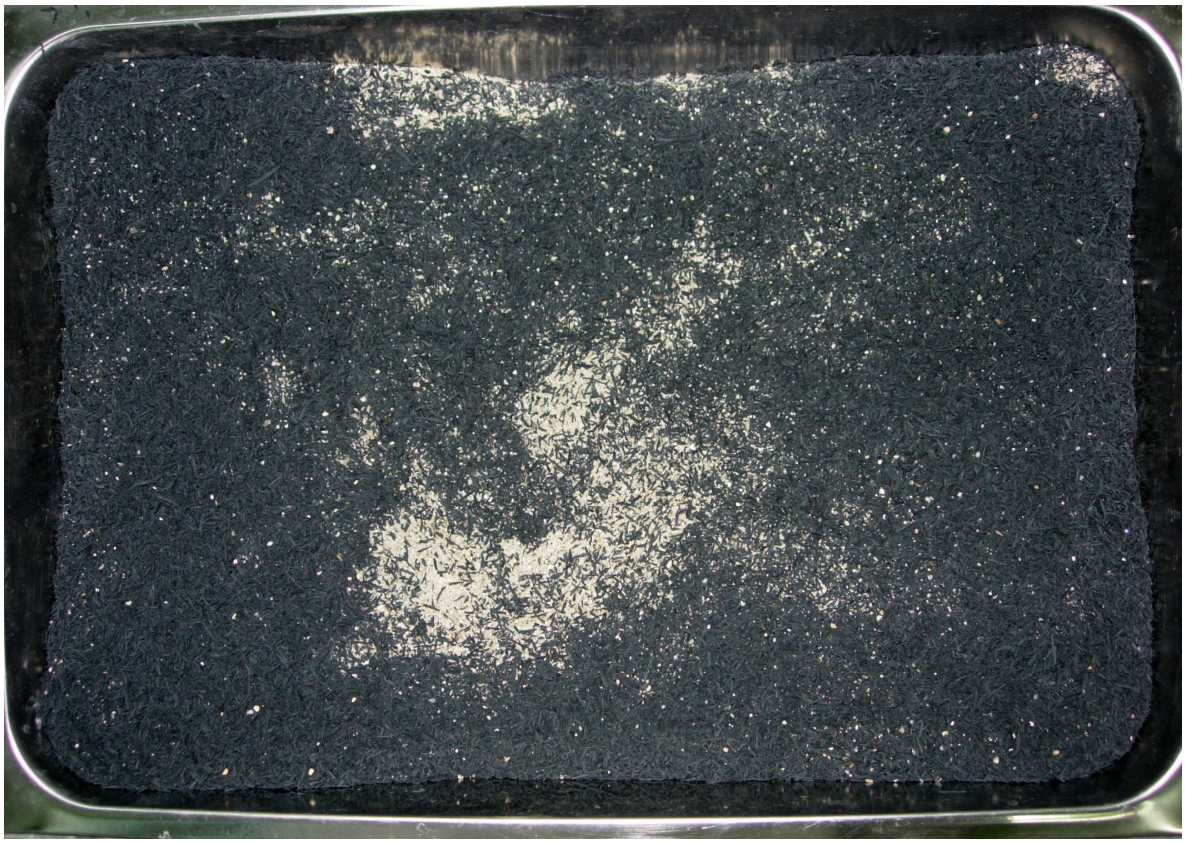

Figure 5.51. Mixture containing 40 per cent tire buffings by weight

5.2.14. Analysis of Quick Triaxial Compression Test Results

A total of 13 sets of quick triaxial compression tests are conducted on dry specimens composed of sand, tire crumb, tire buffings, and mixtures of sand-tire waste with varying tire content. Each test is repeated at three different confining stresses of 40, 100, and 200 kPa. The effects of tire percentage, tire aspect ratio, and tire shape on the shear strength parameters of the specimens are investigated. Tire buffings is a fiber shaped material with an aspect ratio ranging between 3.5 and 4, and tire crumb is a granular material with an aspect ratio ranging between 1 and 1.5. Tire waste-sand specimens are prepared by adding 5, 10, 20, 30, and 40 per cent of tire waste by weight. The stress-strain behaviors and the shear strength parameters of the specimens are investigated.

The test results indicate that, pure sand specimens show well defined peak shear stress values of 221 kPa, 462 kPa, 810 kPa around 5 per cent axial strain (Figure 5.3). On the other hand, no peak shear stress values are observed for specimens composed of pure tire crumb, and pure tire buffings (Figure 5.6, Figure 5.29), and the deviator stress

continues to increase with increasing axial strain. The shear strength of pure tire specimens is defined from the shear stress at 15 per cent axial strain following ASTM D2850-03a, which corresponds to 54, 102, and 184 kPa for pure tire crumb specimens, and 52, 89, and 156 kPa for pure tire buffings specimens. Specimens composed of sand and 5 per cent, 10 per cent, 20 per cent, and 30 per cent tire crumb by weight show peak shear stresses at different axial strains (Figure 5.9, Figure 5.13, Figure 5.17, Figure 5.21). It is determined that as the tire crumb content increases the axial strain value at failure also increases. For the sample prepared by adding 40 per cent tire crumb by weight to sand, no peak stress values are observed, and the deviator stress continued to increase with increasing axial strain for the duration of the test (Figure 5.25). The specimens prepared by adding 5 per cent, 10 per cent, and 20 per cent of tire buffings to sand also show peak values in their deviatoric stress-strain graphs (Figure 5.32, Figure 5.36, Figure 5.40). But it is observed that, specimens containing tire buffings fail at larger axial strains compared to specimens containing the same percentage of tire crumb. So it can be stated that using tire buffings instead of tire crumb as tire inclusions results in a larger axial strain value at failure. In the experiments performed with specimens containing 30 per cent and 40 per cent tire buffings by weight, no peak deviator stress values are observed (Figure 5.44, Figure 5.48), and the shear strength is found using the stress values corresponding to 15 per cent axial strain as described in ASTM D2850-03a.

For the tests performed using tire crumb, the cohesion values vary from 8.10 to 24.65 kPa, and for the tests performed using tire buffings, the cohesion values vary from 9.54 to 14.98 kPa (Table 5.2). It is mentioned by other researchers (Humprey et al., 1993; Gotteland et al., 2005) that the cohesion values are not real cohesions, but apparent cohesion values. The angle of internal friction values varies from 16.89º to 38.19º for specimens with tire crumb additions, and from 14.35º to 41.28º for specimens with tire buffings additions (Table 5.2). To compare and evaluate the test results better, an equivalent friction angle is calculated using regression analysis. The equivalent angle is calculated by fitting the experimental shear data with a straight line through the origin, and forcing the cohesion to be zero. This method was used and suggested by several investigators (Zornberg et al., 2004; Gotteland et al., 2005).

The quick triaxial test results indicate that the greatest shear strength can be achieved by adding 5 per cent tire buffings by weight to sand, which gives a cohesion value of 11.43 kPa, a friction angle of 41.28 degrees, and an equivalent friction angle of 43.18 degrees. The results indicate that the addition of fiber shaped material having an aspect ratio of 3.5-4 gives higher shear strength parameters compared to the addition of granular material with an aspect ratio of 1-1.5. The shear strength value decreases with increasing tire content beyond 5 per cent of tire inclusions by weight.

The summary of test results is shown in Table 5.2. The effects of tire content on shear strength parameters are shown in Figure 5.52, Figure 5.53, and Figure 5.54. Figure 5.39 shows the variation of the cohesion value with changing tire content. Figure 5.52 shows that the maximum cohesion value is obtained from the specimen containing 20 per cent tire crumb by weight as 24.65 kPa, and the minimum cohesion value is obtained from the pure tire crumb specimen as 8.10 kPa. Tire buffings lead to lower cohesion values compared to tire crumb in 5 per cent, 10 per cent, 20 per cent, and 30 per cent additions, and to higher cohesion values in 40 per cent, and 100 per cent additions. Figure 5.53 shows the variation of internal friction angle with the tire content. The equivalent friction angle is a parameter that is calculated from the cohesion and friction angle values obtained from the experimental results by using regression analysis. Several researchers (Zornberg et al., 2004; Gotteland et al., 2005) suggest that the equivalent friction angle is a good representative of the experimental results and it is useful for the comparison of the test results. The shear envelope is forced through the origin by reducing the apparent cohesion to zero. It is shown in Figure 5.54 that the highest equivalent friction angle which is 43.18 degrees is obtained from the specimen composed of 5 per cent tire buffings by weight and sand, and the lowest equivalent friction angle which is 17.74 degrees is obtained from the specimen composed of pure tire buffings.

Table 5.2. Summary of quick triaxial compression test results

Specimen	Deviator Stress (kPa)			c (kPa)	Φ (°)	Φ_{eq} (°)	Unit Weight (kN/m³)
	40 kPa Confining Pressure	100 kPa Confining Pressure	200 kPa Confining Pressure				
Sand	221	462	810	9.97	41.48	43.02	16.0
Tire Crumb	54	102	184	8.1	16.89	19.71	6.5
%5 Tire Crumb	191	408	692	15.10	38.19	40.88	15.1
%10 Tire Crumb	233	428	731	21.02	38.16	41.57	14.5
%20 Tire Crumb	210	355	632	24.65	35.12	39.57	13.3
%30 Tire Crumb	134	262	472	14.21	31.02	34.19	12.5
%40 Tire Crumb	108	210	398	9.28	28.69	30.96	11.2
Tire Buffings	52	89	156	9.54	14.35	17.74	4.6
%5 Tire Buffings	218	454	813	11.43	41.28	43.18	14.7
%10 Tire Buffings	181	336	616	14.98	35.93	38.78	13.7
%20 Tire Buffings	140	275	463	14.04	30.99	34.07	12.1
%30 Tire Buffings	116	218	368	13.63	26.89	30.33	10.3
%40 Tire Buffings	99	174	328	11.18	24.70	27.72	9.1

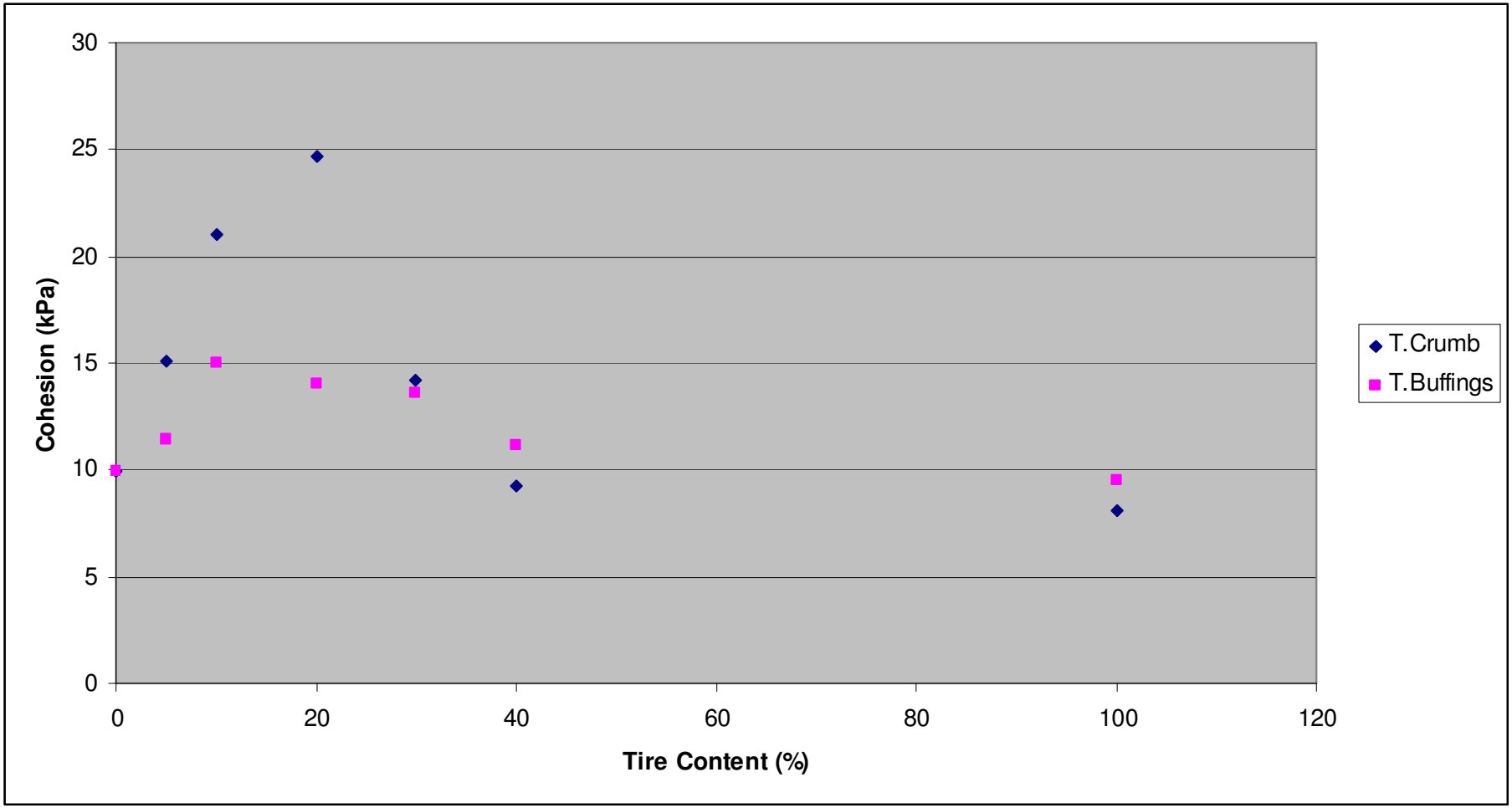

Figure 5.52. Cohesion - tire content diagram of quick triaxial test results

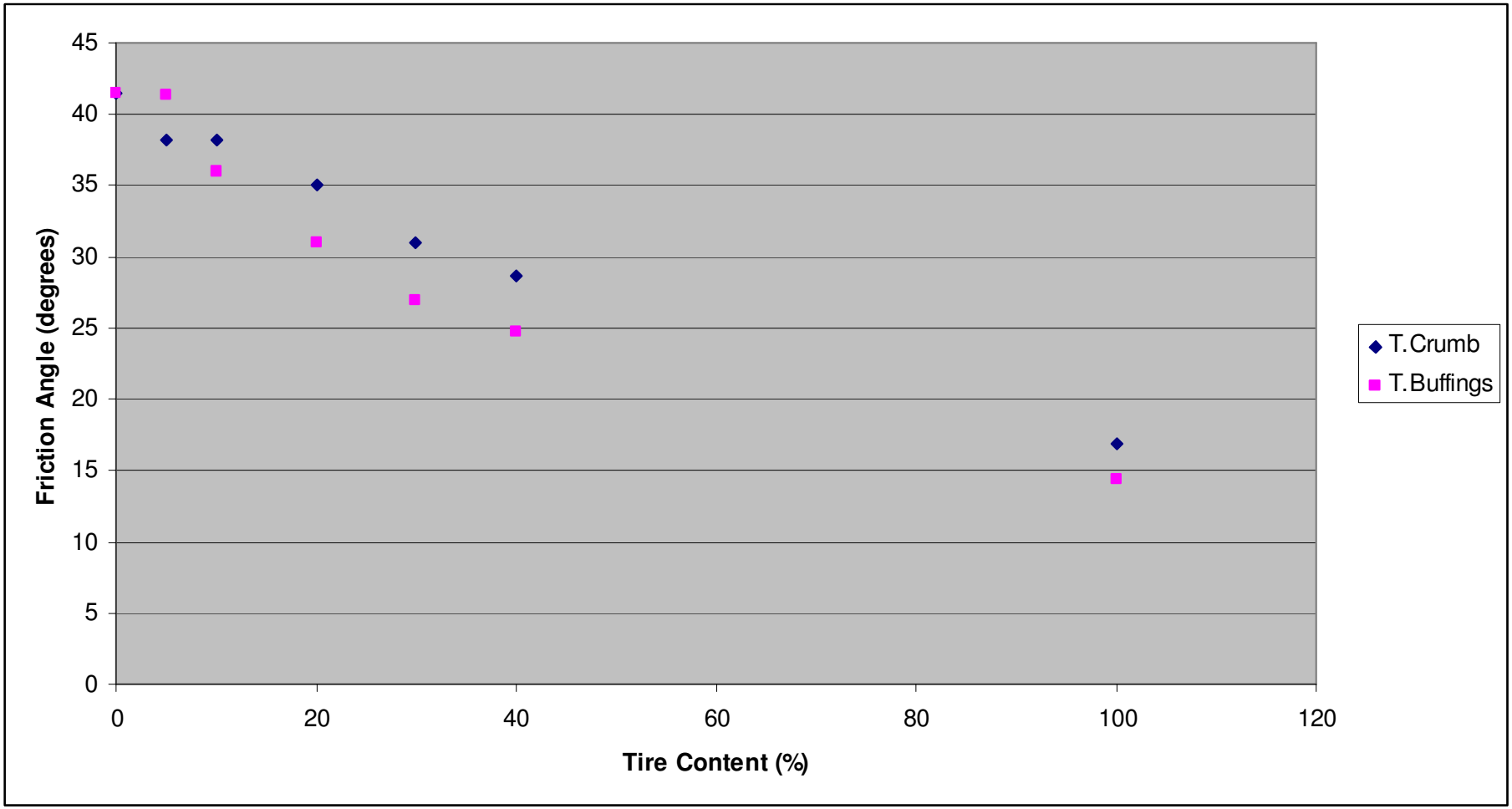

Figure 5.53. Friction angle - tire content diagram of quick triaxial test results

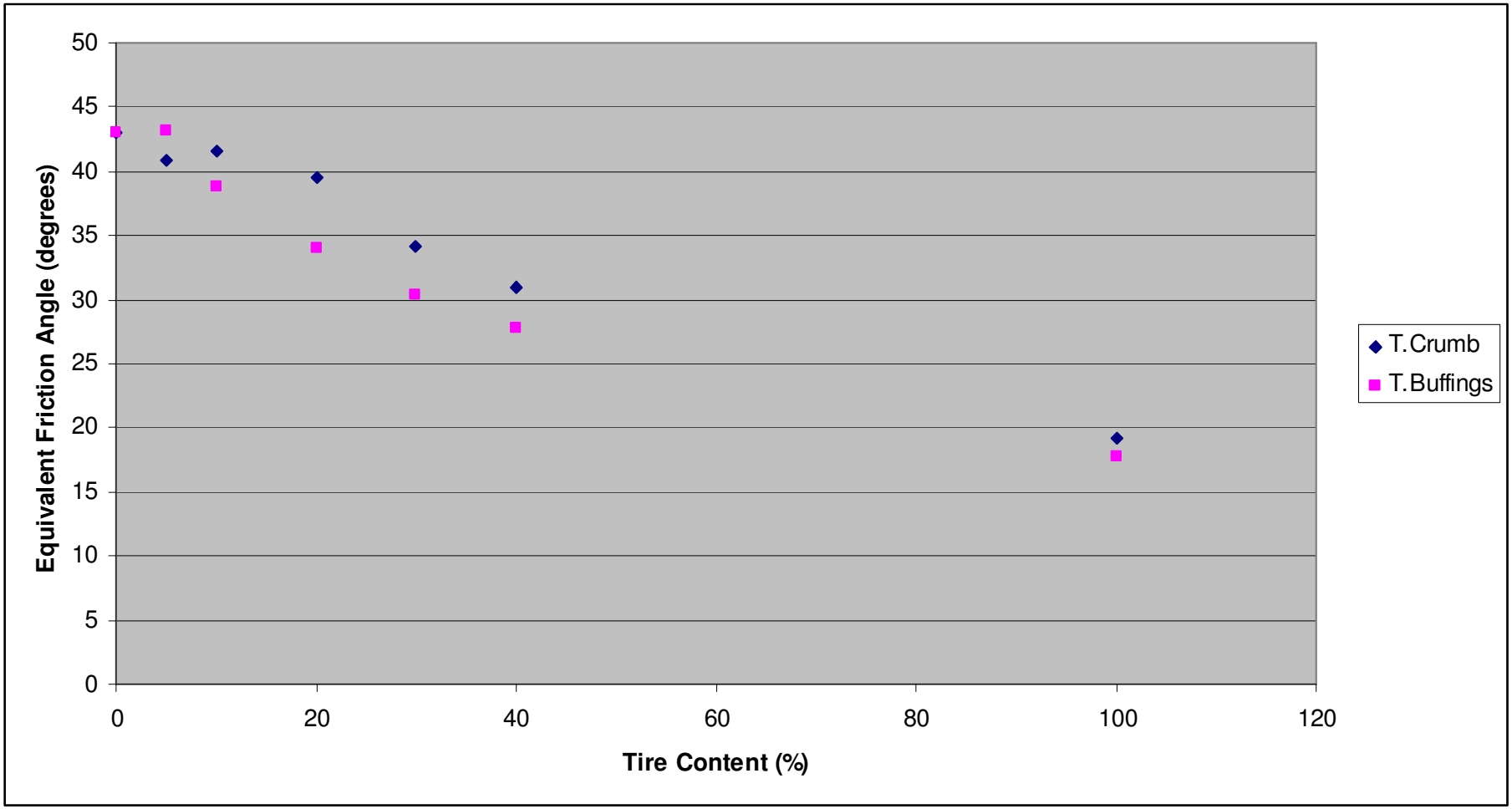

Figure 5.54. Equivalent friction angle - tire content diagram of quick triaxial test results

5.3. Consolidated Drained Triaxial Test Results

Consolidated drained (CD) triaxial tests are conducted on sand, tire crumb, tire buffings, and sand-tire waste compositions with varying tire content. A total of 13 sets of experiments are done, with each test repeated at three different confining pressures of 40, 100, and 200 kPa. The tests are conducted in general accordance with ASTM D4765. Tire waste-sand specimens are mixed at 5, 10, 20, 30, and 40 per cent of tire waste by weight. The strain rate is determined as 0.5 mm/min, at which the pore water pressure remains unchanged at zero for the duration of the compression stage. The B value is around 0.97 in all the tests at the end of the saturation stage. The corrected deviator stress is calculated by Data System 7 as described in ASTM D4765 using the area corrections of the rubber membrane. The consolidated drained (CD) shear strength is most critical for the long-term steady seepage case for embankments, for example an embankment constructed very slowly, in layers.

5.3.1. Mixture Containing 100 per cent Sand

First, sand alone is tested. The unit weight of the sand specimen is determined as 16.0 kN/m³. The deviator stress-strain graph (Figure 5.55) revealed that the peak deviator stress occurs around 5-6 per cent of axial strain. At failure, the maximum deviator stresses are observed as 183.2, 418.1, and 824.2 kPa, corresponding to axial strains of 5.32 per cent, 4.78 per cent, and 6.27 per cent. According to the failure envelope (Figure 5.57), the cohesion is found to be 1.45 kPa, and the friction angle is found as 41.49 degrees. The same shear strength parameters can be obtained from the p-q graph of the specimen which is shown in Figure 5.58. Using regression analysis, the equivalent friction angle is calculated as 41.70 degrees. The specimen shows a dilatant volumetric behavior (Figure 5.56). Also, a more dilatant behavior is observed under lower confining pressures.

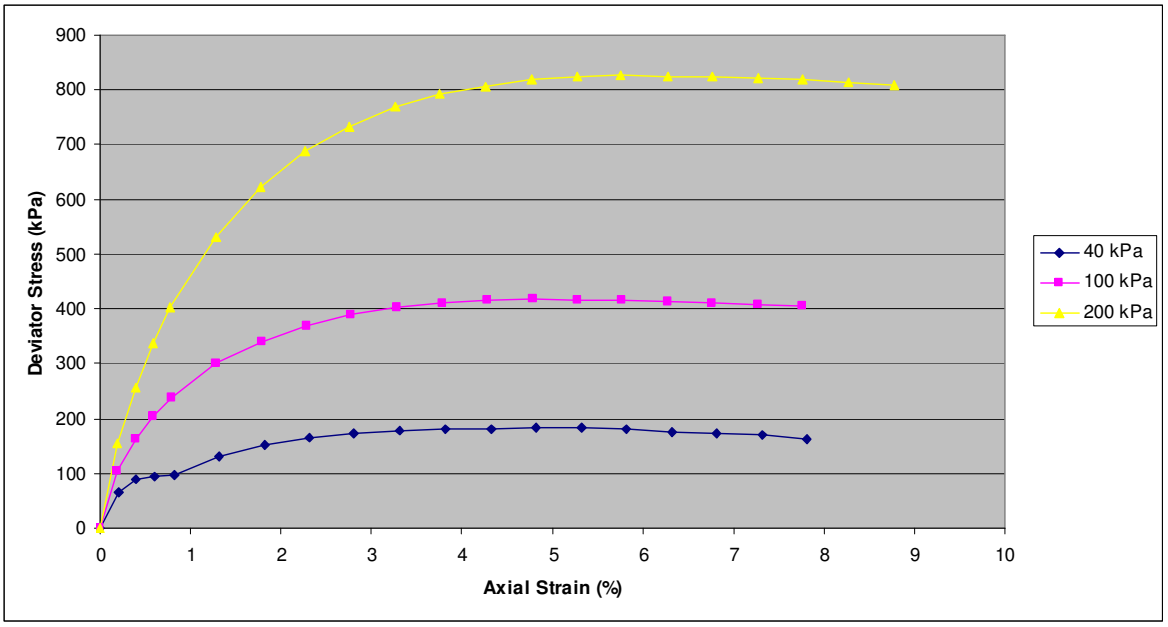

Figure 5.55. Deviator stress-axial strain behavior of specimen containing 100 per cent sand

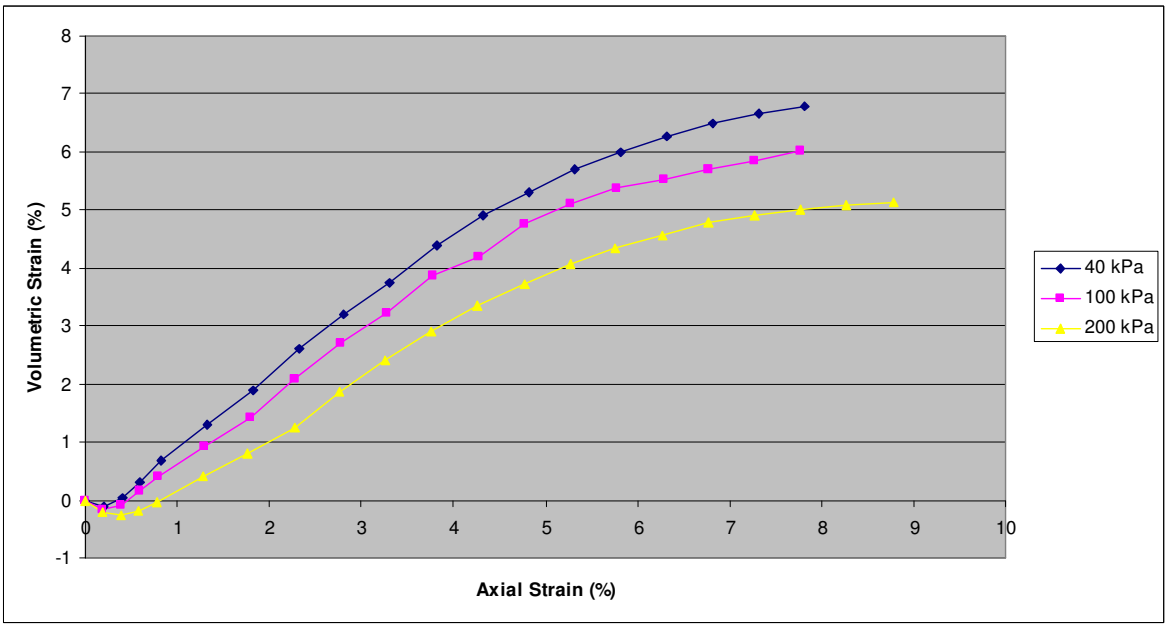

Figure 5.56. Volumetric strain of specimen containing 100 per cent sand

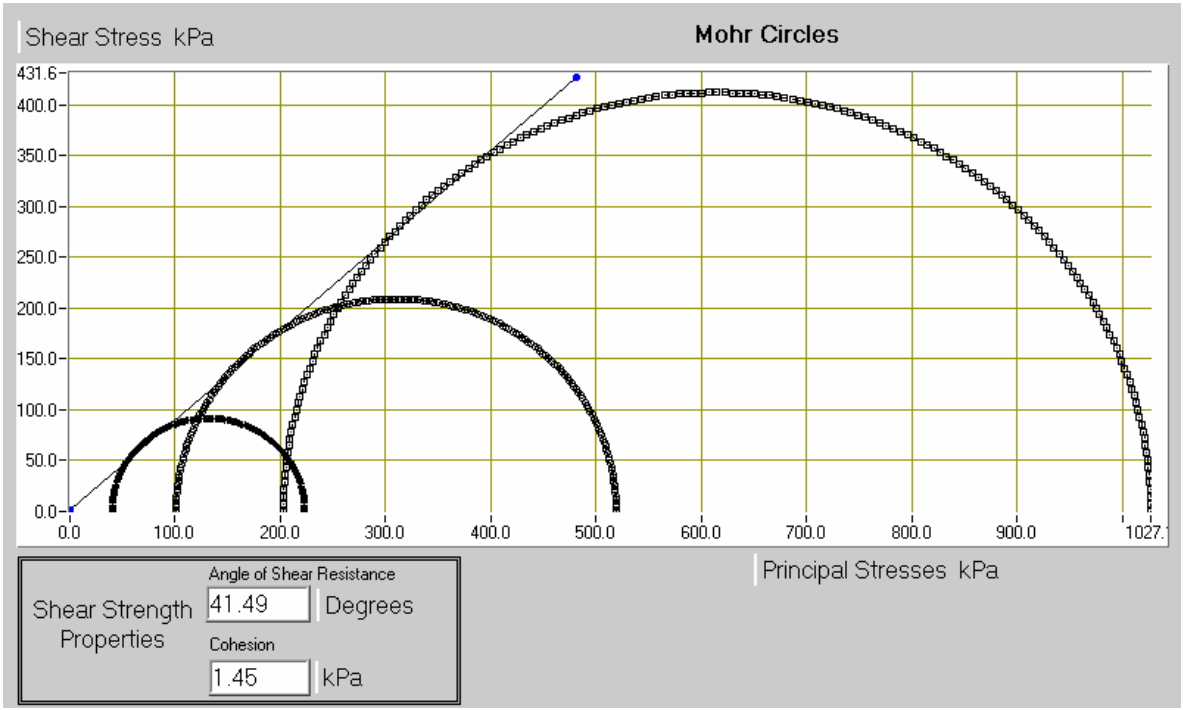

Figure 5.57. Shear strength envelope of specimen containing 100 per cent sand

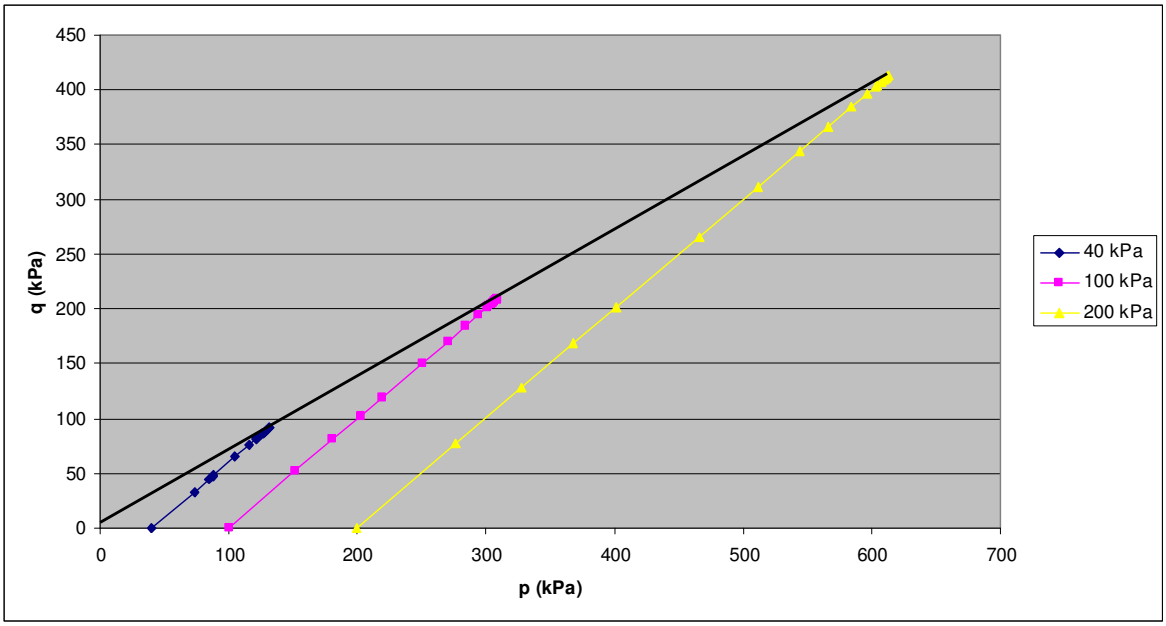

Figure 5.58. p-q graph of specimen containing 100 per cent sand

5.3.2. Mixture Containing 100 per cent Tire Crumb

Next, a specimen composed of only tire crumb is tested. The unit weight of the sample is 6.5 kN/m³. It is seen in the stress-strain diagram of the mixture that the deviator stress continues to increase, with increasing axial strain, and a peak value does not occur (Figure 5.59). All three samples show similar stress behavior up to 1.5 per cent axial strain. The deviator stress values at 15 per cent axial strain are 117.9, 170.3 and 250.9 kPa. From the Mohr-failure diagram (Figure 5.61), the cohesion is determined as 30.17 kPa, and the friction angle as 17.56 degrees. From the experimental data, the equivalent friction angle is calculated as 25.95 degrees. Figure 5.62 shows the p-q graph of the specimen. The same cohesion and friction angle values can be obtained from the p-q graph. The specimen composed of only tired crumb shows a contractive and an approximately linear volumetric strain behavior (Figure 5.60). More contractive behavior is observed under higher confining pressures.

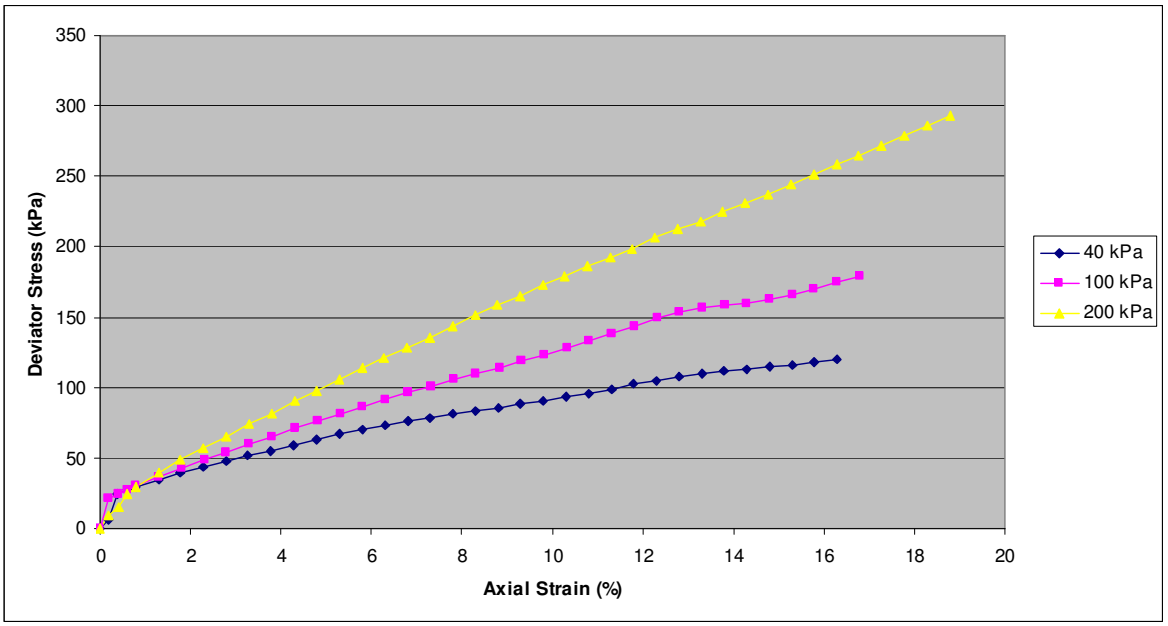

Figure 5.59. Deviator stress-axial strain behavior of specimen containing 100 per cent tire crumb

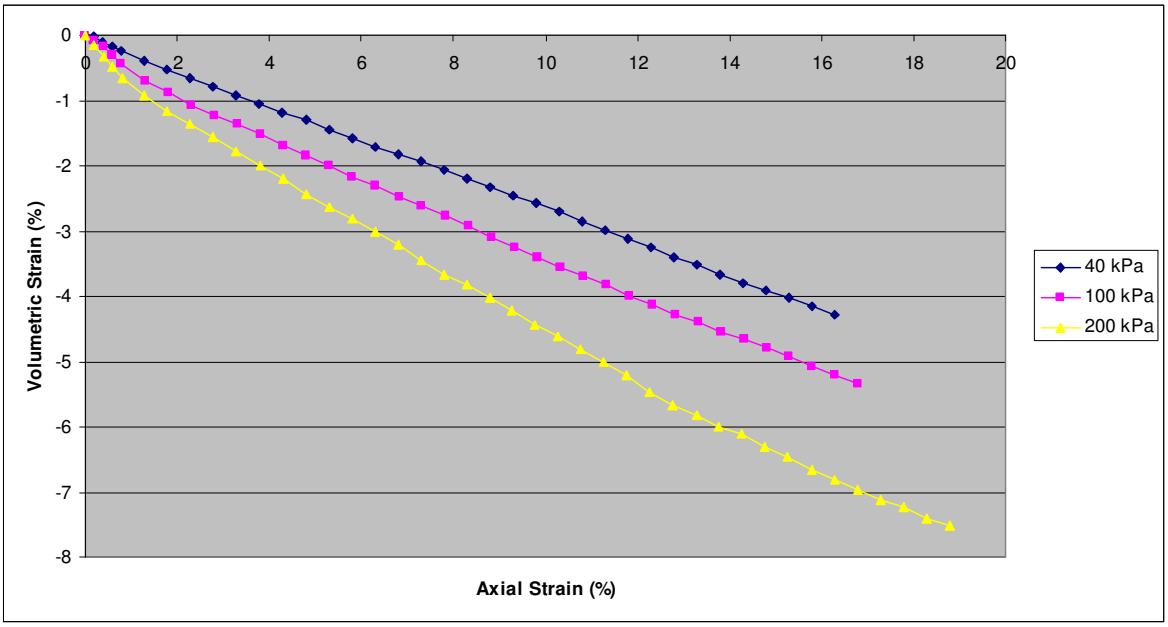

Figure 5.60. Volumetric strain of specimen containing 100 per cent tire crumb

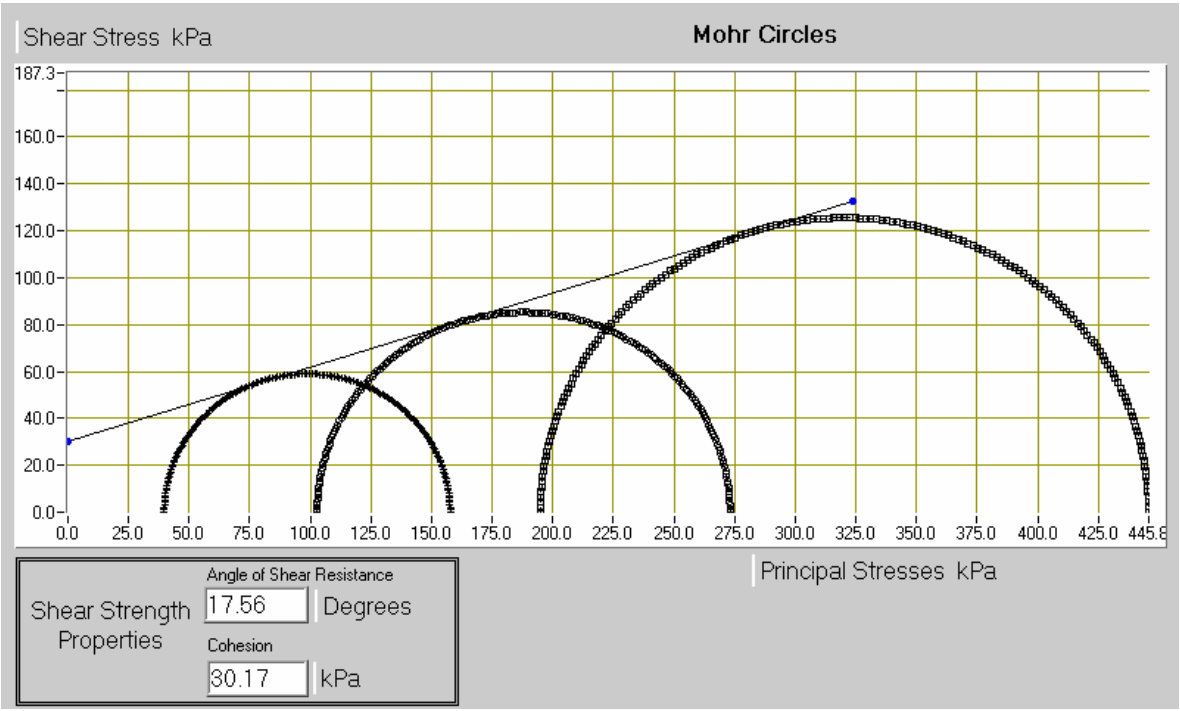

Figure 5.61. Shear strength envelope of specimen containing 100 per cent tire crumb

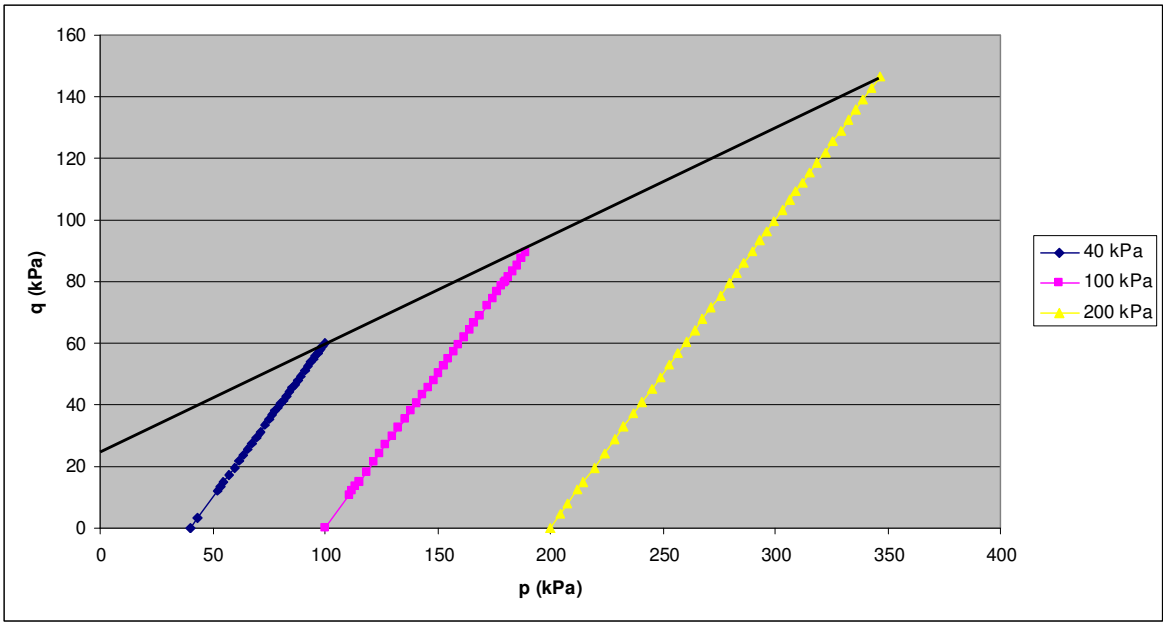

Figure 5.62. p-q graph of specimen containing 100 per cent tire crumb

5.3.3. Mixture Containing 5 per cent Tire Crumb

5 per cent tire crumb by weight is added to sand. The specimen has a unit weight of 15.1 kN/m³. The deviator stress-strain diagram is shown in Figure 5.63. The peak deviator stresses are obtained at different axial strains for different confining pressures. Up to 0.5 per cent axial strain the specimens tested at 100 and 200 kPa confining pressures show similar stress increase. The deviator stress values at failure are 249.9, 417.7, and 751.4 kPa, corresponding to axial strains of 5.79 per cent, 6.81 per cent, and 9.29 per cent. The shear strength envelope is shown in Figure 5.65. The cohesion value is determined as 16.13 kPa, and the friction angle is found to be 39.35 degrees. The same shear strength parameters can be obtained from the p-q graph of the specimen (Figure 5.66). The equivalent angle of internal friction is calculated as 41.99 degrees. The specimen shows a dilatant behavior, and as the confining pressure increases the dilatant volumetric strain decreases (Figure 5.64). Almost a linear dilatant behavior is observed up to axial strains around 6 per cent to 8 per cent , after which the slope of the lines decrease.

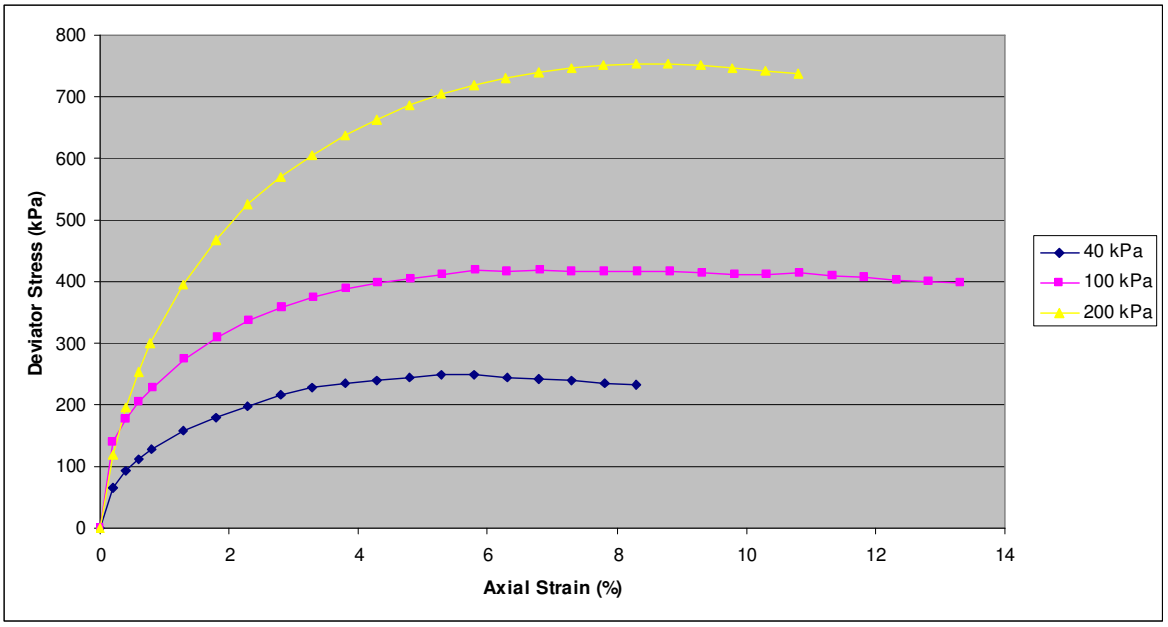

Figure 5.63. Deviator stress-axial strain behavior of specimen containing 5 per cent tire crumb

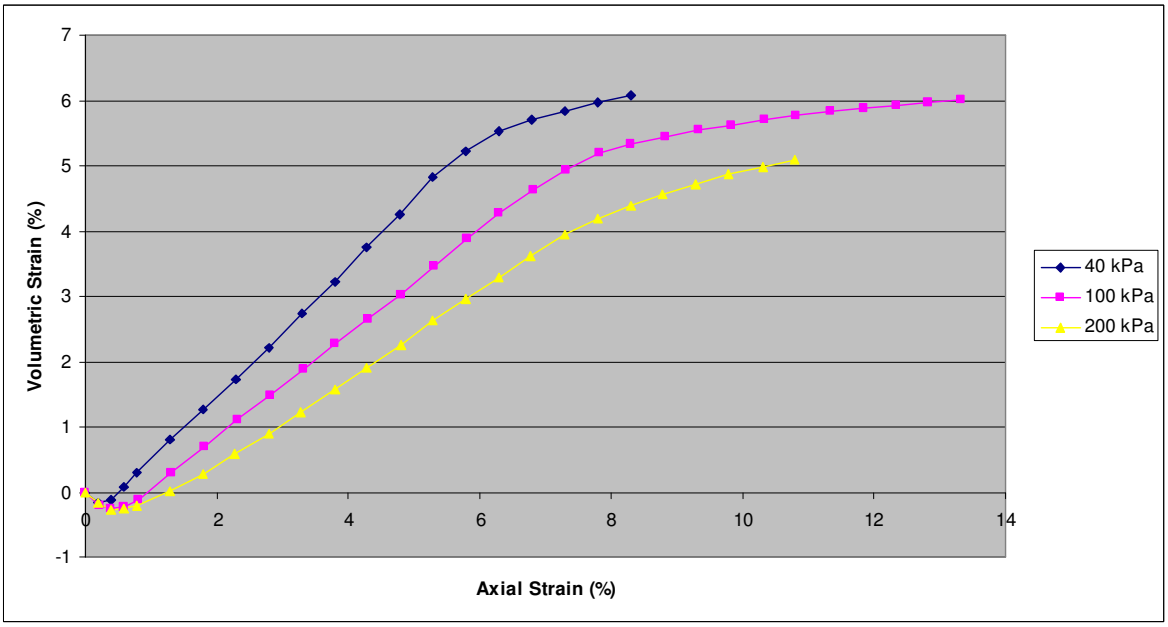

Figure 5.64. Volumetric strain of specimen containing 5 per cent tire crumb

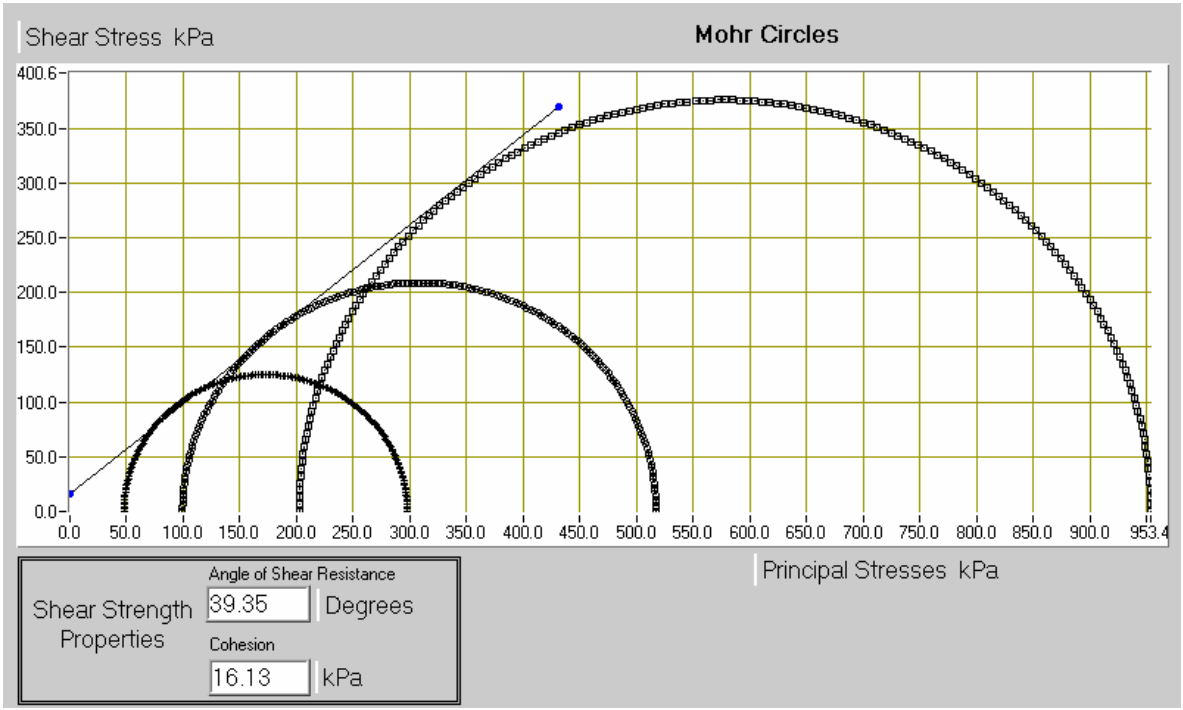

Figure 5.65. Shear strength envelope of specimen containing 5 per cent tire crumb

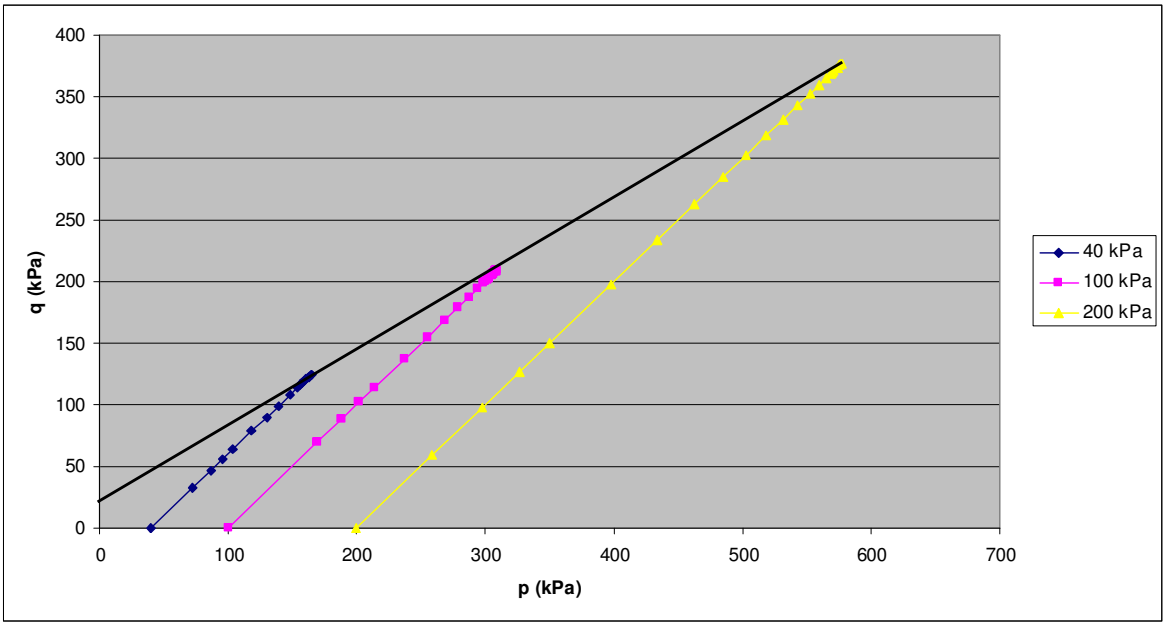

Figure 5.66. p-q graph of specimen containing 5 per cent tire crumb

5.3.4. Mixture Containing 10 per cent Tire Crumb

The sample to be tested is prepared by adding 10 per cent tire crumb by weight to sand. The unit weight of the specimen is 14.5 kN/m³. The peak deviator stresses are obtained at about 8-9 per cent of axial strain (Figure 5.67). The maximum deviator stresses are 179.9, 437.9, and 684.2 kPa. According to the failure envelope (Figure 5.69), the cohesion value is 17.38 kPa, and the angle of internal friction is 38.33 degrees. The p-q graph of the specimen is shown in Figure 5.70. The shear strength parameters obtained from the p-q graph are identical with the values obtained from the Mohr failure diagram. Using regression analysis, the equivalent friction angle is calculated as 41.31 degrees. According to the volumetric strain graph (Figure 5.68), the specimen shows a dilatant behavior. The highest volumetric strain is obtained under the lowest confining pressure.

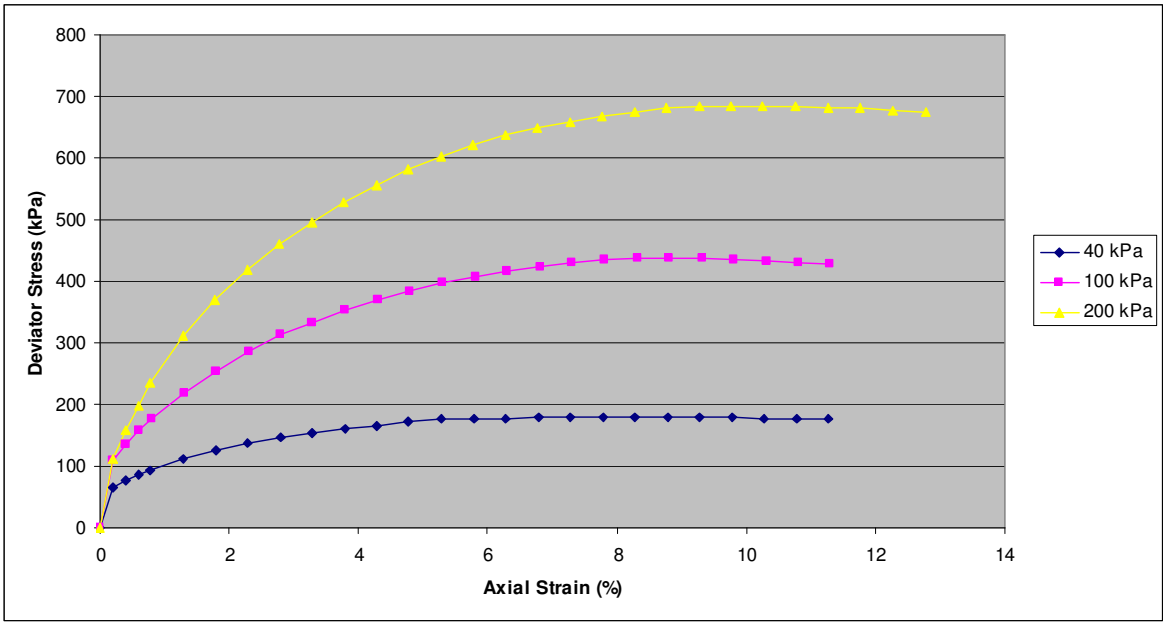

Figure 5.67. Deviator stress-axial strain behavior of specimen containing 10 per cent tire crumb

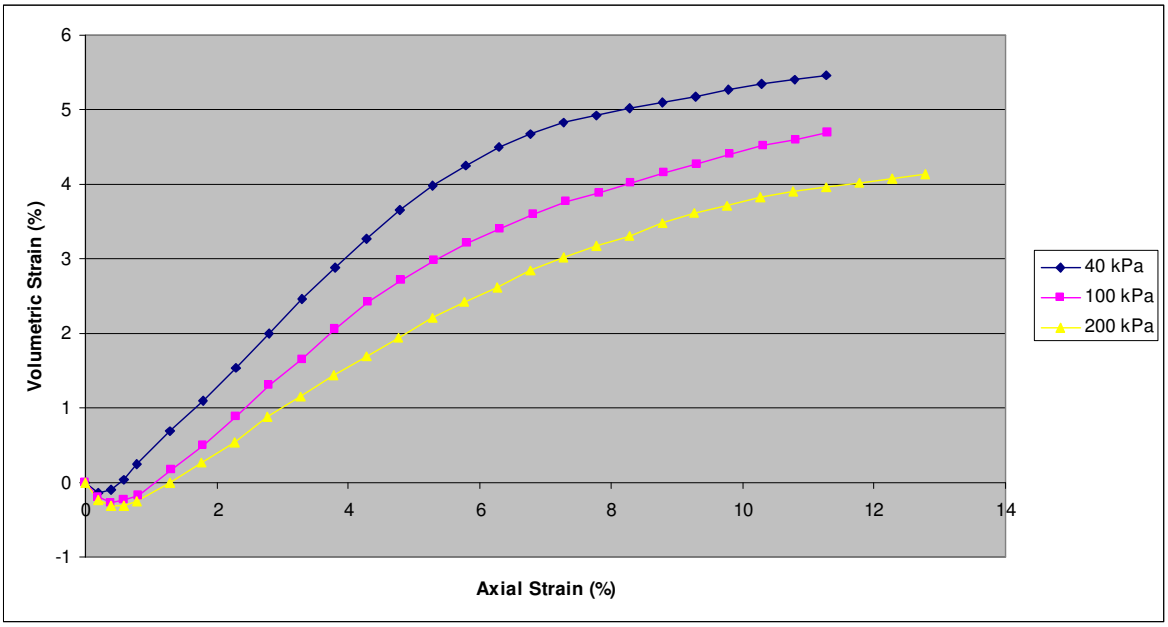

Figure 5.68. Volumetric strain of specimen containing 10 per cent tire crumb

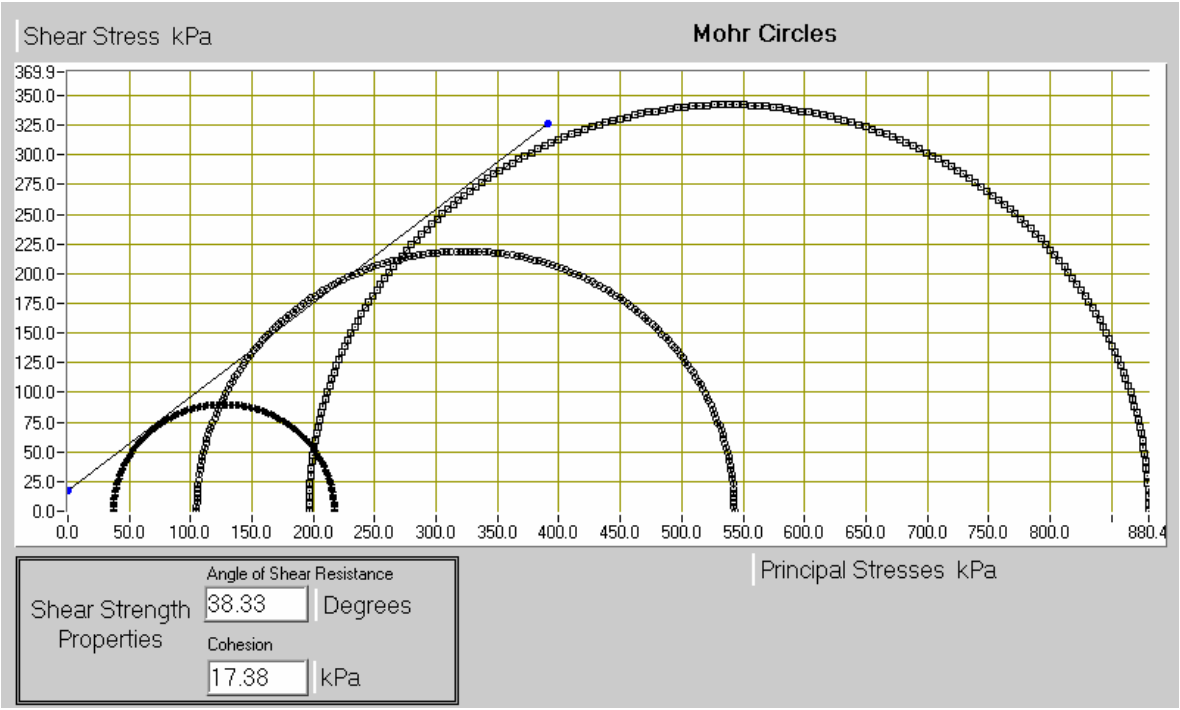

Figure 5.69. Shear strength envelope of specimen containing 10 per cent tire crumb

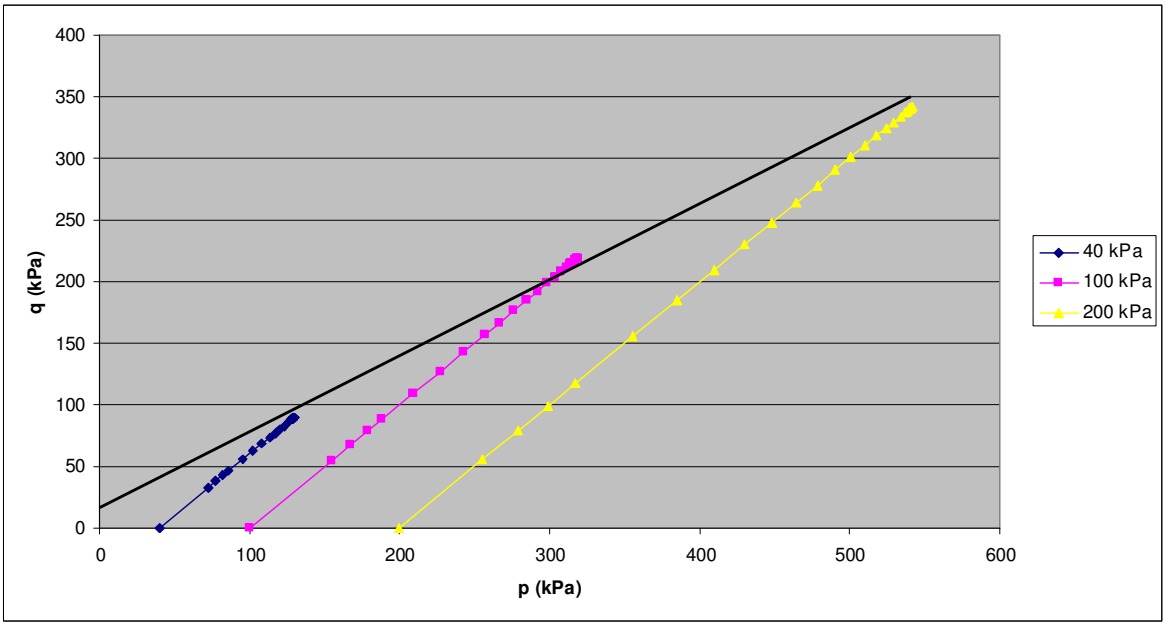

Figure 5.70. p-q graph of specimen containing 10 per cent tire crumb

5.3.5. Mixture Containing 20 per cent Tire Crumb

20 per cent tire crumb by weight is mixed with sand to form the specimen. The mixture has a unit weight of 13.3 kN/m³. The deviator stress-strain graph is drawn to analyze the results (Figure 5.71). Between 0 per cent and 1 per cent axial strain the sample tested under 200 kPa confining pressure shows a slight increase in deviator stress, which gets steeper afterwards. At failure, the peak deviator stresses observed are 177.4, 349.1, and 592.6 kPa, which corresponds to axial strains of 10.32 per cent, 9.81 per cent and 14.26 per cent. From the Mohr-failure envelope (Figure 5.73), the cohesion value is found to be 15.60 kPa, and the friction angle is found to be 35.44 degrees. Figure 5.74 shows the p-q graph of the specimen, from which the same shear strength parameters can be obtained. Using the experimental data, the equivalent angle of internal friction is calculated to be 38.48 degrees. The tire crumb-sand mixture shows a dilatant volumetric strain behavior (Figure 5.72). Under 200 kPa confining pressure, almost a linear behavior is observed up to an axial strain of 12 per cent. Higher volumetric strains are observed under lower confining pressures, however they can not be classified as linear.

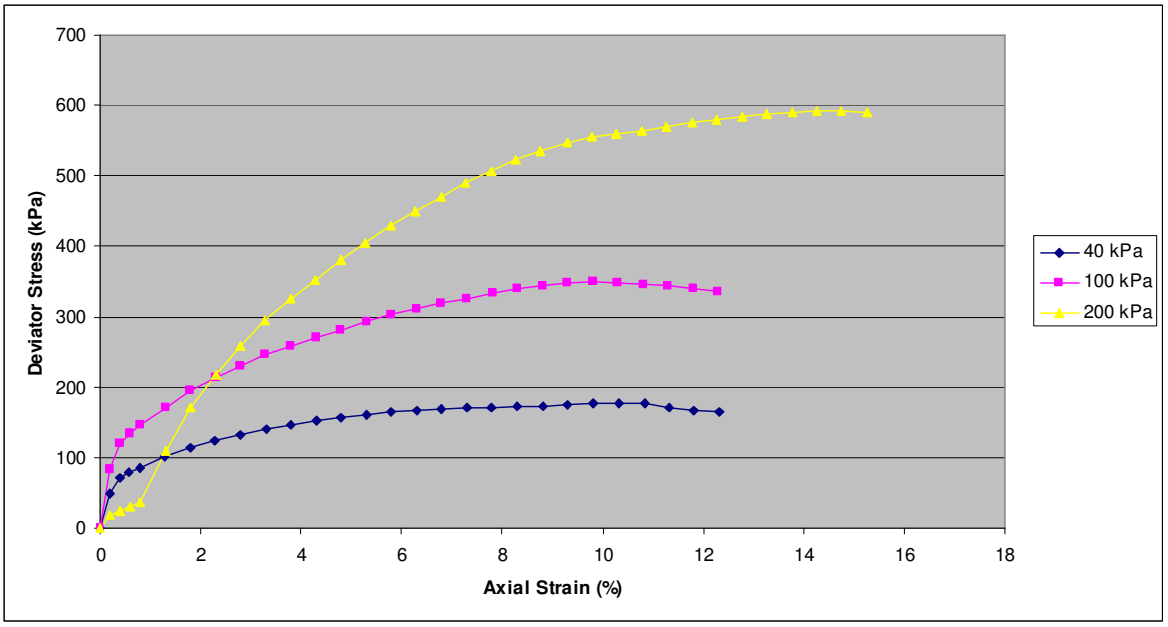

Figure 5.71. Deviator stress-axial strain behavior of specimen containing 20 per cent tire crumb

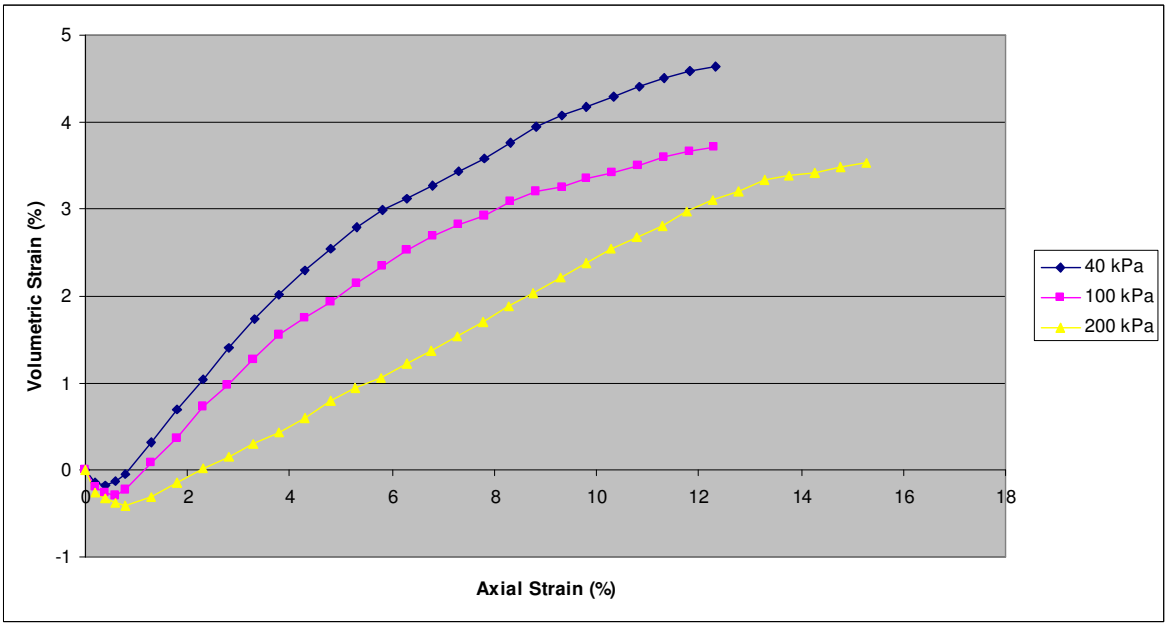

Figure 5.72. Volumetric strain of specimen containing 20 per cent tire crumb

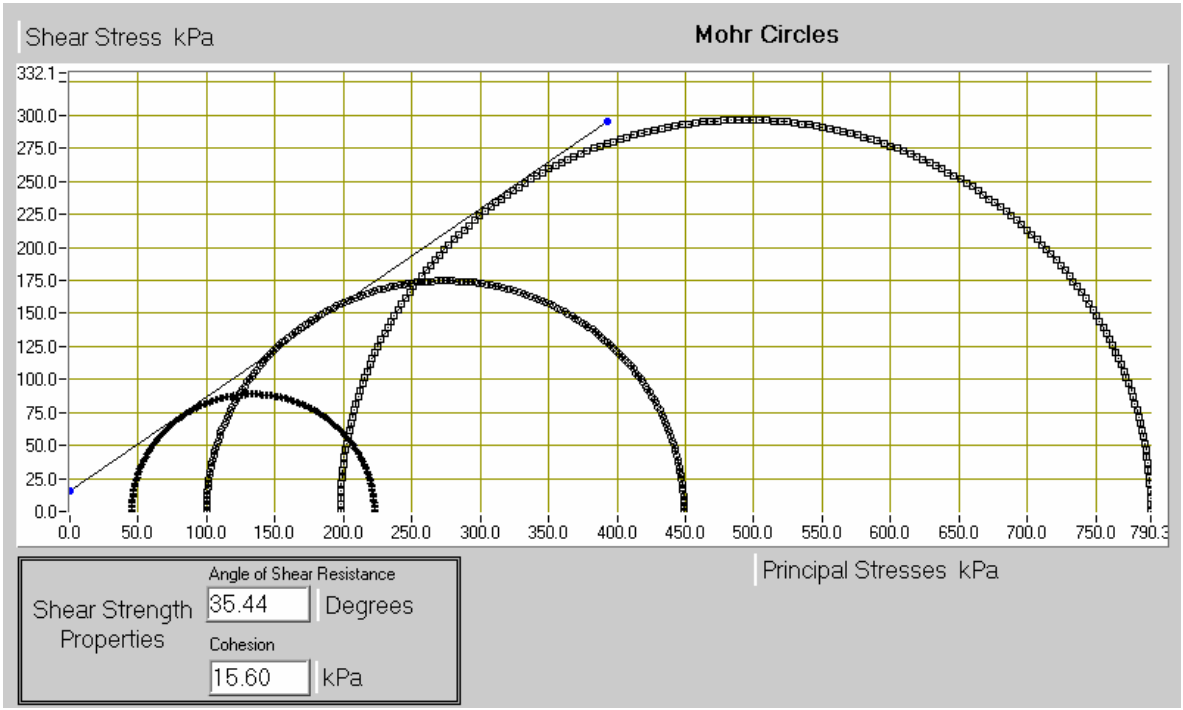

Figure 5.73. Shear strength envelope of specimen containing 20 per cent tire crumb

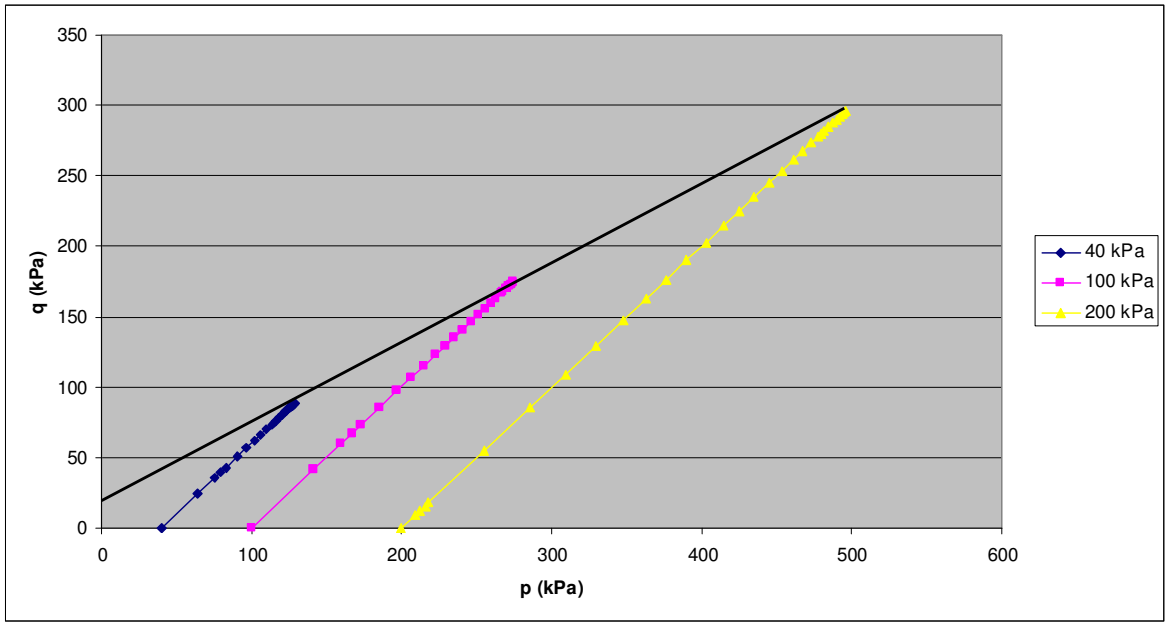

Figure 5.74. p-q graph of specimen containing 20 per cent tire crumb

5.3.6. Mixture Containing 30 per cent Tire Crumb

30 per cent tire crumb by weight is added to sand. The unit weight of the sample is 12.5 kN/m³. From the experimental data, the deviator stress-axial strain graph is drawn (Figure 5.75). Up to 0.5 per cent axial strain the samples tested at 100 and 200 kPa confining pressures show similar stress behavior. The same samples does not show any peak stresses throughout the test and the deviator stresses at 15 per cent axial strain are 325.4,and 618.9 kPa. On the other hand, failure is observed for the specimen tested under 40 kPa confining pressure, corresponding to an axial strain of 12.28 per cent and a deviator stress of 185.2 kPa. From the failure envelope (Figure 5.77), the cohesion value is found as 12.72 kPa, and the friction angle as 36.28 degrees. The shear strength parameters can also be obtained from the p-q graph shown in Figure 5.78. The equivalent friction angle is calculated as 38.67 degrees. The volumetric strain behavior is shown in Figure 5.76. The specimen shows a dilatant behavior, however the ratio of volumetric strain to axial strain is much lower compared to the tests with lower tire content.

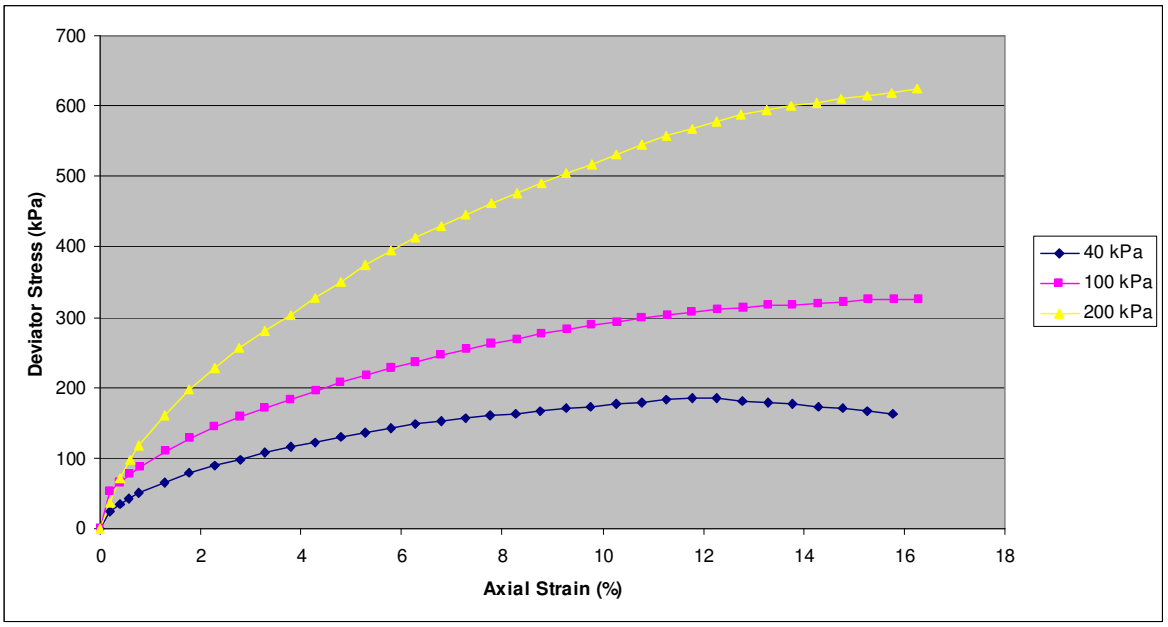

Figure 5.75. Deviator stress-axial strain behavior of specimen containing 30 per cent tire crumb

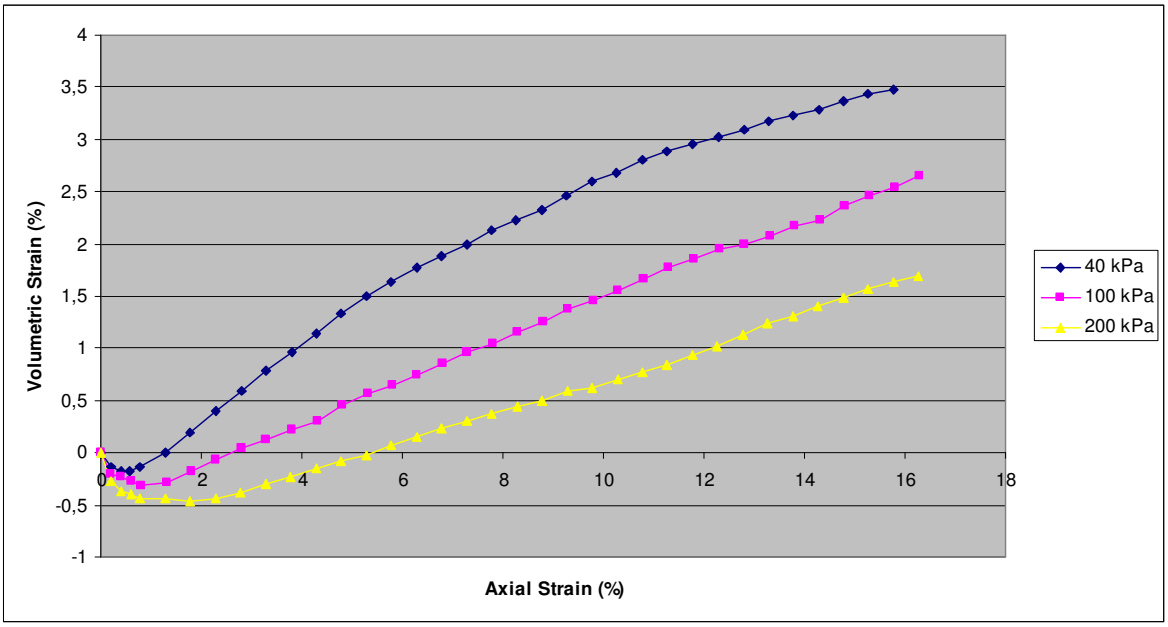

Figure 5.76. Volumetric strain of specimen containing 30 per cent tire crumb

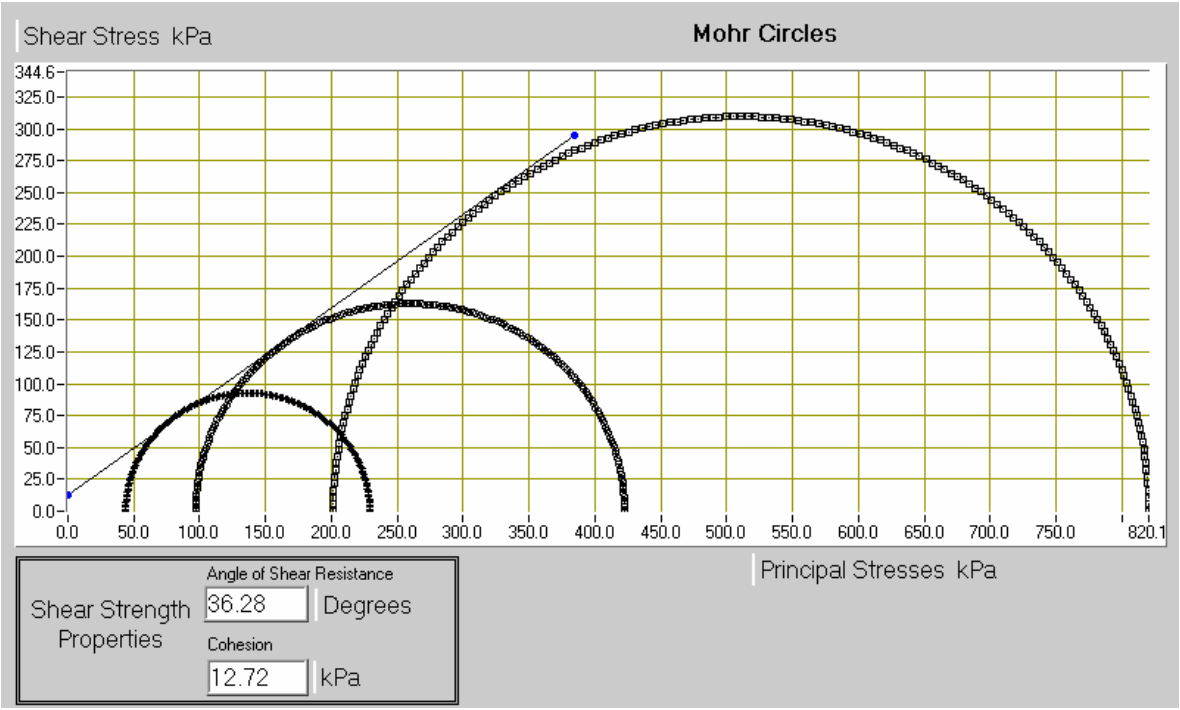

Figure 5.77. Shear strength envelope of specimen containing 30 per cent tire crumb

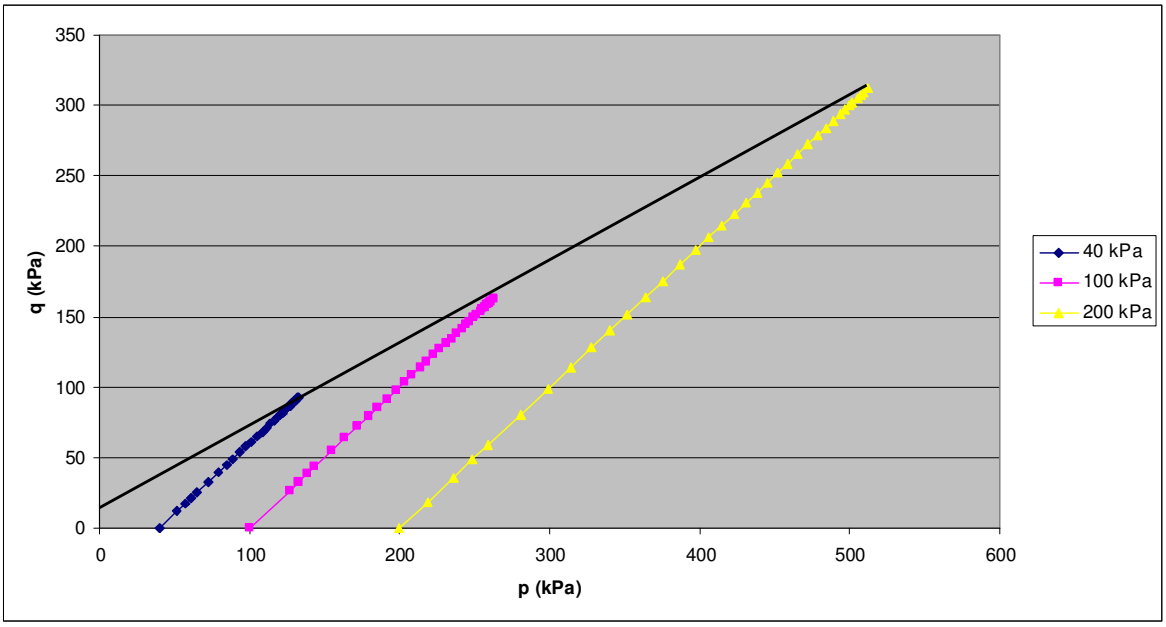

Figure 5.78. p-q graph of specimen containing 30 per cent tire crumb

5.3.7. Mixture Containing 40 per cent Tire Crumb

The specimen to be tested is composed of 40 per cent tire crumb by total weight, and sand. The unit weight of the sample is 11.2 kN/m³. The deviator stress-strain behavior of the specimen is shown in Figure 5.79. All three specimens show similar stress behavior up to 0.8 per cent axial strain. Failure is observed only in the first test under 40 kPa confining pressure, at a deviator stress of 175.1 kPa, and an axial strain of 12.27 per cent. Tests under 100 and 200 kPa confining pressures does not show any peak stresses, and the corresponding deviator stress at 15 per cent axial strain are 256.5, and 422.8 kPa. From the Mohr-circle diagram (Figure 5.81), the cohesion is determined as 27.85 kPa, and the angle of internal friction as 27.57 degrees. The p-q graph of the specimen is shown in Figure 5.82, which gives the same shear strength parameters as the Mohr failure diagram. Using regression analysis, the equivalent angle of internal friction is calculated as 33.90 degrees. The volumetric strain-axial strain graph (Figure 5.80) indicates that, the specimen shows an initial loss of volume and varying levels of dilation can be observed for different confining pressures. A full contractive behavior can be observed under 200 kPa confining pressure.

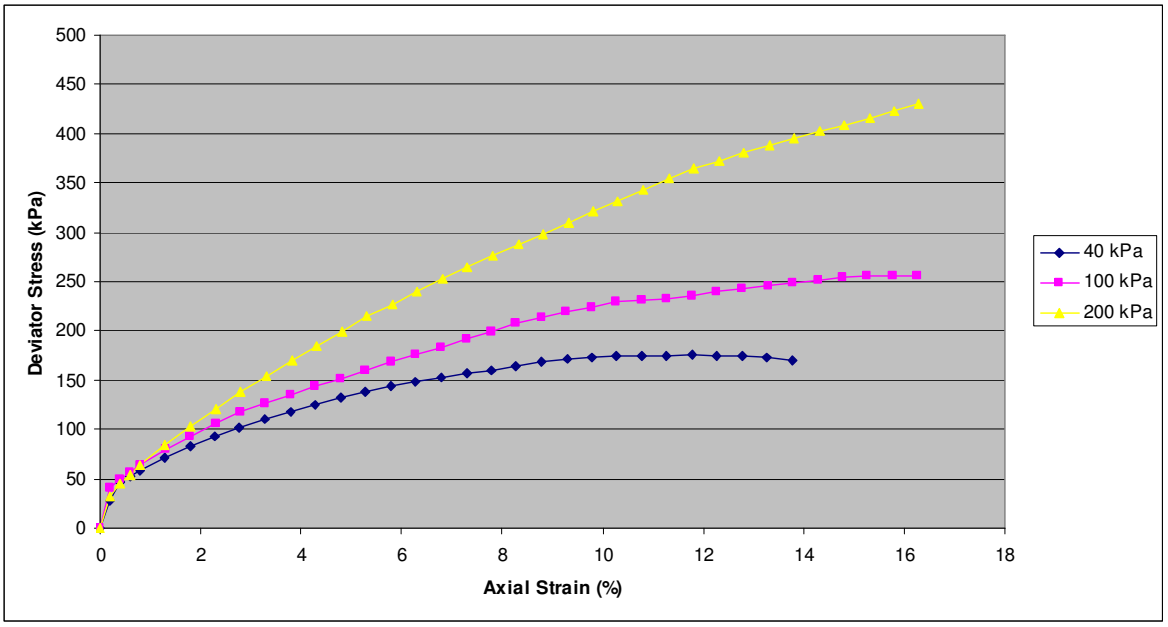

Figure 5.79. Deviator stress-axial strain behavior of specimen containing 40 per cent tire crumb

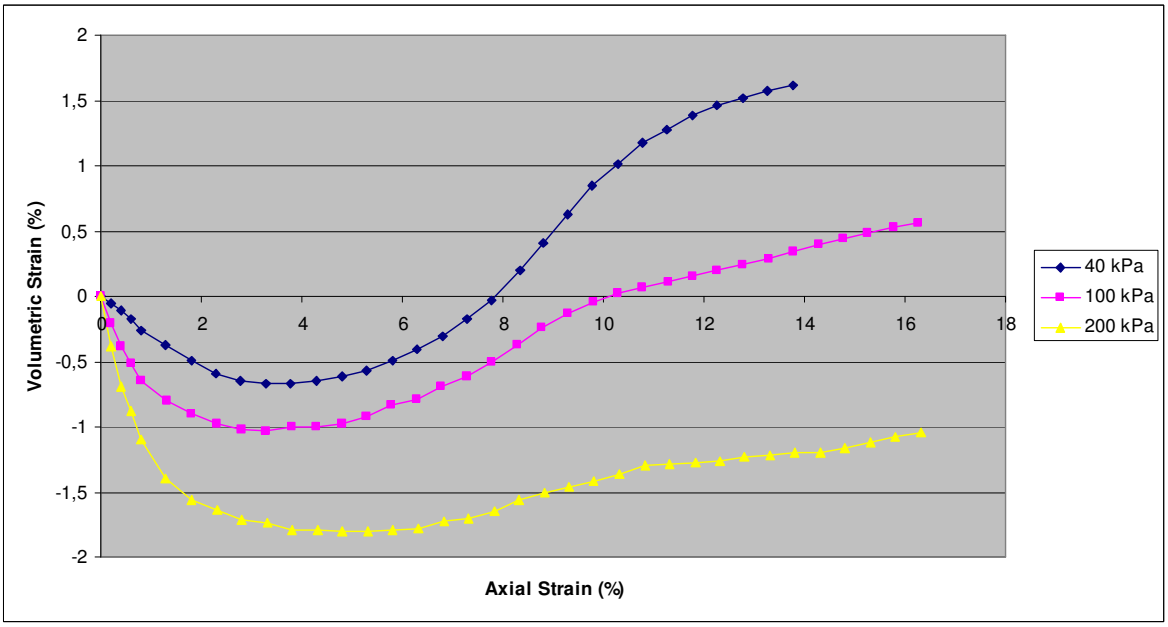

Figure 5.80. Volumetric strain of specimen containing 40 per cent tire crumb

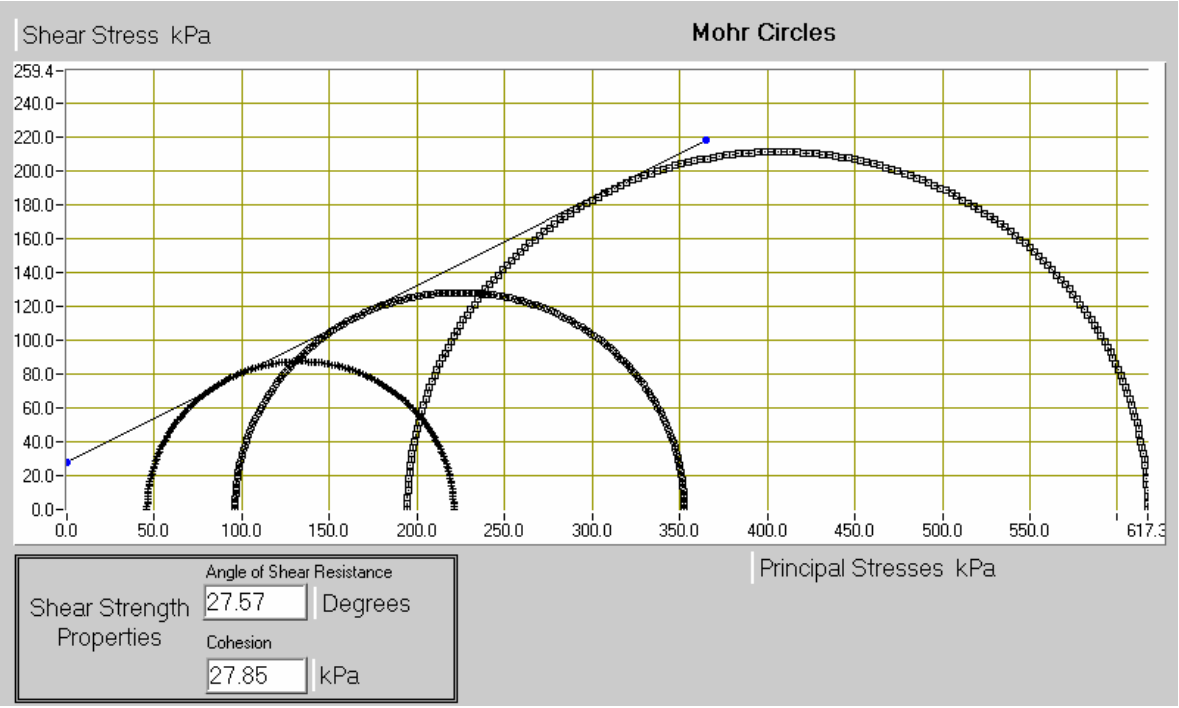

Figure 5.81. Shear strength envelope of specimen containing 40 per cent tire crumb

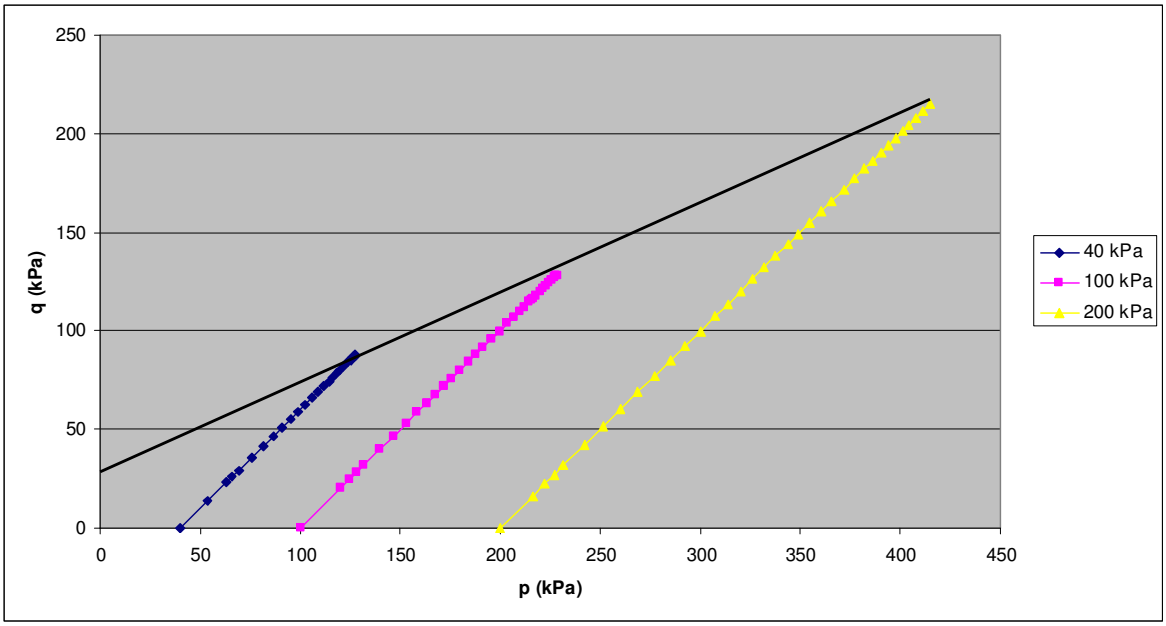

Figure 5.82. p-q graph of specimen containing 40 per cent tire crumb

5.3.8. Mixture Containing 100 per cent Tire Buffings

The specimen to be tested is composed of only tire buffings. The unit weight of the tire buffings sample is 4.6 kN/m³. As it is shown on the deviator stress-strain graph (Figure 5.83) the deviator stress does not make any peaks, and it continues to increase with increasing axial strain. The first two tests (40 and 100 kPa confining pressures) show similar stress behavior up to an axial strain of 2 per cent. The corresponding deviator stress values at 15 per cent axial strain are 110.1, 164.7, and 235.9 kPa. From the failure envelope (Figure 5.85), the cohesion value can be found as 29.51 kPa, and the internal friction angle as 16.62 degrees. The same shear strength parameters are also found by using the p-q graph of the specimen (Figure 5.86). The equivalent angle of internal friction is calculated as 24.89 degrees. The specimen shows a contractive and an approximately linear volumetric behavior (Figure 5.84). More contraction is observed under higher confining pressures.

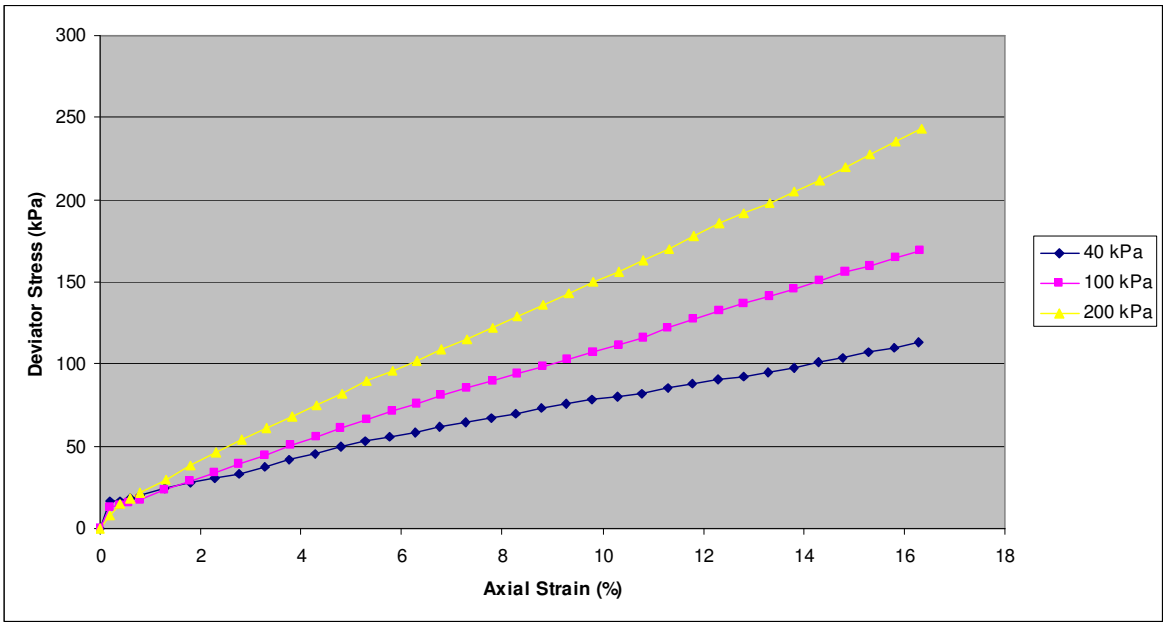

Figure 5.83. Deviator stress-axial strain behavior of specimen containing 100 per cent tire buffings

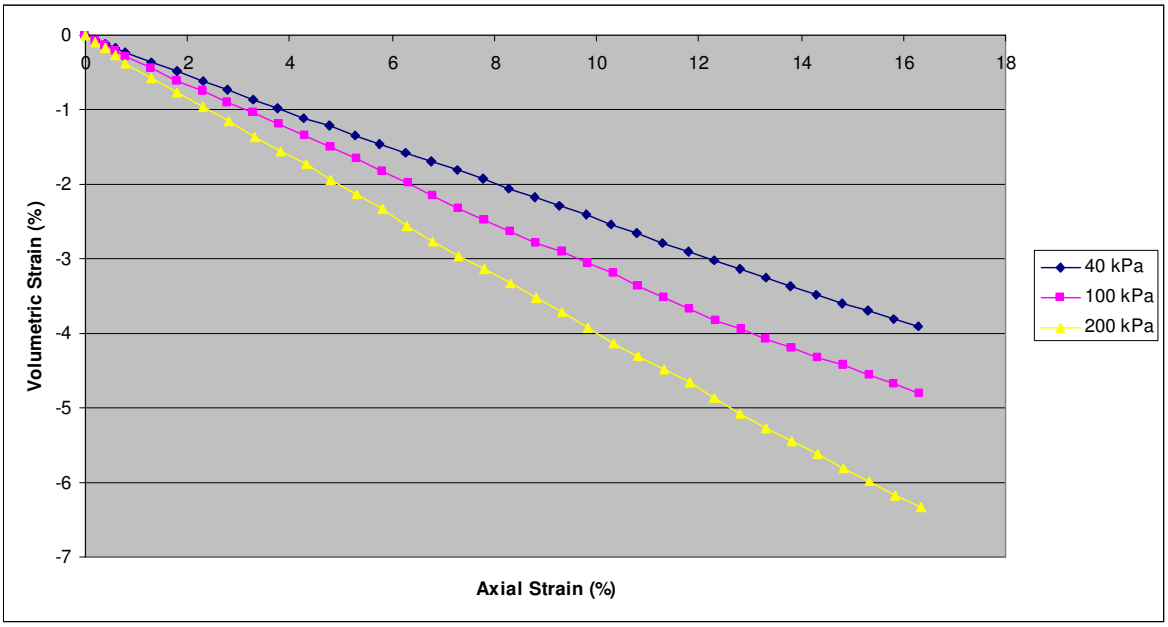

Figure 5.84. Volumetric strain of specimen containing 100 per cent tire buffings

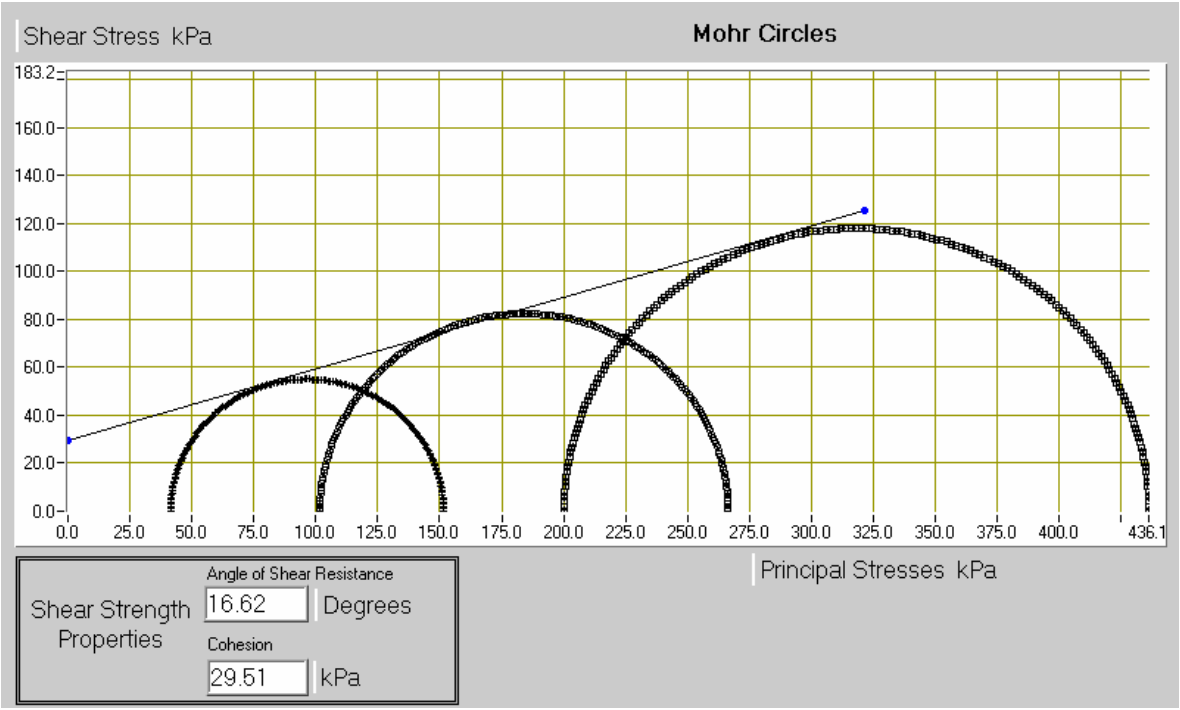

Figure 5.85. Shear strength envelope of specimen containing 100 per cent tire buffings

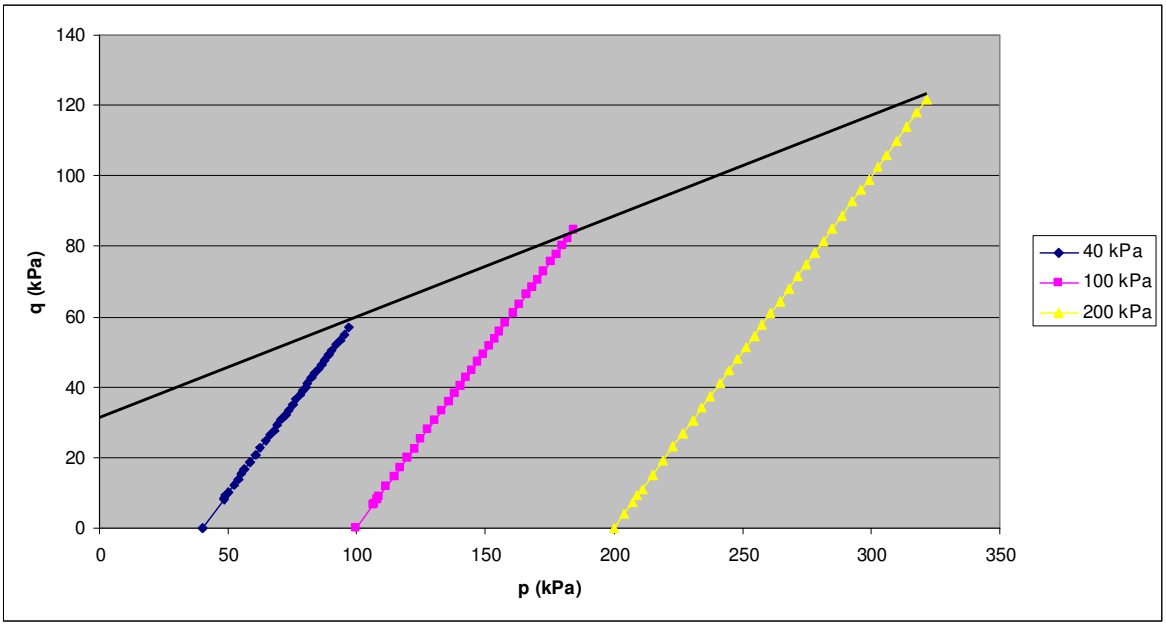

Figure 5.86. p-q graph of specimen containing 100 per cent tire buffings

5.3.9. Mixture Containing 5 per cent Tire Buffings

5 per cent tire buffings by weight is added to sand, to form the specimen to be tested. The sample has a unit weight of 14.7 kN/m³. The deviator stress-strain diagram is shown in Figure 5.87. At failure, the peak deviator stresses are 177.8, 409.7, and 774.9 kPa, and the axial strains are 5.81 per cent, 8.79 per cent, and 12.32 per cent. The Mohr-circle diagram (Figure 5.89) reveals that the cohesion value of the specimen is 5.51 kPa, and the angle of internal friction of the specimen is 41.07 degrees. The p-q graph of the specimen is shown in Figure 5.90. The cohesion and friction angle values can also be obtained from the p-q graph. Using experimental data, the equivalent angle of internal friction is calculated as 42.02 degrees. The specimen shows a dilatant volumetric strain behavior (Figure 5.88). At the same axial strain, higher volumetric strain can be observed under lower confining pressures. The specimens show almost a linear increase up to reaching 4 per cent of volumetric strain.

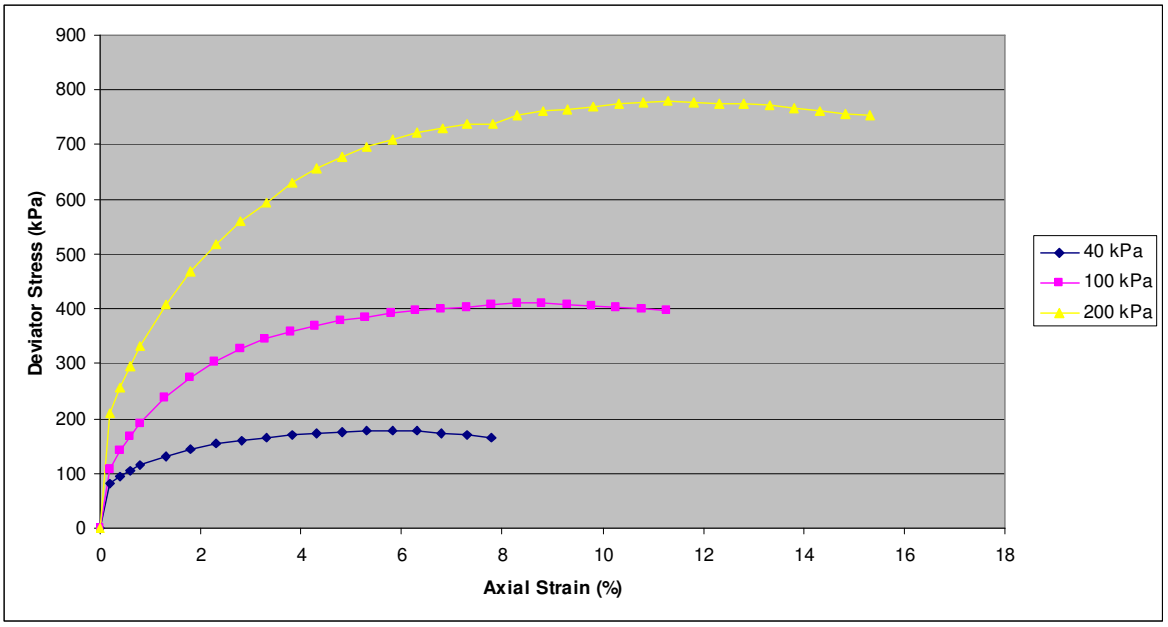

Figure 5.87. Deviator stress-axial strain behavior of specimen containing 5 per cent tire buffings

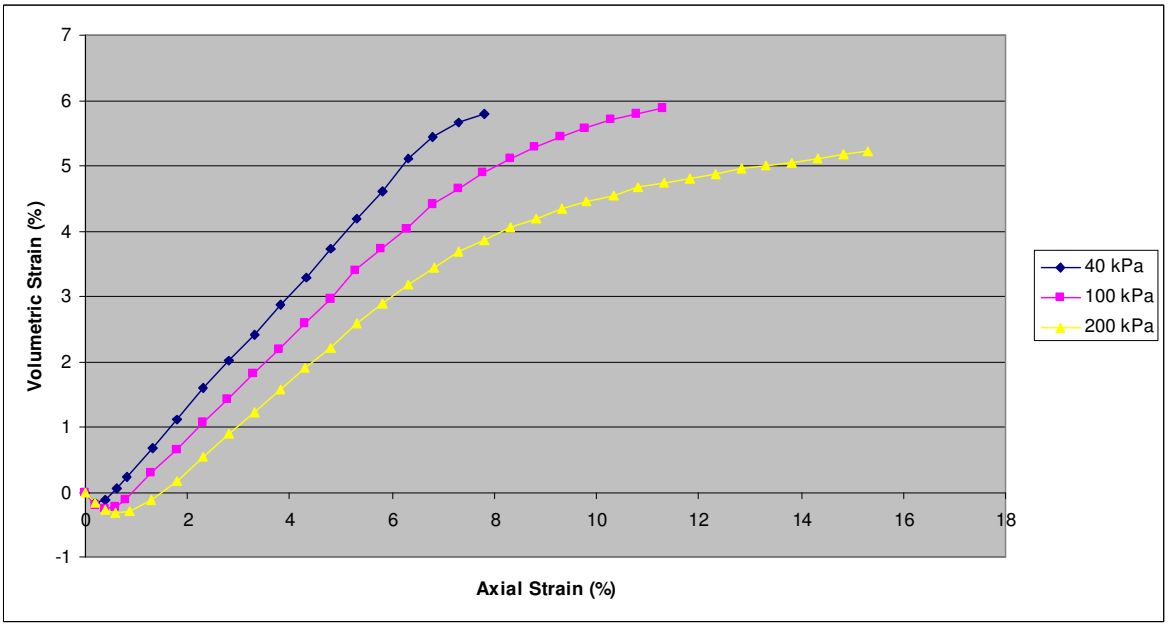

Figure 5.88. Volumetric strain of specimen containing 5 per cent tire buffings

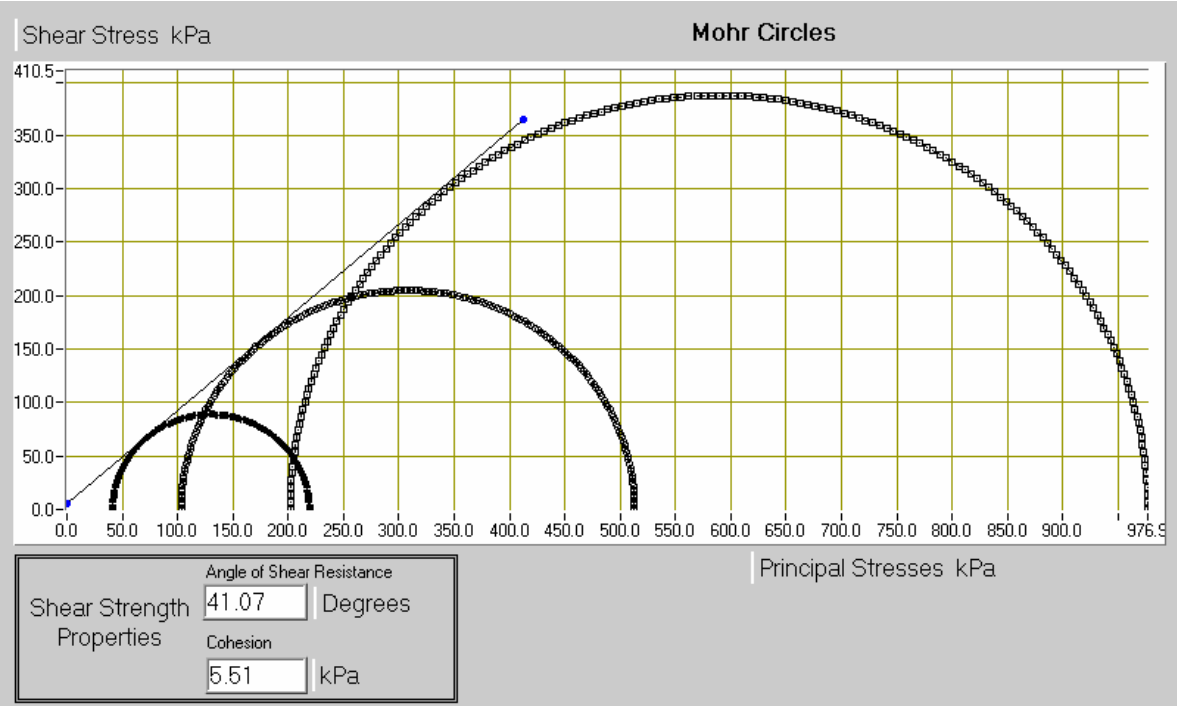

Figure 5.89. Shear strength envelope of specimen containing 5 per cent tire buffings

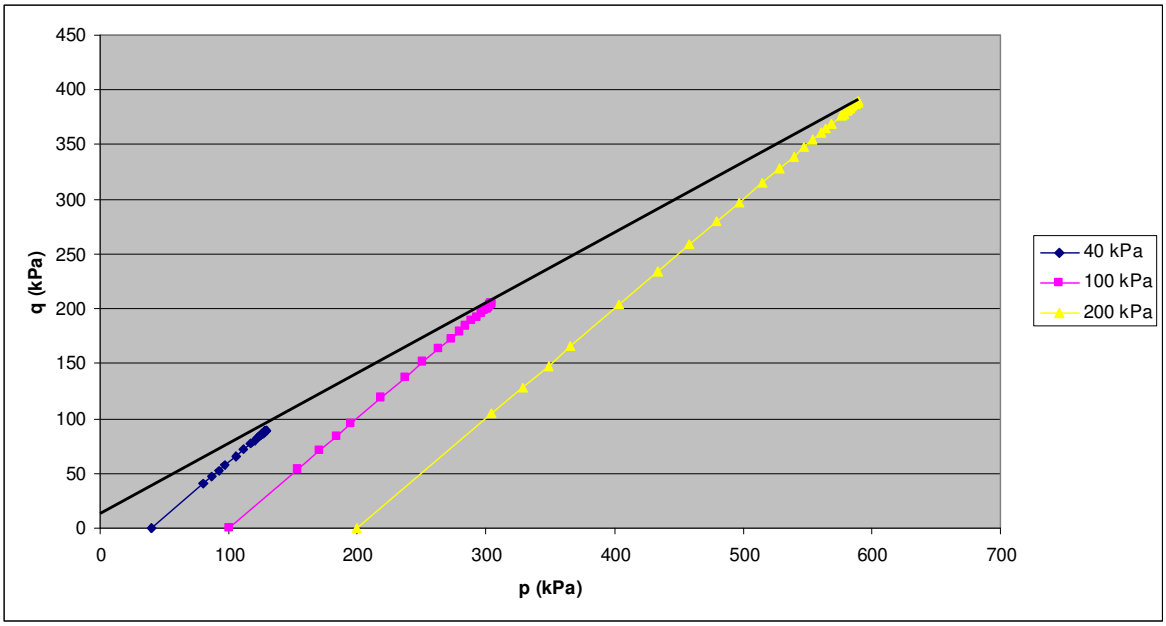

Figure 5.90. p-q graph of specimen containing 5 per cent tire buffings

5.3.10. Mixture Containing 10 per cent Tire Buffings

The specimen to be tested is prepared by adding 10 per cent tire buffings by weight to sand. The unit weight of the mixture is 13.7 kN/m³. At the beginning of the test both the specimen tested under 100 kPa confining pressure and the specimen tested under 200 kPa confining pressure show a sudden increase in stress. Figure 5.91 shows the deviator stress-strain graph of the sample. The maximum deviator stresses observed are 173.7, 352.3, and 591.7 kPa, and the corresponding axial strain values are 9.78 per cent, 13.29 per cent, and 12.30 per cent. From the shear strength envelope (Figure 5.93), the cohesion value is found as 15.64 kPa, and the angle of internal friction as 35.10 degrees. Figure 5.94 shows the p-q graph of the specimen, which gives the same shear strength parameters as the Mohr failure diagram. The equivalent angle of internal friction is computed as 38.12 degrees. The specimen shows a dilatant volumetric behavior (Figure 5.92).

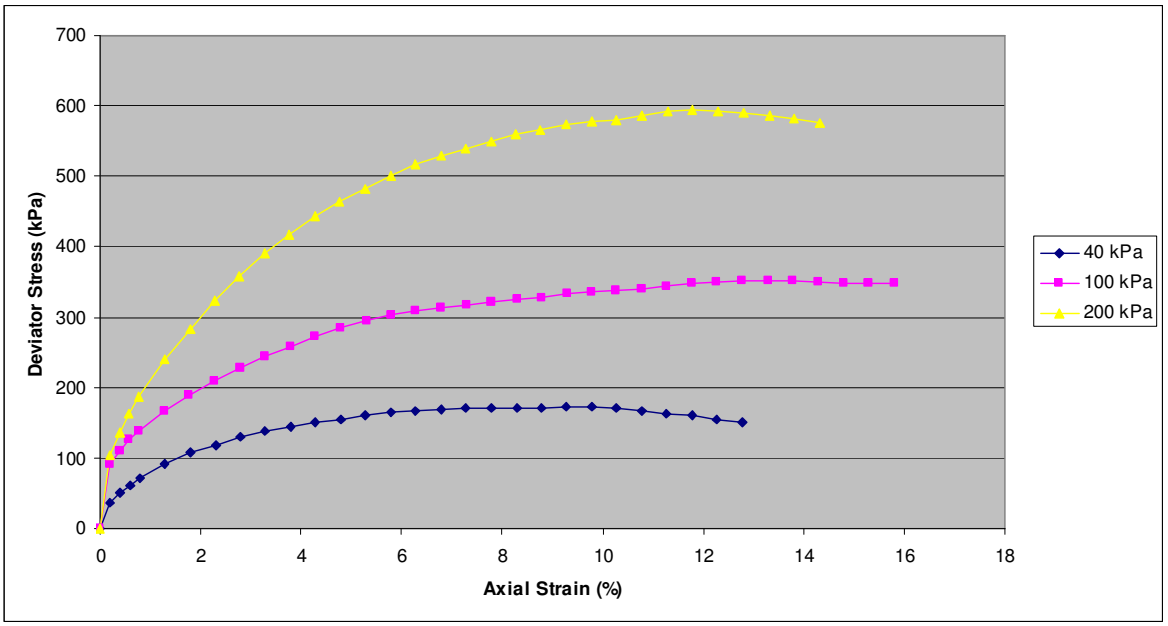

Figure 5.91. Deviator stress-axial strain behavior of specimen containing 10 per cent tire buffings

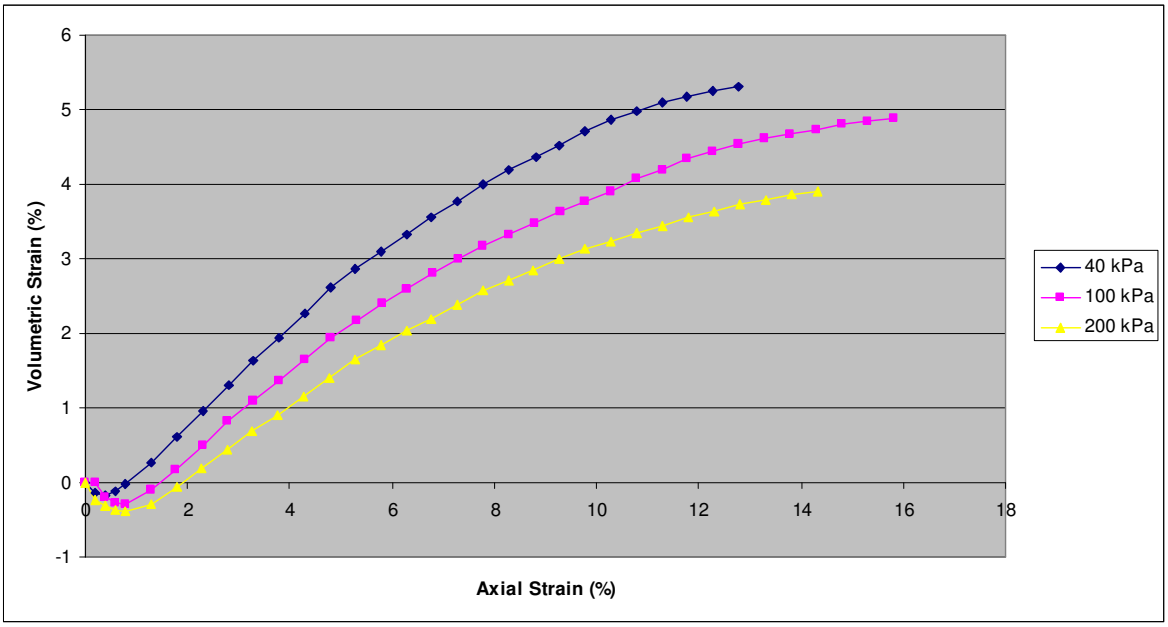

Figure 5.92. Volumetric strain of specimen containing 10 per cent tire buffings

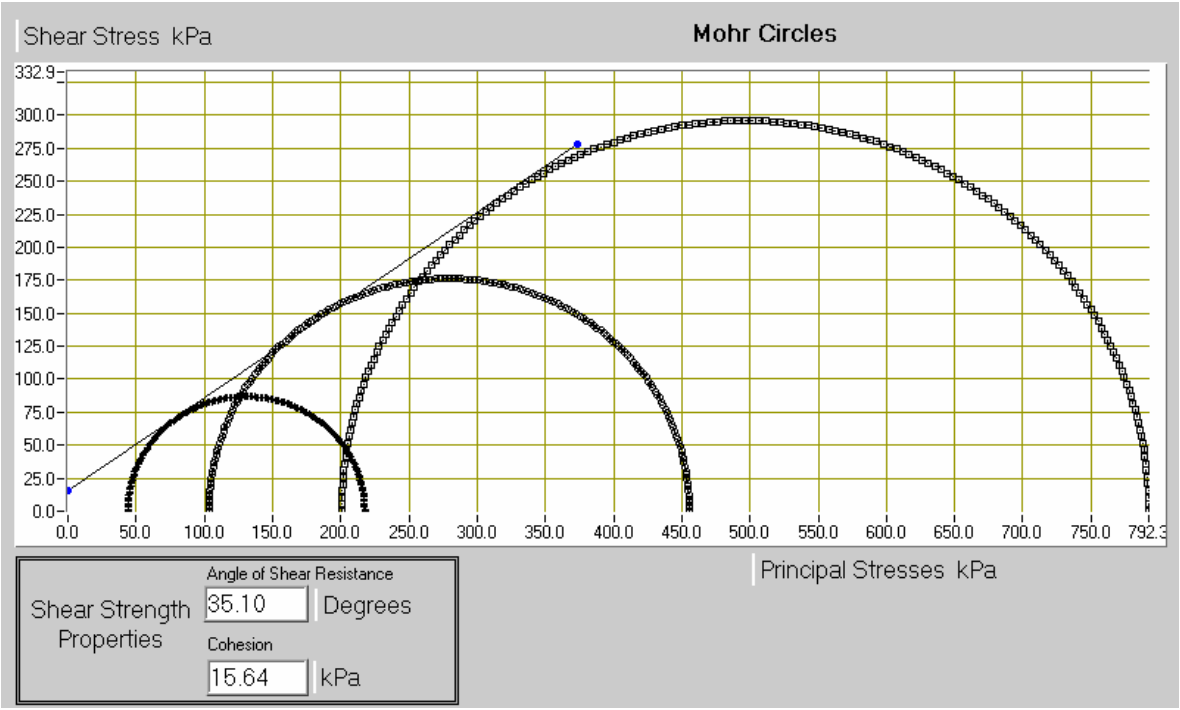

Figure 5.93. Shear strength envelope of specimen containing 10 per cent tire buffings

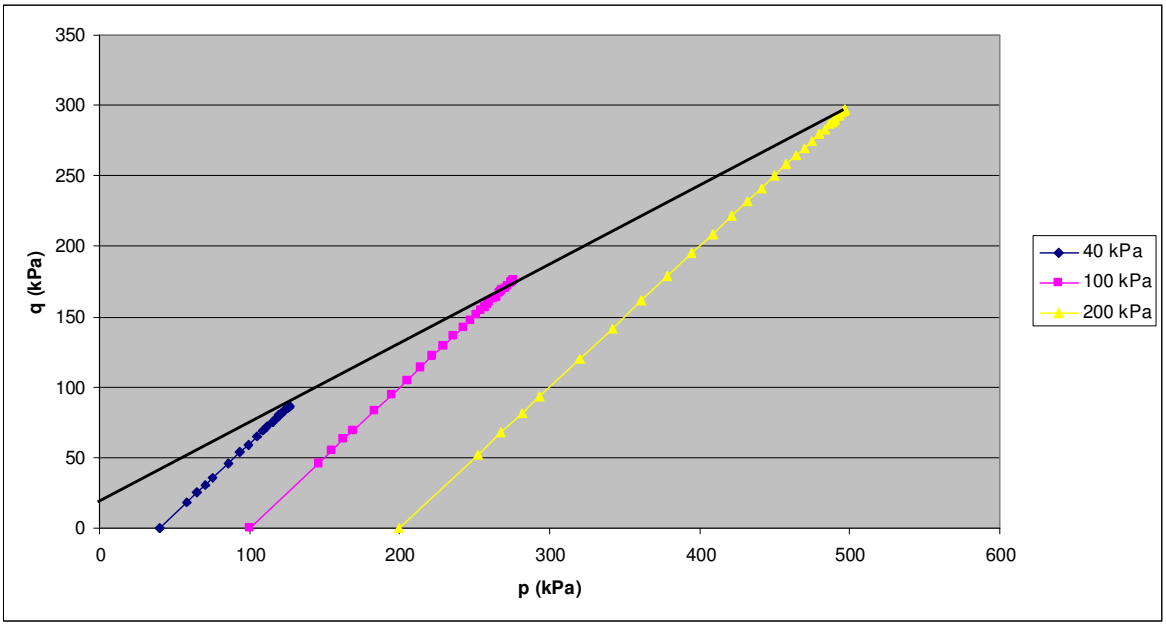

Figure 5.94. p-q graph of specimen containing 10 per cent tire buffings

5.3.11. Mixture Containing 20 per cent Tire Buffings

The specimen is composed of 20 per cent tire buffings by weight and sand. The unit weight of the sample is 14.74 kN/m³. The deviator stress-strain diagram (Figure 5.95) reveals that the peak stress ranges between 10 per cent and 15 per cent axial strains for tests at different confining pressures. Up to 0.8 per cent axial strain the tests conducted at confining pressures of 100 and 200 kPa show similar stress increase. At failure, the maximum deviator stresses observed are 164.6, 320.7, and 547.3 kPa. From the Mohr-circle diagram (Figure 5.97), the cohesion value is observed as 14.74 kPa, and the friction angle as 33.88 degrees. The shear strength parameters can also be obtained from the p-q graph shown in Figure 5.98. Using regression analysis, the equivalent angle of internal friction is 36.78 degrees. The samples composed of 20 per cent tire buffings show a dilatant volumetric strain behavior after a small initial loss of volume (Figure 5.96). The volumetric behavior is approximately linear under a confining pressure of 200 kPa.

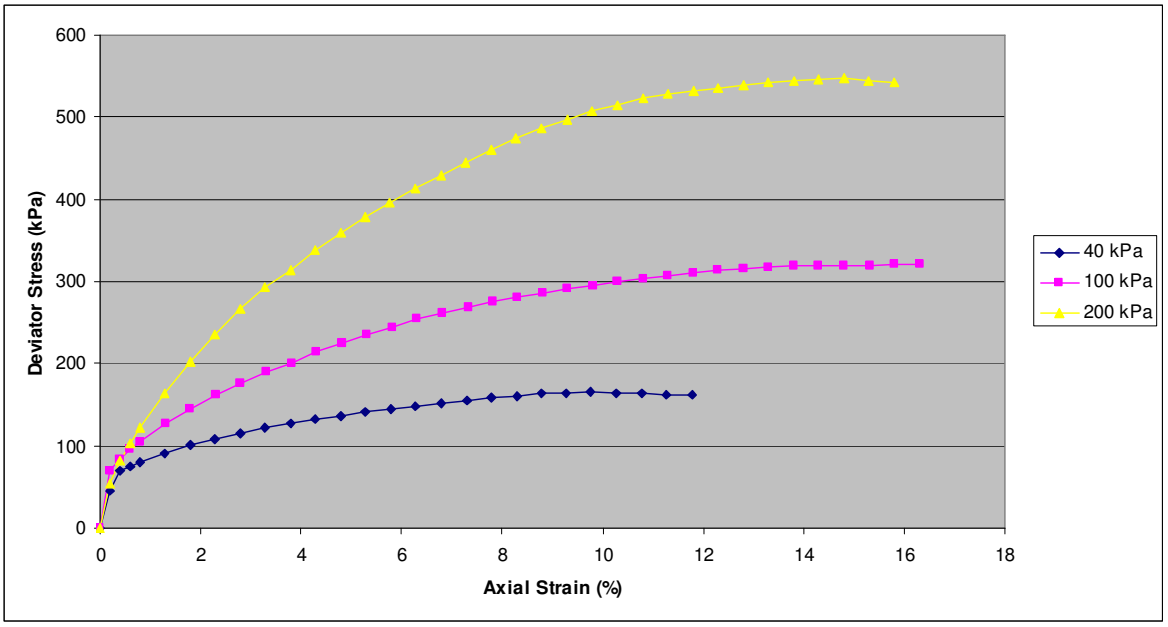

Figure 5.95. Deviator stress-axial strain behavior of specimen containing 20 per cent tire buffings

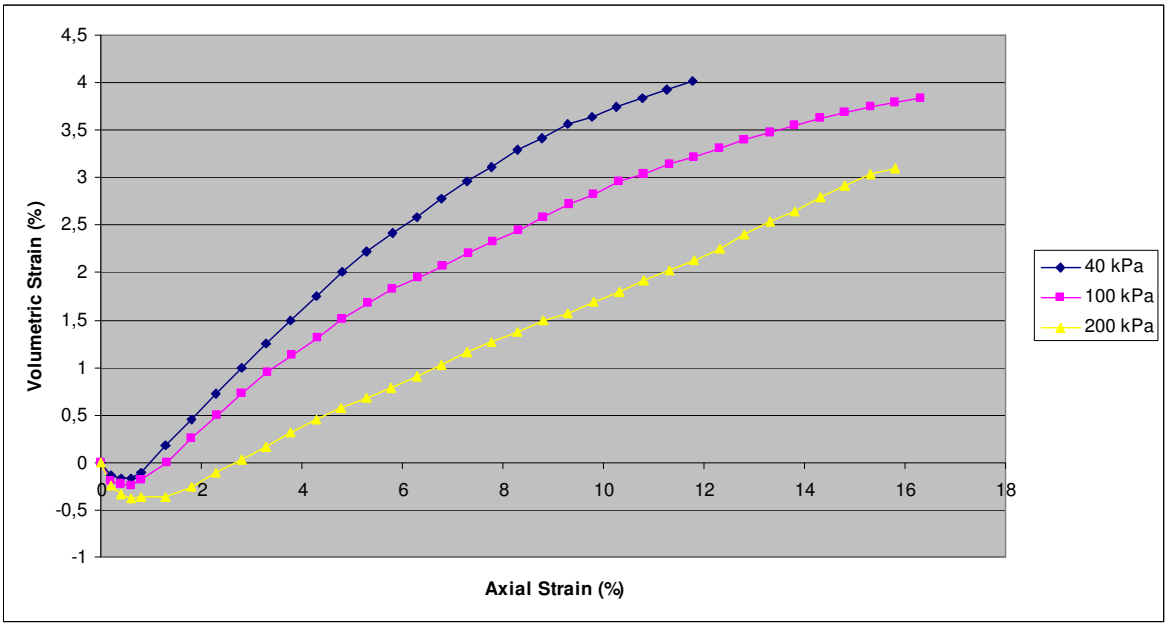

Figure 5.96. Volumetric strain of specimen containing 20 per cent tire buffings

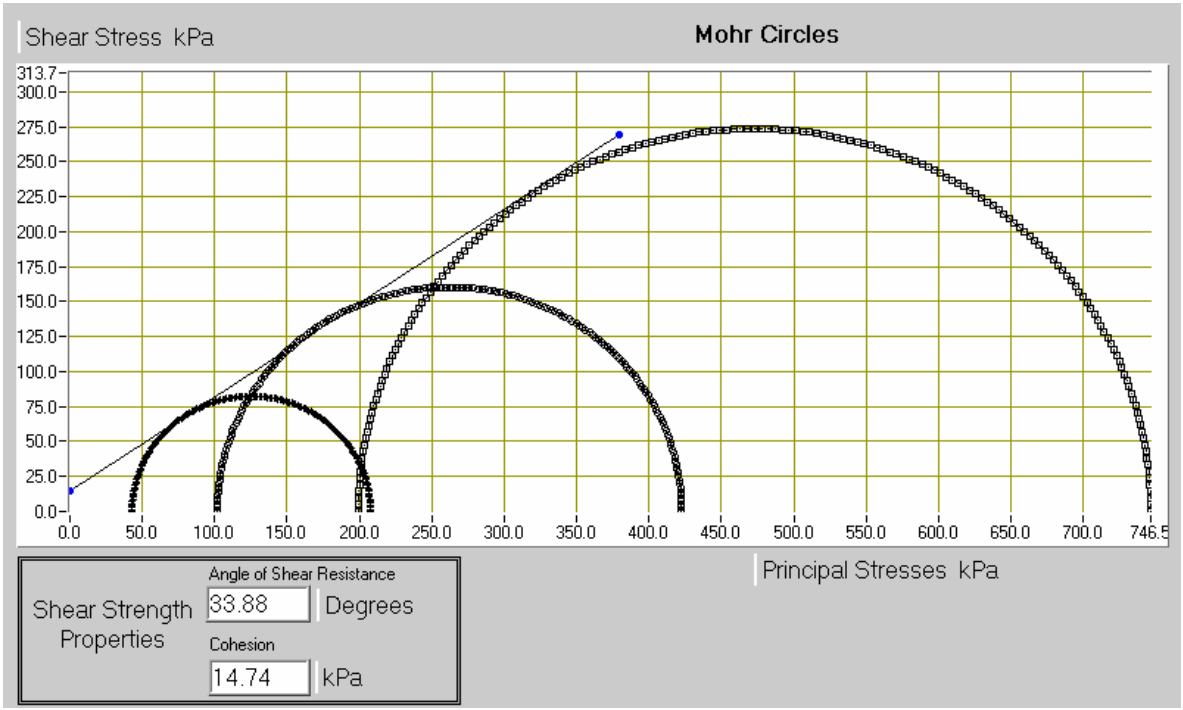

Figure 5.97. Shear strength envelope of specimen containing 20 per cent tire buffings

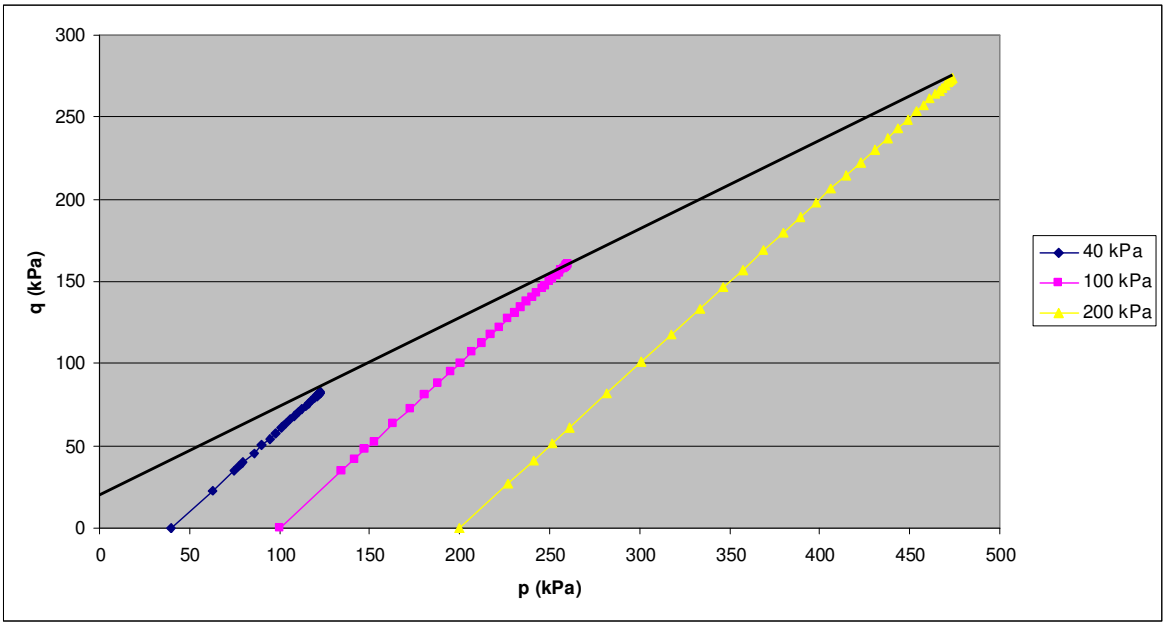

Figure 5.98. p-q graph of specimen containing 20 per cent tire buffings

5.3.12. Mixture Containing 30 per cent Tire Buffings

30 per cent tire buffings by weight is mixed with sand. The mixture has a unit weight of 10.3 kN/m³. No peak stress is observed for all three of the tests up to an axial strain of 15 per cent (Figure 5.99). The test under a confining pressure of 200 kPa shows a steep increase in stress up to 2 per cent axial strain. The corresponding deviator stress values for the tests at 15 per cent axial strain are 130.4, 256.2, and 446.1 kPa. According to the failure envelope (Figure 5.101), the cohesion value is 11.83 kPa, and the angle of internal friction value is 30.47 degrees. Figure 5.102 shows the p-q graph of the specimen, from which the same shear strength parameters can be obtained. The equivalent friction angle is calculated as 33.12 degrees. The specimens show a dilatant volume change behavior after a small initial loss of volume (Figure 5.100). Under a confining pressure of 200 kPa, larger volume loss can be observed at the beginning of the test.

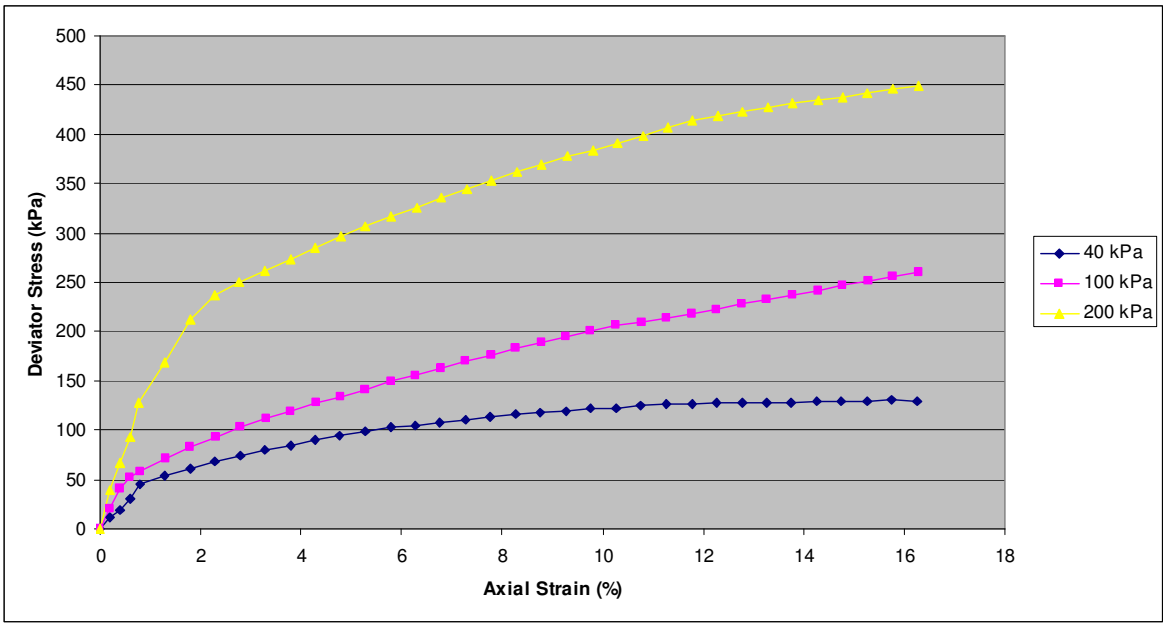

Figure 5.99. Deviator stress-axial strain behavior of specimen containing 30 per cent tire buffings

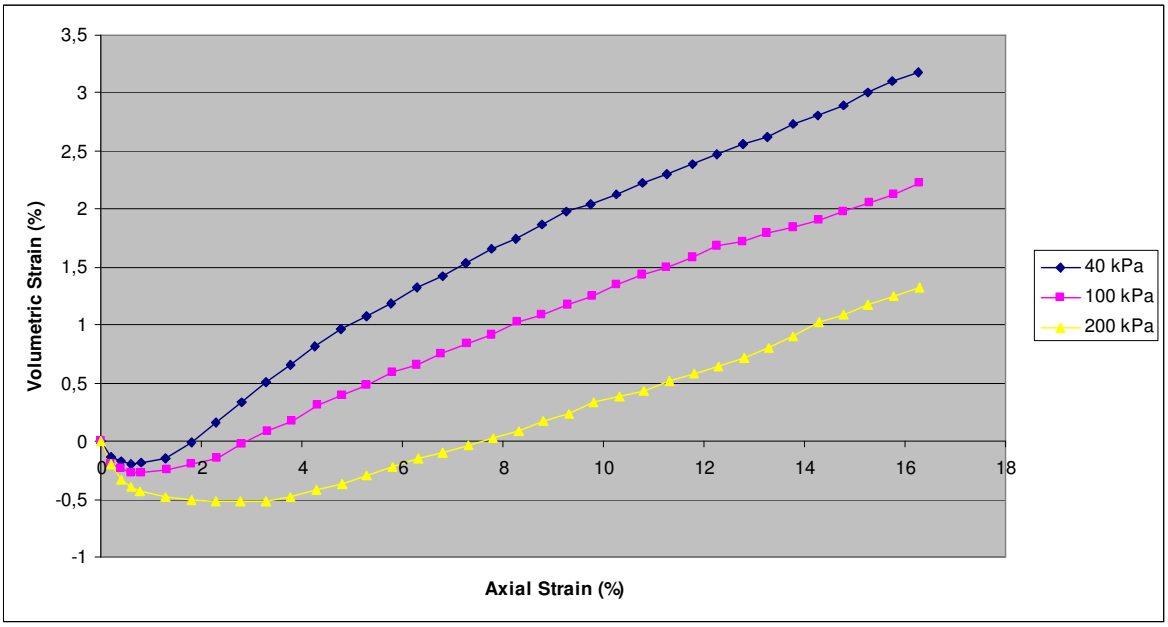

Figure 5.100. Volumetric strain of specimen containing 30 per cent tire buffings

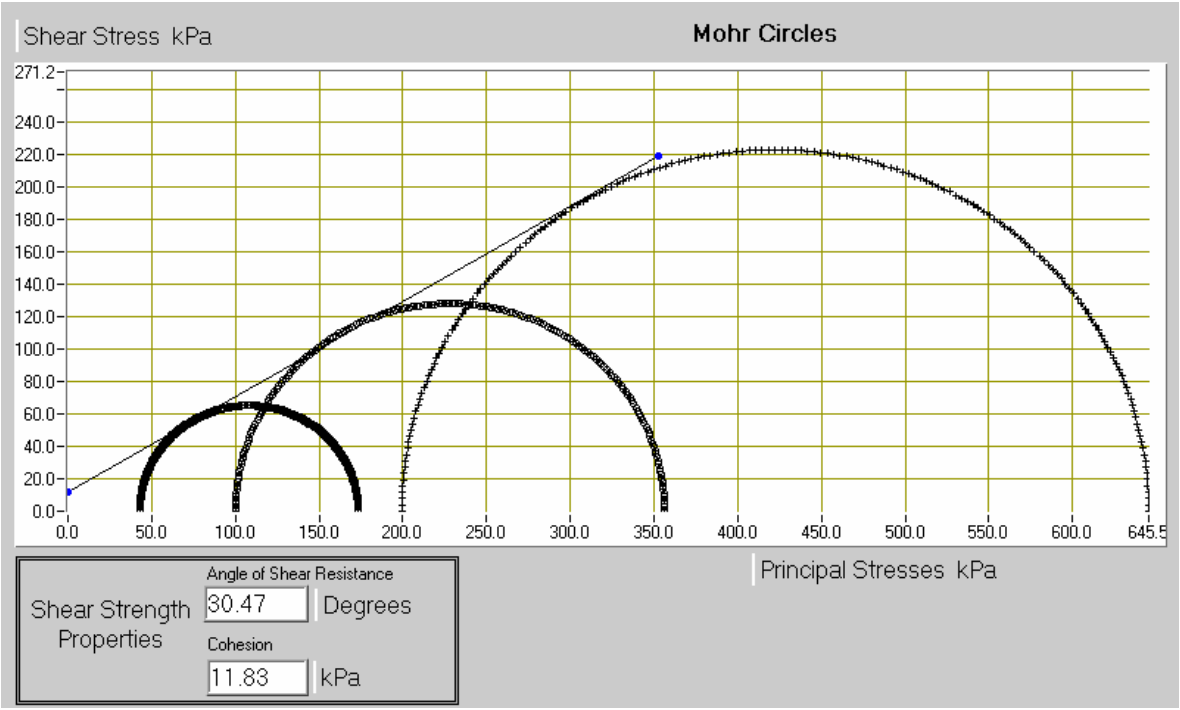

Figure 5.101. Shear strength envelope of specimen containing 30 per cent tire buffings

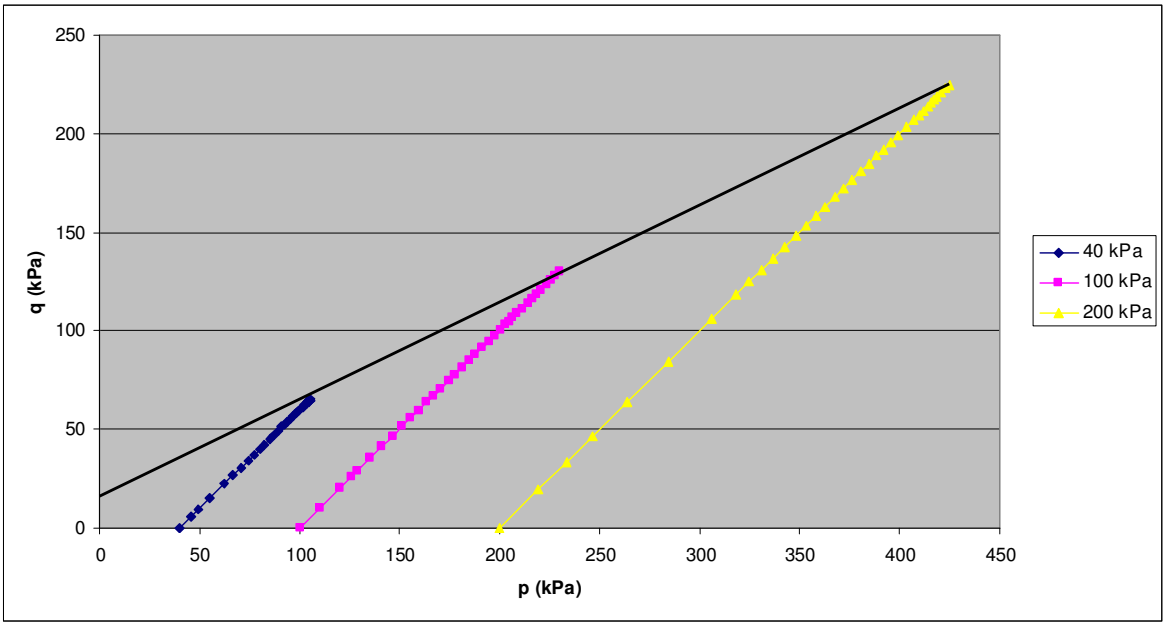

Figure 5.102. p-q graph of specimen containing 30 per cent tire buffings

5.3.13. Mixture Containing 40 per cent Tire Buffings

Finally, 40 per cent tire buffings by weight is added to sand, to form a specimen to be tested. The unit weight of the sample is 9.1 kN/m³. It is shown in the deviator stress-strain graph that (Figure 5.103) no peak deviator stress occurs in any of the three tests, and the stress keeps increasing with increasing strain for the duration of the tests. It is observed that up to 1.5 per cent axial strain the first two tests (40 kPa and 100 kPa confining pressures) show similar stress behavior. The deviator stress values corresponding to 15 per cent axial strain are 145.9, 223.0, and 359.0 kPa. Figure 5.105 shows the shear strength envelope of the specimen. The results lead us to a cohesion value of 28.05 kPa, and an internal friction angle of 24.36 degrees. Using regression analysis, the equivalent angle of internal friction is computed as 31.27 degrees. The p-q graph is also drawn and is shown in Figure 5.106. The same cohesion and internal friction angle values are also found from the p-q graph. The specimen shows an initial loss of volume, showing a contractive behavior first and then varying levels of dilation can be observed for different confining pressures (Figure 5.104). Under 200 kPa confining pressure, the specimen shows a contractive behavior.

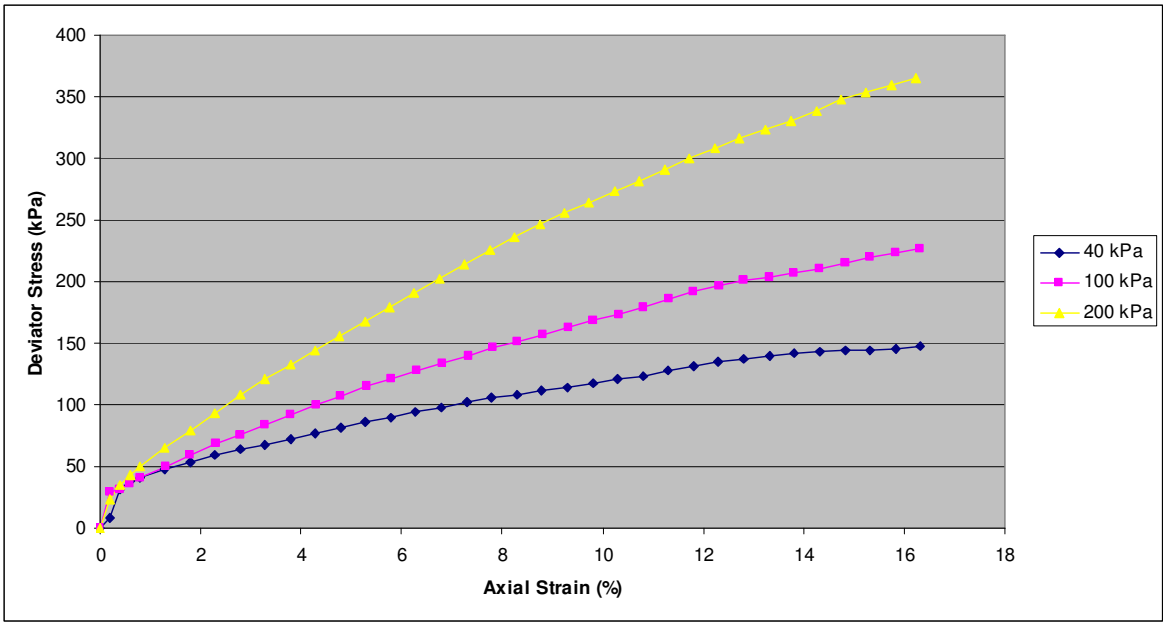

Figure 5.103. Deviator stress-axial strain behavior of specimen containing 40 per cent tire buffings

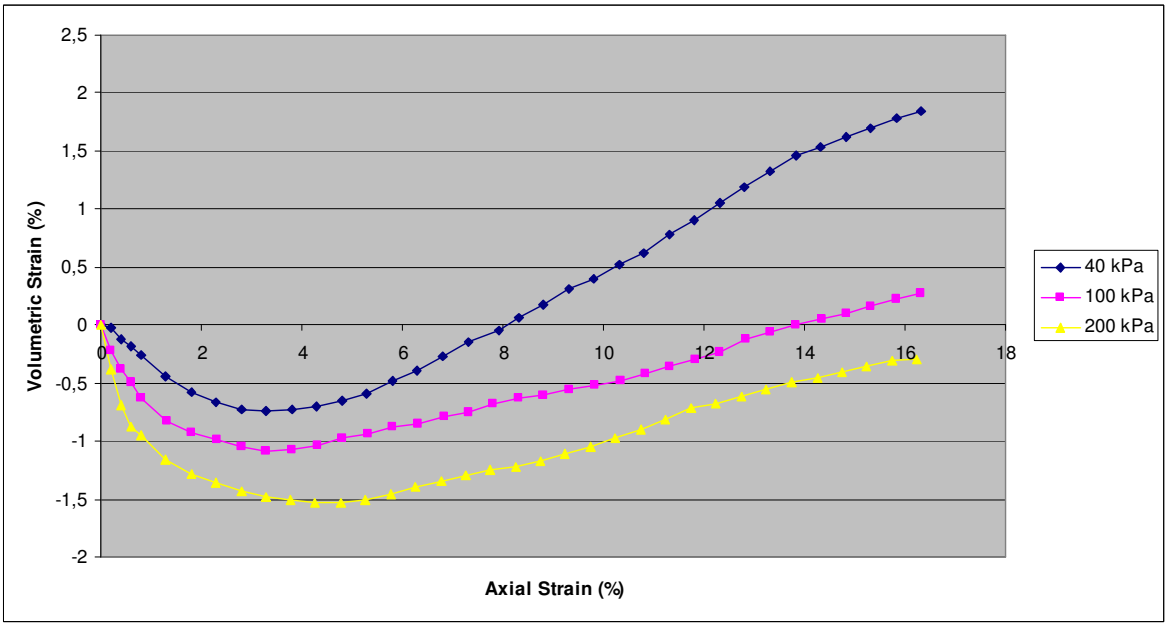

Figure 5.104. Volumetric strain of specimen containing 40 per cent tire buffings

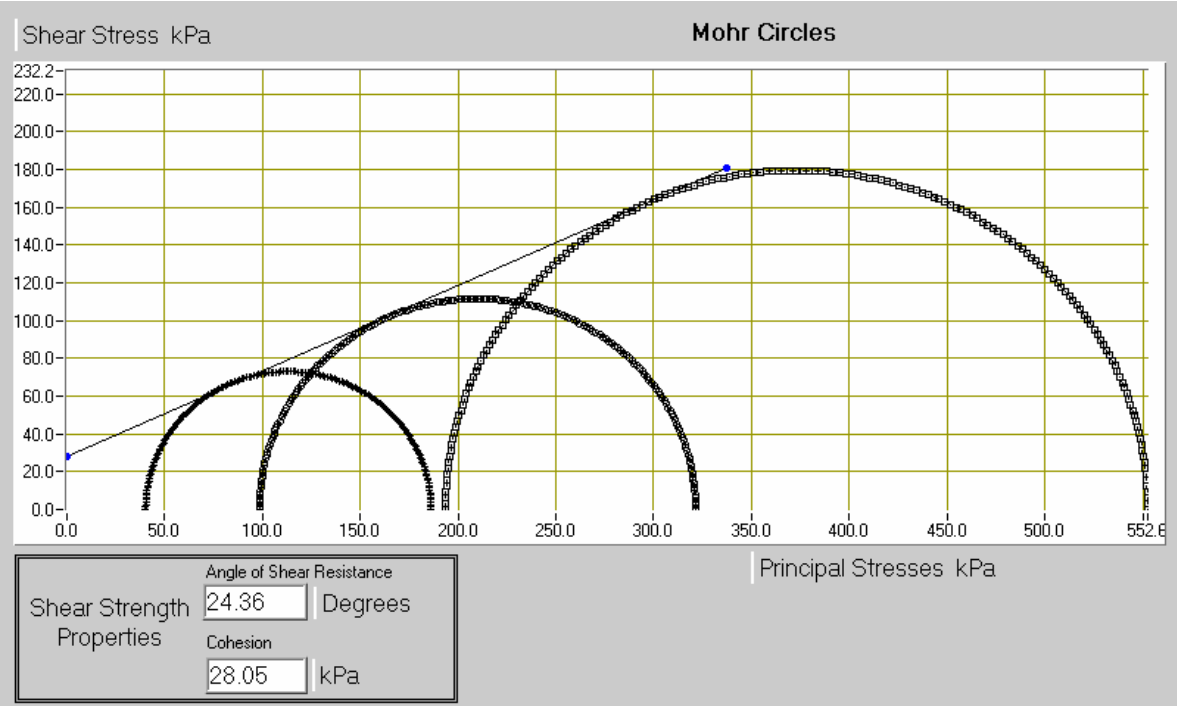

Figure 5.105. Shear strength envelope of specimen containing 40 per cent tire buffings

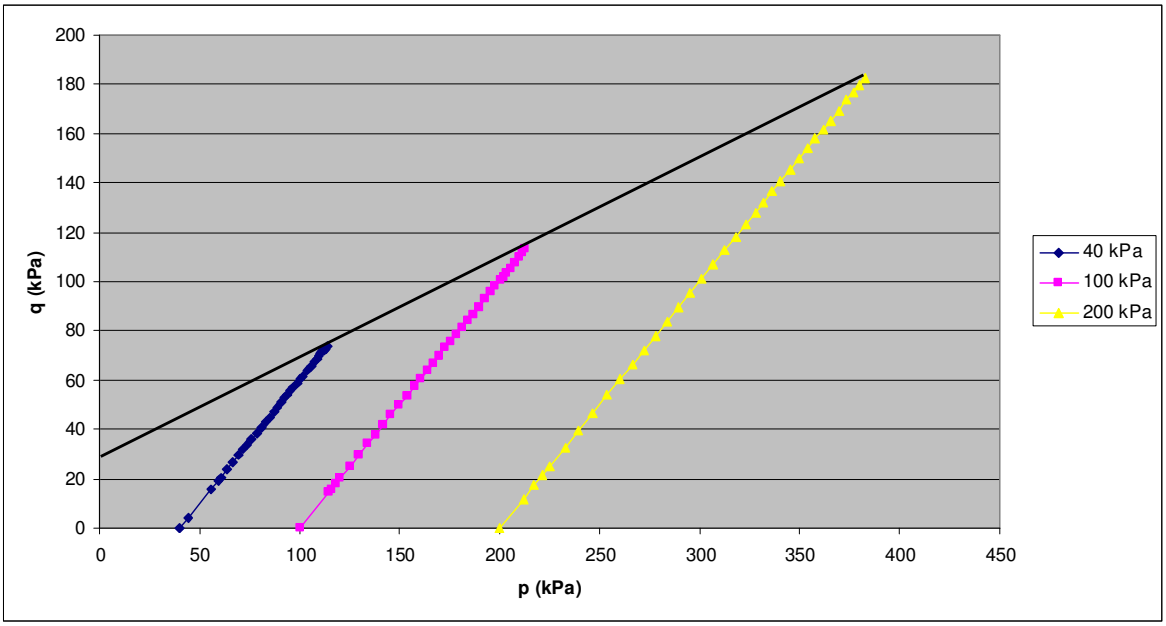

Figure 5.106. p-q graph of specimen containing 40 per cent tire buffings

5.3.14. Analysis of Consolidated Drained Triaxial Test Results

A total of 13 sets of consolidated drained (CD) triaxial tests are conducted on sand, tire crumb, tire buffings, and sand-tire waste compositions with varying tire content. Each test is repeated at three different confining stresses of 40, 100, and 200 kPa. The effect of tire percentage, tire aspect ratio, and tire shape on the shear strength parameters of the specimen is investigated. Tire waste-sand specimens are prepared at 5, 10, 20, 30, and 40 per cent of tire waste content by weight. Tire buffings is a fiber shaped material with an aspect ratio about 3.5-4, and tire crumb is a granular material with an aspect ratio about 1-1.5. The deviatoric stress-strain behaviors, the volumetric strain behaviors and the shear strength parameters of the specimens are investigated.

According to the experimental results, the deviator stress-axial strain graph (Figure 5.55) of pure sand specimens show peak shear stress values of 183.2, 418.1, and 824.2 kPa around 5-6 per cent axial strain. Sand specimens show a dilatant volumetric strain behavior (Figure 5.56). Next, pure tire crumb and pure tire buffings specimens show an approximately linear deviator stress-strain behavior for the confining pressures used in this study (Figure 5.59, Figure 5.83). No peak deviator stresses are observed for both types of the pure tire specimens, so the shear strength is defined from the shear stress at 15 per cent axial strain following ASTM D4767-95. Other investigators (Lee et al., 1999; Zornberg et al., 2004) also reported that pure tire waste specimens show an approximately linear stress-strain behavior regardless of the tire type. The volumetric strain behaviors of pure tire waste specimens are also approximately linear and contractive (Figure 5.60, Figure 5.84). Specimens prepared with 5 per cent, 10 per cent, and 20 per cent tire waste content by weight show a dilatant volumetric strain behavior (Figure 5.64, Figure 5.68, Figure 5.72, Figure 5.88, Figure 5.92, Figure 5.96), and peak deviator stresses (Figure 5.63, Figure 5.67, Figure 5.71, Figure 5.87, Figure 5.91, Figure 5.95). Specimens composed of sand and relatively high amount of (30 per cent and 40 per cent by weight) tire crumb show tire-like stress-strain behavior under high confining pressures, and sand-like stress-strain behavior under low confining pressures (Figure 5.75, Figure 5.79). On the other hand, in the experiments on specimens prepared with mixing a relatively high amount of (30 per cent and 40 per cent by weight) tire buffings and sand, no peak deviator stresses are observed (Figure 5.99, Figure 5.103), and the deviator stress continued to increase with increasing

axial strain at any confining pressure. For both of the tire inclusions, specimens containing 30 per cent tire waste by weight show a dilatant volumetric strain behavior (Figure 5.76, Figure 5.100). However, specimens containing relatively higher amount of tire waste (40 per cent by weight) show a contactive volumetric strain behavior (Figure 5.80, Figure 5.104). An initial loss of volume and some dilatant behavior is observed for specimens containing 40 per cent tire crumb by weight under low confining pressures. It is also determined that in the range of these aspect ratios the volumetric strain behaviors of tire crumb and tire buffings show similar characteristics, which is in good agreement with the report of Zornberg et al. (2004) who investigated the volumetric strain behavior of specimens composed of tire shreds with aspect ratios of 1, 2, 4, and 8. They reported that tire shred specimens having an aspect ratio of 1, 2, and 4 showed similar volumetric strain behaviors. It is also determined that in all tests a higher confining pressure leads to a higher deviator stress, and a less dilatant (more contractive) volumetric behavior.

For the tests conducted using tire crumb, the cohesion values vary from 12.72 to 30.17 kPa, and for the tests performed using tire buffings, the cohesion values vary from 11.83 to 29.51 kPa (Table 5.3). These values are not real cohesions but intercept (apparent) cohesion values resulting from the simplistic Mohr-Coulomb linear model, as mentioned by other researchers (Humprey et al., 1993; Gotteland et al., 2005). The angle of internal friction values varies from 17.56º to 39.35º for specimens with tire crumb additions, and from 16.62º to 41.07º for specimens with tire buffings additions (Table 5.3). To compare and evaluate the test results, the equivalent friction angles are calculated using regression analysis as described before. This method was used and suggested by several investigators (Zornberg et al., 2004; Gotteland et al., 2005).

The effect of tire content, tire aspect ratio, and tire shape on the shear strength of tire waste-sand mixtures is evaluated using the experimental data. The results indicate that for both tire crumb and tire buffings additions the shear strength parameters giving the maximum shear strength can be obtained at a tire content of 5 per cent (Table 5.3). With the addition of 5 per cent tire buffings by weight a cohesion value of 5.51 kPa, a friction angle of 41.07 degrees, and a calculated equivalent friction angle of 42.02 degrees are obtained, and with the addition of 5 per cent tire crumb by weight a cohesion value of 16.13 kPa, a friction angle of 39.35 degrees, and a calculated equivalent friction angle of

41.99 degrees is obtained. The shear strength value decreases for tire contents beyond 5 per cent by weight. However, it is observed that 5 per cent addition of tire buffings, results in a greater increase in the shear strength parameters, compared to the addition of tire crumb (Table 5.3). It can be stated that, the fiber shaped tire inclusions with an aspect ratio of 3.5-4 influences the shear strength parameters better compared to granular tire inclusions with an aspect ratio of 1-1.5. Michalowski et al. (2003) reported that the larger the aspect ratio, the more effective the reinforcements are. Zornberg et al. (2004) reported that at high percentages of tire content, the shear among individual tire particles governs the shear strength of the mixture, leading to a lower overall shear strength.

The summary of test results is shown in Table 5.3. The effects of tire content on shear strength parameters are shown in Figure 5.107, Figure 5.108, and Figure 5.109. Figure 5.107 shows that the maximum cohesion value which is 30.17 kPa is obtained from the specimen containing pure tire crumb. The minimum cohesion value is 1.45 and it is obtained from the specimen containing pure sand. It can also be seen that at low percentages of tire content (5 per cent and 10 per cent), the specimens containing tire buffings have a smaller cohesion value compared to the specimens containing tire crumb. As the tire content increases, the specimens containing both tire buffings and tire crumb show similar cohesion values. Figure 5.108 shows the variation of the internal friction angle with the changing tire content. Figure 5.109 shows the effect of tire content on the equivalent friction angle of the specimens, which is a parameter used by several researchers (Zornberg et al., 2004; Gotteland et al., 2005) who conducted consolidated drained tests on sand-tire waste mixtures. The equivalent friction angle is obtained by forcing the apparent cohesion to be equal to zero. The maximum equivalent friction angle is obtained from specimens containing 5 per cent tire buffings by weight which is 42.02 degrees, and the lowest equivalent friction angle is 24.89 degrees and it is obtained from specimens containing pure tire buffings.

Table 5.4 shows the comparison of results obtained in this study with the studies of other researchers including direct shear tests as well as triaxial tests. Zornberg et al. (2004) conducted large scale consolidated drained triaxial tests on mixtures composed of tire shreds and sand, and Gotteland et al. (2005) carried out large scale consolidated drained triaxial tests on mixtures composed of tire chips and sand. Since consolidated drained tests

are performed in this study using tire crumb and tire buffings as tire inclusions, a graphical comparison of the experimental results with the results obtained by Zornberg et al. (2004) and Gotteland et al. (2005) are presented in Figure 5.110, Figure 5.111, and Figure 5.112. Figure 5.110 shows the variation of cohesion value with varying tire content. The maximum cohesion value is observed as 50 kPa which belongs to the specimen containing 22 per cent tire chips by weight. Figure 5.111 shows the variation of internal friction angle with varying tire content. The maximum internal friction angle is observed for the specimen containing 15 per cent tire chips by weight as 41.1 degrees. Figure 5.112 shows the variation of the calculated equivalent friction angle with varying tire content. The maximum equivalent friction is observed for the specimen containing 22 per cent tire chips by weight as 45 degrees.

Table 5.3. Summary of consolidated drained triaxial test results

Specimen	Deviator Stress (kPa)			c (kPa)	Φ (°)	Φ_{eq} (°)	Unit Weight (kN/m³)
	40 kPa Confining Pressure	100 kPa Confining Pressure	200 kPa Confining Pressure				
Sand	183.2	418.1	824.2	1.45	41.49	41.70	16.0
Tire Crumb	117.9	170.3	250.9	30.17	17.56	25.95	6.5
%5 Tire Crumb	249.9	417.7	751.4	16.13	39.35	41.99	15.1
%10 Tire Crumb	179.9	437.9	684.2	17.38	38.33	41.31	14.5
%20 Tire Crumb	177.4	349.1	592.6	15.60	35.44	38.48	13.3
%30 Tire Crumb	185.2	325.4	618.9	12.72	36.28	38.67	12.5
%40 Tire Crumb	175.1	256.5	422.8	27.85	27.57	33.90	11.2
Tire Buffings	110.1	164.7	235.9	29.51	16.62	24.89	4.6
%5 Tire Buffings	177.8	409.7	774.9	5.51	41.07	42.02	14.7
%10 Tire Buffings	173.7	352.3	591.7	15.64	35.10	38.12	13.7
%20 Tire Buffings	164.6	320.7	547.3	14.74	33.88	36.78	12.1
%30 Tire Buffings	130.4	256.2	446.1	11.83	30.47	33.12	10.3
%40 Tire Buffings	145.9	223.0	359.0	28.05	24.36	31.27	9.1

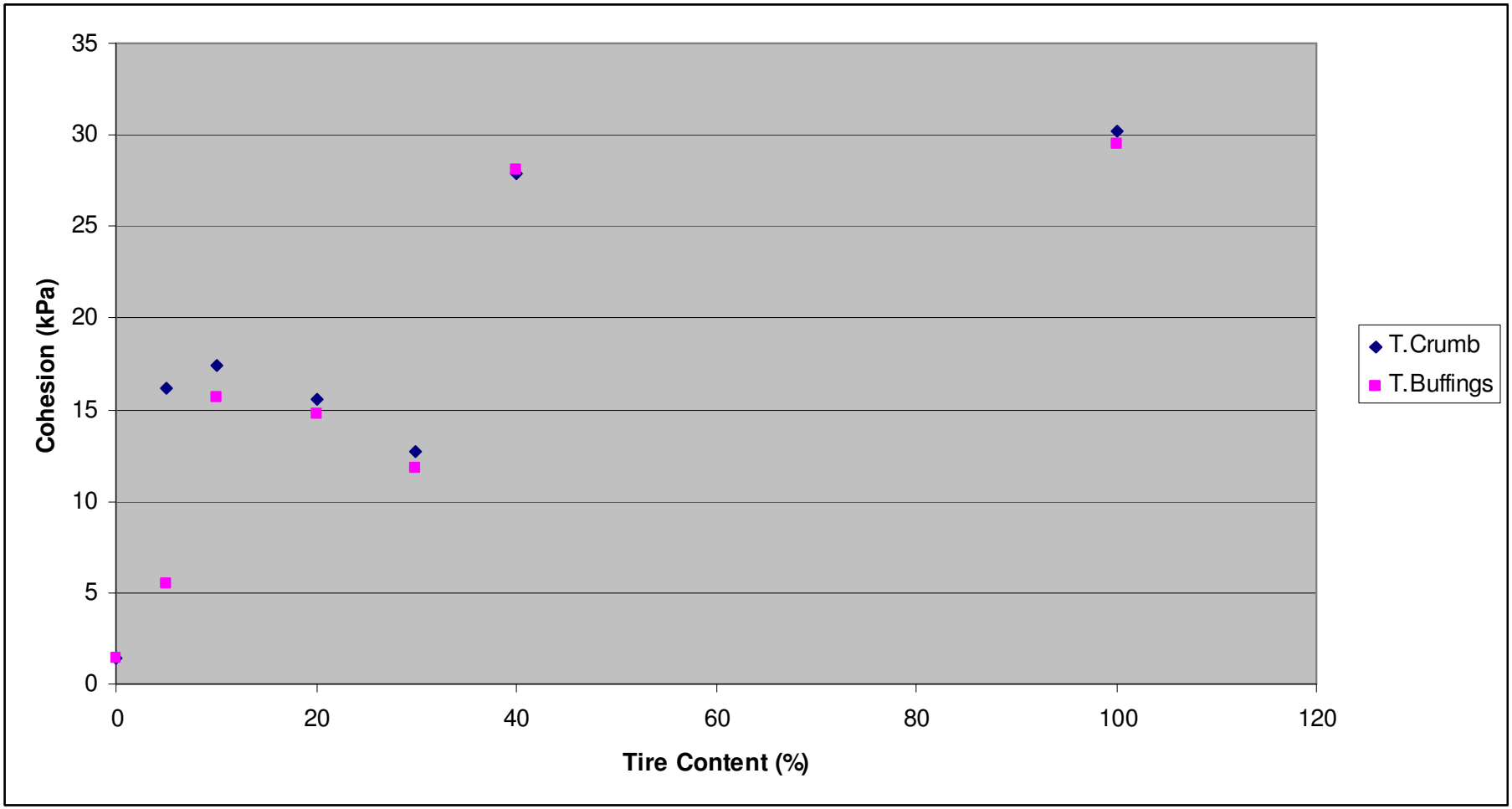

Figure 5.107. Cohesion - tire content diagram of CD triaxial test results

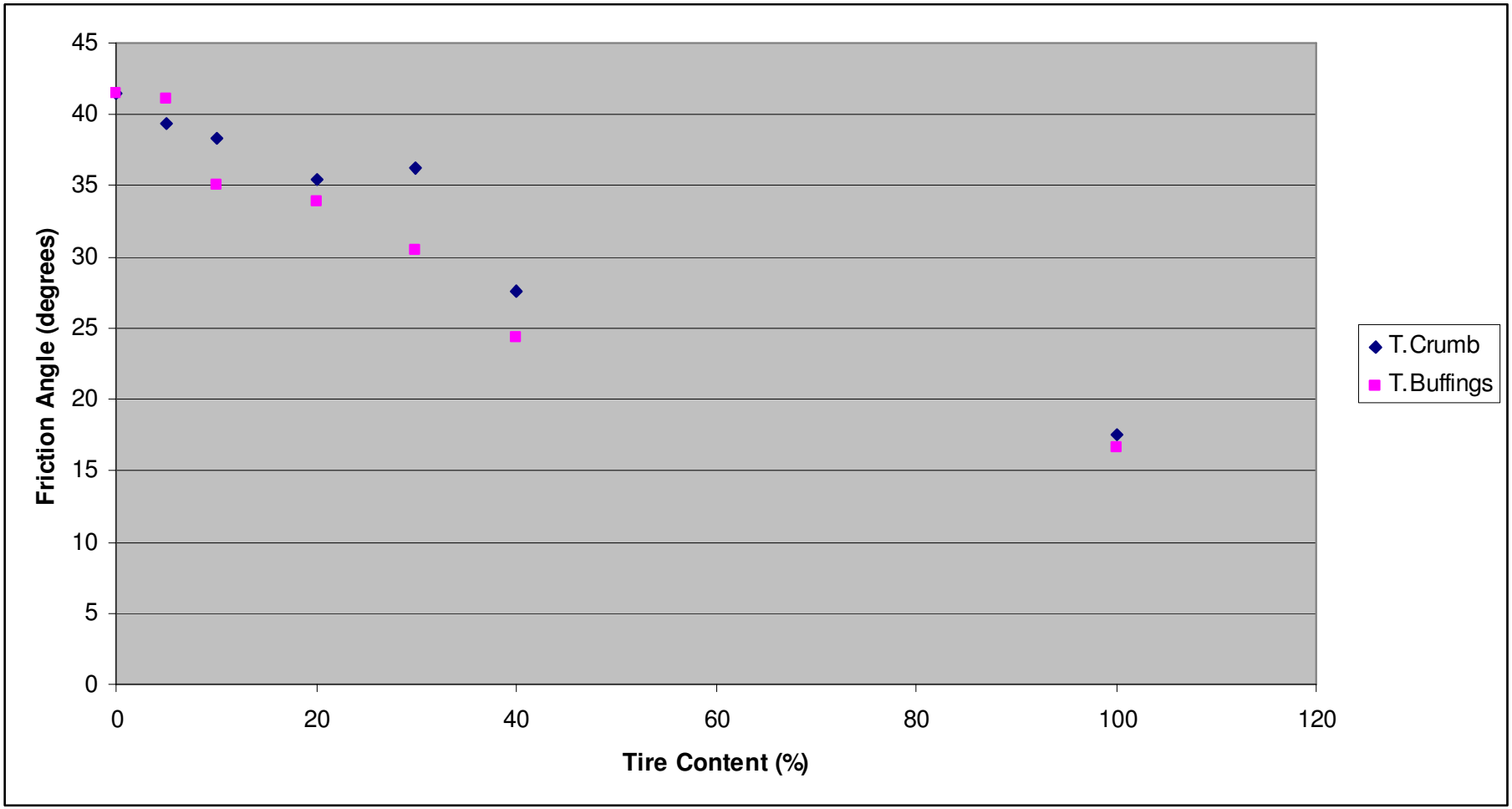

Figure 5.108. Friction angle - tire content diagram of CD triaxial test results

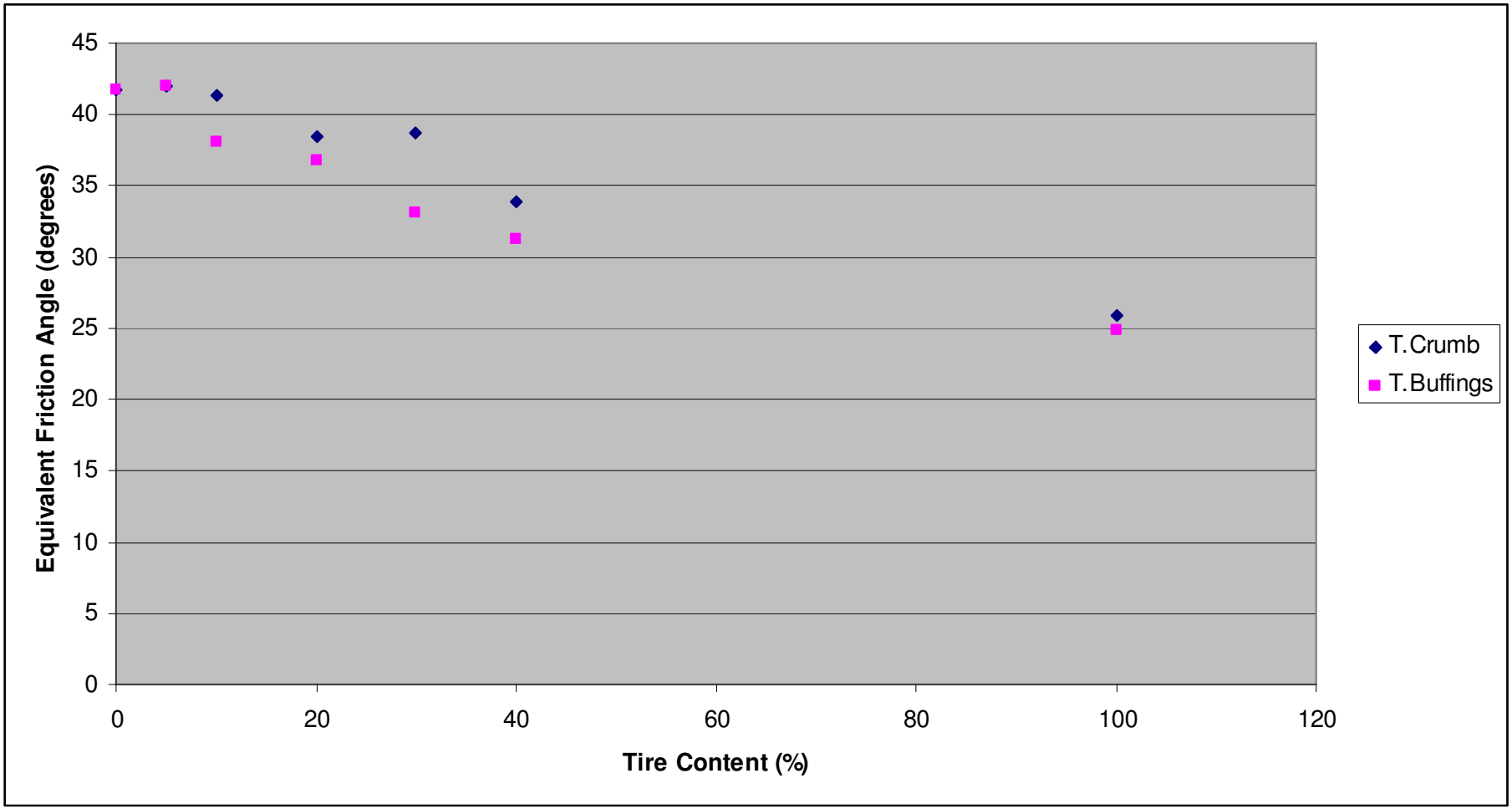

Figure 5.109. Equivalent friction angle - tire content diagram of CD triaxial test results

Table 5.4. Comparison of this study with previous studies

Reference	Test Type	Material	Unit Weight (kN/m³)	c (kPa)	Φ (º)	Φ_{eq} (º)
Edincliler et al. (2004)	Large Scale Direct Shear	Sand	15.3	6.9	33	-
		Tire Buffings	5.1	3.1	22	-
		5% Tire Buffings	15.19	10.4	28	-
		10%TireBuffings	14.89	8.7	29	-
		20% Tire Buffings	14.22	15.5	5	-
		30% Tire Buffings	13.56	10.7	8	-
Zornberg et al. (2004)	Large Scale Triaxial (CD) (48.3, 103.5, 207 kpa) Strain rate= 0.5 mm/min	Sand	15.64	7.8	36.8	37.9
		Sand	16.21	3.8	41.0	41.4
		Tire Shred (12.7mm)	-	22.8	21.4	26.5
		5% Tire Shred	-	7.0	36.1	37.1
		10% Tire Shred	-	21.7	35.7	38.9
		30% Tire Shred	-	30.4	35.7	40.2
		60% Tire Shred	-	18.2	34.4	37.3
		38.3% Tire Shred	-	41.2	36.1	42.0
Gotteland et al. (2005)	Large Scale Triaxial (CD) (50, 75, 100kPa) Strain rate= 2 mm/min	Sand	16.7	0	40.9	40.9
		Tire Chips	6.1	16.3	19	25
		14% Tire Chips	15.5	13.8	39	43
		14% Tire Chips (H)	15.9	15	42.6	44.5
		14% Tire Chips (V)	15.9	7.5	41.7	43.5
		15% Tire Chips (H&V)	15.5	10	41.1	44.5
		22% Tire Chips (H&V)	15.3	50	36.1	45
		50% Tire Chips	11.4	7.5	41.5	43.5

Venkatappa Rao et al. (2006)	Triaxial (CD) (34.5, 69, 138, 276 kPa) Strain rate= 1.016 mm/min (continued)	Sand	16.7 (max.)	0	38	-
		Type 1 Tire Chips (10mm*10mm)				
		5% Tire Chips	-	6.6	39.6	-
		10% Tire Chips	-	9.1	39.7	-
		15% Tire Chips	-	11.5	39.9	-
		20% Tire Chips	-	13.3	40	-
		Type 2 Tire Chips (20mm*20mm)				
		5% Tire Chips	-	9.2	39.5	-
		10% Tire Chips	-	11.6	39.7	-
		15% Tire Chips	-	14.1	39.9	-
		20% Tire Chips	-	15.8	40.1	-
		Type 3 Tire Chips (10mm*20mm)				
		5% Tire Chips	-	15.2	39.2	-
		10% Tire Chips	-	15.9	39.5	-
		15% Tire Chips	-	17.6	39.7	-
		20% Tire Chips	-	18.4	39.9	-
Tatlisoz et al. (1998)	Large Scale Direct Shear	Sandy Silt	18.3	11	30	-
		10% Tire Chips	17.6	8	55	-
		20% Tire Chips	17	38	54	-
		30% Tire Chips	16.3	39	53	-
		Sand	16.8	2	34	-
		Tire Chips	5.9	0	30	-
		10% Tire Chips	15.6	2	46	-
		20% Tire Chips	14.5	2	50	-
		30% Tire Chips	13.3	2	52	-

Humphrey et al. (1993)	Large Scale Direct Shear (continued)	Tire Chips-1 < 76 mm	7.01	8.6	25	-
		Tire Chips-1 < 76 mm	6.82	11.5	19	-
		Tire Chips-1 < 76 mm	7.24	7.7	21	-
		Tire Chips-2 < 76 mm	-	4.3	26	-
Wu et al. (1997)	Triaxial Compression	Tire Chips 38 mm-Flat	5.89	0	57	-
		Tire Chips 19 mm-Granular	5.69	0	54	-
		Tire Chips 9.5 mm-Elongated	4.95	0	54	-
		Tire Chips 9.5 mm-Granular	5.89	0	47	-
		Tire Chips 2 mm-Powder	5.69	0	45	-
Attom (2004)	Large Scale Direct Shear (Sand A)	Sand A	-	0	25	-
		10% Tire Shreds	-	0	30	-
		20% Tire Shreds	-	0	37	-
		30% Tire Shreds	-	0	41	-
		40% Tire Shreds	-	0	45	-
	Large Scale Direct Shear (Sand B)	Sand B	-	0	28	-
		10% Tire Shreds	-	0	35	-
		20% Tire Shreds	-	0	42	-
		30% Tire Shreds	-	0	47	-
		40% Tire Shreds	-	0	49	-
	Large Scale Direct Shear (Sand C)	Sand C	-	0	36	-
		10% Tire Shreds	-	0	42	-
		20% Tire Shreds	-	0	45	-
		30% Tire Shreds	-	0	48	-
		40% Tire Shreds	-	0	50	-

This Study	Triaxial (Quick Compression) (40, 100, 200 kPa) Strain rate= 0.5 mm/min (continued)	Sand	16.0	9.97	41.48	43.02
		Tire Crumb	6.5	8.1	16.89	19.71
		5% Tire Crumb	15.1	15.10	38.19	40.88
		10% Tire Crumb	14.5	21.02	38.16	41.57
		20% Tire Crumb	13.3	24.65	35.12	39.57
		30% Tire Crumb	12.5	14.21	31.02	34.19
		40% Tire Crumb	11.2	9.28	28.69	30.96
		Tire Buffings	4.6	9.54	14.35	17.74
		5% Tire Buffings	14.7	11.43	41.28	43.18
		10% Tire Buffings	13.7	14.98	35.93	38.78
		20% Tire Buffings	12.1	14.04	30.99	34.07
		30% Tire Buffings	10.3	13.63	26.89	30.33
		40% Tire Buffings	9.1	11.18	24.70	27.72
	Triaxial (CD) (40, 100, 200 kPa) Strain rate= 0.5 mm/min	Sand	16.0	1.45	41.49	41.70
		Tire Crumb	6.5	30.17	17.56	25.95
		5% Tire Crumb	15.1	16.13	39.35	41.99
		10% Tire Crumb	14.5	17.38	38.33	41.31
		20% Tire Crumb	13.3	15.60	35.44	38.48
		30% Tire Crumb	12.5	12.72	36.28	38.67
		40% Tire Crumb	11.2	27.85	27.57	33.90
		Tire Buffings	4.6	29.51	16.62	24.89
		5% Tire Buffings	14.7	5.51	41.07	42.02
		10% Tire Buffings	13.7	15.64	35.10	38.12
		20% Tire Buffings	12.1	14.74	33.88	36.78
		30% Tire Buffings	10.3	11.83	30.47	33.12
		40% Tire Buffings	9.1	28.05	24.36	31.27

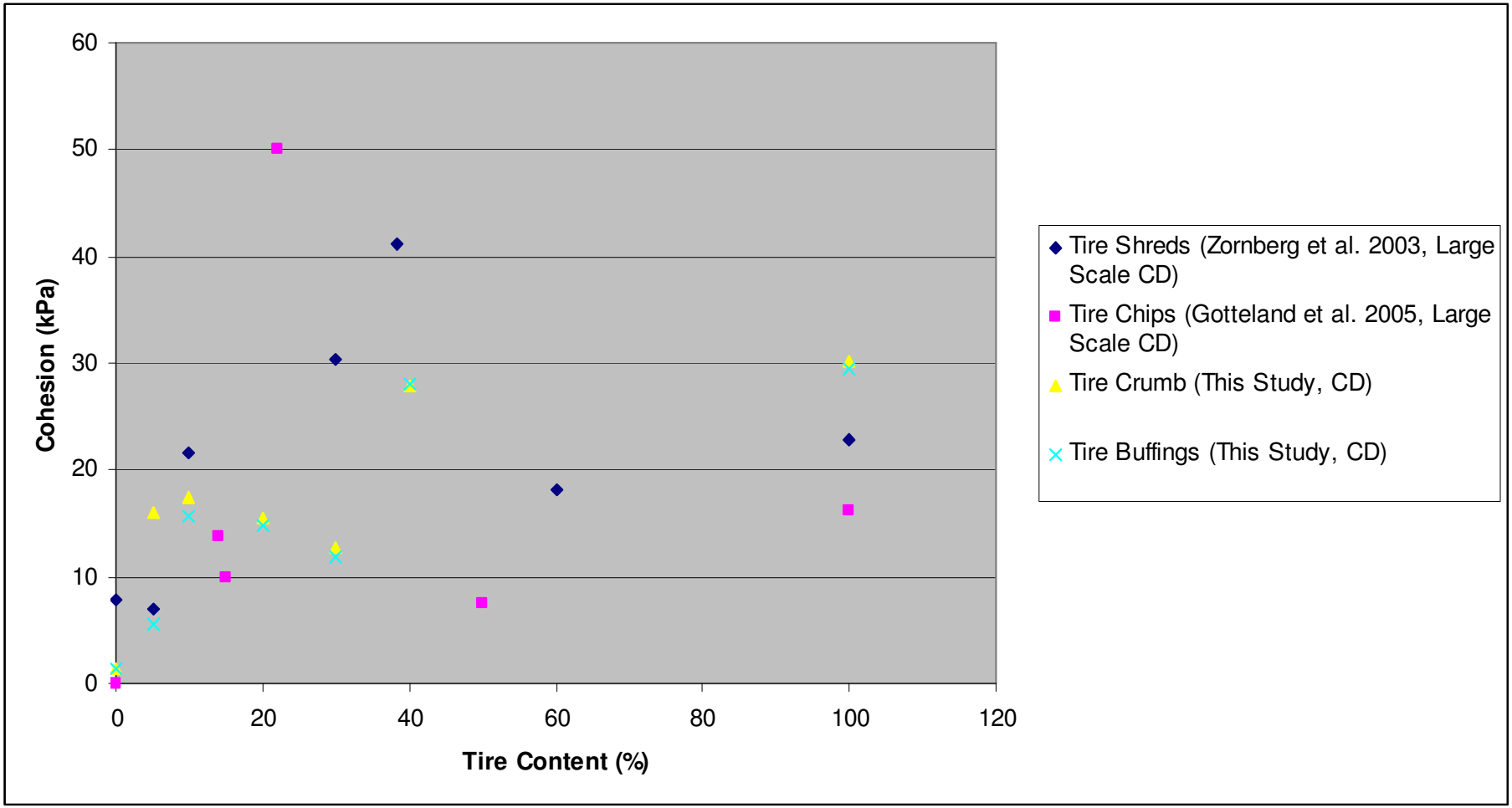

Figure 5.110. Cohesion- tire content graph with literature comparison

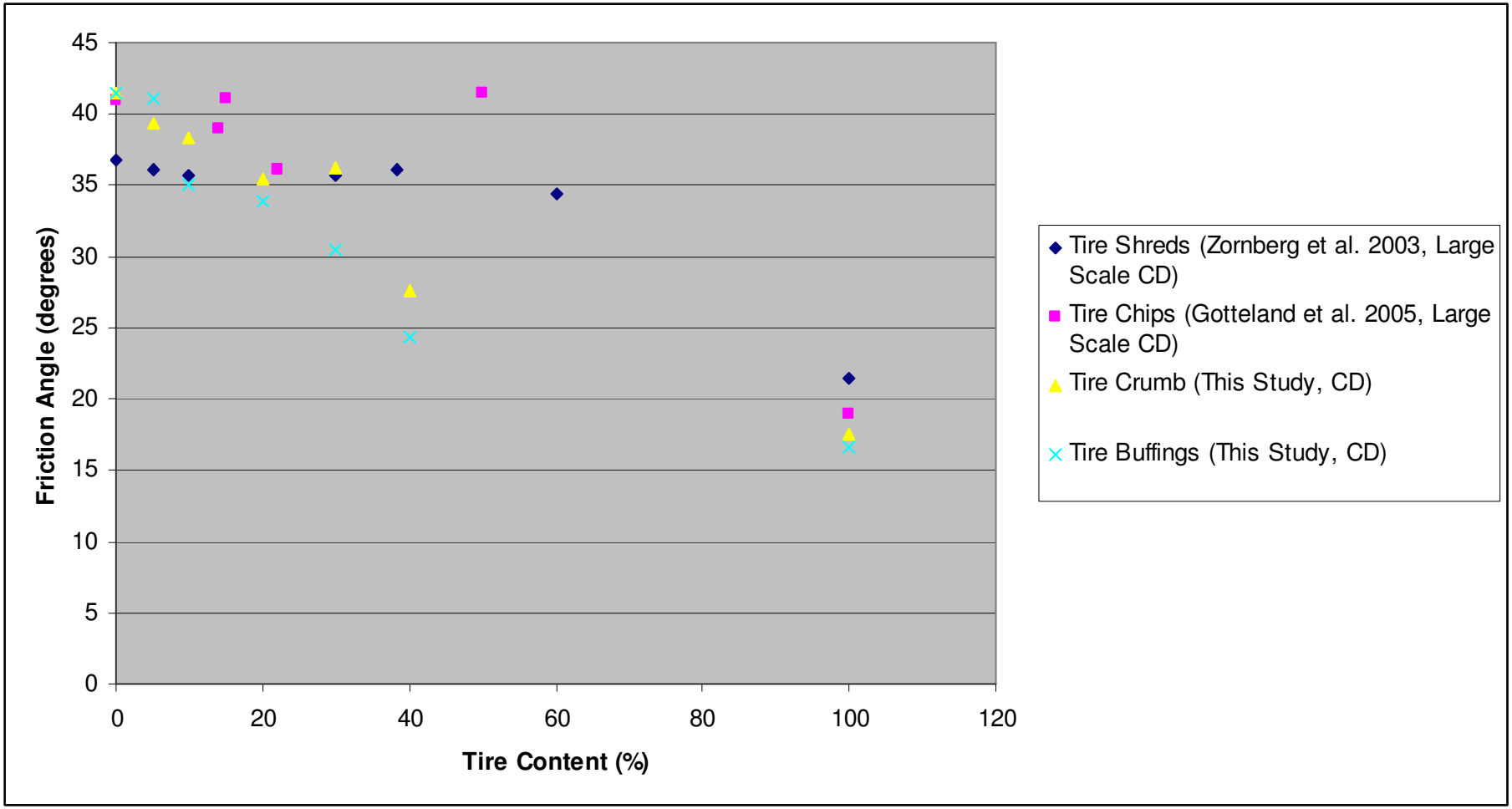

Figure 5.111. Friction angle - tire content graph with literature comparison

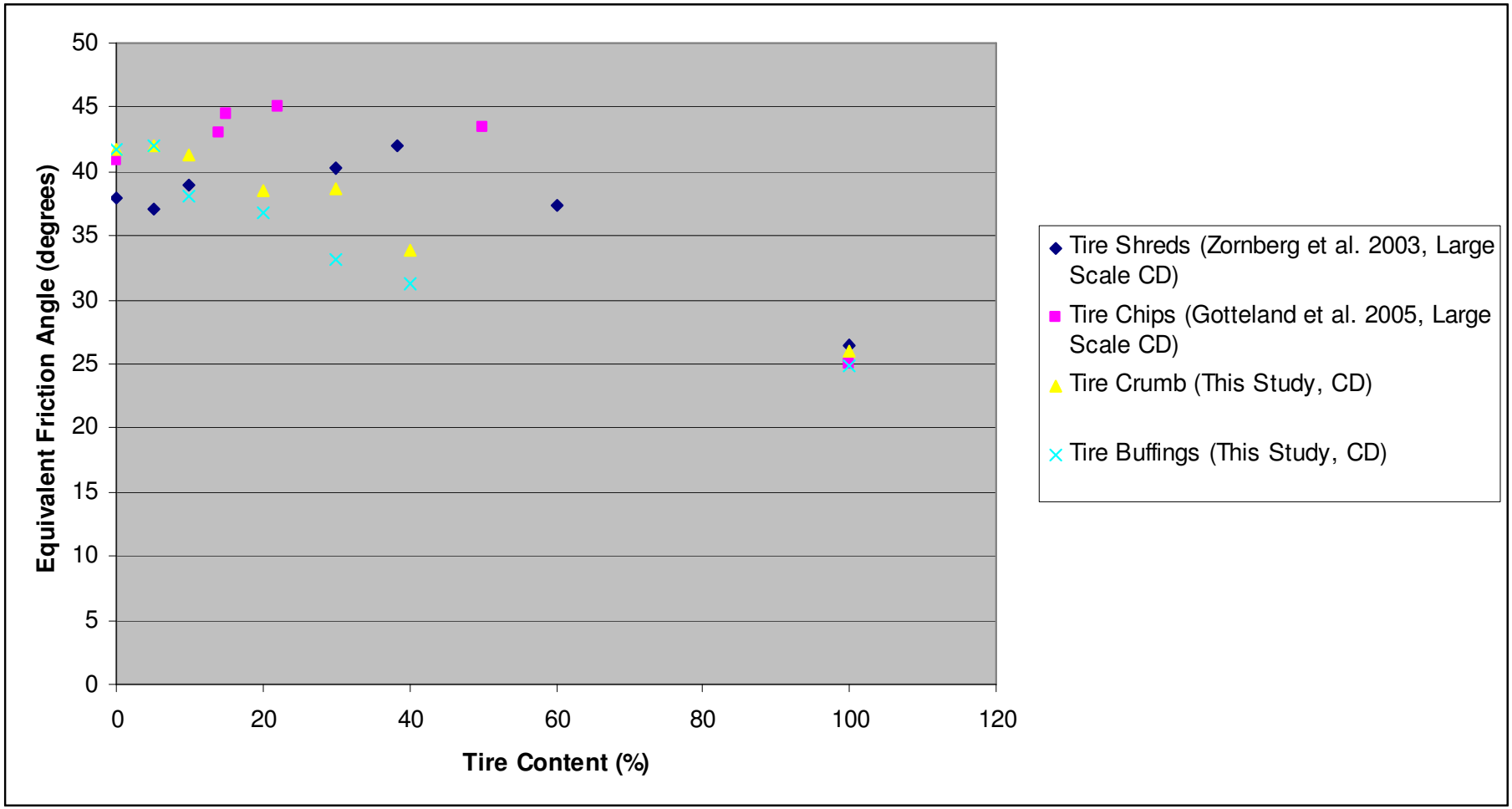

Figure 5.112. Equivalent friction angle - tire content graph with literature comparison

6. CONCLUSION

Tire wastes and tire waste-sand mixtures can be used as an alternative lightweight fill material to construct highway embankments. The reuse of tire wastes help to solve environmental problems by consuming stockpiles of scrap tires, and geotechnical problems by enhancing the shear strength of weak soils. The aim of this study is to evaluate the effect of tire waste inclusions to sand on the shear strength of the mixture. A series of quick triaxial compression tests are performed on dry specimens and a series of consolidated drained (CD) triaxial tests are conducted to investigate the effects of tire content, tire aspect ratio, and tire shape on the shear strength parameters of the sand-tire waste mixtures. California bearing ratio (CBR) tests are also conducted to evaluate the effect of tire waste inclusions on the CBR value. Tire crumb, and tire buffings are the types of tire wastes used in the experiments. Tire crumb are granular materials with an aspect ratio ranging between the values 1 and 1.5, and tire buffings are fiber shaped materials with an aspect ratio ranging between the values 3.5-4.

In the first part of the experimental program, a set of CBR tests are conducted on sand and mixtures of sand and tire waste with varying tire content. Mixtures are prepared at tire contents of 5, 10, 20, 30, and 40 per cent tire waste by weight. Three different inclusions are tested which are tire crumb, tire buffings having an aspect ratio of 3.5-4, and tire buffings having an aspect ratio of 7.5-8. Experimental results showed that the addition of tire buffings increased the CBR value of the mixture, however the addition of tire crumb decreased the CBR value. The addition of 30 per cent tire buffings having an aspect ratio of 7.5-8 to sand increased the CBR value from 7.98 to 15.77, which is a 98 per cent increase, and the addition of tire buffings having an aspect ratio of 3.5-4 resulted in a 44 per cent increase, increasing the CBR value from 7.98 to 11.48. Use of tire buffings with a higher aspect ratio resulted in a higher CBR value in all of the experiments.

In the next part of the experimental program, 13 sets of quick triaxial compression tests are performed on dry specimens composed of sand, tire crumb, tire buffings, and mixtures of sand and tire waste with varying tire content. The mixtures were prepared at 5, 10, 20, 30, and 40 per cent tire waste by weight. The tests are conducted under three

different confining stresses that are 40, 100, and 200 kPa. A strain rate of 0.5 mm/min is used in the experiments. According to the test results the optimum reinforcement is fiber shaped tire buffings with an amount of 5 per cent by weight. 5 per cent tire buffings addition to sand leads to a cohesion value of 11.43 kPa, and an internal friction angle of 41.28 degrees, where the calculated equivalent friction angle is determined as 43.18. Addition of tire crumb is not as effective as addition of tire buffings. Using fiber shaped tire wastes with an aspect ratio of 3.5-4 leads to higher shear strength parameters compared to granular tire wastes with an aspect ratio of 1-1.5. It is also determined that as the tire crumb content increases the axial strain value at failure also increases, but the use of tire buffings instead of tire crumb as tire inclusions results even in a larger axial strain value at failure.

In the last part of the experimental program, 13 sets of consolidated drained triaxial tests are performed on specimens having same ratios of compositions as the quick triaxial compression tests. Same confining stresses (40, 100, 200 kPa) are used, and the test is conducted at a strain rate of 0.5 mm/min at which the pore pressure remains zero for the duration of the test. The results showed that addition of 5 per cent tire crumb or 5 per cent tire buffings both increased the shear strength of sand. However, the greatest shear strength was obtained by adding 5 per cent of tire buffings to sand. The specimen prepared by adding 5 per cent tire buffings to sand has a cohesion value of 5.51 kPa, and an internal friction angle of 41.07 degrees, where the equivalent internal friction angle can be calculated as 42.02 degrees. The shear strength decreases for tire contents beyond the value 5 per cent by weight. The results of consolidated drained tests indicate that fiber shaped tire buffings at an amount of 5 per cent by weight should be added to sand as reinforcement for geotechnical applications. The stress-strain behavior and the volumetric strain behavior of tire waste-sand mixtures change from sand-like behavior to tire-like behavior at a tire waste content of 40 per cent. It is also determined that in all tests a higher confining pressure leads to a higher deviator stress, and a more contractive volumetric behavior. Specimens prepared with both types of tires show similar volumetric strain behavior in the range of the aspect ratios used in this study (1-1.5 and 3.5-4). It is observed that pure sand specimens, and specimens containing 5 per cent, 10 per cent, 20 per cent, and 30 per cent tire waste show dilative volumetric behavior. Pure tire waste specimens, and specimens containing 40 per cent tire waste show contractive volumetric behavior.

The test results are in good agreement with the study of Zornberg et al. (2004) regardless of the type of tire used. It is reported by Zornberg et al. (2004) that various specimens containing tire shreds having aspect ratios of 1, 2, and 4, showed similar volumetric strain behavior.

The results indicate that use of tire buffings additive will improve the performance of highway embankments under the traffic load. Adding 5 per cent of fiber shaped tire buffings by weight to sand will form a reinforced lightweight fill composition to be used in geotechnical applications improving both the shear strength and the CBR value of soil. Tire shape, tire aspect ratio, and tire content have a significant effect on the shear strength parameters of the composition. Fiber shaped tire inclusions influences the shear strength parameters and the CBR value better compared to granular tire inclusions. The optimum tire content is determined as 5 per cent from the triaxial test results. The CBR test results indicated that as the aspect ratio increases, the reinforcements become more effective.

Because of the ASTM standard limitations tire buffings with higher lengths and aspect ratios could not be tested in this study. To evaluate the possible effects of fiber shaped tire waste additions on the shear strength parameters of sand and to determine if boundary effects influence the test results, further study is required. Both drained and quick large scale triaxial compression tests must be conducted on mixtures of sand and tire buffings, using fibers with higher lengths and aspect ratios.

REFERENCES

Acosta, H. A., T. B. Edil and C. H. Benson, 2003, *Soil Stabilization and Drying Using Fly Ash*, Geo Engineering Report No. 03-03, University of Wisconsin-Madison.

Ahmed, I. and C. W. Lovell, 1993, "Rubber Soils as Lightweight Geomaterial", *Transportation Research Record*,1422, pp. 61-70.

Akbulut, S., S. Arasan and E. Kalkan, 2007, "Modification of Clayey Soils Using Scrap Tire Rubber and Synthetic Fibers", *Applied Clay Science*, 38, pp. 23-32.

ASTM D 1883-07, 2007, *Standard Test Method for CBR (California Bearing Ratio) of Laboratory-Compacted Soils*, American Society for Testing and Materials.

ASTM D 2850-03a, 2007, *Standard Test Method for Unconsolidated-Undrained Triaxial Compression Test on Cohesive Soils*, American Society for Testing and Materials.

ASTM D 4767-04, 2004, *Standard Test Method for Consolidated Undrained Triaxial Compression Test for Cohesive Soils*, American Society for Testing and Materials.

ASTM D 6270-98, 1998, *Standard Practice for Use of Scrap Tires in Civil Engineering Applications*, American Society for Testing and Materials.

Attom, M. F., 2005, "The Use of Shredded Waste Tires to Improve the Geotechnical Engineering Properties of Sands", *Environmental Geology*, 49, pp. 497-503.

Benson, C. H., 1995, "Using Shredded Scrap Tires in Civil and Environmental Construction", *Resource Recycling*, October.

Benson, C. and M. V. Khire, 1994, "Reinforcing Sand with Strips of Reclaimed High-Density Polyethylene", *Journal of Geotechnical and Geoenvironmental Engineering*, Vol. 120, No. 5, ASCE, pp. 838-855.

Bernal, A., 1996, *Laboratory Study on the Use of Tire Shreds and Rubber-Sand in Backfills and Reinforced Soil Applications*, Ph.D. Thesis, Purdue University.

Duffy, D.P., 1995, "Using Tire Chips as a Leachate Drainage Layer", *Waste Age*, Vol. 26, No. 9, pp. 113-122.

Edil, T. B. and P. J. Bosscher, 1994, "Engineering Properties of Tire Chips and Soil Mixtures", *Geotechnical Testing Journal*, Vol. 17, No. 4, pp. 453-464.

Edincliler, A., G. Baykal and K. Dengili, 2004, "Determination of Static and Dynamic Behavior of Recycled Materials for Highways", *Resources, Conservation and Recycling*, 42, pp. 223-337.

Ferguson, G., 1993, "Use of Self Cementing Fly Ashes as a Soil Stabilization Agent", *Geotechnical Special Publication*, No. 36, ASCE New York, pp. 1-15.

Foose, G. J., C. H. Benson and P. J. Bosscher, 1996, "Sand Reinforced with Shredded Waste Tires", *Journal of Geotechnical and Geoenvironmental Engineering*, Vol. 122, No. 9, ASCE, pp. 760-767.

Ghazavi, M., 2004, "Shear Strength Characteristics of Sand-Mixed with Granular Rubber", *Geotechnical and Geological Engineering*, 22, pp. 401-416

Ghazavi, M. and M. A. Sakhi, 2005, "Optimization of Aspect Ratio of Waste Tire Shreds in Sand-Shred Mixtures Using CBR Tests", *Geotechnical Testing Journal*, Vol. 28, No. 6.

Ghiassian, H., G. Poorebrahim and D. H. Gray, 2004, "Soil Reinforcement with Recycled Carpet Wastes", *Waste Management Research*, 22, pp. 108-114.

Gotteland, P., S. Lambert and L. Balachowski, 2005, "Strength Characteristics of Tyre Chips-Sand Mixtures", *Studia Geotechnica et Mechanica*, Vol. 17, No. 1-2.

Gray, T., *Preliminary Directional Plan for CIWMB Market Development/ Demonstrations Contract*, California Integrated Waste Management Board, February.

Gray, D. H. and H. Ohashi, 1983, "Mechanics of Fiber Reinforcing in Sand", *Journal of Geotechnical Engineering Division*, ASCE 109, pp. 335-353.

Hataf, N. and M. M. Rahimi, 2005, "Experimental Investigation of Bearing Capacity of Sand Reinforced with Randomly Distributed Tire Shreds", *Construction and Building Materials*, 20, pp. 910-916.

Humphrey, D. N., 1999, *Civil Engineering Application of Tire Shreds,* The Tire Industry Conference, Hilton Head, South Carolina, March.

Humphrey, D. N., L. E. Katz and M. Blumenthal, 1997, "Water Quality Effects of Tire Chip Fills Placed Above the Groundwater Table", *Testing Soil Mixed with Waste or Recycled Materials*, ASTM STP 1275, pp. 299-313.

Humphrey, D. N. and W. P. Manion, 1992, "Properties of Tire Chips for Lightweight Fill", *Proceedings of the Conference on Grouting, Soil Improvement, and Geosynthetics*, ASCE, Vol. 2, pp. 1344-1355.

Jang, J., T. Yoo, J. Oh and I. Iwasaki, 1997, "Discarded Tire Recycling Practices in the United States, Japan and Korea", *Resources, Conservation and Recycling*, 22, pp. 1-14.

Lawrence, B., D. Humphrey and L. H. Chen, 1998, "Field Trial of Tire Shreds as Insulation for Paved Roads", *Proceedings of the Tenth International Conference on Cold Regions Engineering: Putting Research into Practice*, ASCE, pp. 428-439.

Li, C. and J. G. Zornberg, 2003, "Validation of Discrete Framework for Fiber-Reinforcement", *Proc. Two Rivers Conference,* North American Geosynthetics Society, Winnipeg, Canada, Session 10E.

Maher, M. H. and D. H. Gray, 1990, "Static Response of Sands Reinforced with Randomly Distributed Fibers", *Journals of Geotechnical Engineering Division*, ASCE 116, pp. 1661-1667.

Masad, E., R. Taha, C. Ho and T. Papagiannakis, 1996, "Engineering Properties of Tire/Soil Mixtures as a Lightweight Fill Material", *Geotechnical Testing Journal*, Vol. 19, No. 3, pp. 297-304.

Michalowski, R. L. and A. Zhao, 1996, "Failure of Fiber-Reinforced Granular Soils", *Journal of Geotechnical and Geoenvironmental Engineering*, Vol. 122, No. 3, ASCE, pp. 226-234.

Michalowski, R. L. and J. Cernak, 2003, "Triaxial Compression of Sand Reinforced with Fibers", *Journal of Geotechnical and Geoenvironmental Engineering*, Vol. 129, No. 2, ASCE, pp. 125-136.

Moo-Young, H., K. Sellasie, D. Zeroka and G. Sabnis, 2003, "Physical and Chemical Properties of Recycled Tire Shreds for Use in Construction", *Journal of Geotechnical and Geoenvironmental Engineering*, Vol. 129, No. 10, ASCE, pp. 921-929.

Narejo, D.B. and M. Shettima, 1995, "Use of Recycled Automobile Tires to Design Landfill Components", *Geosynthetics International*, Vol. 2, No. 3, pp. 619-625.

Ozkul, Z. H. and G. Baykal, 2007, "Shear Behavior of Compacted Rubber Fiber-Clay Composite in Drained and Undrained Loading", *Journal of Geotechnical and Geoenvironmental Engineering*, Vol. 133, No. 7, ASCE, pp. 767-781.

Palmer, B. G., T. B. Edil and C. H. Benson, 2000, "Liners for Waste Containment Constructed with Class F and C Fly Ashes", *Journal of Hazardous Materials*, 76, pp. 193-216.

Ranjan, G., R. M. Vasan and H. D. Charan, 1996, "Probabilistic Analysis of Randomly Distributed Fiber-Reinforced Soil", *Journals of Geotechnical Engineering Division*, ASCE 122, pp. 419-426.

Reddy, K. R. and A. Marella, 2001, "Properties of Different Size Scrap Tire Shreds: Implications on Using as Drainage Material in Landfill Cover Systems", *The Seventeenth International Conference on Solid Waste Technology and Management*, October, Philadelphia, USA.

RMA, 2006, *Scrap Tire Markets in the United States*, Rubber Manufacturers Association, November.

Santoni, R., J. Tingle and S. L. Webster, 2001, "Engineering Properties of Sand-Fiber Mixtures for Road Construction", *Journal of Geotechnical and Geoenvironmental Engineering*, Vol. 127, No. 3, ASCE, pp. 258-268.

Shalaby, A. and R. A. Khan, 2004, "Design of Unsurfaced Roads Constructed with Large-Size Shredded Rubber Tires: A Case Study", *Resources, Conservation and Recycling*, 44, pp. 318-332.

Tatlisoz, N., C. H. Benson and T. B. Edil, 1997, "Effect of Fines on Mechanical Properties of Soil-Tire Chip Mixtures", *Testing Soil Mixed with Waste or Recycled Materials*, ASTM STP 1275.

Tatlisoz, N., T. B. Edil and C. H. Benson, 1998, "Interaction between Reinforcing Geosynthetics and Soil-Tire Chip Mixtures", *Journal of Geotechnical and Geoenvironmental Engineering*, Vol. 124, No. 11, ASCE, pp. 1109-1119.

Toth, P., H. Chan and C. Cragg, 1988, "Coal Ash as Structural Fill with Special Reference to Ontario Experience", *Canadian Geotechnical Journal*, Vol. 25, No. 4, pp. 694-704.

Trzebiatowski, B. D., T. B. Edil and C. H. Benson, 2004, "Case Study of Subgrade Stabilization Using Fly Ash: State Highway 32, Port Washington, Wisconsin", *Recycled Materials in Geotechnics,* No. 127, pp. 123-136.

Venkatappa Rao, G. and R. K. Dutta, 2006, "Compressibility and Strength Behaviour of Sand-Tyre Chip Mixtures", *Geotechnical and Geological Engineering*, 24, pp. 711-724.

Waldron, L. J., 1977, "Shear Resistance of Root-Permeated Homogeneous and Stratified Soil", *Soil Sci Soc Am Proc*, 41:843–9.

Wu, T. H., 1976, *Investigation of Landslides on Prince of Wales Island, Alaska*, Geotechnical Engineering Report No. 5, Department of Civil Engineering, OH State University.

Wu, W. Y., C. C. Benda and R. F. Cauley, 1997, "Triaxial Determination of Shear Strength of Tire Chips", *Journal of Geotechnical and Geoenvironmental Engineering*, Vol. 123, No. 5, ASCE, pp. 479-482.

Yetimoglu, T. and O. Salbas, 2003, "A Study on Shear Strength of Sands Reinforced with Randomly Distributed Discrete Fibers", *Geotextiles and Geomembranes*, 21, pp. 103-110.

Yoon, S., M. Prezzi, N. Z. Siddiki and B. Kim, "Construction of a Test Embankment Using a Sand-Tire Shred Mixture as Fill Material", *Waste Management*, 26, pp. 1033-1044.

Zimmerman, P. S., 1997, *Compressibility, Hydraulic Conductivity, and Soil Infiltration Testing of Tire Shreds and Field Testing of a Shredded Tire Horizontal Drain*, M.S. Thesis, Iowa State University.

Zornberg, J. G., 2002, "Discrete Framework for Limit Equilibrium Analysis of Fiber-Reinforced Soil", *Geotechnique,* Vol. 52, No. 8, pp. 593-604.

Zornberg, J. G., A. R. Cabral and C. Viratjandr, 2004, "Behaviour of Tire Shred-Sand Mixtures", *Canadian Geotechnical Journal*, 41, pp. 227-241.